CALCIUM SIGNALLING
IN
NEUTROPHIL BEHAVIOUR

by

Esther Joy Saltmarsh

A dissertation submitted to Cardiff University in candidature for the degree of Doctor of Philosophy

Neutrophil Signalling Group
Department of Surgery
Wales College of Medicine
Cardiff University

September 2008

UMI Number: U584323

All rights reserved

INFORMATION TO ALL USERS
The quality of this reproduction is dependent upon the quality of the copy submitted.

In the unlikely event that the author did not send a complete manuscript
and there are missing pages, these will be noted. Also, if material had to be removed,
a note will indicate the deletion.

UMI U584323
Published by ProQuest LLC 2013. Copyright in the Dissertation held by the Author.
Microform Edition © ProQuest LLC.
All rights reserved. This work is protected against
unauthorized copying under Title 17, United States Code.

ProQuest LLC
789 East Eisenhower Parkway
P.O. Box 1346
Ann Arbor, MI 48106-1346

DECLARATION

This work has not previously been accepted in substance for any degree and is not concurrently submitted in candidature for any degree.

Signed ..... (candidate) Date 23rd Sept 2008

STATEMENT 1

This thesis is being submitted in partial fulfilment of the requirements for the degree of PhD.

Signed..... .....(candidate) Date 23rd Sept 2008

STATEMENT 2

This thesis is the result of my own independent work/investigation, except where otherwise stated. Other sources are acknowledged by explicit references.

Signed ..... (candidate) Date 23rd Sept 2008

STATEMENT 3

I hereby give consent for my thesis, if accepted, to be available for photocopying and for inter-library loan, and for the title and summary to be made available to outside organisations.

Signed ..... (candidate) Date 23rd Sept 2008

Acknowledgements

The studies described in this thesis were conducted in the Department of Surgery, Wales College of Medicine, Cardiff University. There are several people I would like to thank for making this research project as enlightening a journey as it has been. Firstly, many thanks go to my supervisor, Professor Maurice Hallett, for his unfailing support, encouragement and enthusiasm for research. I would also like to thank Dr Sharon Dewitt and Iraj Laffafian for their laboratory expertise and informative discussions, some of which were about science.

Many thanks must go to the blood donors, without whom this project would not have been possible. For those who let me practise on them and those who let me take their blood before morning coffee, I am truly grateful. Also my gratitude goes to all the other members of the department for their input in conversations over coffee each morning.

Thank you to Bill Luskanskas for the ICAM-1-GFP plasmid, to Iraj for sharing his CHO cells, and most importantly to Cardiff University for funding the research.

An enormous thank you goes to my friends and family who have persevered with me through moments of madness alongside moments of inspiration. Their support has been as invaluable as the distractions they provided. A special thank you must go to Mark, my husband. Ever since we got married he has endured sleepless nights and tyrannical rants while also sharing the joys of achievement. Through everything he has been a rock of constancy that has kept me grounded and probably sane.

PUBLICATIONS

Some of the work presented in this thesis has previously been published. Early work appeared under my maiden name of Hillson.

Hillson E, Hallett MB (2006) **Localised and Rapid Ca^{2+} Micro-Events in Human Neutrophils: Conventional Ca^{2+} Puffs and Global Waves Without Peripheral-Restriction Or Wave Cycling.** *Cell Calcium*

Hillson E, Dewitt S, Hallett MB (2006) **IP_3-Induced Cell Spreading of Human Neutrophils Requires Ca^{2+} Influx.** *Proceedings of the American Society of Cell Biology Annual Meeting*

Hillson EJ, Dewitt S, Hallett MB (2007) **Optical Methods for the Measurement and Manipulation of Cytosolic Free Calcium in Neutrophils.** *Methods Mol Biol. 412:125-37 (invited chapter)*

Hillson-Saltmarsh EJ, Hallett MB (2008) **Addressing Controversy in the Ca^{2+} Signalling in Human Neutrophils.** *European Journal of Clinical Investigation*

Some of the work presented in this thesis has previously been presented:

Mar 2008: **Addressing Controversy In Ca^{2+} Signalling in Human Neutrophils.** ESCI Annual Meeting, Geneva, Switzerland

Dec 2006: **IP_3-Induced Cell Spreading of Human Neutrophils Requires Ca^{2+} Influx.** ASCB Annual Meeting

Nov 2006: **Human Neutrophil Spreading Requires Ca^{2+} Influx.** Cardiff University Postgraduate Research Day (1st Prize)

May 2006: **Calcium Sparks Ignite Human Neutrophil Behaviour.** SET for Britain, House of Parliament, Westminster, UK

May 2006: **Ca^{2+} Puffs Trigger Human Neutrophil Activity.** Speaking Of Science (1st Prize)

Nov 2005: **Fast Localised Ca^{2+} Signalling In Human Neutrophils.** Cardiff University Postgraduate Research Day

SUMMARY

Neutrophils are at the front line of defence in humans against attack by invading pathogens. They undergo complex behaviours, many of which are controlled by changes in the concentration of cytosolic free calcium ions (Ca^{2+}). However, the control and mechanisms of these behaviours are still the subject of much research and debate. Ca^{2+} is known to be important in many different cell systems. There are a plethora of Ca^{2+} signalling events in the "Ca^{2+} toolkit", but not all cells have each element. It is not fully understood elements of the toolkit that neutrophils employ to make up their well-characterised global Ca^{2+} changes.

This thesis is an investigation into the involvement of Ca^{2+} in neutrophil behaviours that underlie much of their functionality, particularly focussing on subcellular Ca^{2+} release events (puffs) and Ca^{2+} signalling during neutrophil spreading on surfaces and during phagocytosis.

Reports were published by Petty et al of a travelling zone of elevated Ca^{2+} (z-wave) in neutrophils. However, research laid out in this thesis demonstrates that these z-waves are questionable in neutrophils. Instead, conventional Ca^{2+} puffs and waves were seen and characterised in response to fMLP stimulation and uncaging IP_3.

Neutrophils undergo dramatic, rapid morphological changes during Ca^{2+} signals triggered by both fMLP and uncaging IP_3, representative of behaviour during adhesion and extravasation. It was shown that the high concentration of Ca^{2+} under the plasma membrane that results from Ca^{2+} influx activated the protease calpain, which released the membrane from the cytoskeleton for rapid shape change. Similar signals and behaviours are seen when neutrophils are stimulated by binding of β-integrins. Indeed, adhesion to ICAM-1 expressing cells and phagocytosis resulted in global Ca^{2+} signals and Ca^{2+} influx accompanied by rapid shape change. However, no Ca^{2+} puffs were seen in these latter experiments, implying that the signalling in these conditions occurs through a different pathway, possibly PIP_3.

In conclusion, neutrophils utilise conventional Ca^{2+} signalling events (release puffs and influx waves) not z-waves to control many of their functions. They are capable of producing Ca^{2+} puffs, but the lack of ER means this is unlikely to be a primary signalling pathway. Binding through β-integrins does trigger Ca^{2+} signals, possibly through the PIP_3 pathway, but not store release. The characterisation of Ca^{2+} puffs and the functionality of the Ca^{2+}-activated protease calpain in these conditions are novel and merit future investigation. The findings in this thesis enhance the general understanding of how neutrophil behaviours are regulated by Ca^{2+} and provide a new methodology for further research.

CONTENTS

ABBREVIATIONS

AM	Acetotoxymethyl Ester
AO	Acridine Orange
ATP	Adenosine Triphosphate
BSA	Bovine Serum Albumin
BSS	Balanced Saline Solution
Ca^{2+}	Cytosolic free Ca^{2+} ion
CAM	Calmodulin
cAMP	Cyclic Adenosine Monophosphate
C3bi	Complement fragment 3b (inactive)
cADPR	Cyclic Adenosine Diphosphate Ribose
CCD	Charged Coupled Decide Camera
CFU-GEMM	Colony Forming Unit – Granulocyte, Erythroid, Monocyte, Megakaryote
CFU-GM	Colony Forming Unit – Granulocyte, macrophage
CFU-G	Colony Forming Unit – Granulocyte
CHO	Chinese Hamster Ovary carcinoma cell line
CICR	Ca^{2+} Induce Ca^{2+} Release
CNP	Circulating Neutrophil Pool
CRAC	Ca^{2+} Release Activated Ca^{2+} (channel)
CSF	Colony Stimulating Factor
CTC	Chlortetracycline
DAG	Diacylglycerol
DMSO	Dimethylsulfoxide
ECIS	Electric Cell-Substrate Impedance Sensing
EF-hand	Ca^{2+} binding motif on a protein
EGTA	Ethylene Glycol Aminoethyl Ester Tetraacetic Acid
EM	Electron Microscope
ER	Endoplasmic Reticulum
fMLP	Formyl-methionyl-leucyl-phenylalanine (formlyated peptide)

FRAP	Fluorescence Recovery After Photobleaching
GFP	Green Fluorescent Protein
GMCSF	Granulocyte-Monocyte Colony Stimulating Factor
GPI	Glycosylphosphatidylinositol
GPN	Glycylphenylalanine-B-Naphthalamide
HAEC	Human Aortic Endothelial Cell
HEPES	Hydroxyethylpiprazine Ethanesulphonic Acid
HUVEC	Human Umbilical Endothelial Cell
ICAM-1	Intercellular Adhesion Molecule-1
IL-1	Interleukin-1
IP_3	Inositol 1,4,5 Triphosphate
IP_3R	Inositol 1,4,5 Triphosphate Receptor
Kd	Dissociation Constant
Km	Michaelis Constant
LCSM	Leica Confocal Scanning Microscope
LPS	Lipopolysaccharide
LUT	Look Up Table
MNP	Marginal Neutrophil Pool
NADPH	Nicotinamide Adenine Dinucleotide Phosphate, reduced form
NPP	Neutrophil Proliferative Pool
NSP	Neutrophil Storage Pool
PAF	Platelet Activating Factor
PI-3-Kinase	Phosphatidylinositide-3-Kinase
PIP_2	Phosphatidylinositol 4,5 bisphosphate
PIP_3	Phosphatidylinositol 3,4,5 trisphosphate
PKC	Protein Kinase C
PLC	Phospholipase C
PMN	Polymorphonuclear neutrophilic leukocytes (neutrophils)
PMT	Photomultiplier Tube
PTP	Permeability Transition Poor
RSCM	Resonant Scanning Confocal Microscopy

RyR	Ryanodine Receptor
SD	Standard Deviation of the Mean
SERCA	Sarco-Endoplasmic Reticulum Ca^{2+} ATP-ase
SLAM	Simple Lipid Assisted Microinjection
7TM	Seven Transmembrane Spanning Domain Receptor
TNFα	Tumour Necrosis Factor α
TnC	Troponin C
UV	Ultraviolet
z-waves	Travelling zone of elevated Ca^{2+} reported by Petty et al (occasionally PW for Petty Wave)

CHAPTER 1

Introduction

1.1 Immune System

1.1.1 Introduction

The human body, like many higher organisms has an immune system out of necessity; to protect it from attack by micro-organisms, such as bacteria, viruses, fungi and parasites. In humans the immune system also acts to prevent damage by the body's own cells, such as cancerous, senescent or damaged cells, which need removing. This system must be able to distinguish between non-self micro-organisms and self, and also between damaged cells and healthy ones. Therefore, every element must be tightly controlled and regulated to ensure only the intended targets are destroyed.

1.1.2 Innate and Acquired Immunity

The human immune system is divided into three branches: barriers, innate and acquired immunity. Each branch contains of both cells and molecular components. The barriers to infection range in complexity, from the relatively simple skin, to more complicated mucosal membranes. Few microbes are capable of penetrating intact skin and antimicrobial chemicals are secreted in the sweat and by sebaceous and lachrymal glands. The presence of some microbes on the skin surface and also in the gastrointestinal tract keeps other potentially harmful microbe growth in check. Hairs at the entrance to the nasal passage and microscopic hairs along the respiratory and upper gastrointestinal tract help to prevent entry into body cavities. The microscopic hairs sweep any microbes that become trapped in the viscous mucus that lines these areas up into the throat by ciliary action. They are then swallowed and destroyed in the acidic stomach (Vander et al, 1994). However, if micro-organisms do manage to

bypass all these barriers, the human body has the highly specialised, regulated and coordinated innate and acquired immune systems.

The innate immune system is so called because all humans are born with this complete system. It is relatively non-specific compared to the acquired immune system. However, it is still highly regulated and has high specificity for the range of targets of this branch of immunity. Many higher organisms also have components of the innate immune system. The innate immune system is comprised of both cellular and molecular components, which act in coordination to rid the body of any potentially hazardous cells or micro-organisms. Table 1.1.2 lists the components of the innate system and indicates points of cross-talk with the acquired system. Complement is a series of proteins that circulate in the blood stream. They act in a cascade, cleaving the next protein in the chain to reveal active and/or binding sites, ultimately culminating in the formation of pores in the surface of target cells and coating of cells and particles to encourage ingestion by phagocytic cells. The former causes lysis of the target cell or micro-organism. The debris is then also cleared by phagocytic cells. As this suggests, the major cellular component of the innate system is made up of phagocytic cells, including neutrophils, which are the focus of this thesis. Phagocytes are discussed in more detail in the following section.

The acquired immune system is unique to vertebrates and is considered more specialised. Certainly the responses are more specific to the particular pathogen that has managed to bypass the body's barriers. The first time a body encounters a pathogenic micro-organism a sequence of events is triggered resulting in the production of antibodies specific to that micro-organism. The system also produces

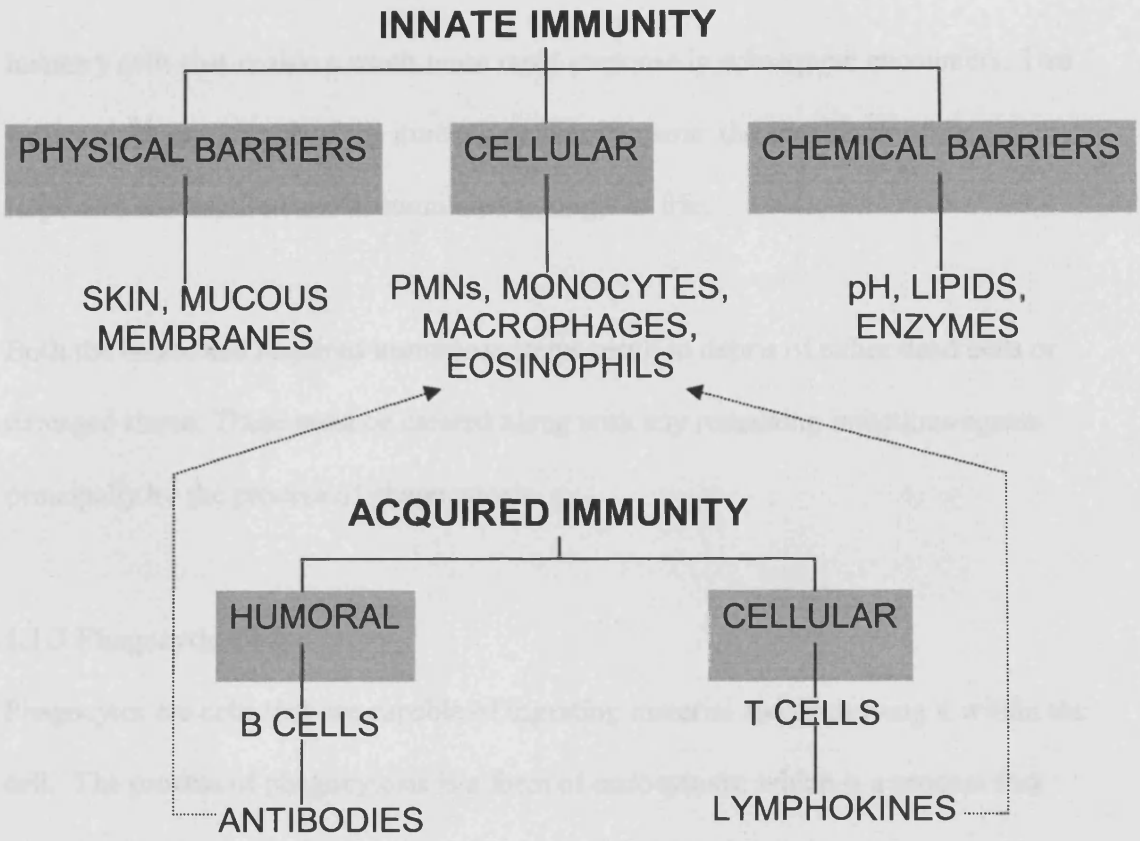

Table 1.1.2 Components of the Immune System – Crosstalk Between Innate and Acquired

A basic schematic illustrates the major point of cross talk between innate and acquired arms of the immune system is via the antibodies and lymphokines that act to enhance the activity of the cellular components of the innate system.

memory cells that enable a much more rapid response in subsequent encounters. This ability gives this branch of the immune system its name: the specificity of the responses are acquired and accumulated throughout life.

Both the innate and acquired immune systems result in debris of either dead cells or damaged tissue. These must be cleared along with any remaining infectious agents principally by the process of phagocytosis.

1.1.3 Phagocytic Cells

Phagocytes are cells that are capable of ingesting material and destroying it within the cell. The process of phagocytosis is a form of endocytosis, which is a process that many types of cells perform. For example, the primitive free-living amoeba *Dictyostelium discoideum* performs phagocytosis as a means of sustenance. Dictostelia engulf bacteria or fungi into a vacuole within the cell, where they are digested and absorbed for nourishment. Some lower animals, such as coelentrates have an inner cavity that is lined with phagocytic cells that provide nutrition to the whole organism by digesting food that is phagocytosed from the inner cavity (Brown, 1995). Higher animals have a more complex digestive system, which no longer uses phagocytic cells for the purposes of digestion and sustenance. Instead, phagocytic cells are used for the removal and destruction of unwanted material. This function is the principle responsibility of the bone marrow derived white blood cells: monocytes, macrophages and polymorphonuclear leukocytes (PMNs, or neutrophils).

1.2 Neutrophils (PMN)

White blood cells were originally divided into different groups by Paul Ehrlich on the basis of their distinctive morphologies (Fig 1.2.1). He initially observed that one group had multiple nuclei within each cell, although closer inspection revealed that these were lobes on a single nucleus connected by very fine connections. Ehrlich named this group "cells with polymorphous nuclei" (Ehrlich, 1898). However, they were soon renamed in 1905 as polymorphonuclear leukocytes by Elie Metchnikoff to better reflect the cell type being referred to. To this day the family of leukocytes are still referred to by this name.

The polymorphonuclear cells were then subdivided into three different cell types according to the distinctive staining properties of the granules within the cells. Basophils stain strongly with basic stain, eosinophils stain with eosin, and neutrophils stain with neutral dyes. Thus, the full terminology for what is often just referred to as a neutrophil was established: polymorphonuclear neutrophilic leukocyte (PMNL).

1.2.1 The Neutrophil

Neutrophils are the most abundant of the white blood cells, representing 40-80 % of the circulating white blood cells in humans ($7x10^9$ cells/L) (Dace and Lewis, 1995). However, establishing a role for these small cells was the cause of much debate in the 19^{th} century. It was originally thought that neutrophils are spontaneously generated at the site of infection, or that they act as agents of infection by carrying accumulated bacteria to the inflamed site. These conclusions were reached from the observation that neutrophils were abundant at sites of infection and inflammation and in pus, and were often engorged with bacteria in these sites.

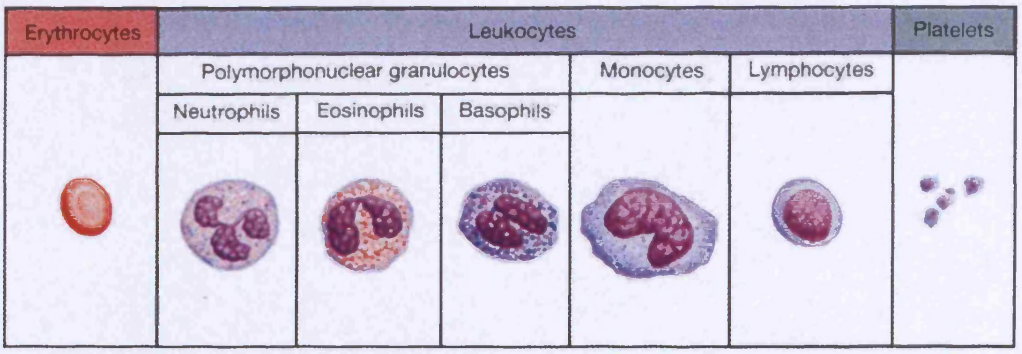

Fig 1.2.1 Cellular Constituents of Blood.

Blood contains red blood cells (erythrocytes), white blood cells (leukocytes) and platelets. Leukocytes can be divided into 2 groups, the polymorphonuclear granulocytes, whose nuclei consist of multiple interconnected lobes (neutrophils, eosinophils, basophils) and mononuclear leukocytes (monocytes and lymphocytes). (Figure taken from Vander et al, 1994)

The theory of spontaneous generation of neutrophils at infected sites was disproved by Waller (1846) who showed that neutrophils were found in the blood stream and moved from the blood vessels by a process called "diapedesis" (Cohnheim, 1867a,b). However, the true role of neutrophils was not established until Metchinkoff used his knowledge of phagocytic cells in the digestive process to study these neutrophils and their purpose at sites of infection. Metchinkoff believed that neutrophils played a beneficial role in the clearance of microbes and the resulting damaged tissue at infected areas. He conducted an experiment, dubbed "thorn in the starfish" where he inserted a thorn into the transparent starfish embryo and observed that the phagocytic cells had migrated to the site of injury. Metchinkoff concluded that this experiment confirmed his theory that phagocytic neutrophils migrate to sites of injury and inflammation, where they removed microbes by ingesting and digesting them through the process of phagocytosis (Metchinkoff 1892, 1901, 1905). Indeed, all subsequent studies have reached the same conclusions as to the role of neutrophils in clearance of infection.

1.2.2 Production – Myelopoiesis

Neutrophils have a short half life of between 4-10 hours in circulation, and therefore must be constantly produced from the bone marrow throughout the lifespan of an individual. The process of neutrophil production is termed myelopoiesis, since they are derived from myeloid stem cells in the bone marrow, along with the other granular leukocytes, eosinophils and basophils, and monocytes, platelets and erythrocytes.

The bone marrow contains pluri-potent stem cells that undergo a series of mitotic divisions to give rise to the various stem cell lines that make up these different cellular components of the blood (Fig 1.2.2).

These pools of stem cells within the bone marrow are at various stages of development. The myeloid progenitor pool contains several dynamic cell pools, from some containing cells that are not committed to their final phenotype up through various stages of division and maturation that become progressively committed before undergoing maturation. For neutrophils specifically, the myeloid stem cell loses the ability to self-replicate, but undergoes the following differentiation stages. The stem cell is referred to as CFU-GEMM (colony forming unit-granulocyte, erythrocyte, monocyte, megakaryocyte), which differentiates into CFU-GM (colony forming unit-granulocyte, macrophage), then CFU-G (colony forming unit-granulocyte), becoming more committed with each mitotic division. These cells, along with the stem cells constitute the neutrophil progenitor pool.

The CFU-G cells have the potential to become any of the granulocytes. The first three cell stages that are specifically committed to neutrophil production are the myeloblast, promyelocyte and neutrophilic myelocyte. These cells along with the progenitor pool constitute the neutrophil proliferative pool. Each of these different cell types are the product of mitotic divisions that take a total of about a week to complete. After this the post-mitotic maturation begins.

Neutrophils at various stages of post-mitotic maturation form the neutrophil storage pool (NSP), consisting of metamyelocytes, band cells and neutrophils. As neutrophils

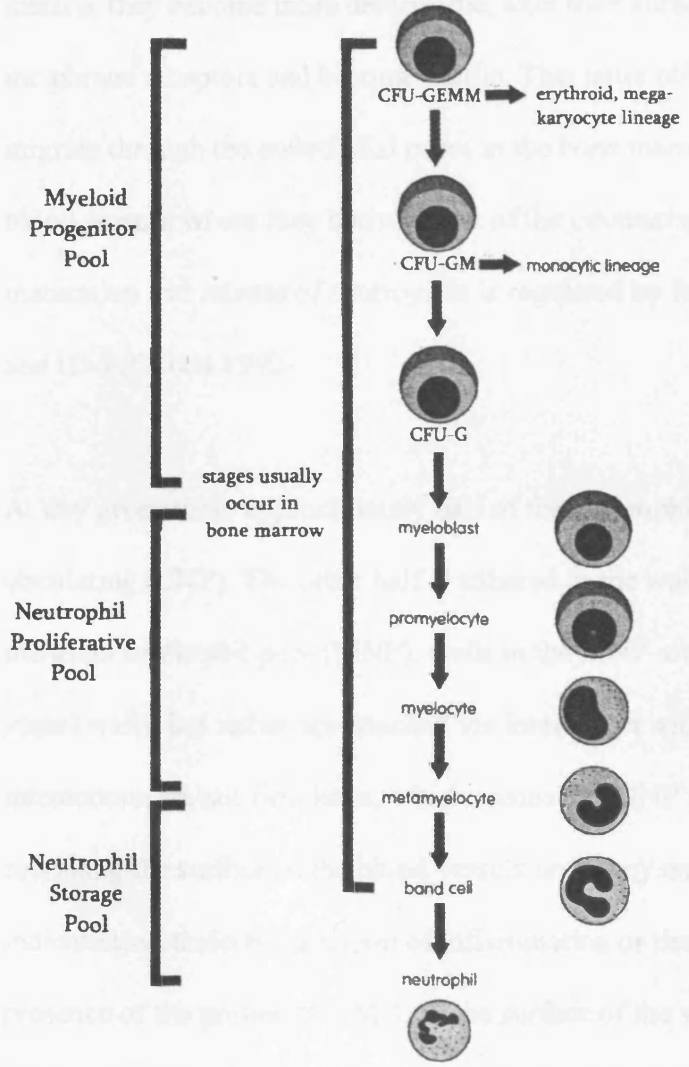

Fig 1.2.2 Myelopoiesis

Neutrophils originate from the myeloid stem cell, CFU-GEMM (colony forming unit – granulocyte, erythroid, monocyte, megakaryocyte), which is also capable of producing erythrocytes, monocytes and megakaryocytes. This differentiates several times, becoming progressively more committed to the final cell type: CFU-GM (colony forming unit – granulocyte, macrophage), CFU-G (colony forming unit – granulocyte). The myeloblast is committed to neutrophil production, and this continues through a series of mitotic divisions within the bone marrow, which is followed by the final phase of neutrophil maturation (adapted from Arif and Mufti, 1998).

mature, they become more deformable, alter their surface charge, acquire new plasma membrane receptors and become motile. This latter ability enables the neutrophil to migrate through the endothelial pores in the bone marrow sinusoids and enter the blood stream, where they become part of the circulating neutrophil pool (CNP). The maturation and release of neutrophils is regulated by factors such as GM-CSF, CSF, and IL-3 (Okuda 1992).

At any given time, approximately half of the neutrophils in the circulation are freely circulating (CNP). The other half is adhered to the walls of small blood vessels, the marginal neutrophil pool (MNP). Cells in the MNP are not firmly adhered to the vessel walls, but rather are attached via interaction with 'selectin' proteins. These interactions are not firm links, which means the MNP neutrophils are not static, but roll along the surface of the blood vessels until they encounter a particular signal indicating an underlying region of inflammation or tissue damage. This signal is the presence of the protein ICAM-1 on the surface of the vascular endothelium, which binds to the β-integrin on the neutrophil. This signals the neutrophil to extravasate between the endothelial cells into the tissue and migrate to the site of inflammation (Ley et al, 2007),

1.2.3 Neutrophil Cellular Structure

Neutrophils are very specialised cells and have a cellular structure that is designed to enable them to fulfil these specialised functions with maximum efficiency. Neutrophils are small cells with a spherical shape, diameter approximately 10μm, when they are in the circulation (Wintrobe, 1967). When spread, their morphology dramatically changes (Fig 1.2.3.1).

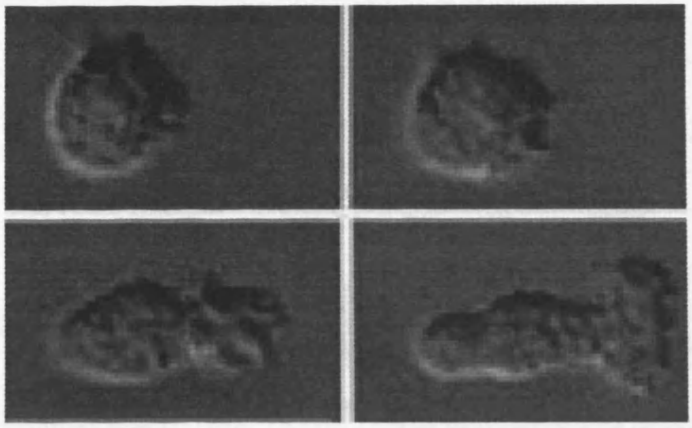

Fig 1.2.3.1 Neutrophil in Round and Spread Form

In the circulation neutrophils adopt a roughly spherical shape. However, when they marginate to the vascular endothelium or are migrating towards a site of inflammation they adopt a more spread form (figure taken from HR Bourne Lab web-site).

There are three immediately striking features of the neutrophil organelles: (i) the multilobed nucleus, (iii) the lack of mitochondria and (iii) the abundance of granules. The multilobed nucleus occupies a significant percentage of the cytosol (~20 %) and an easily recognisable distinguishing characteristic of this class of cells when stained. The second feature is the distinct lack of mitochondria. In neutrophils, mitochondria occupy only 0.6% of the organelle volume of isolated neutrophil organelles, compared to a liver cell in which mitochondria occupy around 20 % of the whole cell volume (Hallett and Lloyds, 1997). This is indicative that neutrophils do not use mitochondria for their usual functions; namely energy production, Ca^{2+} storage, protein synthesis. Indeed, energy produced in neutrophils is almost exclusively from glycolysis, Ca^{2+} is stored in other organelles, and there is little, if any *de novo* protein synthesis. The third feature that is very striking is the abundance of granules within the cytosol. Electron micrographs (Fig 1.2.3.2) indicate that there are at least 3 different types of granules: azurophilic, specific and small storage or gelatinase. These can be differentiated by their contents, which is determined at the time of their production (Abramson and Wheeler, 1993). A later publication indicates a fourth subset of neutrophil granules that arise from endocytosis, named secretory vesicles (Lominadze et al, 2005). The endocytic origin of the secretory vesicles dictates that the membranes are rich in receptors, signalling proteins and adhesion molecules with a lumen containing plasma. In contrast azurophil, specific and gelatinase granules contain various enzymes and host defence proteins in their luminal spaces, whilst their membranes contain receptors, signalling proteins, adhesion molecules and enzymes (Borregaard and Cowland 1997). Borregaard *et al* have shown that the targeting of proteins to each of the different granule compartments is determined by the timing of protein synthesis during myeloid progenitor cell differentiation, not by specific granule-specific sorting.

Fig 1.2.3.2 Electron Micrograph of Neutrophil

This EM reveals nuclear lobes with chromatin rich and chromatin light regions, different types of granules ubiquitously spread through the cytoplasm. It is worth noting the lack of endoplasmic reticulum or golgi apparatus and mitochondria. (Image from Ohio State University, Microscopy and Imaging Facility)

This can lead to overlaps in the time of synthesis and therefore overlap occurs in the protein contents among granule subsets. A full proteomic analysis of human neutrophil granules was carried out by Lominadze et al (2005).

Another distinguishing feature of neutrophils that becomes apparent in electron micrographs is the abundance of plasma membrane. The surface of spherical neutrophils has a "wrinkly" appearance (Fig 1.2.3.3). Neutrophils have approximately 85 % more plasma membrane than they need to enclose the volume of the cell if it were a simple sphere (Hogg 1987). This massive excess of plasma membrane belays the ability to make the dramatic changes to the morphology of the cell that often accompany functions such as chemotaxis, extravasation and phagocytosis. Indeed these morphological changes are a characteristic trait of neutrophils, and the ability to easily deform, extend and withdraw regions of cell membrane allow the neutrophil to readily squeeze between vascular endothelial cells, travel through tissue spaces to sites of inflammation, and send out projections of their membrane to enclose a particle to be phagocytosed, occasionally up to 50 % of their size.

The excess of membrane allows neutrophils to be easily deformed and to rapidly change their morphology. However, the membrane cannot control its own directionality. Rather, it relies on the dynamic underlying cytoskeleton beneath the membrane to push or retract it as necessary. The primary component of the cytoskeleton beneath the plasma membrane is actin (Stossel 1989). Indeed, actin is reportedly one of the most abundant proteins in mammalian leukocytes (Southwich and Stossel 1983) as is illustrated in Fig 1.2.3.4. Actin exists in two forms: globular (g-actin) and assembled into filaments (f-actin). The polymerisation of g-actin into f-

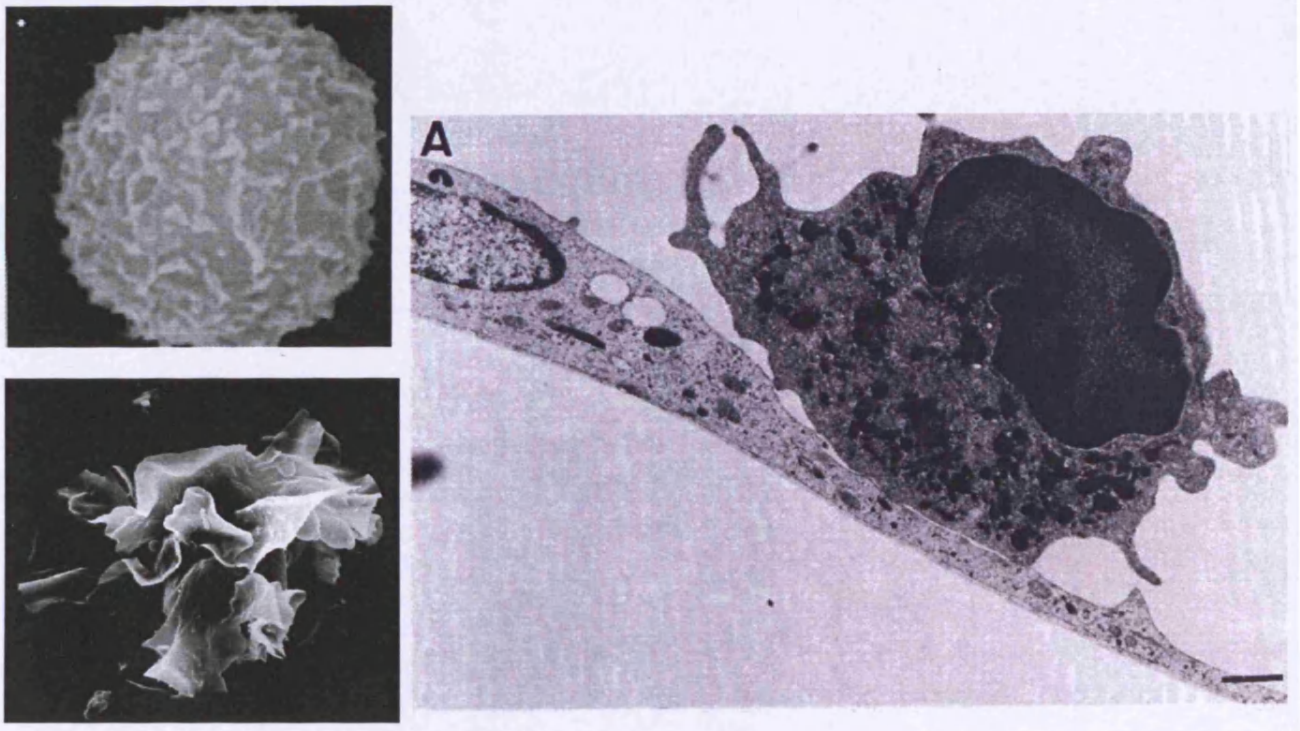

Fig 1.2.3.3 Wrinkly Surface of Neutrophil

Neutrophils have a massive excess of plasma membrane relative to their volume, which they keep in folds, as seen in the upper scanning EM image, and the EM through a neutrophil attached to an endothelial cell (HUVEC). The lower scanning EM was a rare image of a neutrophil that had unfolded all of its plasma membrane during the fixing process. (Figures were taken from neutrophils web sites)

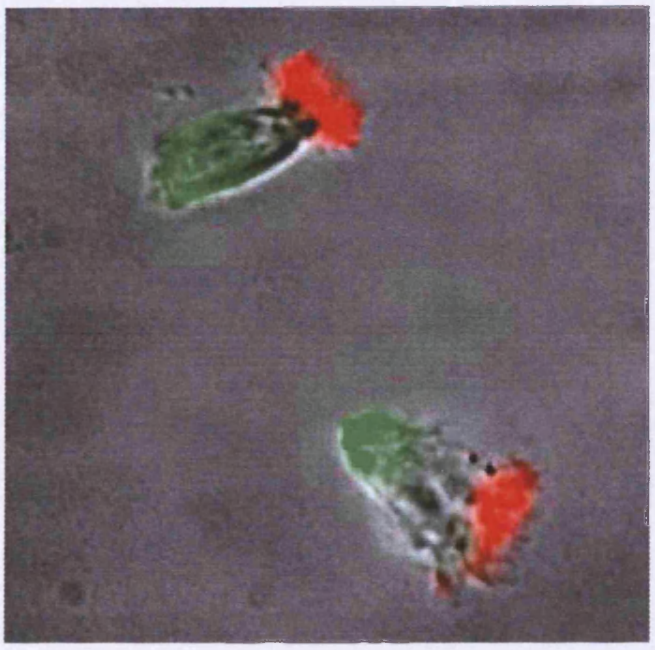

Fig 1.2.3.4 Actin Cytoskeleton

This pseudocoloured image reveals the extensive actin cytoskeleton inside a the neutrophil-like HL60s. In this case f-actin (red) has localised to the leading edge of the HL60 polarised by chemotaxis. The lower image shows neutrophils stained for f-actin. The tail of the neutrophil is indicated with an arrow, again indicating localisation of f-actin in the leading edge. (Figures taken from H Bourne, UCSF and Niggli et al 1992)

actin and disassembly back to g-actin is a dynamic process that is constantly taking place within the cytoskeleton.

Activation of neutrophils by various stimuli often results in changes in morphology, which involves polymerisation of g-actin to f-actin, shifting the ratio towards f-actin by up to 4-fold (Stossel 1989). Naturally, stimuli can cause the opposite where the f-actin suddenly fragments. This process is extensively regulated in neutrophils by several proteins leading to their ability to rapidly respond to stimuli with sudden and dramatic changes in shape.

The neutrophil cytoskeleton has also been implicated in other cellular events such as regulation of expression and localisation of membrane receptors, connecting receptor events to intracellular signalling cascades, forming isolated submembrane signalling compartments, and regulating granule fusion with the plasma membrane.

The uniquely wrinkly plasma membrane of the neutrophil is also worthy of note for its composition. It has a unique combination of lipids, proteins and carbohydrates that make it a neutrophil membrane rather than any other cell. It is rich in receptors that enable the neutrophil to detect minute changes in the chemical composition of the extracellular medium; bind to various surfaces such as endothelial cells, matrix proteins and opsonised particles; and to sense gradients of chemotactic molecules as shallow as 0.1% over the length of the neutrophil. Often these receptors are linked to intracellular signalling molecules, which transduce the signals and direct the appropriate cellular responses, including polymerisation of actin, fragmentation of f-actin, polarisation, upregulation of receptors, degranulation, and secretion.

1.2.4 Neutrophil Behaviour

Different research groups would identify alternative functions of the neutrophil as "primary". The most commonly of these is the phagocytic ability of the neutrophil. Neutrophils complete this task with great efficiency, and have been dubbed "professional phagocytes" (Rabinovitch, 1995). However, to accomplish phagocytosis, neutrophils must first be released from their site of production in the bone marrow, into the circulation. Once in the circulation there are two sub-populations – the circulating neutrophil pool (CNP) and the marginal neutrophil pool (MNP). The neutrophils can freely interchange between the two pools. The marginal neutrophils roll along the vascular endothelium until they reach an area that has been stimulated by the underlying tissue to express intercellular adhesion molecule-1 (ICAM-1) on the luminal surface. The neutrophils then firmly adhere and migrate towards a junction between endothelial cells where they can extravasate into the tissue via the process diapedesis. Once inside the tissue, the neutrophils migrate along a gradient of chemotactic peptides towards the region of infection or tissue damage. Only when they have completed all of these steps are they at the site of inflammation, can they complete their "primary function" of phagocytosis. These steps are illustrated in Fig 1.2.4.1, each of which is described in more detail below.

(a) Detection of Inflammatory Indicators

Neutrophils transfer from the CNP to MNP by engaging protein expressed on their surface with proteins expressed on the surface of the vascular endothelial cells, namely interactions between selectins. The interactions are temporary, involving lose binding such as hydrogen-bonds, and therefore easily broken by the sheer forces exerted on the neutrophil by the flow of circulating blood. This flow keeps the

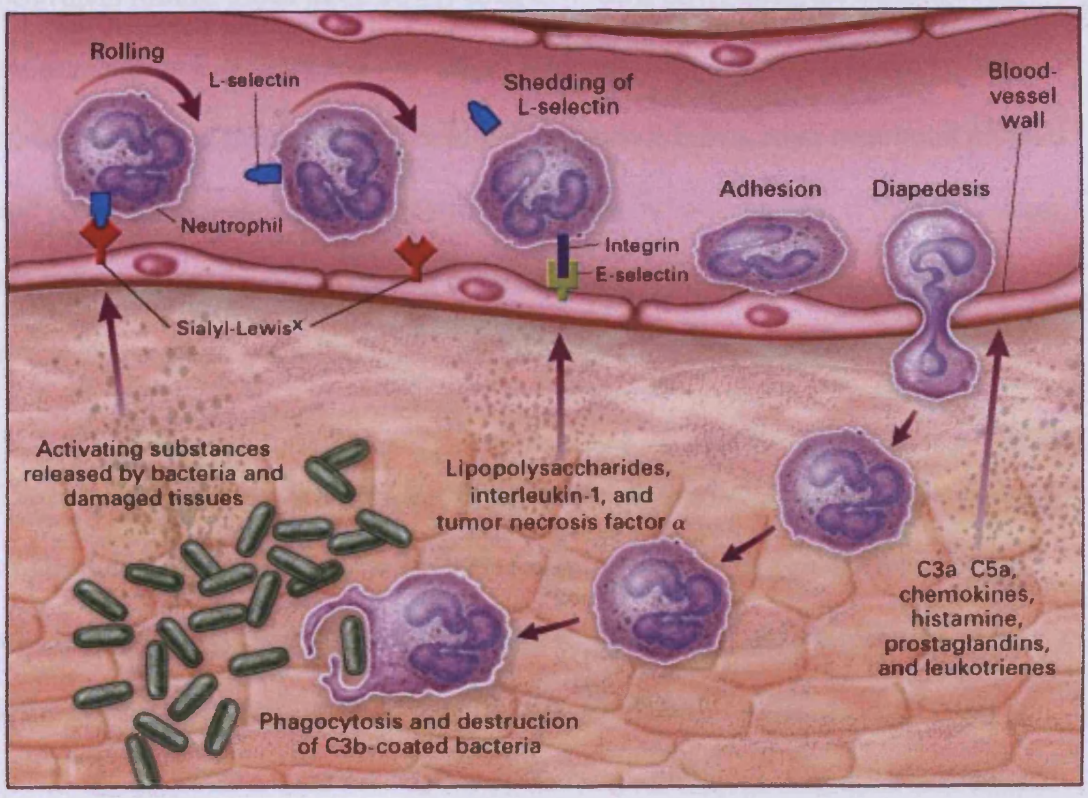

Fig 1.2.4.1 Neutrophil Migration From Circulation Into Inflammed Tissue

Neutrophils move from free circulation by loosely binding to proteins expressed on the surface of the vascular endothelial cells. These loose interactions allow the neutrophil to roll along the surface of the blood vessel by making and braking bindings with selectins until they reach a region of endothelium that has upregulated ICAM-1 surface expression in response to inflammatory mediators in the underlying tissue. The neutrophil halts, assumes a flattened morphology, migrates to a space between endothelial cells and undergoes diapedesis. Once in the underlying tissue, it migrates along the chemotactic gradient to the site of inflammation where it will phagocytose and destroy invading micro-organisms and damaged tissue. (Figure taken from chronicprostatitis.com)

neutrophil rolling, albeit more slowly than CNP cells flow, along the surface of the endothelium as it engages and disengages selectins. This close contact allows the neutrophil to read the state of the endothelium since it brings other neutrophil proteins and receptors into close proximity with the endothelial membranes. If further binding between neutrophil receptors and endothelial proteins does not occur, then the neutrophil continues to roll along.

Tissue damage caused by invading pathogens or other injury, together with any micro-organisms and cells proximal to the infected and/or damaged region release factors, which diffuse through the tissue to signal an inflammatory response. These inflammatory mediators include lipopolysacharide (LPS), tumour necrosis factor-α (TNF- α), and interleukin-1 (IL-1), and cause endothelial cells that line blood vessels to increase their surface expression of vascular inflammatory mediators, such as ICAM-1 and other lipid mediators including platelet activating factor (PAF). The rolling neutrophil detects this change because the neutrophil membrane-bound integrins bind to ICAM-1. This binding is firm, unlike the transient selectin interactions and coupled with the stimulatory effect of PAF and other chemical mediators increases the adhesiveness of the neutrophil surface receptors (Lorant et al 1991, Lawrence and Springer 1991). This halts the rolling neutrophil and induces a morphological change to a more flattened appearance. The neutrophil membrane then begins to ruffle and the whole cell moves towards a space between the endothelial cells, where it passes between them into the underlying tissue by a process called diapedesis.

(b) Migration to Site of Inflammation

Once in the tissue, the neutrophil is attracted to the site of inflammation by chemotactic peptides such as the complement fragment C5a, interleukin-8 and leukotriene B4 that are both released by cells, and fMLP that is secreted by bacteria. These form a concentration gradient that the neutrophil detects via surface receptors and migrates up it towards the source, i.e. towards the bacteria and/or damaged tissues, through tissue spaces. It has been proposed that these chemicals may increase the life span of neutrophils in the tissue to 1-2 days compared to 4-10 hours in the circulation.

(c) Phagocytosis

At the site of inflammation the primary function of neutrophils is to dispose of micro-organisms and safely destroy them without causing more damage to the surrounding tissue than is necessary. The neutrophil follows the concentration gradient of chemotactic peptides from the micro-organisms until it comes into contact with them. Upon contact the neutrophil sends out extensions of its plasma membrane called pseudopodia, which progressively enclose the particle. Once closed, the new vacuole containing the particle is referred to as the phagosome. An arsenal of cytotoxic chemicals is then unleashed along with the activation of an array of enzymes, which destroy the ingested particle. Many of these chemicals and enzymes are stored in granules in an inactive form until they fuse with the phagosome. The pH of the phagosome drops (becomes acidic; Segal and Jones, 1978), which activates the enzymes. This is referred to as degranulation of the neutrophil (Hirsch and Cohn 1960, Pryzwansky et al 1979). In the membrane of the phagosome are also proteins that aggregate to form the NADPH oxidase. This oxidase produces reactive oxygen

species that break down and irreparably damage the structural components of the particle. The combination of the degranulation with the oxidase response forms an extremely powerful and efficient killing mechanism.

(d) Apoptosis

The neutrophil then undergoes programmed cell death, apoptosis, and is ingested by macrophages or other phagocytic cells. This ensures the neutrophil and its potentially toxic contents are safely disposed of (Haslett, 1992).

1.3 Calcium Signalling

Calcium, or more specifically the Ca^{2+} ion, is a ubiquitous intracellular messenger across a broad range of cell types. It controls a diverse range of cellular processes ranging from gene transcription, muscle contraction, cell proliferation and death. On a wider scale, Ca^{2+} is the fifth most abundant element in the earth's crust; only oxygen, silicon, aluminium and iron have greater mass (Case RM et al, 2007). All of these ions are stringently controlled in biological systems. However, the control of Ca^{2+} was crucial due to its propensity to interact with biological molecules. These interactions are promoted by the specific properties of the Ca^{2+} ion, namely high affinity for carboxylate oxygen such as in amino-acids, rapid binding kinetics, flexible coordination chemistry with greater tolerance in the number, angle and distance of coordination bonds, etc (Jaiswal et al 2001, Saris & Carafoli, 2005). High concentrations of Ca^{2+} are therefore incompatable with life, leading to aggregation of proteins and nucleic acids, altered lipid membrane integrity, and precipitation of phosphates and other ions such as sulphate and carbonate. Specifically, Ca^{2+} at high concentrations within an aqueous solution that also contains high levels of phosphate will quickly react to produce calcium phosphate, which is the primary insoluble component of bone. Since most eukaryotic cells use adenosine tri-phosphate (ATP) as their energy currency, the level of free Ca^{2+} inside the cell must be kept low. However, the extracellular milieu often has a higher level of Ca^{2+} than would be compatible with life. Therefore, cells have a homeostatic system to pump Ca^{2+} out of the cell to maintain a comfortably low concentration of approximately 100 nM.

The intracellular low background level of Ca^{2+} results in a massive concentration gradient across the plasma membrane. This is ideal for a signalling molecule, since

trace amounts of Ca^{2+} entering the cytosol would significantly change the free Ca^{2+} concentration, especially close to the channel mouth that facilitated the entry (Saris and Carafoli 2005).

1.3.1 General Principles of Calcium Signalling

The ability of a simple ion, Ca^{2+}, to control a wide variety of functions indicates that there must be a complex array of signals and interpretation pathways that vary between cell types according to the functions of that particular cell.

Ca^{2+} gradients exist in some of the most primitive prokaryotes, such as *Escherisha coli*, whose cytosolic free Ca^{2+} concentration is around 100nM (Gandola & Rosen 1987, Watkins et al 1995). It is therefore conceivable that Ca^{2+} channels even in primitive prokaryotes could serve a signalling function, allowing influx that creates a zone of elevated Ca^{2+}. The signal would be terminated by the closure of the Ca^{2+} pore, and subsequent extrusion of Ca^{2+} ions. Indeed, prokaryotes have a prototypic Ca^{2+} signalling system where fluctuations in Ca^{2+} are involved in regulation of movement, chemotaxis and phototaxis, certain survival reactions and sporulation (Kippert 1987).

Eukaryotic cells have a more complicated cellular structure with intracellular membrane-bound compartments. These compartments often have a Ca^{2+} gradient across the membrane and have distinct mechanisms for Ca^{2+} handling (reviewed in Michelangeli, 2005). These are discussed below in the Ca^{2+} toolkit (sect 1.3.2).

Humans are complex multi-cellular organisms comprised of many different, diverse cell types. Across the whole spectrum cell types within the human body there is a

wide variety of Ca^{2+} signalling pathways, involving different intermediates, receptors, ligands and ultimately outcomes. In general, Ca^{2+} signalling follows the same basic structure of any signalling pathway (Fig 1.3.1.1) with a signal that is interpreted by a receptor, which triggers a cascade of events resulting in the desired outcome(s) (Lehninger, 2005). In most cases, the Ca^{2+} acts as a secondary messenger, relaying information down a pathway. However, the trigger resulting in the Ca^{2+} signal and the outcome of the subsequent change in Ca^{2+} varies widely. This ability of such a simple ion to cause such a variety of responses has incited much curiosity over the years and inspired many research projects.

1.3.2 Calcium Toolkit

Ca^{2+} signals inside cells can be generated in two different ways: (i) release from intracellular stores or (ii) influx from the extra-cellular medium. The Ca^{2+} must then be extruded from cells since, as previously discussed, high levels of intracellular Ca^{2+} are incompatible with life. The Ca^{2+} stores also need to be refilled to allow further Ca^{2+} release events and signals to occur. All of these are strictly regulated, although the exact control mechanisms of some pathways are still a matter of ongoing investigation. Although these general principles are followed in all cell types, the mechanisms and molecules involved in achieving these principles vary from cell-to-cell.

The term "Ca^{2+} signalling toolkit" is therefore useful to describe all the elements of Ca^{2+} signalling used by an organism, which are potentially available to each cell. All cells do not use all components of the toolkit, but rather "choose" the tools suitable for the specific functions they must carry out. This ability to mix and match elements

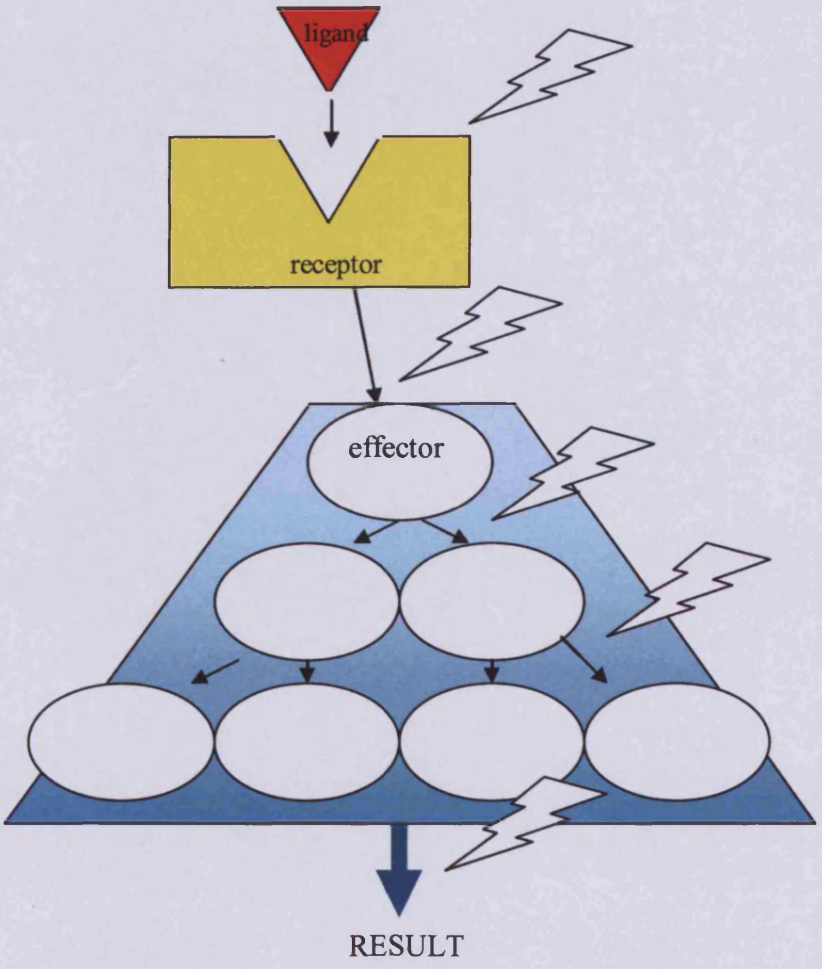

Fig 1.3.1.1 General Signalling System

Biological signalling systems are widely varied but the general principles tend to apply in different combinations. That is a signal detected by a receptor that transduces the signal to the appropriate signalling pathway, often involving a cascade (shown as the accumulation of blue 'product', ultimately leading in the desired result. There are complex elements of control at each stage of the pathway (shown as lightening bolts) and cross-talk with other pathways.

from the toolkit goes some way to explaining how cells can use the relatively simple Ca^{2+} ion as a signalling messenger for such a wide variety of functions.

The elements of the toolkit comprise responses to stimuli, intermediate Ca^{2+}-mobilising messengers, Ca^{2+} binding proteins, release from intracellular stores and their subsequent refilling, influx from the extracellular milieu, and Ca^{2+} homeostasis (Fig 1.3.2.1). These will be discussed in general here and then more relevant details that are pertinent to the topic of this thesis will be covered in the following sections (1.4-1.7).

(i) Ca^{2+} Homeostasis

Ca^{2+} homeostasis is important to cell viability. Both low and high concentrations of Ca^{2+} dramatically hinder the normal functions of the cell. Therefore the cell expends a great deal of energy on maintaining a relatively constant level of free Ca^{2+}. This is achieved by pumping Ca^{2+} out of the cytosol into the extracellular milieu by Na^{2+}/Ca^{2+} exchangers and by the plasma membrane Ca^{2+} ATPase. Ca^{2+} is also sequestered into intracellular compartments and organelles such as the sarco-endoplasmic reticulum Ca^{2+} ATPase (SERCA) pumps, which transport Ca^{2+} into the sarco- or endoplasmic reticulum. Ca^{2+} may also be sequestered by mitochondria, which have Na^{2+}/Ca^{2+} exchangers and Ca^{2+} channels on their surface although the relevance of this, and whether physiological or pathological, remains unclear at this time. However, Ca^{2+} released from stores and entering the cytoplasm through plasma membrane channels, may be quickly removed into mitochondria or other stores, pumped from the cell or buffered by Ca^{2+} buffering proteins. Thus, the concentration of free Ca^{2+} within a cell is maintained within the tight boundaries of the acceptable limits compatible with life.

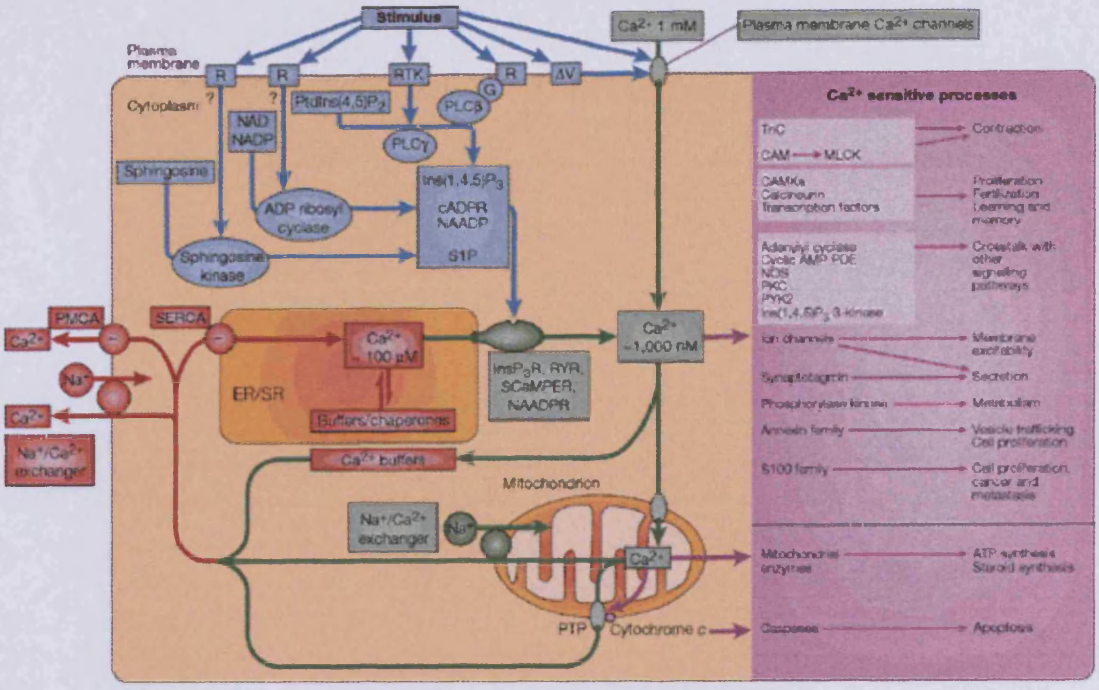

Fig 1.3.2.1 Ca^{2+} Toolkit

Comprising stimuli, intermediate Ca^{2+} mobilising messengers, Ca^{2+} binding proteins, release from Ca^{2+} stores and subsequent refilling, influx, Ca^{2+} homeostasis. (Figure adapted from Berridge, 2000).

(ii) Ca^{2+} Buffering

Most cells have the ability to buffer free Ca^{2+} ions by binding or chelating them into other molecules. The properties of Ca^{2+} were extensively characterised and compared to Mg^{2+} and other cations by R.J.P. Williams (1970, 1976, 1994). Ca^{2+} is preferentially bound to multidentate anions and strong acid anions (Williams 1970). Ca^{2+} has greater binding flexibility, which means dehydrated Ca^{2+} can permeate membranes and reach binding sites deeper inside proteins. These Ca^{2+} binding proteins vary in their function from contractile to regulatory to those involved in transport processes. One of the earliest of these proteins to be characterised was Parvalbumin, which was derived by X-ray crystallography (Kretsinger & Nockolds 1973). Nucleotides such as ADP and ATP strongly chelate Ca^{2+} and Mg^{2+} with association constants of 4.0 and 4.2 respectively for ATP, which is subsequently released by hydrolysis of the ATP. Other proteins that buffer the Ca^{2+} concentration include calbindin D and calretinin (Berridge, Lipp, Bootman 2000).

(iii) Ca^{2+} Movement Across Plasma Membrane

Ca^{2+} enters the cell by crossing the plasma membrane. A certain amount of Ca^{2+} can diffuse across a lipid membrane due to its binding properties. However, this is accounted for in the Ca^{2+} homeostasis and is counteracted by the constant action of the Na^{2+}/Ca^{2+} exchangers and plasma membrane Ca^{2+}-ATPase pumping Ca^{2+} from the cell. Larger changes in Ca^{2+} concentration used for signalling purposes are achieved through the activity of Ca^{2+} channels in the plasma membrane. These can be divided into three groups according to the nature of their activation: voltage operated, receptor operated and store operated channels (VOCs, ROCs and SOCs respectively). When

open, these channels allow Ca^{2+} to flow down the concentration gradient into the cytoplasm.

As the name suggests, voltage operated channels (VOCs) respond to changes in the potential difference (voltage) across the plasma membrane. These channels are expressed and particularly active in excitable cells such as neurons and muscle cells. Smooth muscle cells have L-type VOC (α_{1S}), which undergoes a conformational change when the membrane depolarises. This allows Ca^{2+} to flow through the channel. There is also a direct action on the ryanodine receptor (RyR) 1 on the endoplasmic reticulum causing Ca^{2+} release through the RyR1. It is worth noting that in cardiac cells L-type VOC (α_{1C}) acts on RyR2 indirectly where a small Ca^{2+} influx from the VOC induces RyR2 opening in a process dubbed Ca^{2+} induced Ca^{2+} release.

Receptor operated channels (ROCs) are common channels in non-excitable cells such as pancreatic acinar cells, leukocytes, and endothelial cells. They can be activated in two ways: by binding of the ligand to the receptor on either the extracellular or intracellular domain of the protein. Acetylcholine, glutamate and ATP are examples of extracellular ligands, while diacylglycerol and aracadonic acid are examples of intracellular ligands for plasma membrane bound ROCs. When these ligands bind they result in a conformational change that opens the channel allowing influx of Ca^{2+}. ROCs can also be coupled with other proteins such as kinases, phosphatases, enzymes, etc, which have their activity linked to the status of the ROC. This is the case in the pancreas where acetylcholine or cholecytokinin bind to the ROC resulting in Ca^{2+} influx but also the production of the second messengers IP_3, NAADP, cADPR. These act on the IP_3R or RyR on the intracellular Ca^{2+} store causing Ca^{2+} efflux from

the store. In pancreatic cells these processes mediate down stream processes such as fluid and enzyme secretion.

The third type of channel is the store operated channel (SOC), also referred to as the Ca^{2+} release activated Ca^{2+} (CRAC) channel. Elucidating the exact structure and functional mechanism of this channel has been difficult since it appears to be inherently unstable, thus hindering its isolation and characterisation. However, it has long been known that the phenomenon exists that emptying of cellular Ca^{2+} stores results in the opening of Ca^{2+} channels in the plasma membrane to allow the Ca^{2+} stores to refill, thus restoring the ability of the cell to respond to further stimuli. This phenomenon is important because the influx of Ca^{2+} also acts as a signal for many processes. As Ca^{2+} stores empty, an unknown messenger is produced or released, which stimulated the SOC to open and allow Ca^{2+} influx to refill the store. Parakh (2007) has proposed that the primary method of store refilling is through the direct interaction of the endoplasmic reticulum (ER) bound protein STIM-1 with a novel protein Orai/CRACM1. The latter was reported by two groups at the same time. For the purpose of clarity it will be referred to as Orai in this thesis. The mechanism of action of these proteins is still unknown, although it is accepted that they are capable of direct contact to stimulate Ca^{2+} channel opening.

(iv) Ca^{2+} Release From Stores

Ca^{2+} is stored within a number of different organelles within cells. These stores vary extensively between cell types. However, they can be roughly divided into the sarco/endoplasmic reticulum (referred to as ER), mitochondria, and membrane bound

vesicles. In general, each of these has pumps that move Ca^{2+} into the luminal space and regulated channels that allow Ca^{2+} to be released upon appropriate stimulation.

The ER is more commonly known for housing the protein production machinery. However, there is also a selection of other functions carried out by this organelle. Electon micrographs (Fig 1.3.2.2) indicate that a large proportion of the cytoplasm of a range of cells is occupied by the ER. The ER often appears to be continuous with the nuclear envelope, suggesting that signalling may also be continuous between those two compartments. Ca^{2+} is transported into the ER by the sarco/endoplasmic reticulum Ca^{2+} ATPase (SERCA) pump. Ca^{2+} is released from the ER through receptor operated channels. The most widely studied of these are the IP_3R and RyR. The activity of IP_3R and RyR are also mediated directly by Ca^{2+} on both the luminal and cytosolic sides of the pump. When there are high levels of Ca^{2+} within the lumen, the IP_3R and RyR become increasingly active. IP_3R sensitivity to Ca^{2+} is also modulated by the levels of IP_3, switching from a bell shaped sensitivity curve at low levels of IP_3 to a sigmoidal curve shape at higher levels (Fig 1.3.2.3). There may be other channels regulated by IP_3, NAADP, S1P, and other ligands, although the molecular nature of these has yet to be defined.

Mitochondria are complex, multifunctional organelles with a double membrane comprising the inner and outer lipid layers. The mitochondrial inner membrane has a much increased surface area through invaginations into the mitochondrial luminal space. There is a pH gradient between the lumen and the intermembrane space generated by the transport of H^+ ions. This gradient is used to drive ATP production but also plays a part in Ca^{2+} transport. Ca^{2+} is taken up very rapidly by mitochondria

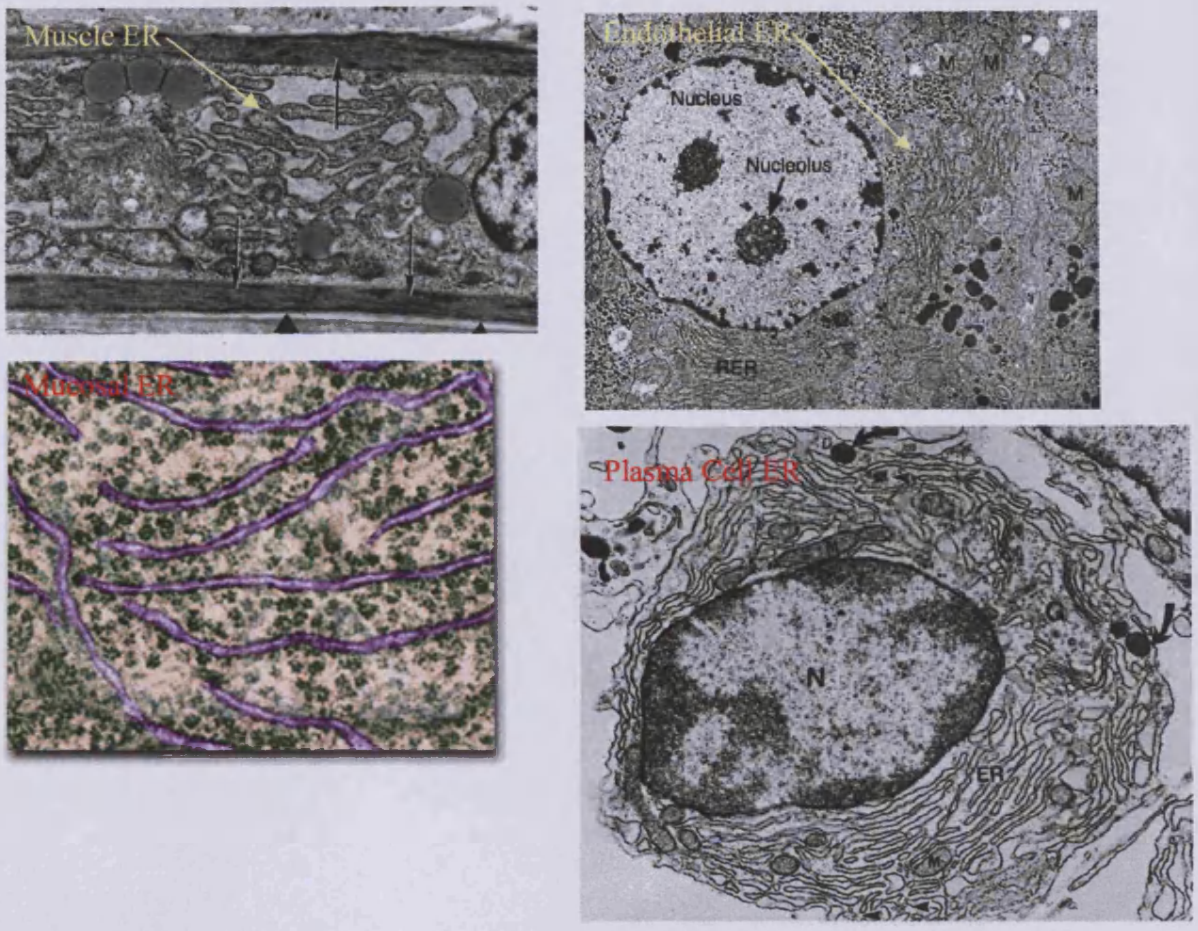

Fig 1.3.2.2 Electron Micrographs Reveal a Plethora of ER in Many Cell Types

In a variety of cells, a large proportion of the cytosol is occupied by endoplasmic reticulum, as seem above in transverse electron micrographs of muscle, endothelial, mucosal and plasma cells.

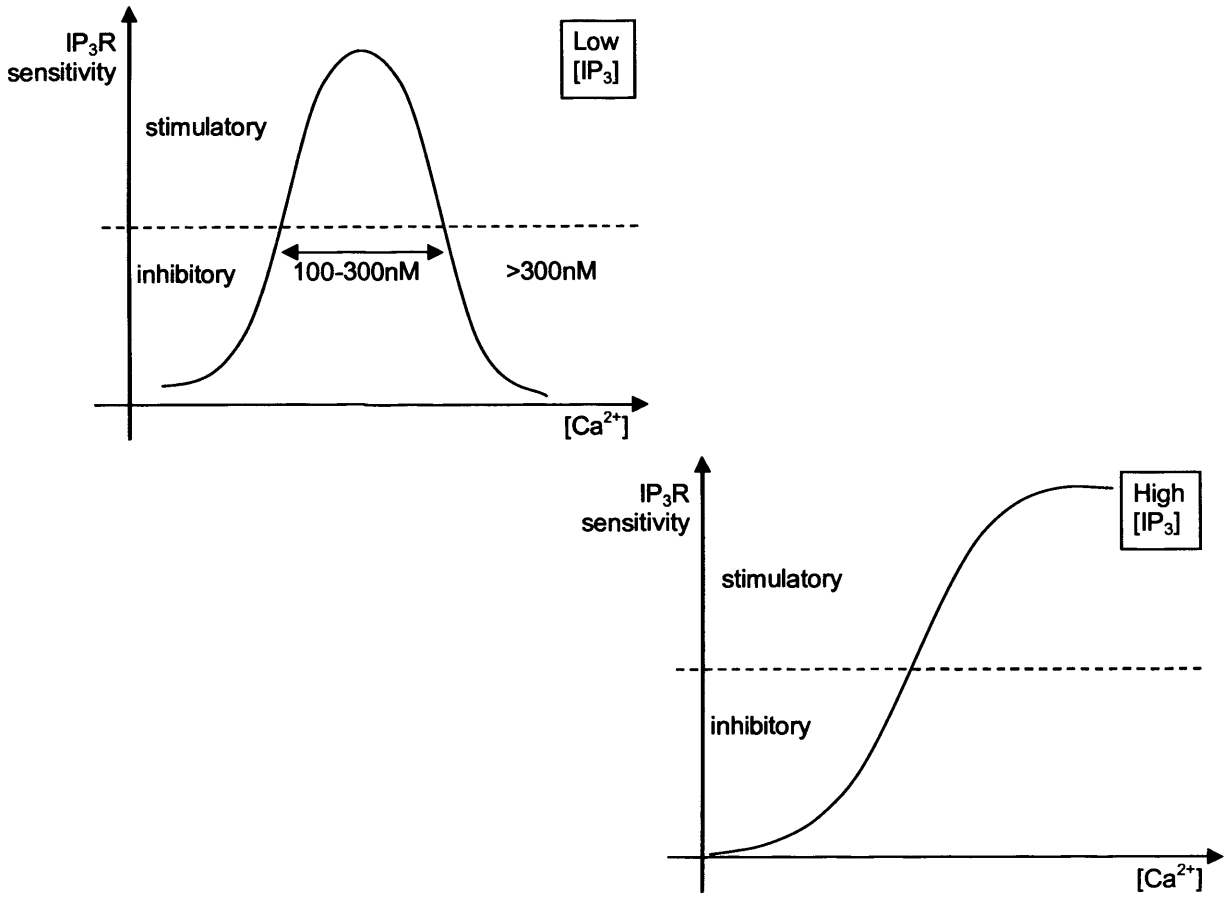

Fig 1.3.2.3 IP_3R Sensitivity to Ca^{2+} at High and Low Levels of IP_3.

At low IP_3 the sensitivity of the IP_3R is a bell shaped curve with a window of 100-300nM of Ca^{2+} acting to stimulate the IP_3R. At both higher and lower concentrations of Ca^{2+}, it decreases the sensitivity of the receptor. However, at high concentrations of IP_3 the response curve is sigmoidal such that above a given Ca^{2+} level, the Ca^{2+} continues to act to stimulate the IP_3R.

through the uniporter (Saris 2005, Michelangeli 2005). The mitochondrial lumen has proteins that bind and buffer the Ca^{2+} concentration as in the cytosol. During uptake the Ca^{2+} release channels close to prevent uncontrolled Ca^{2+} leakage out of the mitochondria. The mitochondrial Na^{+}/Ca^{2+} exchanger traverses both the inner and outer mitochondrial membranes. This pump extrudes Ca^{2+} from the mitochondrial into the cytosol to be taken up by the ER/SR to refill their stores, or to be further extruded from the cell by the plasma membrane Ca^{2+} ATPase and Na^{+}/Ca^{2+} exchanger. However, if the concentration of Ca^{2+} in the mitochondria reaches a critically high level the permeability transition pore (PTP) opens. This process is similar to Ca^{2+} induced Ca^{2+} release from other stores where increases in Ca^{2+} directly induces Ca^{2+} release. PTP activity is divided into two states: low and high conductance. At low conductance the PTP can act reversibly. It has been proposed that low conductance PTP may help generate Ca^{2+} waves. However, at high conductance the PTP remains open, collapsing the transmembrane potential, stopping ATP production, releasing cytochrome c and ultimately causing the programmed cell death process of apoptosis to occur. Mitochondria play specialist roles in some cells because of their ability to quickly sequester Ca^{2+}. For example, in pancreatic acinar cells, mitochondria are arranged across the centre of the cell in such a way that they prevent propagating Ca^{2+} waves from traversing the entirety of a cell, but is quenched at the line of mitochondria (Peterson, 2002)

Membrane bound vesicles are enormously varied across the plethora of different cell types. However, in general they all have the potential to be stores of Ca^{2+}. These vesicles may constitute secretory vesicles in neurons, granules in leukocytes, buds from the golgi apparatus and so on. The protein content, plasma membrane

composition and function is widely varied. In terms of Ca^{2+} signalling, many vesicles have Ca^{2+} pores and/or channels that enable them to act as Ca^{2+} stores. Channel opening can be stimulated in similar ways to those for the ER, since vesicles often form by budding off from the golgi apparatus. The distribution of these vesicles is also varied between cell types. In some cells they are located at one end of a polarised cell, such as a neuron, allowing their secretion into the synaptic space rather than all around the cell. In other cells, vesicles are uniformly and ubiquitously spread throughout the cytoplasm with no particular order to their arrangement. An example of Ca^{2+} regulation of vesicles is in neurones, which contain vesicles with the Ca^{2+} sensitive protein synaptotagmin in their membrane. The synaptotagmin is the Ca^{2+} sensor for controlling exocytosis of those vesicles.

(v) Ca^{2+} Sensors

Within the cytoplasm of cells, and luminal spaces of organelles, there are proteins that act as Ca^{2+} sensors, i.e. they detect changes in the Ca^{2+} and consequently undergo conformational changes that regulate pathways. The two examples that will be discussed here are troponin C (TnC) and Calmodulin (CAM) since these are relatively ubiquitous across cell types. TnC regulates the interaction of actin and myosin fibres during the contraction cycle of cardiac and skeletal muscle cells. CAM regulates many different processes including contraction of smooth muscle, crosstalk between signalling pathways, gene transcription, ion channel modulation, and metabolism. For example, CAM stimulates phosphorylase kinase to increase production of ATP to enable the cell to carry out specific functions with sufficient energy supplies. Both TnC and CAM have a protein domain referred to as EF-hand-like domains. This EF

hand has a Ca^{2+} binding domain made of basic residues. The newly described STIM1 also has an EF-hand that may account for it's Ca^{2+}-dependent functions.

1.4 Ca^{2+} Signalling in Neutrophils

Signalling within neutrophils must involve a complex interaction of events in order to control co-ordinated autonomous behaviour of individual cells. There may also be special features about the neutrophil which need to be considered in order to gain insight in to how the various inputs to the cell are interpreted by the neutrophil and result in a particular response. Some of these specific aspects of Ca^{2+} signalling in neutrophils are explored here, and provide the back-drop to the results presented in future chapters.

1.4.1 Repertoire of Neutrophil Behaviour

The repertoire of neutrophil responses must be signalled accurately for the cell to perform its function. During the physiological response to a local infection, the neutrophil follows a defined course of activity (Fig 1.4.1). From the circulation, neutrophils are signalled to leave at specific sites by the interaction of neutrophil surface adhesion molecules with molecules on the endothelial cells. Initially selectins bind to provide a weak interaction, which slows down the cell and permits it to roll along the endothelial wall (McEver 1991; Bevilacqua et al, 1991). This enables the neutrophil to sample the environment near the endothelial cell, and possibly respond to PAF or other local inflammatory factors (Lorant et al, 1995: Abbassi et al, 1993) by increasing externalisation of integrin receptors (CD11b/CD18). TNF, generated locally by tissue macrophages in response to infection or cell injury, causes the upregulation on ICAM-1 on local endothelial cells (Macconi et al, 1995). These molecules provide a local "flag" for neutrophil extravasation, directing neutrophils to leave the blood stream specifically at sites near the infection. The TNF-rich environment causes priming of the cells; a preliminary step, which results in a greater

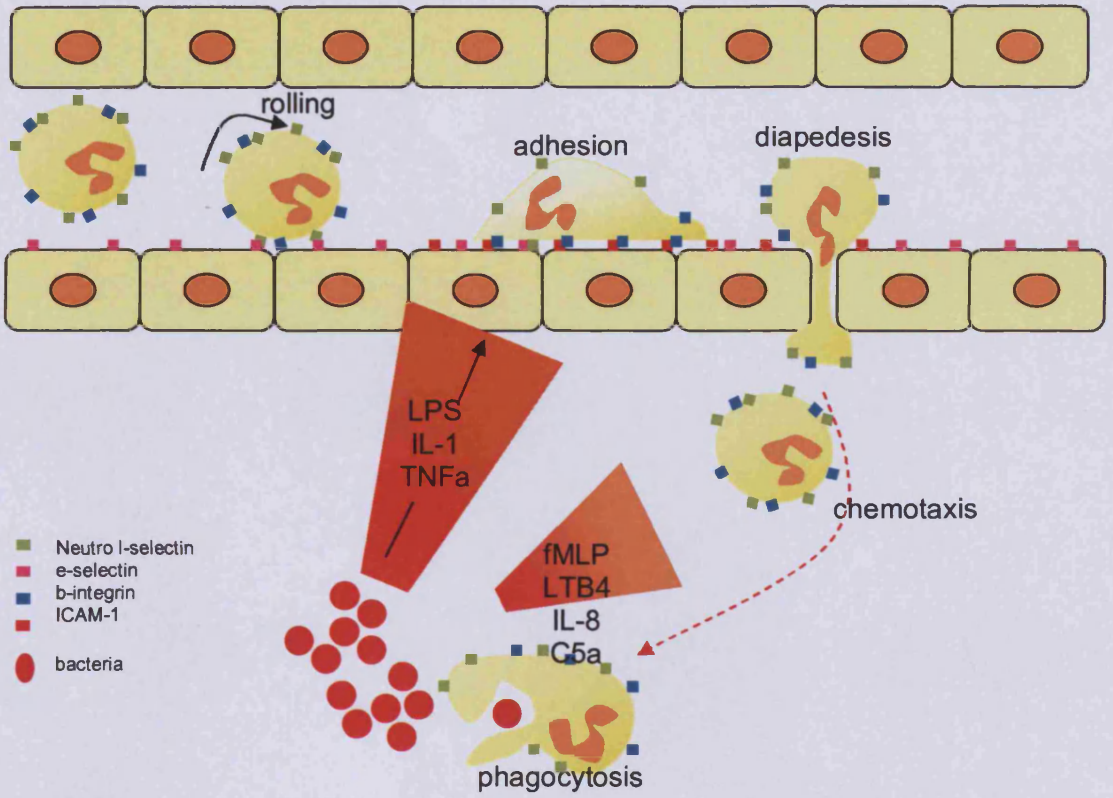

Figure 1.4.1 The Behaviour of the Neutrophil From Blood to Site of Action

The diagram shows (a) engagement of selectins on endothelial surface and exposure to PAF, (b) the engagement of integrins and firm adherence and cell shape change, (c) extravasation, (d) chemotaxis through the extracellular matrix and (e) phagocytosis of an infecting microbe.

oxidative response to subsequent stimulation (Lloyds et al, 1995: Hallett et al, 1995). Once in the extravascular space, the neutrophil is signalled both by adhesive contact with the extracellular matrix (Hynes, 1992) but also by a gradient of chemoattractant: either formylated peptides, the complement component C5a or IL-8 (Zigmond, 1977: Murphy, 1994: Gerard and Gerard, 1994). These gradients cause the neutrophil to migrate towards their source, where the neutrophil encounters the infecting microbes. Binding between the microbe and the neutrophil occurs as a result of an interaction between the opsonin, either C3bi or antibody, and receptors on the neutrophil, either integrin CD11b/CD18 or Fc receptors (IIa and III) respectively (Anderson, et al, 1986: Arnaout 1990). This interaction also results in the local formation of pseudopodia and phagocytosis (Anderson et al, 1993). Finally the phagosome fuses with a granule intracellularly and the non-mitochondrial NADPH oxidase is activated to generate toxic oxygen species (Babior , 1984: Baggiolin & Wymann, 1990). The neutrophil thus has a repertoire of responses (Table 1.4.1), which must be individually controlled and signalled.

1.4.2 Diversity of Signalling Mechanism in Neutrophils

In order to achieve this diversity of activity the surface of the neutrophil contains a wide range of receptor types (Table 1.4.2). There are, however, distinct receptor classes, which can be divided into three major groups according to their structure, activation mechanism and function.

The amino-acid sequences of a number of receptors for a number of agonists from a number of cell-types have now been determined. There is a clearly a major group of receptors which belong to the same "family" and have structural similarity.

Table 1.4.1 Repertoire of Neutrophil Responses

Stimulus	Cell Response	Signalling Event
Integrin engagement	shape change: "priming"	Ca^{2+}, tyrosine phosphorylation
7TM	chemotaxis, oxidase activation	Ca^{2+}, tyrosine phosphorylation
TNF	"priming"	tyrosine phosphorylation
Phagocytosis Initiation	shape change	Ca^{2+}, tyrosine phosphorylation
CD59	complement resistance	Ca^{2+}, tyrosine phosphorylation

Table 1.4.2 Diversity of Signalling Mechanisms

Receptor Type	**Activation Mechanism**
single transmembrane protein	Aggregation/cross-linking
seven transmembrane domain receptor	Occupancy
GPI-linked protein	Aggregation/cross-linking
adenosine A2 receptor	Occupancy
TNF receptor	Occupancy & Aggregation

They all have seven distinct transmembrane spanning domains (7TM receptors). On the neutrophil, there are several receptors that fall into this class, including the receptors for formylated peptides (FPR: Boulay et al, 1990) C5a (C5aR: Gerard & Gerard, 1991), PAF (PAFR: Nakamura et al, 1991), IL-8 (IL-8R: Murphy et al, 1991) and probably substance P (SP-R) (Table 1.4.3). Variants of these receptors have also been found including, IL-8 like receptor (IL-8LR). All these receptors have some strong homology with each other and with other receptors not expressed on neutrophils, especially in the transmembrane spanning domains (Table 1.4.3). The major difference between neutrophil 7TM receptors and those on other cells is to be found on the third intracellular loop. In some other receptors this has been identified as being involved with binding to adenyl cyclase (Strosberg, 1991) and hence the production of cAMP. In the neutrophil 7TM receptors, this loop is very much shortened and the elements thought to be involved in adenyl cyclase binding are absent. Instead, it has been demonstrated that this region is important for G-protein binding (Prossnitz et al, 1993: Holmes et al, 1991).

Receptors of this class may be considered as "classical" pharmacological receptors. They are activated by binding a ligand and involve heterotrimeric G-proteins in their mechanism of signal transduction. All the receptors of this class on neutrophils are for chemoattractants. They are also able to trigger oxidase activation and degranulation in neutrophils that have been treated with cytochalasin B (Hallett, 1989: Al-Mohanna & Hallett, 1991).

The second major group of receptors on the neutrophil are diverse in their structure but are grouped because of the mode of activation. These are receptors that are not

Table 1.4.3 Some Receptors on Neutrophils

Receptor	**Class**
formylated peptide receptor	7 TM
IL-8 receptor	7 TM
PAF receptor	7 TM
C5a receptor	7 TM
Substance P	7 TM
integrin receptor(CD11b/CD18)	dimer single TM
Phagocytic receptor: - CD32 - CD16	 1 TM GPI-linked
TNF receptor	trimer single TM
CD59 (complement inhibitor)	GPI-linked

TM= transmembrane spanning domain

"classical" pharmacological receptors, but produce an intracellular signal when the receptors are immobilised relative to each other (Metzger, 1992). Although there are ligand binding sites, their occupancy is not required for signalling. Experimentally the receptors can be immobilised or cross-linked by antibodies directed to any part of the receptor. The antibody must be immobilised either to a solid surface (Pettit & Hallett, 1996) or by the use of a second antibody, to bind to the first antibody (Ng-Sikorski et al, 1991: Petersen et al, 1993: Morgan et al, 1993). The manner in which the stimulus is presented to the neutrophil is thus distinct from the "classical" occupancy receptors (Table 1.4.2).

Although receptors in this class are activated by similar mechanisms, there are two structurally distinct types. There are those in which there is contact between the extracellular and the intracellular domains of the protein with a single transmembrane spanning region (Fig 1.4.2a). In the case of integrins, the single integrin is composed of two sub-units, the α and ß sub-units (Fig 1.4.2c), each with a transmembrane spanning region (Uedaet al, 1994: Lee et al, 1995). The second structural type are those in which there is no direct contact from the extracellular binding domain with the cytosol (Selvaraj et al, 1988), as the protein is linked to the outer face of the lipid bilayer only by a GPI-linkage (Fig 1.4.3). The mechanism by which these receptors transmit the aggregation signal across the plasma membrane remains to be established. However, it is possible that the transmission of information involves a secondary transmembrane signalling molecule, the "transducer" (Fig 1.4.4). However, no such molecule has yet been unambiguously discovered. Its existence could, however, have important implication for signalling for all receptors in the group, as the same "transducer" may be involved in transmission for many, if not all of the aggregation

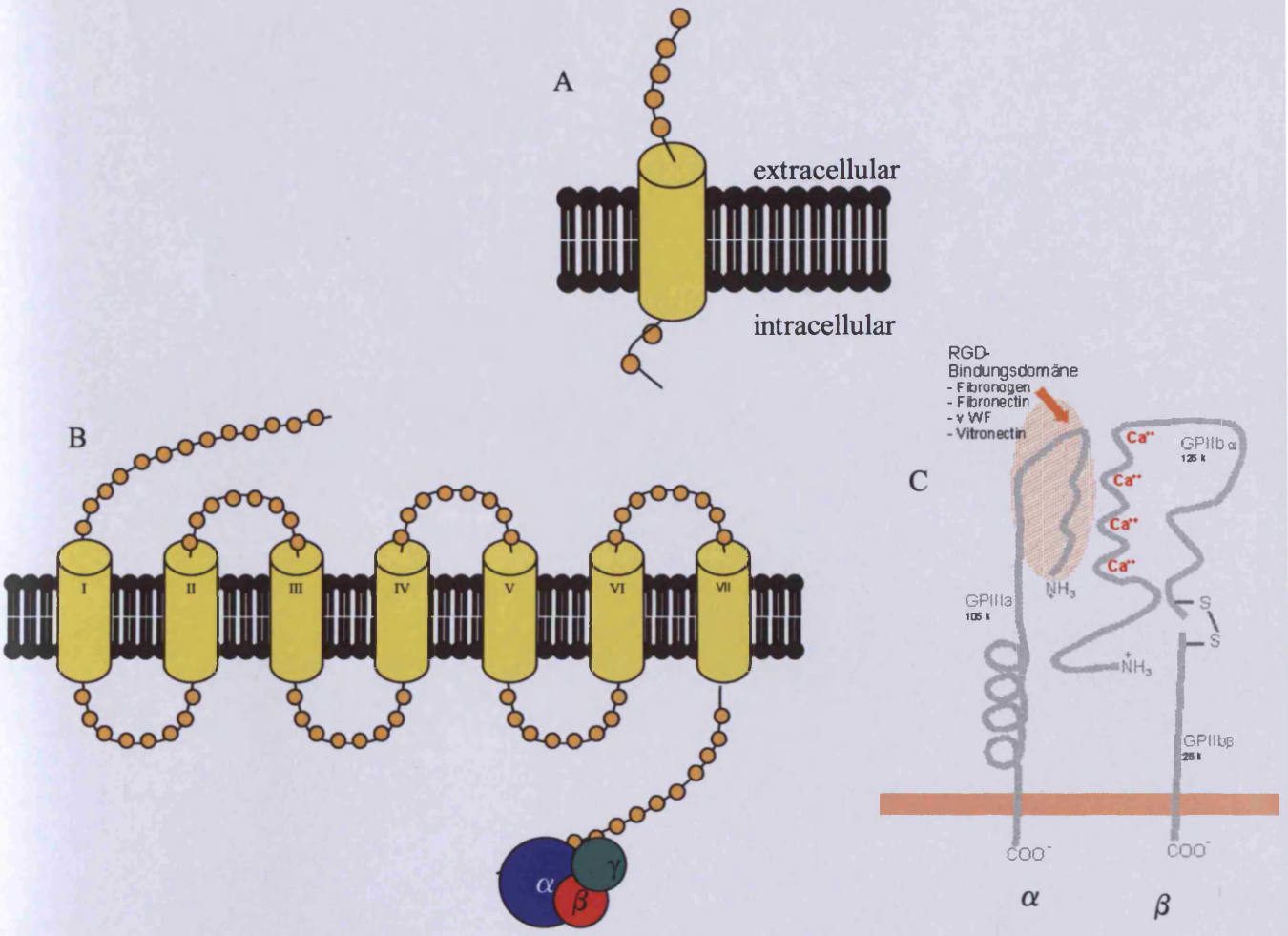

Figure 1.4.2 The Structures of Some Neutrophil Receptors

(A) Single transmembrane spanning domain allows communication between the extracellular environment and the intracellular space. (B) The seven transmembrane spanning domain receptor for the chemoattractants is shown, with the seven transmembrane spanning domains numbered. (C) The α and ß sub-units of the integrins are also labelled.

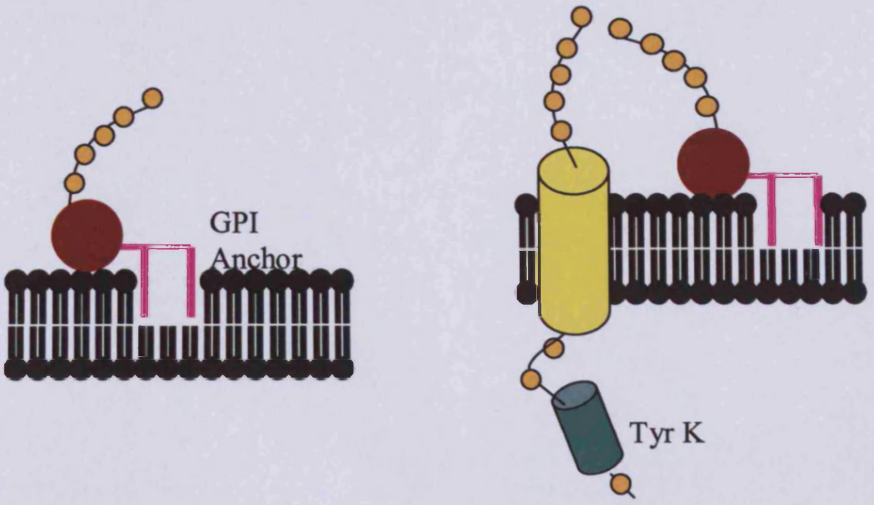

Figure 1.4.3 GPI-Linked Receptor Requires Transducer to Signal Trans-membrane

GPI linkage is shown in purple. The signal is often transduced through the plasma membrane by another molecule, such as here a tyrosine kinase linked receptor.

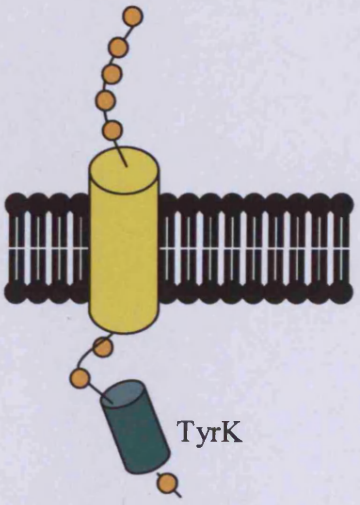

Figure 1.4.4 Receptors Linked with Tyrosine Phosphorylation Rather Than Ca^{2+} Production

A single transmembrane spanning domain transudces the signal from the extracellular binding domain to the intracellular region where there is a tyrosine kinase. This causes phosphorylation of local tyrosine residues, this altering their protein structures. Examples include the receptor for TNF and GMSCF.

signals and thus provide a common underlying signalling mechanism for all the receptors in this class.

On the neutrophil there are also other receptors, involved with "priming" and associated with tyrosine phosphorylation rather than Ca^{2+} signalling. These receptors could be called "growth factor-like" receptors (Ding & Porteu, 1992: Hallett & Lloyds, 1995) and include the receptor for TNF and GMCSF (Fig 1.4.4).

The cellular events associated with activation by each class of receptors are not unique to that class. However, the cross-linking activated receptor seems to be mainly associated with local events, such as cell shape change during adhesion and phagocytosis together with localised oxidase activation. 7TM receptors are generally involved in responses of the whole cell, such as chemotaxis, global degranulation and global oxidase activation. However, no receptor class is strictly coupled to single cellular outputs. There is also overlap in the cellular response (cellular output) from each receptor. For example, occupancy of the formylated peptide receptors results in neutrophil chemotaxis, oxidase activation or degranulation, the proportion of each depending on the concentration of peptide and the experimental condition (Hallett, 1989: Al-Mohanna & Hallett, 1991). The intracellular signalling events associated with stimulation by each of the receptors classes also overlap (Table 1.4.4), and include cytosolic free Ca^{2+} signalling, tyrosine phosphorylation and possibly cyclic nucleotide generation.

Table 1.4.4 Intracellular Signal in Neutrophils

Intracellular Chemical Event	Stimuli
Ca^{2+}	7TM, GPI-linked and cross-linking
Tyrosine phosphorylation	TNF, 7TM, GPI-linked & cross-linking
cAMP	7TM, adenosine receptor
pH	shape change, oxidase activation
actin polymerisation	integrin, 7TM

1.4.3 Local and Global Responses and Signalling in Neutrophils

Many of the responses of neutrophils are characterised by their specific occurrence in one part of the cell (local). For example, the process of phagocytosis occurs only at that part of the cell in direct contact with the particle. Similarly, fusion of a granule with the phagosome, and activation of the oxidase is specifically signalled locally to occur in just one phagosome (Petty, et al, 1992). Local changes also occur during adhesion, and chemotaxis (Fig 1.4.5). This raises an issue of particular importance for neutrophil signalling, namely how can local signalling molecules be restricted.

As the neutrophil has both local and global cellular responses, there must be underlying mechanisms that can signal either locally or globally. For localised neutrophil responses, signalling would have to be restricted in some way to a small volume of the cell. One such mechanism could be related to the hydrophobicity of the signalling molecule. A hypothetical hydrophobic signalling molecule, such as a lipid signalling molecule, would be restricted to the membrane. If the membrane formed an enclosed structure such as the phagosomal membrane, the signalling lipid would be restricted to this phagosome alone (Fig 1.4.5). For such a mechanism to be possible, either the signalling lipid molecule would have to have formed after the formation of the phagosome, or the rate of diffusion of the signalling lipid must be slower than the rate at which the enclosed phagosome formed.

Restriction of signalling could also be achieved in proteins associated with the membrane, such as that of tyrosine or serine/threonine kinases. PKC becomes associated with the plasma membrane by binding to phosphatidyl serine (Bell,1986) and is activated by membrane associated di-acyl glycerol. Its lateral diffusion around

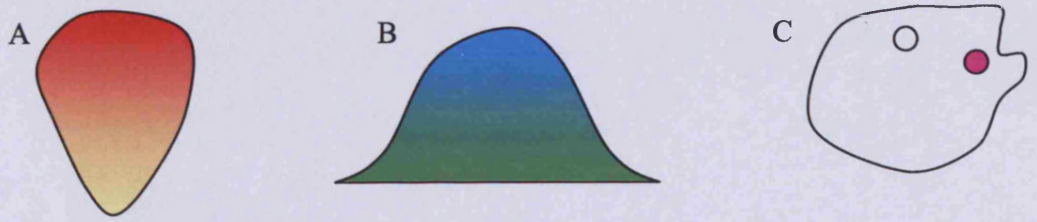

Figure 1.4.5 Localisation of Signals to Sites of Activation Such as Phagosomal Membrane

Many signals are localised to the site of their triggering or action. For example during chemotaxis (A), adhesion (B) and phagocytosis (C) the signals are located to the leading edge, the contact site and specific phagosome respectively. Actin polymerisation is highest at the leading edge (red in A). β2-integrin engagement and Ca^{2+} signalling occurs at the site of surface contact during adhesion (green in B). Only the new phagosome has Ca^{2+} triggered NADPH oxidase activity (purple in C) compared to inactive phagosome (white).

the neutrophil plasma membrane may be limited by the diffusion of the associated lipids and may thus have similar diffusional properties to those described for the lipids. If the signalling molecule were a transmembrane protein, these often have diffusion constants an order of magnitude (or two) lower than lipid (Alberts et al, 1994). The protein would then be even further restricted than PKC. Both types of membrane associated protein could therefore provide a mechanism for fast local signalling from a localised stimulus.

Another hypothetical mechanism for providing localised signalling is for the signalling molecule to be immobile, i.e. have zero (or virtually zero) diffusion. Immobilisation, and hence restriction, could be achieved in proteins, such that tyrosine or serine/threonine phosphorylation of an immobilised protein, perhaps attached to the cytoskeleton, would represent a purely localised signal.

However, many of the signalling molecules and ions identified as signals in neutrophils are not restricted proteins, but small diffusible messengers like Ca^{2+} and IP_3. The question thus arises whether any of the small diffusible messengers have characteristics that enable them to act as localised signals in neutrophils. There are usually considered to be two important factors. For a gradient of a signalling agent to be established, there must be a spatially separated source and sink of the messenger, i.e. the place where the signal is generated must be separate from the place where the signal is destroyed. This condition would seem to be satisfied in neutrophils during phagocytosis, adherence and chemotaxis, as the stimulus acts preferentially only on one part of the cell. If this represents the source of the signal then, in theory, the destruction of the signal as it diffuses through the cytosol either by enzymatic

destruction as for IP_3 or by "buffering" as for Ca^{2+} would represent the sink spatially separate from that site. A stable gradient could be produced. The second consideration is whether the distance over which the gradient would form would result in a restriction of the signal to within the dimension of the neutrophil. Obviously the effective "diffusion distance" would be related to both the rate of diffusion (i.e. the diffusion constant of the messenger, D, μm^2/sec) and its rate of destruction in the cytosol (i.e. the reciprocal of the life-time of the messenger in the cytosol, t, sec). The function Dt has the units of distance (μm) and is the space constant or "effective diffusion length" (Meyer & Stryer, 1991: Allbritton et al, 1992). The theoretical values for the parameter for some of the signalling molecules within neutrophils are given in Table 1.4.5. An estimate of the metabolite destruction rate of membrane associated lipid signalling molecules, together with an estimate of their diffusion in the membrane suggests that they could signal local events. It will be seen that whereas IP_3 can only act as a global signalling molecules within neutrophils (i.e. cell diameter 10 μm), only Ca^{2+} could act locally in the cytosol (Fig 1.4.6). Table 1.4.5 indicates the ranges of various signalling molecules in neutrophils. Many of them have properties that lend them to global signalling events. However, the properties of Ca^{2+} and lipids are the most restricted. Lipids remain to be restricted within hydrophobic environments rather than the general cytosol. This would seem to place Ca^{2+} as the preferential local signalling system in neutrophils.

1.4.4 Integration of Neutrophil Activity

The additional feature that must be considered in neutrophil signalling is how the cellular activity is co-ordinated. An individual neutrophil can migrate and phagocytose at the same time. Is there cross-talk between these signalling systems?

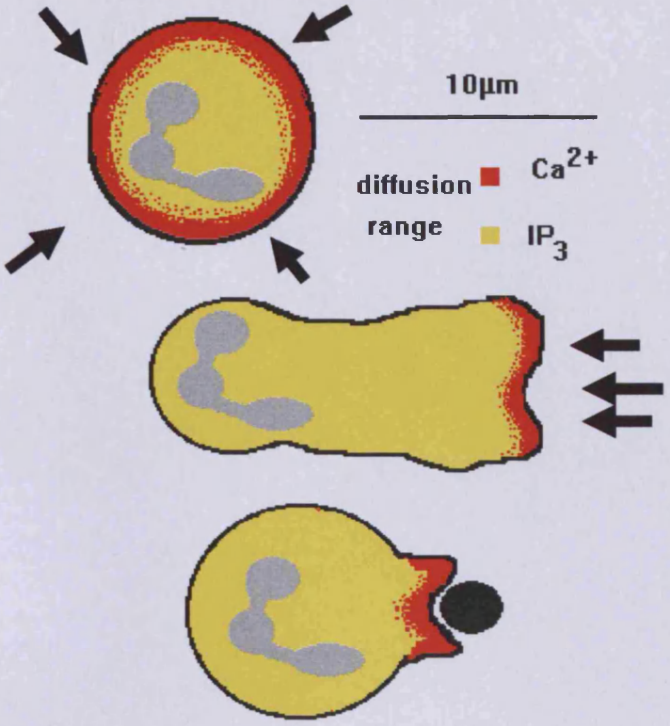

Figure 1.4.6 Range of Signalling Molecules in Neutrophils

The signalling ranges for Ca^{2+} and IP_3 are shown to scale on a spherical neutrophil, a migrating neutrophil and a neutrophil in the act of phagocytosis. In each case the darker shading shows the range of cytosolic free Ca^{2+} diffusion and the lighter shading that of IP_3.

Table 1.4.5 Range of Signalling Molecules in Neutrophils

Messenger	**Diffusion constant (D, $\mu m^2/s$)**	**Lifetime (t,s)**	**Diff Dist(ΔDt) (μm)**	**Local/Global**
ATP	720	1-60	30-200	Global
cAMP	780	1-60	30-200	Global
cGMP	500	1-60	20-170	Global
IP_3	283	1	17	Global
Ca^{2+}				
- free	233	3.10^{-5}	0.1	Local
- buffered	13	1	3.6	Local
Na^+	1320	>60	>200	Global
K^+	1870	>60	>200	Global
*Lipids	~1	~1-10	1-3	Local (laterally)

*Plasma membrane associated lipids:

PIP_3, diacylglycerol, phosphatidic acid and sphingosine metabolites

Data from Hallett & Lloyds 1997

An example where cross-talk between signalling systems may exist is "priming" (Hallett & Lloyds, 1995). Here, the "primer" acts to modify the effectiveness of a subsequent stimulation. However, the question remains whether the neutrophil needs to perform a specific programme of activity, i.e. experience a series of stimuli in a defined order? For example, is the polarisation of the neutrophil, which occurs after adhesion and results in chemotaxis, necessary for subsequent efficient signalling via phagocytosis? These ideas lead to the possibility that, physiologically, the neutrophil follows a programme of activity whereby each activity sets up the appropriate intracellular conditions appropriate for the next response. Thus, signalling and event sequences in neutrophils are important for their appropriate activity.

1.5 Cytosolic Free Ca^{2+} Homeostasis in the Neutrophil

As in all mammalian cells, the concentration of cytosolic free Ca^{2+} in neutrophils is regulated in the both the resting and activated cell. In the resting state, cytosolic free Ca^{2+} concentration is maintained at approximately 100nM, whereas extracellular Ca^{2+} concentration is in the millimolar range. There is thus a 10,000 fold difference in Ca^{2+} concentration across the neutrophil membrane. This difference is maintained by balance between the low permeability of the resting plasma membrane to Ca^{2+} and the pumping out of Ca^{2+} ions back into the extracellular environment. The cytosol is also highly buffered, so that potential fluctuations in cytosolic free Ca^{2+} concentration are reduced. This is achieved by both soluble cytosolic Ca^{2+} buffers and organelles, which actively sequester Ca^{2+}.

As a result, Ca^{2+} is maintained at disequilibrium at a number of sites within the cell. In this section, the mechanism for homeostatic maintenance of this disequilibrium in neutrophils is discussed.

1.5.1 Ca^{2+} Distribution in the Neutrophil

The distribution of Ca^{2+} in the human neutrophil has not been fully established. However, the total Ca^{2+} in the rabbit "neutrophil" is equivalent to roughly 1mM (Petroski et al, 1963). The total amount of Ca^{2+} releasable by ionophore from guinea-pig "neutrophils" has been reported to be 0.91 nmol/4.10^6 cells (Hamachi et al, 1986), equivalent to about 0.5 mM. This means about 50 % of the Ca^{2+} in the neutrophil is releasable from "stores" and other sites. At the electron microscopic level, staining by antimony reveals that the nucleus is a high Ca^{2+} region in the neutrophil (Hoffstein 1979: Cramer & Gallin, 1979) in keeping with the expectation that about 50 % of the

cell calcium in a "typical" cell would be bound in the nucleus (Campbell & Hallett, 1983). However, neutrophils are hardly typical cells as far as Ca^{2+} is concerned, as some classical "calcium-containing organelles", such as the endoplasmic reticulum and mitochondria, are virtually absent (Schmid-Schonbein et al, 1980). Electron microscopic studies, however, located two other regions of high Ca^{2+} in the neutrophil (Hoffstein 1979: Cramer & Gallin, 1979), one located in a subpopulation of granules and the second at specific sites at the plasma membrane. The distribution of the fluorescent Ca^{2+} chelator, chlortetracycline (Caswell, 1979) also identifies a sub-plasma membrane Ca^{2+} storage site (Pettit et al, 1997: Al-Mohanna et al, 1997). Although, this compound cannot be used for the measurement of cytosolic free Ca^{2+}, its Ca^{2+} chelator property makes it potentially useful for mapping-out the subcellular distribution of Ca^{2+} storage sites (see later). The compound binds to Ca^{2+} with a Kd of about 0.4mM, (Caswell & Hutchinson , 1971) to form a complex which is membrane impermeant. Therefore, chlortetracycline accumulates in organelles with high levels of free Ca^{2+}, and its subcellular distribution thus reflects the distribution of Ca^{2+} storage in the cell. As the nucleus does not stain, it can be concluded that the nuclear Ca^{2+} is tightly bound and not available, whereas the staining at the cell periphery, and a second region of high Ca^{2+} storage close to the nucleus may represent physiological storage sites. These locations thus account for virtually all (~95%) of the cell calcium in the neutrophil (Fig 1.5.1). The cytosol also contain small organelles, called "calciosomes" (Volpeet al, 1980: Krauses et al, 1989), which are mobile (Stendahl et al, 1994: Favre et al, 1996). They may contain 5% of the total neutrophil Ca^{2+}(Table 1.5.1). There is also Ca^{2+} in the cytosol, both free and bound, with the cytosolic free Ca^{2+} concentration being consistently around 100nM in the neutrophils from a number of species (Table 1.5.2).

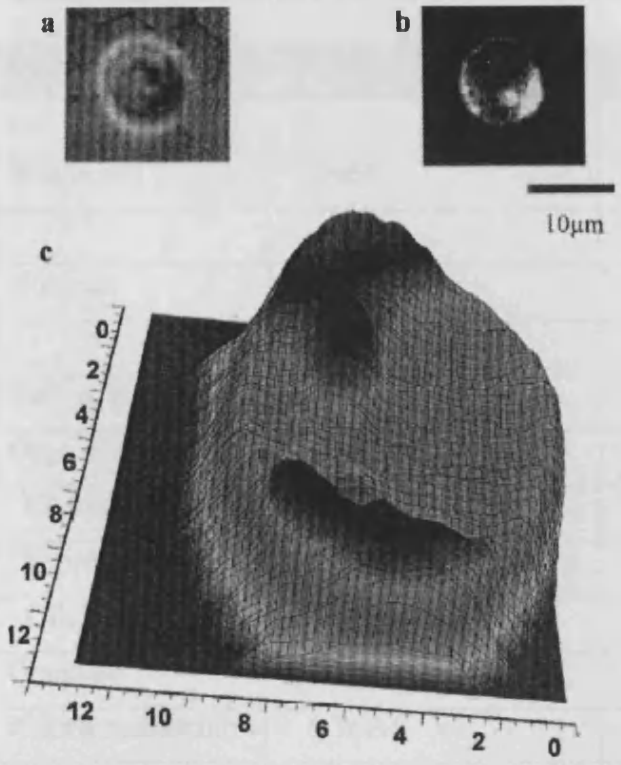

Figure 1.5.1 Chlortetracycline Staining Identifies Distinct Loci of Ca^{2+}

Ca^{2+} store location imaged by CTC fluorescence. (a) Bright-field and (b) fluorescent images of a human neutrophil after incubation with chlortetracycline (45 min, 1:50 chlortetracycline-saturated DMSO solution). (c) An intensity map of the cellular distribution of CTC fluorescence showing the relationship of the central and peripheral high Ca^{2+} zones. (data from Al Mohanna, 1997).

Table 1.5.1 Distribution of Calcium in the Neutrophil

Organelle	**Ca^{2+} Concentration**	**Percentage**
Whole cell	2mM	100
Nucleus	1mM	50
Ca^{2+} storage		
Organelles:-		
Central	0.3mM	15
Peripheral	0.34mM	17
Calciosomes	0.1mM	5
Granules	0.16mM	8
Plasma membrane	0.1mM	5
Cytosol:-		
Bound	10μM	0.5
Free	100nM	0.005%

Table 1.5.2 Resting Membrane Permeability to Ca^{2+}

Cell	Resting influx (mole/cm^2/sec)	Extracellular Ca^{2+}conc (mM)	Permeability Coefficient (10^{-9}cm.sec^{-1})	Reference
Squid giant axon	76	10.7	7.1	Hodgkin & Keynes, 1957
Frog Heart cells	36	4	9	Niedergerke, 1963
Guinea Pig atria	10	1.25	8	Wingrad & Shanes, 1962
Mast Cell	8	1	8	Foreman et al, 1977
Neutrophil	8	1	8	Naccache et al, 1977

* The Permeability Coefficient is independent on the extracellular Ca^{2+} concentration and was calculated from the references as:-

(Ca^{2+} flux)/(extracellular Ca^{2+} concentration) giving units of (moles/cm^2/sec)/(moles/cm^2)= cm/sec.

1.5.2 Resting Ca^{2+} Permeability

The resting plasma membrane from a variety of sources have similar Ca^{2+} permeability properties, all having a permeability coefficient of about $8x10^{-9}$ cm/sec (Table 1.5.2). In the neutrophil, with a surface area of 300 μm^2 and in a medium with 1 mM Ca^{2+}, this corresponds to a resting Ca^{2+} influx of about $2.4x10^{-20}$ moles/sec. As no net cytosolic free Ca^{2+} concentration change occurs, this resting permeability is balanced by Ca^{2+} efflux. The Ca^{2+} efflux pump must have an equal rate to this, or 8.10^{-23} mole/μm^2 /sec, or just 48 Ca^{2+} ions extruded/μm^2/sec. Presumably the resting Ca^{2+} influx partly results from "leakage" across the lipid bilayer or at points of protein insertion where the bilayer is disturbed. Another source of resting Ca^{2+} influx may be the occasional spontaneous opening of ion channels. Thus, the extrusion rate may be higher than the resting influx to maintain a constant level of cytosolic Ca^{2+}.

The maintenance of the resting cytosolic free Ca^{2+} concentration in the resting cell must result from a balance between the "leak" of Ca^{2+} into the neutrophil and the pumping of cytosolic Ca^{2+} out of the cell. In neutrophils, a Mg^{2+}, Ca^{2+}- activated ATP-ase, which is detectable in the plasma membrane, represents this Ca^{2+} pump (Jackowski et al, 1979: Schneider et al, 1979: Volpi et al, 1982). Mg^{2+} is required to provide Mg-ATP, and the Ca^{2+} is actively transported across the membrane from the cytosolic face to the exterior (Volpi et al, 1983). The Km for this transport rate was determined to be 2.8 μM, indicating that this transport system would operate best at cytosolic free Ca^{2+} concentration up to about 5 μM, which is in excess of the bulk cytosolic free Ca^{2+} concentration experienced under physiological conditions. However, such high concentrations may be experienced locally or just under the plasma membrane during Ca^{2+} influx. The efflux system is modulated by calmodulin (Volpi et al, 1983) acting as a switch to activate the pump as cytosolic free Ca^{2+}

concentration rises in the cell. Ca^{2+} pumping may also stimulated by PMA, presumably by acting through protein kinase C, and can cause a measurable decrease in the resting cytosolic free Ca^{2+} concentration (Lagast et al, 1985: Rickard & Sheterline, 1985: Cooke et al, 1989). The Km for Ca^{2+} of the ATP-ase is about 0.2 μM (Volpi et al, 1983). So at a resting cytosolic free Ca^{2+} concentration (0.1 μM), the ATPase (and hence the pump rate) would be operating at approximately 25 % of its maximum rate.

1.5.3 Ca^{2+} Buffering Capacity in Neutrophils

The buffering capacity of the neutrophil cytoplasm for Ca^{2+} is an important parameter in understanding the role of this ion in neutrophil cell physiology. It is often given as the ratio of bound Ca^{2+}:free Ca^{2+} in the cytosol and is defined at any free Ca^{2+} as:- L/kd, where L is the concentration of free ligand and kd the dissociation constant. The concentration of free ligand can be calculated from $L=L_t/[1+(Ca^{2+}/kd)]$, where L_t is the total ligand concentration.

It is important to know the parameters of the buffering capacity for (i) establishing the required influx of Ca^{2+} for a given cytosolic free Ca^{2+} change, (ii) determining the apparent diffusion constant of Ca^{2+} in the neutrophil cytosol and (iii) quantifying the effect of experimental manipulations, such as the inclusion of fluorescent Ca^{2+} chelator indicators on the measured cytosolic free Ca^{2+} concentration. As in other cells, there will be a fast component of Ca^{2+} buffering, which results from binding to proteins, citrate and other cellular components. In squid axons this occurs on the msec time scale and accounts for about 1 % of the total buffering capacity. The remainder of the buffering capacity results from slower processes (over seconds rather than

milliseconds) such as uptake into storage organelles and binding to proteins in the nucleus. Neutrophils respond within time scales of seconds rather than milliseconds, so this total buffering capacity is the effective parameter of interest. In squid giant axon cytoplasm, which is devoid of nuclei and is often used as a standard compare Ca^{2+} parameters to, Baker (1976) estimated that the total cytoplasmic Ca^{2+} concentration was 400 μM whereas the cytosolic free Ca^{2+} concentration was only 0.1 μM. This gives a buffering capacity of 4000:1. From the apparent diffusion constant of Ca^{2+} in the squid axon (DiPoloet al, 1976), it was estimated that only 0.1 % of Ca^{2+} ions were free, giving a buffering capacity of 1:1000.

In neutrophils, it is more difficult to obtain this parameter, but a rough estimate can be made from knowledge of total Ca^{2+} transported into the cell and the actual cytosolic free Ca^{2+} concentration change. In rabbit neutrophils, a $^{45}Ca^{2+}$ influx of 36 fmoles/cm^2/cell over a 10 second period (Naccache et al, 1977) would give a total Ca^{2+} increase of 3 mM. As the cytosolic free Ca^{2+} concentration rise is only about 1 μM, the buffering capacity for the rabbit neutrophil is about 3000:1. In human and rat neutrophils, intracellular fura2 has been used to estimate the Ca^{2+} buffering capacity making use of both the buffering and measuring properties of this molecule. With intracellular fura2 at 100 μM, and a resting Ca^{2+} (100 nM), the resting buffering capacity is about 300:1. Thus 300 ions of Ca^{2+} will be bound to fura2 for every one free in the cytosol. During stimulation, the buffering capacity for rat and human neutrophil increases to about 3000:1 and 2000-3000:1 respectively (Al-Mohanna & Hallett, 1988: Hallett et al, 1996). von Tscharner et al (1986a) reported that the Ca^{2+} buffering was equivalent to a buffer with kd 0.55 μM at a concentration of 0.76 mM, corresponding to a buffering capacity of about 1300:1. Thus all estimates of

neutrophil buffering capacity are in reasonable agreement, with the effective Ca^{2+} buffering capacity being between 1000:1 and 3000:1 (Table 1.5.3). Thus on entry of Ca^{2+} into the cytosol of the neutrophil either from the extracellular space or from Ca^{2+} storage sites, for every free Ca^{2+} ion generated in the cytosol there would be approximately 1000 to 3000 Ca^{2+} ions bound.

1.5.4 Ca^{2+} Stores in Neutrophils

When the plasma membrane is permeabilsed, the contribution of the plasma membrane Ca^{2+} ATP-ase pumps to Ca^{2+} homeostasis and signalling is removed. However, the permeabilisd neutrophil remains able to reduce the ambient Ca^{2+} (Prentki et al, 1984) to a "set point". This is due to pumping into organelles to achieve the set point of less than 200 nM, which is near the resting cytosolic free Ca^{2+} concentration in the intact cell (Prentki et al, 1984). In cell fractional studies, there was found to be correlations of Ca^{2+} uptake with markers of endosomes, the plasma membrane and "golgi" (Krause et al, 1987). The organelle uptake sites probably correspond with the "calciosomes", the subplasma membrane site and the juxta-nuclear central organelle discussed earlier. Another study (Klempner, 1986) also suggested that granules actively pumped Ca^{2+}, in agreement the Ca^{2+} rich granules identified by electron microscopy.

There are known to be several isoforms of the Ca^{2+}-ATPase (SERCAs). In neutrophils, SERCA 3 has been identified by proteomics (Lominadze et al, 2005), and SERCA II isoforms have been identified immunologically with SERCaIIb being associated with the "calciosome" organelles (Favre et al, 1996).

Table 1.5.3 Ca^{2+} Buffering Capacity in Neutrophils

Species	Buffering Capacity	Reference
rabbit	3000:1	Naccache et al, 1977
rat	3000:1	Al-Mohanna & Hallett, 1988
human	2000-3000:1	Hallett et al, 1996
human	1300:1	Von Tscharner et al, 1986
squid axon	1000-4000:1	DiPolo et al, 1976; Baker, 1976

The storage organelles also contain the Ca^{2+}-binding protein, calreticulin (Volpe et al, 1988: Krause et al, 1989: Stendahl et al, 1994: Favre et al, 1996). This protein is widely distributed within the small "calciosome" organelles. The presence of both Ca^{2+} pumps and Ca^{2+} storage protein gives these structures the two functional molecules required for Ca^{2+} store activity. Furthermore, they also contain IP_3 receptors, which strongly suggest that they also have a Ca^{2+} release mechanism for contributing to Ca^{2+} signalling.

1.6 Cytosolic Free Ca^{2+} Signalling in Neutrophils

The major intracellular change that occurs within neutrophils when appropriately stimulated is the change in cytosolic free Ca^{2+} concentration. The cytosolic free Ca^{2+} concentration increases approximately 10 fold, from 0.1 μM to 1 μM, and probably represents the most significant chemical change within the neutrophil. Although both the seven transmembrane spanning domain receptors and the cross-linking stimuli (discussed earlier) trigger an elevation of cytosolic free Ca^{2+} concentration, the mechanism is distinct at a number of key stages.

The Ca^{2+} signal in neutrophils, as in other cell-types, is generated by both release of Ca^{2+} from intracellular Ca^{2+} storage sites and by an increase in the influx of Ca^{2+} from the extracellular environment. This involves the generation of signals, such as IP_3 and possibly other lipid messengers, such as PIP_3, which signal release from intracellular Ca^{2+} storage sites. The Ca^{2+} influx phase is necessary for the full activation of many of the neutrophil responses, as simple removal of extracellular Ca^{2+} is sufficient to inhibit the response (Hallett & Campbell, 1984). However, although the amount of Ca^{2+} released from the intracellular Ca^{2+} stores may be insufficient to fully activate the neutrophil, it may provide sufficient Ca^{2+} for local activation. The release of intracellular Ca^{2+} from some Ca^{2+} storage sites also has a key role to play in the activation of the Ca^{2+} influx pathway.

Upon stimulation, the membrane Ca^{2+} permeability increases dramatically, and is mainly responsible for the magnitude and duration of the neutrophil Ca^{2+} signal. The comparison of stimulated Ca^{2+} influx rates in different cell-types is more variable but is still within reasonably tight limits (Table 1.5.2). As the Ca^{2+} signal in the absence of

extracellular Ca^{2+} is greatly attenuated, the Ca^{2+} influx phase is known to be of significance. The relative contributions of influx and store release may vary with the stimulus class. For example, for the seven transmembrane spanning domain (7TM) receptors, Ca^{2+} influx and Ca^{2+} store release are tightly coupled, whereas with the cross-linking stimuli they are not. In some cell types, it has been suggested that the release of Ca^{2+} from stores represents the major source for cytosolic free Ca^{2+} changes. However, in neutrophils Ca^{2+} influx is important for effective signalling.

1.6.1 Cytosolic Free Ca^{2+} Signalling by Seven Transmembrane Spanning Domain Receptors

At low concentrations, ligand binding causes activation of seven transmembrane spanning domain (7TM) receptor signal chemotaxis. However, at higher concentrations, global cytosolic free Ca^{2+} rises are provoked (Thelen et al, 1993) and are responsible for triggering oxidase activation (Thelen et al, 1993), but probably not cell movement (Laffafian & Hallett, 1995).

Activation of the 7TM receptors is coupled to release of Ca^{2+} from the Ca^{2+} storage site (Pettit & Hallett, 1996b), an event that precedes the opening of Ca^{2+} influx channels (Pettit & Hallett, 1995) and probably triggers it. As the Ca^{2+} storage site is remote from the plasma membrane, the signal for Ca^{2+} release from here must be a diffusible signal. As with 7TM receptors on other cell-types, activation of those on neutrophils causes activation of phospholipase C-ß, which cleaves PIP_2 and liberates IP_3 (Cockcroft, 1998). Both IP_3 generation in neutrophils after stimulation with agonists of 7TM receptors and the presence of IP_3 receptors (Cockcroft, 1998:

Stendahl, et al, 1994: Favre, et al, 1996) have been detected, indicating both elements are necessary for release of Ca^{2+} from stores are in place.

In the neutrophil (Davies et al, 1991), the human giant myeloid cell (Roberts et al, 1995) and the newt giant eosinophils (Brundage et al, 1993) the Ca^{2+} release site correlates with the location of an organelle that stains with $DiOC_6$. This agent stains the Golgi apparatus and the endoplasmic reticulum (Terasaki et al, 1984), two organelles for which there is evidence of involvement in Ca^{2+} release in other cell types. At the EM level, a membranous structure similar to smooth endoplasmic reticulum or Golgi apparatus is visible in neutrophils, nestling between the nuclear lobes (Cline, 1975: Hallett et al, 1996).

1.6.1a Signalling Delay With fMLP

Monitoring the Ca^{2+} response in small mammalian cells with sufficient time resolution to distinguish the earliest Ca^{2+} events has been difficult. Sage and colleagues using stopped-flow techniques with fura2 loaded neutrophils (1990). With this technique, a delay between addition of stimulus and response is detectable. However, as the technique employs populations of cells, only population "cell-averaged" data can be derived (Sage et al, 1990) However, laser scanning techniques permits cytosolic free Ca^{2+} changes in individual neutrophils to be measured with a time resolution of 12.5 msec (Petit & Hallett, 1995). With this approach it was discovered that individual neutrophils vary in the lag time before Ca^{2+} influx resulted in a global Ca^{2+} rise. The explanation for the asynchrony may lie in the mechanism underlying stimulus-response coupling. One possibility is that the underlying stochasticity of the events that trigger the Ca^{2+} signal are apparent at the individual neutrophil level. The

distribution of lag times is similar to that predicted from a multi-step series of stochastic processes occurring with a stochastic rate similar to that expected for diffusion of a limited number of intracellular signalling molecules (Hallett & Pettit, 1997).

1.6.2 Cytosolic Free Ca^{2+} Signalling by Cross-Linking Stimuli

The mechanism by which cytosolic free Ca^{2+} is signalled by cross-linking is yet to be resolved, but it is clear that it differs from that of the 7TM receptor agonists in several ways: (i) it can be selectively inhibited by inhibitors of tyrosine phosphorylation, which have no effect on Ca^{2+} signalling by 7TM receptor agonists (Morgan et al, 1993), (ii) it can be selectively inhibited by BPB, an inhibitor of l-plastin (Rosales et al, 1994) and other inhibition strategies which have no effect on Ca^{2+} signalling by 7TM receptor agonists (Rosales et al, 1994: Davies & Hallett, 1995a), and (iii) the release of stored Ca^{2+} is not temporally so tightly coupled to Ca^{2+} influx as stimulation via 7TM receptors (Petersen et al, 1993: Davies & Hallett, 1995: Pettit & Hallett, 1996:).

1.6.2a Signalling Delay With Cross-Linking

With the cross-linking stimuli, the delay before Ca^{2+} signalling is not in the millisecond time scale, but in the seconds range. This longer delay is due to the need for aggregation of molecules on the surface before the Ca^{2+} signal is initiated. This has been demonstrated by using the anti-antibody technique (Petersen et al, 1993: Roberts et al, 1997). By allowing saturation binding of antibodies to the receptor, e.g. β2-integrin or CD32, addition of the cross-linking anti-antibody provides a synchronised stimulus for aggregation. Both the delay before initiation of the Ca^{2+} signal and the

magnitude of the Ca^{2+} signal under these circumstances is dependent on the concentration of the second cross-linking antibody (Roberts et al, 1997). This is consistent with the delay being caused by the diffusion of signalling molecules to form the multi-aggregate complexes before signalling. At lower cross-linking antibody concentrations, the probability of a bound anti-antibody coming within binding range of another (first) antibody, which has already cross-linked with another antibody, is low, and would require more time to achieve the equivalent degree of cross-linking. This was confirmed directly, by decreasing the diffusion time for the ligand in the plasma membrane without affecting the second anti-antibody concentration. This was achieved by covalently cross-linking surface proteins on the neutrophil surface, so that their apparent molecular size was increased with the result that diffusion rate was decreased (Roberts et al, 1997). Under these circumstances, the magnitude of the Ca^{2+} signal was unaffected, but the delay time was extended by many seconds (Roberts et al, 1997), an effect predicted from the diffusion rates of proteins in the membrane (DeLisi, 1980). An insight into the formation of the signalling complex may also be gained from the insertion of exogenous GPI-linked molecules into neutrophils (van der Berg et al, 1995). In U937 cells, the exogenously added GPI-linked CD59 molecule initially does not signal Ca^{2+}. However, with time the exogenous molecule associates with tyrosine kinases in the membrane, and forms micro-aggregates in cholesterol rich regions of the membrane (van der Berg et al, 1995). At this point the exogenous molecule acquires the ability to signal Ca^{2+}. As signalling by cross-linking in neutrophils is also dependent on tyrosine phosphorylation (van der Berg et al, 1995) and may involve tyrosine phosphorylation of PLC-γ (Hellberg et al, 1996) there is a strong possibility that similar effects underlie cross-linking signalling in neutrophils.

1.6.3 Capacitative Ca^{2+} Influx in Neutrophils

The release of the small amount of intracellularly stored Ca^{2+} by the seven transmembrane spanning domain (7TM) receptors, acts as a trigger for the larger global Ca^{2+} signal, which is derived from Ca^{2+} influx. The mechanism of coupling between the release of Ca^{2+} from intracellular Ca^{2+} storage sites and influx remains unclear, but is often referred to as capacitative Ca^{2+} influx. It is clear that in neutrophils, this coupling depends on the Ca^{2+} content of the Ca^{2+} stores. When Ca^{2+} is allowed to leak from the stores by the inhibition of the SERCA pumps, using thapsigargin or cyclopiazonic acid (Foder et al, 1998: Demaurex et al, 1992), plasma membrane Ca^{2+} channels are opened. This has led to the suggestion that Ca^{2+} influx occurs in response to the "need" to refill the Ca^{2+} store.

Similarly, with a physiological stimulus, such as fMLP, there is a causal relationship between Ca^{2+} store release and Ca^{2+} influx (Demaurex et al, 1994). The Ca^{2+} influx phase can be resolved by rapid laser scanning (Pettit & Hallett, 1995) or by the use of Mn^{2+} (Merritt et al, 1989), as a surrogate for extracellular Ca^{2+}. Mn^{2+} quenches fura2, so its influx can be observed separately from the release of stored Ca^{2+} (Merritt et al, 1989). A small molecule with the appropriate properties to act as a messenger between the empty Ca^{2+} stores and plasma membrane Ca^{2+} channels has been identified in several cells (Randriamampita & Tsein, 1993: Parekh et al, 1993) and has been isolated from neutrophils (Davies & Hallett, 1995). More recently interest has focussed on STIM-1 and Orail as proteins involved in Ca^{2+} release activated Ca^{2+} influx (see Chapter 4 for more detail). These proteins bridge the gap between Ca^{2+} stores and the plasma membrane and signal directly between the Ca^{2+} content of store and the Ca^{2+} influx channel (CRAC channel). As neutrophils have very little ER and

none close the plasma membrane, it is unlikely that this mechanism is significant in neutrophils.

1.6.4 Ca^{2+} Channels

The opening of Ca^{2+} channels on the plasma membrane represent an important key step in Ca^{2+} signalling in neutrophils, yet surprisingly little is established about them. von Tscharner et al (1986a) showed that in clamped membrane patches, the addition of fMLP did not cause Ca^{2+} channel opening, demonstrating that the receptor status was not directly coupled to receptor occupancy, but required cytosolic components that were missing in the patch. This may be explained by the need for the release from the Ca^{2+} store to trigger Ca^{2+} channel opening. The physiological Ca^{2+} channels are not voltage sensitive channels, and are insensitive to inhibitors of such channels (Demaurex et al, 1994), although membrane potential can play a role (DiVirgilio et al, 1987).The only agent that von Tscharner et al (1986b) found could open the Ca^{2+} channels was Ca^{2+} itself. This raised the possibility that the channels were Ca^{2+} activated Ca^{2+} channels. However, buffering the cytosolic free Ca^{2+} concentration so that it is below the resting Ca^{2+} level does not prevent Ca^{2+} influx (Nasmith & Grinstein, 1987), suggesting that this is not the case in the intact neutrophil. When stimulated to open, there were two type of channel current observed, with conductances of 18-25pS and 4-6pS. These channels were equally permeable to K^+, Na^+ and Ca^{2+}, but not Cl^- (von Tscharner et al, 1986b). Whether the opening of these channels accounts for intracellular changes in K^+, Na^+ and Ca^{2+} is not established. Although the molecular identity of these channels is not fully established there is strong electrophysiological and mRNA evidence for the expression of several members of the TRP family of ionic channels. (Table 1.6.1)

Table 1.6.1 Members of the TRP Family Identified in Neutrophils and HL60 Cells

TRP family names	Detection method	Cell type used
TRPC1	m-RNA	HL-60
TRPC2	m-RNA	HL-60
TRPC6	m-RNA	Neutrophil
TRPM2 (aka LTRPC2, TRPC7)	m-RNA & electrophysiology	neutrophil/ HL60
TRPV1	m-RNA	neutrophil/ HL60
TRPV2	m-RNA	neutrophil/ HL60
TRPV5	m-RNA	neutrophil/ HL60

Data from Heiner et al, 2003a,b

TRP or TRP-like channels have been speculated to be part of the capacitative Ca^{2+} influx route (Putney & McKay, 1999). Neutrophils, and HL60 neutrophilic cells express a number of TRP channels (Heiner et al, 2003a,b) listed in Table 1.6.1. However, TRPM2, also known as TRPC7 and LTRPC2, has been most studied in neutrophils and other "immunocytes" (Sano et al, 2001) and myeloid cells such as U937 cells (Perraud et al, 2001) in which it is expressed. Like other TRP channels, TRPM2 has relatively poor selectivity for Ca^{2+} and can be permeated by a number of ions. Ca^{2+} influx into neutrophils in general also lacks Ca^{2+} selectivity and is often associated with the influx of other ions (Table 1.6.2) and inhibited by Ni^{+}. There is no obvious correlation between the ionic or hydrated radii of the ion and their ability to permeate or block, apart from with the Group II ions where smaller hydrated ions permeate more easily. Mn^{2+} seems anomalously large to permeate in the resting cell and there may be another as yet unknown conductance pathway for this ion. However, it also enters the neutrophil via a physiologically opened channel (Merritt et al, 1989). The organic inhibitors of the channels include SKF 96365 (Merritt et al, 1990) and the structurally closely related compound econazole (Demaurex et al, 1994). They may act at a similar site, and econazole is claimed to be an inhibitor of store operated Ca^{2+} entry mediated by CIF (Randriamampita & Tsein, 1993).

The LTRPC2 channel is opened in response to ADPR, (and NAD^{+}), which acts through a NUDIX-like motif on the channel (Perraud et al, 2001). When expressed in cells that do not normally express these channels, there is a marked increase in conductance in response to ADPR (Heiner et al, 2003b). Furthermore, in immune cells that do naturally express this channel, namely lymphoid cells (such as T-lymphocytes)

Table 1.6.2 Ion Selectivity of TRP Channels In Neutrophils and HL-60s

TRP Channel	Ion Selectivity* $P_{Ca}:P_{Na}$	Control Mechanism
TRPC1	Non-selective	Store depletion: stretch
TRPC2	2.7	Diacylglycerol
TRPC6	5	DAG, PIP3
TRPM2	0.3	ADP-ribose, NAD, H_2O_2
TRPV1	9.6	Vanalloids, PIP_2
TRPV2	3	Osmotic swelling
TRPV5	100	Low intracellular Ca^{2+}

* selectivity for Ca^{2+} expressed as a ratio of permeability to Na^{+}.

From Venkatachalam and Montell, 2007

and myeloid cells (including neutrophils), an elevation of cytosolic ADPR increases Ca^{2+} influx and elevates cytosolic free Ca^{2+} (Heiner et al, 2003a,b). There is no overlap in the activity of ADPR with the Ca^{2+} releasing molecule, cyclic ADP-ribose, the latter releasing Ca^{2+} from membranous stores within some cells but having no effect on this plasma membrane channel (Heiner et al, 2003a,b). In contrast ADPR (and NAD^+) has no effect on releasing Ca^{2+} from membranous stores, being specific for opening LTRPC2 channels at the plasma membrane. Although the existence of the ADPR (NAD^+)-activated channel in cells of the immune system is becoming increasingly recognised, its physiological function remains obscure without a mechanism for regulation of its activators. It would seem unlikely that the concentration of cytosolic NAD^+ would have a large dynamic range, whereas the fold increase in cytosolic ADPR released from mitochondria could be dramatic and act as a Ca^{2+} channel opening signal.

1.6.5 Cytosolic Free Ca^{2+} Diffusion in the Neutrophil Cytosol

Once liberated into the cytosol, the rate at which Ca^{2+} mixes with the cytosol will be determined by its diffusion coefficient for Ca^{2+} (D). In aqueous solution, this parameter has been measured at 520μm^2/sec, 600μm^2/sec, 780μm^2/sec, or 1335μm^2/sec (Robinson & Stokes, 1968). In the cytosol however, the corresponding D value are far less. Meyer and colleagues has provided a value of D for Ca^{2+} in squid axoplasm of 233μm^2/sec (Meyer & Stryer, 1991: Allbritton et al, 1991) giving a severe restriction to the spread of Ca^{2+} released from a "point" source. Ca^{2+} diffusion in neutrophil cytosol is more restricted than many other cells and certainly more than in aqueous solutions.

1.6.5a Is the Neutrophil Nucleus a Barrier to Ca^{2+} Diffusion?

Since the nucleus in neutrophils occupies a significant fraction of the cytoplasm, the question of whether the nucleus represents a barrier to Ca^{2+} diffusion is important. The nucleus membrane could either act as physical barrier to Ca^{2+} movement or the buffering capacity within the nucleus could differ from the rest of the cytoplasm and hence cause asynchrony in free Ca^{2+} concentration changes. In neuronal cells, this latter effect has been documented (Al-Mohanna et al, 1994). Although, these workers reported an effect on the Ca^{2+} wave as it passed the nuclear region, others have suggested alternative (artefactual) explanations for the observation. It has also been suggested that the nucleus could signal Ca^{2+} separately from the cytosol, by release of Ca^{2+} into the nucleoplasm (Stehno-Bittel et al, 1995). However, in the neutrophil, there is no evidence for any influence of the nucleus on Ca^{2+} signalling, and its presence would seem to be neutral. Firstly, fluorescent diffusible dyes such as fura2, fluo4 and fluorescein, all diffuse uniformly throughout the neutrophil cytoplasm, with no exclusion from the nucleus. As the nuclear membrane is permeable to these dyes, it is also probable that it is permeable to small ions. Secondly, when cytosolic free Ca^{2+} concentration is measured and imaged in neutrophils, the cytosolic free Ca^{2+} concentration is uniform throughout the cytosol. This is seen both with conventional and confocal imaging techniques. Also, when cytosolic free Ca^{2+} concentration is triggered to rise, there is no detectable difference in the rate at which the bulk cytosolic free Ca^{2+} concentration changes and that in the nucleus, even using high time resolution laser-scanning confocal techniques. Taken together, these observations suggest that the nucleus within the neutrophil does not contribute a significant barrier to Ca^{2+} diffusion or play a role in differentially signalling Ca^{2+}.

1.6.6 Do Classic (or Other) Ca^{2+} Waves Exist in Neutrophils?

As Ca^{2+} diffusion is restricted in neutrophils, it is possible that this would give rise to differences between local and regional signalling. Ca^{2+}-induced Ca^{2+} release (CICR) is observed in other cell types and causes a wave of elevated Ca^{2+} to spread across the cell. If such a mechanism were in place in the neutrophil, there could be no restriction of elevated Ca^{2+} since local Ca^{2+} rises would spread throughout the cell, not by diffusion but by CICR mechanisms. This mechanism produces a wave of high Ca^{2+} travelling through the cytosol as Ca^{2+} is released from sites progressively distant from the initiation site. The velocity of the Ca^{2+} waves reported in some other cells are in the range 6-60 μm/sec (Kasai & Augustine, 1990: Rooney et al, 1990: Cornell-Bell et al, 1991) and would sweep across the neutrophil in 200 msec-2 sec. However, this has not been observed by fast laser scanning, where store release that generates a localised high Ca^{2+} signal is followed by a global influx of Ca^{2+} with no evidence of a Ca^{2+} wave (Pettit & Hallett, 1995:1996b). This may not be surprising as the mechanism of Ca^{2+} wave generation in other cell types, involves caffeine and ryanodine sensitive release receptors. In neutrophils, these agents have no effect, either alone or on the subsequent stimulation of Ca^{2+} signalling.

However, the production of a Ca^{2+} wave in neutrophils has been reported following phagocytosis (Schwab et al, 1992). In elongated neutrophils engaged in phagocytosis, a Ca^{2+} wave was detected with a velocity of 17 μm/sec, which swept down the cell away from the site of phagocytosis (Schwab et al, 1992). However, it is unclear whether this was truly a Ca^{2+} wave as it was visualised non-ratiometrically and non-confocally. A second group failed to detect the wave using ratiometric techniques (Theler et al, 1995) and suggested that the increased fluoresence ascribed to Ca^{2+} in

the non-ratiometric analysis was the result of cell shape change as the neutrophil moved towards the particle. The question of conventional Ca^{2+} waves in neutrophils thus remains unresolved.

More recently, Petty's group have reported the existence of an entirely novel form of Ca^{2+} waves in neutrophils, which are discussed in more detail in Chapter 4. These Ca^{2+} waves were reported to travel around the periphery of the neutrophil and phagosome as a defined zone of elevated Ca^{2+}. Their existence was unsuspected but has not been reproduced by the work presented in this thesis or by others who have attempted this (Leibedz, 2008- personal communication). The evidence for the non-existence of these Ca^{2+} phenomena will be the subject of chapters 3 and 4.

1.7 Phospholipid Signalling of Ca^{2+} in Neutrophils

Cytosolic free Ca^{2+} signalling is the major chemical event in the neutrophil that triggers its activity. It could therefore be argued that the mechanisms controlling the Ca^{2+} signal are more fundamental. When Hokin and Hokin in 1953 first discovered that receptor-mediated activation stimulated phospholipid metabolism in some cells (Hokin & Hokin, 1953), it is unlikely that they realised the full significance of their discovery. However, it now clear that phospholipid lipid metabolism in neutrophils, as in other cells, is the key signalling event that underlies Ca^{2+} signalling. In this section the role of phospholipid metabolism, especially in the generation of IP_3 and diacylglycerol, in neutrophil signalling is discussed.

1.7.1 Phospholipases

The significance of the work of Hokin and Hokin in 1953 took twenty years to be appreciated. However, a strong hint that similar events were occurring in neutrophils was provided by Karnovsky (Sbarra & Karnovsky, 1960: Karnovsky & Wallach, 1961). He demonstrated the incorporation of phosphate into phosphatides during neutrophil activation, and that lipid turnover was a key feature. This provided clear evidence of a role for phospholipases in neutrophil activation.

The phospholipases can be divided into three main classes according to where they cleave the phospholipid (Fig 1.7.1). The phospholipase A enzymes cleave at the lipid chain, releasing fatty acid, whereas both phospholipase C and D cleave at the phospho-linkage to the head group. The substrate for the inositol-specific phospholipase C is phosphatidyl-inositol-bis-phosphate (PIP_2). However, phospholipase D is less specific and acts on a number of phospholipids, the most

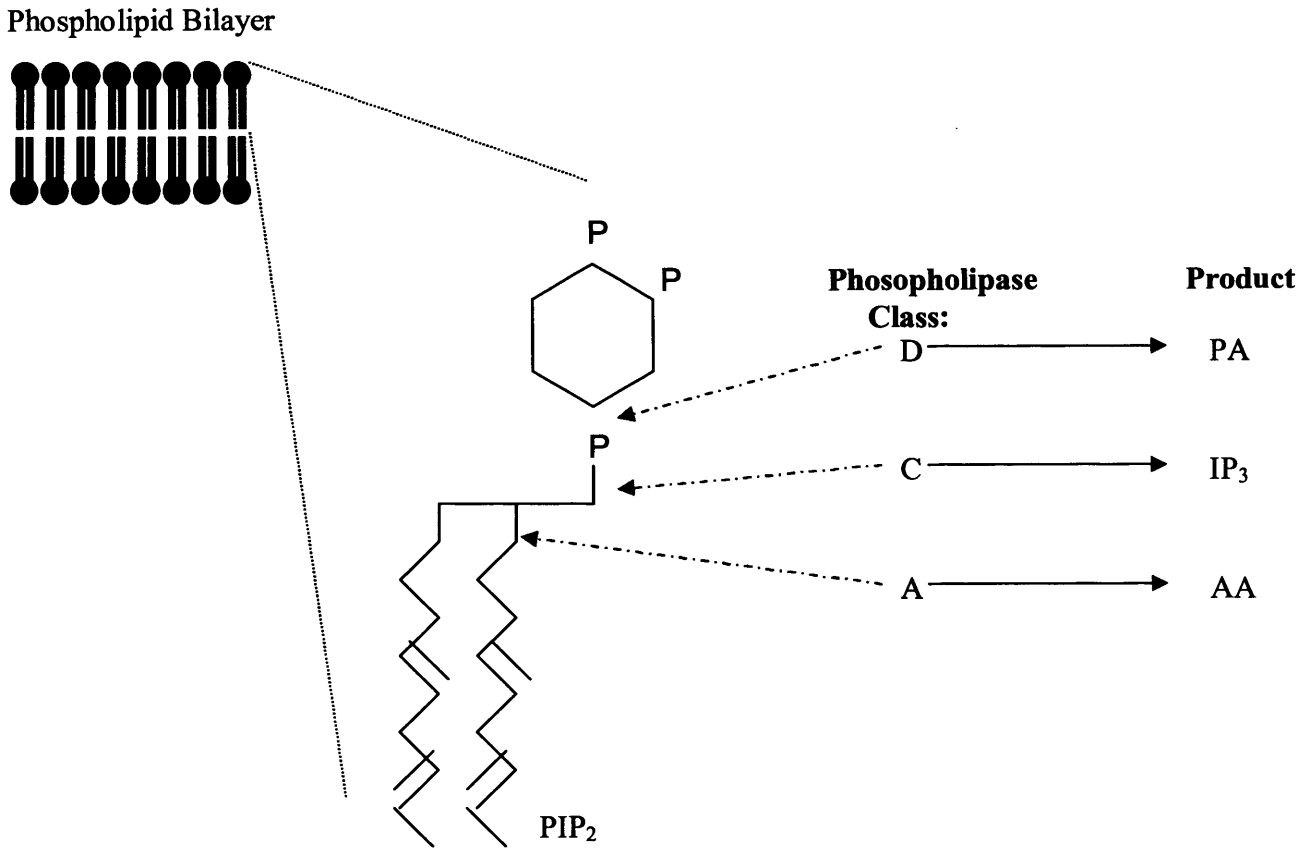

Figure 1.7.1 Classes of Phospolipase

Phospholipase A, C, and D cleave phopsphatidyl ionsitol bis phosphate (PIP_2) at three distinct sites as indicated to generate phosphatidic acid (PA), IP_3 (inositol tris phosphate) or arachidonic acid (AA).

prominent being phosphatidyl-choline. Whereas phospholipase A is involved in the production of arachidonates and inflammatory mediators, phospholipases C and D are more likely to be involved in neutrophil intracellular signalling, as both are capable of generating signalling molecules, particularly diacylglycerols (DAGs). The cleavage of PIP_2 by inositol-specific phospholipase C will release from the membrane associated PIP_2 molecule, the water soluble $Ins(1,4,5)P_3$ (Fig 1.7.2). This molecule is, of course, the biologically active isomer that releases Ca^{2+} from some Ca^{2+} stores in neutrophils. Furthermore, the membrane associated, diacylglycerol is also biologically active, causing activation of protein kinase C.

1.7.2 IP_3 Generation and Phospholipase C Activation

In neutrophils that have been labelled with radioactive ^{32}P, a demonstrable fall in the level of the phospholipase C substrate PIP_2 has been reported to occur within 5 to 10 seconds of addition of fMLP (Volpi et al, 1983, 1985: Dougherty et al, 1984: Bradford & Rubin, 1985: Ohta et al, 1985). The fall is transient and returns to the resting level within 60 seconds. Similarly, activation with PAF, which also acts on a 7TM receptors, causes the fall in PIP_2 level, and ConA, which probably acts by cross-linking Fc receptors, has also been reported to cause such a decrease (Naccache et al, 1985: Verghese et al, 1985). However, leukotriene B4, which also liberates stored Ca^{2+}, does so without a detectable fall in PIP_2 level (Volpi et al, 1984), suggesting that it may act on different storage sites. This might point to an alternate Ca^{2+} release mechanism by these stimuli, although IP_3 generation by this stimulus has also been reported (Andersson et al, 1986: Mong et al, 1986).

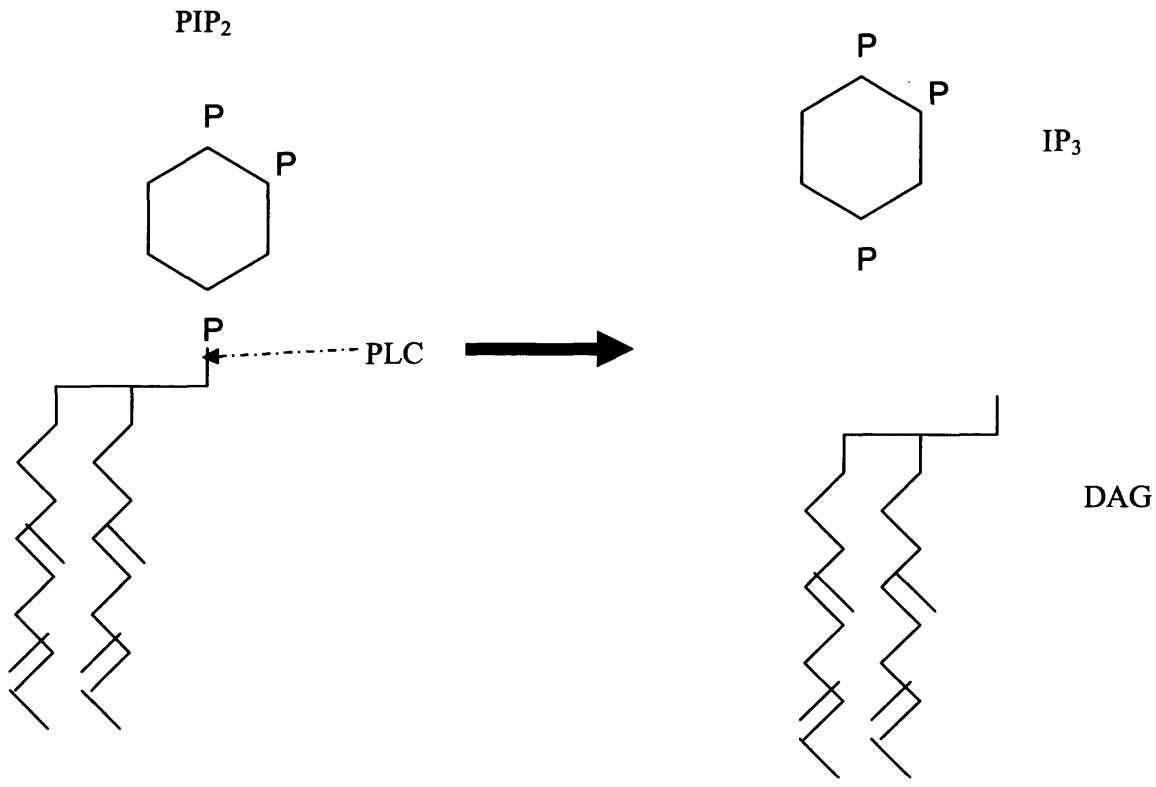

Figure 1.7.2 Cleavage of PIP_2 to Produce IP_3 and DAG

PIP_2 in membranes is cleaved by phospholipase C (PLC) to form IP_3 and diacylcgycerol (DAG), both of which can act as localised messengers in the cell.

The direct formation of IP_3 has also been reported for fMLP (Lew et al, 1986: Di Virgilio et al, 1985), with the rise in IP_3 level peaking at about 20-30 seconds after stimulation. In HL60 cells, IP_3 levels have been more clearly resolved. The increase in Ins(1,4,5)P_3 began at 5 seconds and was maximal at 10 seconds (Lew et al, 1986: Burgess et al, 1985). Surprisingly the level of IP_3 remained elevated for many minutes, returning to control level only after 2 minutes.

1.7.3 Phopholipase C ß and Phopholipase C γ

There are at least two forms of phospholipase C (PLC) in neutrophils, PLC-ß (Cockcroft, 1998) and the γ2 isoform of PLCγ (Krause et al, 1985: Hellberg et al, 1996) both of which are sensitive to the "PLC-inhibitor" U73122 (Hellberg et al, 1996). PLC-ß is activated by 7TM receptors and involves activation by heterotrimeric α β γ G-proteins. In neutrophils, it involves a pertussis toxin sensitive G protein, as this agent inhibits inositol signalling in neutrophils (Lad et al, 1985: Krause et al, 1985: Becker et al, 1985). In contrast, the mechanism for activation of PLC- γ is not fully established, but is probably triggered by tyrosine phosphorylation (Rhee et al, 1992). Tyrosine phosphorylation of PLC- γ 2 has been demonstrated to accompany CD32 (Dusi et al, 1994) and integrin β 2 cross-linking (Hellberg et al, 1996).

1.7.4 IP_3 Production and Ca^{2+} Signalling

One of the earliest demonstrations of the potential role of IP_3 as a molecule that signals the release of Ca^{2+} from stores in neutrophils was provided by Prentki, Wollheim and Lew (1984). Although IP_3 has no effect when added to normal neutrophils, when added the cells in which the plasma membrane was permeabilised, IP_3 caused an immediate release of Ca^{2+}. This indicated not only that IP_3 could release

Ca^{2+} from stores in neutrophils, but that its action was purely intracellular. The effect was specific for the Ins(1,4,5)P_3 isomer, suggesting that it would occur physiologically from the action of PLC on phosphatidyl inositol bis phosphate (PIP_2). Inhibition of IP_3 binding by the microinjection of heparin into intact human neutrophils has also been shown to inhibit fMLP-induced Ca^{2+} signalling (Davies-Cox et al, 2001). IP_3 is thus established as an intracellularly generated messenger for the release of Ca^{2+} from Ca^{2+} stores in neutrophils. However, while the evidence is strong for this being the physiological route utilised by 7TM receptor agonists, the evidence for the cross-linking stimuli is not secure. Cross-linking of surface CD32 receptors has been reported to mobilise Ca^{2+} without a detectable elevation of IP_3 (Rosales & Brown, 1992), and bromophenacyl bromide inhibits Ca^{2+} mobilisation by this cross-linking, but does not affect the release route by fMLP (Rosales et al, 1994: Davies & Hallett, 1995). Also cross-linking β2 integrins generates very little (if any) IP_3 compared to fMLP (Fallman et al, 1993).

1.7.5 PI-3-Kinase

PI-3-kinase activity increases during neutrophil activation, including during β2 integrin engagement (Lofgren et al, 1993). PI-3-kinase activity is triggered by the monomeric G-proteins p21ras and p21rho (Marshall 1995), and it subsequently activates another G-protein, p21rac. This sequence may have significance to neutrophil behaviour and, in addition, PI-3-kinase may be upstream of Ca^{2+} signalling triggered by cross-linking stimuli. This could be the alternative pathway from that used by 7TM receptor agonists.

1.8 Ca^{2+} Regulation of Neutrophil Function

As has been previously discussed, global Ca^{2+} signalling is known to accompany many neutrophil activities. Ca^{2+} has a biphasic signal during phagocytosis and is necessary for closure of the phagocytic cup. Interruption to this signal fatally interferes with the process, which is aborted by the neutrophil. Ca^{2+} accompanies engagement of integrins during settling of neutrophils onto CD38 coated coverslips. However, to date, these changes in global Ca^{2+} have been observed simply as corresponding events. Only phagocytic induced changes in Ca^{2+} have been studied in any depth. It remains unclear whether the global increases in Ca^{2+} are made up of sub-cellular signalling events and what the mechanism of inducing Ca^{2+} changes are. Neutrophils are notoriously difficult to study since they are small, active cells. Therefore, it would be necessary to image the Ca^{2+} changes rapidly and take advantage of technology such as micromanipulation in order to study these phenomena. Rapid imaging would also elucidate whether the changes in Ca^{2+} occur before, during or after corresponding changes in morphology, thus revealing whether the Ca^{2+} is causal or an effect of the particular neutrophil activity. This information would give insights to the mechanisms that drive neutrophil behaviour. For example, if Ca^{2+} rises before the neutrophil spreads out, it may be due to Ca^{2+} activation of actin-polymerisation pathways. Or, if the Ca^{2+} rises after the neutrophil spreads, the action of spreading may cause tension on the membrane resulting in an increase in channel opening or membrane leakiness. These are important distinctions to be able to make.

1.9 Aims of the Thesis

The foregoing summary of previous work investigating the relationship between localised and global Ca^{2+} signalling in neutrophils leads to the question of whether these phenomena are related to neutrophil behaviour. ***The main aim of the work presented in this thesis, therefore, was to investigate the roles of global and sub-cellular Ca^{2+} events in neutrophil shape change during cell spreading and phagocytosis.***

In order to achieve this main aim, it was necessary (i) to establish cytosolic free Ca^{2+} imaging conditions with sufficient speed and spatial resolution to detect rapid and localised sub-cellular Ca^{2+} events; (ii) to establish techniques for manipulating cytosolic free Ca^{2+} rapidly using photolytic uncaging of cytosolic caged IP_3; and (iii) to correlate cytosolic free Ca^{2+} changes with neutrophil morphology and dynamic shape changes. During the course of this work, it became obvious that the rapid sub-cellular Ca^{2+} "waves" reported by Petty's group, which were thought to be important in neutrophil signalling, were not detectable. Although it has now been admitted that the published reports by Petty's group are entirely fraudulent (Lebiedz, 2008 - personal communication), considerable time was lost in failing to demonstrate their existence. Despite this, the establishment of high speed confocal imaging of cytosolic free Ca^{2+} changes and photolytic uncaging of IP_3 have permitted the novel discovery of conventional (IP_3-generated) Ca^{2+} puffs in neutrophils and in establishing the relationship between global cytosolic free Ca^{2+} elevation and rapid neutrophil spreading.

CHAPTER 2

Materials and Methods

2.1 Materials

2.1.1 Reagents

Acridine Orange	Sigma Chemicals, Poole, U.K.
Bovine Serum Albumin (BSA)	Sigma Chemicals, Poole, U.K.
$CaCl_2$	Sigma Chemicals, Poole, U.K.
Caged-IP_3 salt	Invitrogen, Carlsbad, California, U.S.A.
Caged-IP_3-PM	Alexis Biochemical, U.S.A.
Calpeptin	Calbiochem, Nottingham, U.K.
CHO cells	European Cell Culture Collection
Cytochalasin B	Sigma Chemicals, Poole, U.K.
Dextran	Sigma Chemicals, Poole, U.K.
dimethyl sulphoxide (DMSO)	Sigma Chemicals, Poole, U.K.
DMEM	Flow Laboratories, Paisley, U.K.
EDTA	Sigma Chemicals, Poole, U.K.
EGTA	Sigma Chemicals, Poole, U.K.
Ficoll-Paque	Amersham Biosciences, Uppsala, Sweden
Fluo-4 salt	Invitrogen, Carlsbad, California, U.S.A.
Fluo-4-AM	Invitrogen, Carlsbad, California, U.S.A.
FMLP	Sigma Chemicals, Poole, U.K.
Fura-2 dextran	Molecular Probes, Eugene, Oregon, U.S.A.
Fura-2-AM	Invitrogen, Carlsbad, California, U.S.A.
Fura-2-AM	Molecular Probes, Eugene, Oregon, U.S.A.
Gly-Phe-B-Naphthalamide	Sigma Chemicals, Poole, U.K.
Heparin	CP Pharmaceuticals Ltd, Wrexham, U.K.
Hepes	Fisher Scientific, Leicester, U.K.
Hydrogen Peroxide (H_2O_2)	Sigma Chemicals, Poole, U.K.
Hydroxylamine	BDH Laboratory Supplies, Poole, U.K.
ICAM-1 antibody	Santa Cruz, Calne, UK
ICAM-1-GFP constructs (complete and tailless)	W. Luchikas, Harvard Medical School, U.S.A.
Ionomycin	Calbiochem, Nottingham, U.K.
KCl	Sigma Chemicals, Poole, U.K.
KH_2PO_4	Sigma Chemicals, Poole, U.K.
Lucifer yellow	Sigma Chemicals, Poole, U.K.
LY294002	Calbiochem, Nottingham, U.K.
Lysotracker	Invitrogen, Carlsbad, California, U.S.A.
Methanol	Fisher Scientific, Leicester, U.K.

$MgSO_4$	Sigma Chemicals, Poole, U.K.
Mitotracker	Invitrogen, Carlsbad, California, U.S.A
MOMO	Teflabs, Texas, USA
Na_2CO_3	BDH Laboratory Supplies, Poole, U.K.
Na_2HPO_4	Sigma Chemicals, Poole, U.K.
NaCl	Sigma Chemicals, Poole, U.K.
$NaHC0_3$	Fisher Scientific, Leicester, U.K.
NaOH	Sigma Chemicals, Poole, U.K.
$NiCl_2$	Sigma Chemicals, Poole, U.K.
Nitra-5 salt	Calbiochem, Nottingham, U.K.
PD 150606	Calbiochem, Nottingham, U.K.
Phosphate Buffer (pH6.8) tablets	BDH Laboratory Supplies, Poole, U.K.
Pluronic-F127	Molecular Probes, Eugene, Oregon, U.S.A.
Succimidyl ester of 2'7' dichlorodihydrofluorescein diacetate (DCDHF)	Molecular Probes, Eugene, Oregon, U.S.A.
Trypsin	Sigma Chemicals, Poole, U.K.
ZR cells	European Cell Culture Collection
Zymosan A	Sigma Chemicals, Poole, U.K.

2.1.2 Equipment

Eppendorf Injectman micromanipulator	Eppendorf, Hamburg, Germany
Eppendorf 5629 micromanipulator	Eppendorf, Hamburg, Germany
WPI micromanipulator	WPI, Florida, U.S.A.
Eppendorf Femtojet pressure controller	Eppendorf, Hamburg, Germany
Pre-pulled femtotips	
Phagocytosis - tip diameter 1μm	WPI, Stevenage, U.K.
SLAM - tip diameter 0.5μm	
Micropipette Puller P2000	Sutter Instruments, Novato, California, U.S.A.
Micropipette capillaries	Sutter Instruments, Novato, California, U.S.A.
Rapid monochromator - Delta RAM	PTI, Surbiton, U.K.
Nikon Eclipse inverted microscope	Nikon, Kingston-upon-Thames, U.K.
IC100 Intensified CCD camera	PTI, Surbiton, U.K.
Red sensitive camera	Watec, Tsuruoka-shi, Japan
LPS-220b lamp power supply	PTI, Surbiton, U.K.
Filters, dichroic mirrors	Omega Optical Inc Filters, Stanmore, U.K.
Beam Splitter	Cairn Research Instruments, Faversham, U.K.
Microscope stage heater	Linkam Scientific Instruments, Tadworth, U.K.
Video monitor	Sony, Basingstoke, U.K.
VHS video recorder	JVC, Cardiff, U.K.
CLSM Confocal microscope SP2	Leica, Milton Keynes, U.K.
Single 488nm line laser	Laser Physics, Milton Green, U.K.
ISIS Intensified CCD camera	Photonic Science Ltd, Robertsbridge, U.K.
Fluorimeter Fluolog 3	SPEX CertiPrep, Metuchen, Watford, U.K.
UV filter	Chroma Filters, Stanmore, UK

2.1.3 Software

Image Master 1.4b8	PTI, Surbiton, U.K.
Microsoft Excel 2000	Microsoft, Redmond, Washington, U.S.A.
Paintshop Pro Version 4.15 SE	Jasc Software Inc., Minnesota, U.S.A. Eden Prairie,
Microsoft PhotoEditor 3.0	Microsoft, Redmond, Washington, U.S.A.
Gif Animator (32-bit)	Alchemy Mindworks Inc., Ontario, Canada
HyperCam Version 1.34.00	Shareware
Microsoft Paint Version 5.1	Microsoft, Redmond, Washington, U.S.A.
Adobe Photoshop 7.0	Adobe Systems Inc, San Jose, California, U.S.A.
Microsoft Word 2002	Microsoft, Redmond, Washington, U.S.A.
Image J	NIH, Bethesda, U.S.A.

2.2 Buffer Composition

2.2.1 Balanced Salt Solution (BSS)

0.13 M NaCl

2.6 mM KCl

8 mM Na_2HPO_4

1.83 mM KH_2PO_4

Batches of 5 litres were made up by dissolving 40 g NaCl, 1 g KCl, 5.75 g Na_2HPO_4 and 1 g KH_2PO_4 in ddH_2O and adjusted to pH 7.4 with concentrated NaOH. 0.5 L aliquots were stored in sterile bottles until use.

2.2.2 HEPES Buffered Krebs Medium (Krebs)

120 mM NaCl

25 mM HEPES

4.8 mM KCl

1.2 mM KH_2PO_4

1.2 mM $MgSO_4.7H_2O$

1.3 mM $CaCl_2.2H_2O$ – *optional, inclusion assumed unless otherwise stated*

0.1 % Bovine Serum Albumin (BSA) – *optional, indicated by "(+BSA)"*

Stock solutions of each component were made up in ddH_2O and stored at -20 °C for all except NaCl and HEPES, which were kept at 4 °C. Stocks were as follows: 1.2 M NaCl (7.04 g/100 ml), 2.5 M HEPES (59.6 g/100 ml), 0.48 M KCl (3.58 g/100 ml), 0.12 M KH_2PO_4 (1.63 g/100 ml), 0.12 M $MgSO_4.7H_2O$ (2.95 g/100 ml), 0.13 M $CaCl_2.2H_2O$ (1.90 g/100 ml). BSA was made up to 10% w/v. NaCl was dispensed into 10 ml aliquots. BSA was dispensed in 100 µl aliquots. All other stock solutions were dispensed into 1ml aliquots. One of each aliquot was used to make 100 ml of Krebs.

N.B. The $CaCl_2$ was added when the solution had been made up to approximately 90% to prevent the formation of Ca_2PO_4. The medium was then adjusted to pH 7.4 with concentrated NaOH.

For Ca^{2+}-free Krebs medium (Ca^{2+}-free Krebs), no $CaCl_2$ was added to the medium. Instead 1 mM of the calcium chelator EGTA was added, thus retaining the osmolarity of the medium. This resulted in an estimated free Ca^{2+} concentration below 10 mM.

1 mM $NiCl_2$ was added to Krebs (+ BSA) in some experiments. Nickel blocks Ca^{2+} channels in the plasma membrane of cells and can be used to prevent influx of Ca^{2+} from Krebs containing Ca^{2+}.

2.3 General Methods

2.3.1 Isolation of Neutrophils From Whole Peripheral Human Blood

Neutrophils were isolated as previously described (Pettit & Hallett, 1998). Briefly, 10-20 ml of peripheral blood was taken from a healthy human volunteer using a needle and syringe and decanted into a universal container with 200 µl heparin. This was gently mixed by inversion with 25% v/v Dextran (6% 80 K, in BSS), i.e., 10 ml of blood was mixed with 2.5 ml of Dextran, 20 ml of blood with 5 ml Dextran. The blood was allowed to separate by sedimentation at room temperature for 30-50 min resulting in 3 distinct layers, represented in Fig 2.3.1.1. The middle "buffy" layer was removed carefully to avoid disturbing the erythrocytes or collecting too much of the top platelet-rich layer. The cells in this section were pelleted by centrifugation at 800 x g for 1 minute. Any contaminating erythrocytes were removed by hypotonic lysis. The pellet was resuspended in 1 ml of ddH2O for exactly 10 seconds. Osmolarity was restored by the addition of an excess of BSS, approximately 20 ml. The cells were repelleted by centrifuging at 800 x g for 30 seconds. The cells were resuspended in Krebs buffer containing BSA (0.1% w/v). This suspension was used for some experiments where it was necessary to have as many cells as possible without activating them by further isolation steps. This was especially applicable to single cell experiments where the morphologically distinct neutrophils could be identified from other monocytes, lymphocytes or eosinophils. However, when a purer sample of neutrophils was required a further separation step was used. This was another relative sedimentation step. The cells were resuspended in Krebs buffer (+BSA) and 3-5 ml of Ficoll-Paque medium was pipetted underneath the suspension. The Ficoll-Paque medium has a higher density than Krebs buffer (+BSA). Centrifugation at 400 x g for 20 minutes separated the cells according to their density. Fig 2.3.1.2 represents the

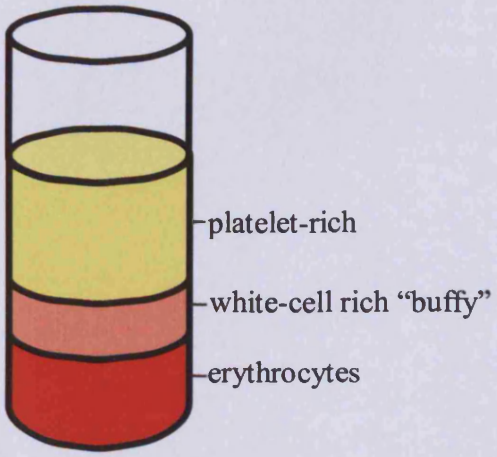

Fig 2.3.1.1 Distinct Layers or Sedimented Heparinised Blood

Heparinised blood (200 µl heparin/20 mls blood) was mixed with 5 mls 6 % dextran (80K in BSS) for 30-50 minutes until 3 distinct layers formed as above. The middle "buffy" layer is enriched for white blood cells.

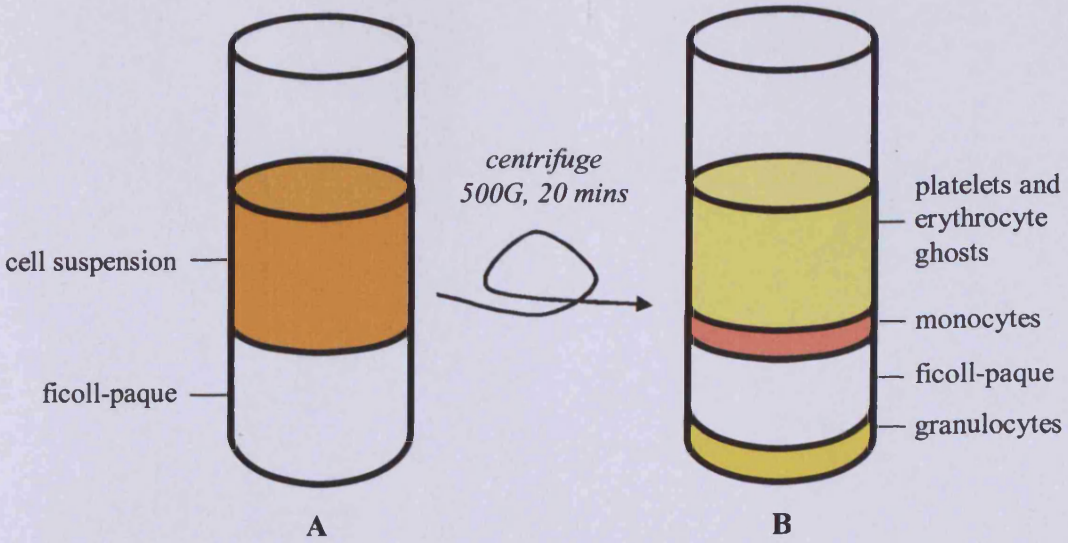

Fig 2.3.1.2 Sedimentation Through Ficoll-Paque

The "buffy" layer is spun down, contaminating erythrocytes removed by hypotonic lysis, and then resuspended in Krebs (+BSA). Ficoll-Paque medium is then gently pipetted underneath the cell suspension, as seen in (A). This is centrifuged for 20 mins resulting in (B) where 4 distinct layers are seen. The layer of interest at the bottom of the tube contains the pelleted cells. This is the neutrophil enriched section. It is necessary to be very gently in removing upper layers so as not to create vortexes between layers causing mixing.

layers before and after this centrifugation step. The Krebs (+BSA) contains most of the platelets and any erythrocyte ghosts remaining from the hypotonic lysis. The interface between Krebs (+BSA) and Ficoll-Paque retains the monocytes, which are dense enough to travel through the Krebs (+BSA) but do not have the density to migrate through the Ficoll-Paque. The granulocytes migrate through the Ficoll-Paque and pellet on the bottom of the centrifuge tube. The supernatants were carefully removed to avoid any mixing of the cell layers. The neutrophil-enriched granulocyte pellet was washed by resuspension in Krebs (+BSA), centrifugation at 800 x g for 30 seconds, and then resuspension in a final volume of 1-2 ml of Krebs (+BSA). The cell suspension was kept on ice until use.

2.3.2 Loading Neutrophils with Ester-Conjugates

Neutrophils were optimally loaded while in suspension in Krebs buffer. Stock solutions of the ester-conjugated molecules were made up to a concentration that allowed 1 µl of stock solution to be added to 1 ml of neutrophil suspension. As most of these molecules were made up in DMSO it was important to keep the stock concentration high so that the final amount of DMSO remained as low as possible – preferably below 1 %. Thus, having stocks that got diluted 1:1000 to the working concentration allowed the addition of multiple probes, each in DMSO, without affecting the viability of the neutrophils.

Fluo-4-AM was made up to 1 mM, Fura-2-AM 1 mM, MOMO-AM 1 mM, Mitotracker 5 mM, Lysotracker 5 mM, Acridine Orange (AO) 1 mM, caged-IP_3-AM 1 mM.

Loading occurred optimally at room temperature to ensure that the cellular esterases were active. Single loading times were as follows: Fluo-4-AM 40 min, Fura-2-AM 30 min, MOMO-AM 30 min, Mitotracker 10 min, Lysotracker 30 min, AO 2-5 min and caged-IP_3-AM 60 min (dark). When more than one probe was loaded for an experiment they were either loaded concurrently, such as with MOMO-AM and caged-IP_3-AM, or sequentially, such as caged-IP_3-AM and Fluo-4-AM. In this case the caged-IP_3-AM was loaded for 30 min before the Fluo-4-AM was added to ensure that sufficient caged-IP_3 was loaded into the cells.

Once the ester-conjugate is added to the cell suspension, it diffuses passively into the neutrophils. Once inside the cells the ester bonds are cleaved by non-specific esterases. This releases the native molecule, which no longer has an effect on the diffusion gradient of the ester-conjugated molecule. The ester-conjugated groups mask any charged moieties on the surface of the molecule and allow it to passively diffuse across the neutral plasma membrane. The native molecule is trapped inside the cell by its charge. Therefore, more of the ester-conjugate diffuses into the cell leading to accumulation of the molecule inside the cell. The concentration of the molecule within the cell ends up much higher than the concentration in the surrounding medium. This has the added benefit that the background fluorescence outside the cell is minimal. The process is represented in Fig 2.3.2.1 along with the structure of Fluo-4-AM.

2.3.3 Loading Neutrophils Via Microinjection

When it was not possible to load the neutrophils via ester-linked molecules, it was necessary to inject the molecule. This allowed higher concentrations of molecules of interest to be introduced into the cells. However, neutrophils have a complex

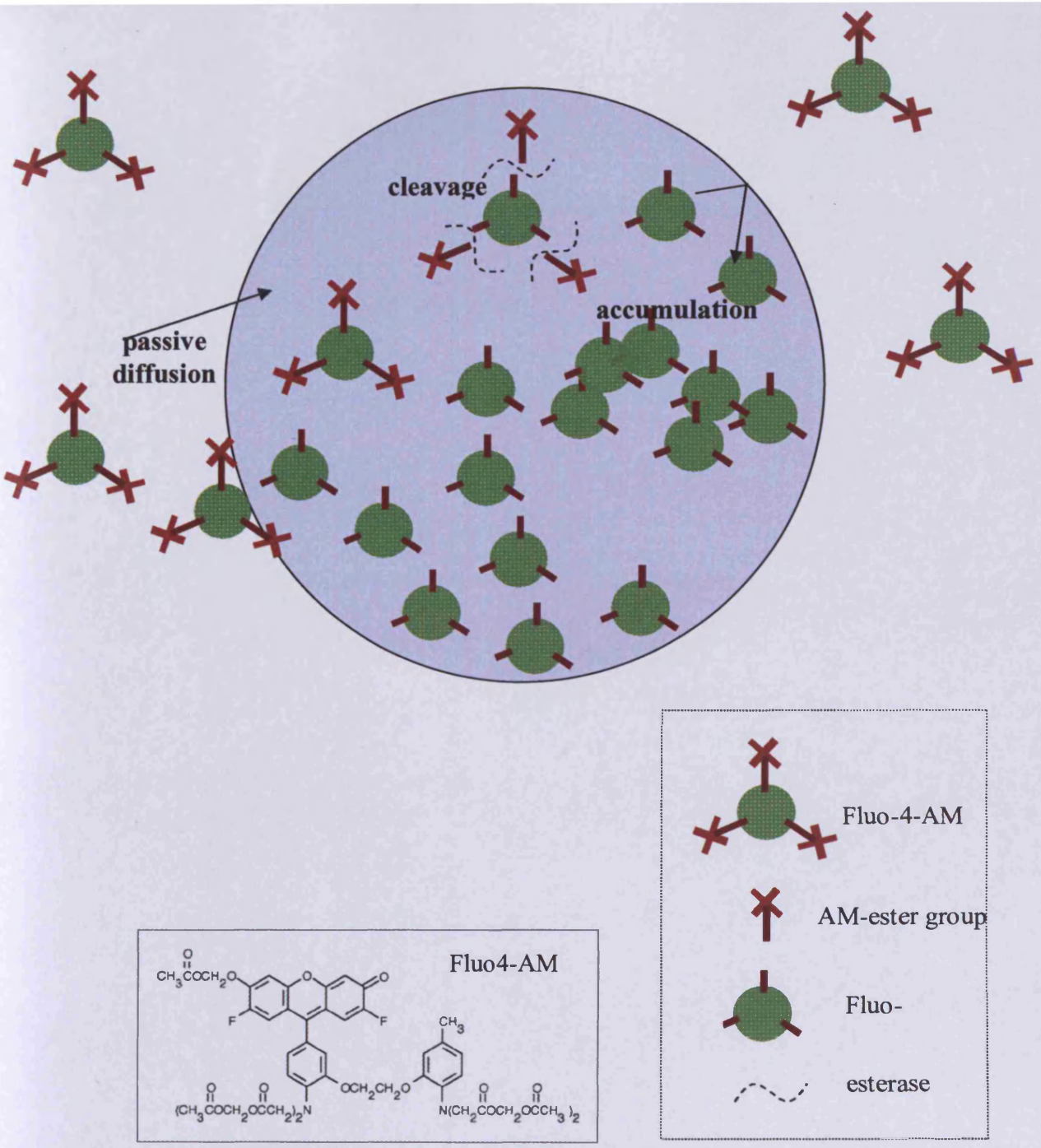

Fig 2.3.2.1 Ester-Conjugate Loading into Neutrophils

Fluo-4-AM is used here as an example of how ester-conjugated loading works. The Fluo-4-AM structure is shown in the box. It passively diffuses across the plasma membrane. Once inside the neutrophil, nonspecific esterases cleave the AM-ester groups releasing Fluo-4. Fluo-4 is charged and cannot cross the plasma membrane. Thus it does not act on the diffusion gradient of the Fluo-4-AM, which continues to diffuse across the membrane. This leads to accumulation of Fluo-4 inside the neutrophil, resulting in a much higher concentration of the molecule in the cytosol compared to the surrounding medium. This process is the same for loading other ester conjugated molecules.

intracellular structure. This makes them very difficult to inject. In most cases once the tip of the microinjection needle penetrates the plasma membrane the cell dies, thus becoming invalid for further study.

Fortunately, Iraj Laffafian has been able to develop a technique in our lab that enables microinjection without piercing the plasma membrane. This technique has been dubbed SLAM (Soft Lipid Assisted Microinjection). The tips of the microinjector pipettes are coated with phospholipid under argon gas. When the tip of one of these microinjector pipettes is placed on the surface of a cell the lipid on the pipette fuses with the lipid of the plasma membrane and this allows the contents of the pipette to be introduced into the cell. Gentle retraction of the pipette allows the plasma membrane to re-fuse without bursting the cell. This does not interfere with the underlying cytoskeleton of the neutrophil and therefore does not induce necrosis or apoptosis. Fig 2.3.3.1 illustrates the basics of this technique.

SLAM was employed when loading the cells with multiple compounds. Loading with ester-conjugated molecules results in by-products as the cellular non-specific esterases cleave off the ester groups and these can compromise the cellular functionality. Cells were also microinjected when it was not possible to obtain an ester-conjugated version of the probe or molecule of interest.

Microinjection requires highly concentrated stock solutions as the volume of the cell is small and therefore it is also only possible to inject tiny volumes, usually less than 10% of the cell volume, without causing decrease in cell viability.

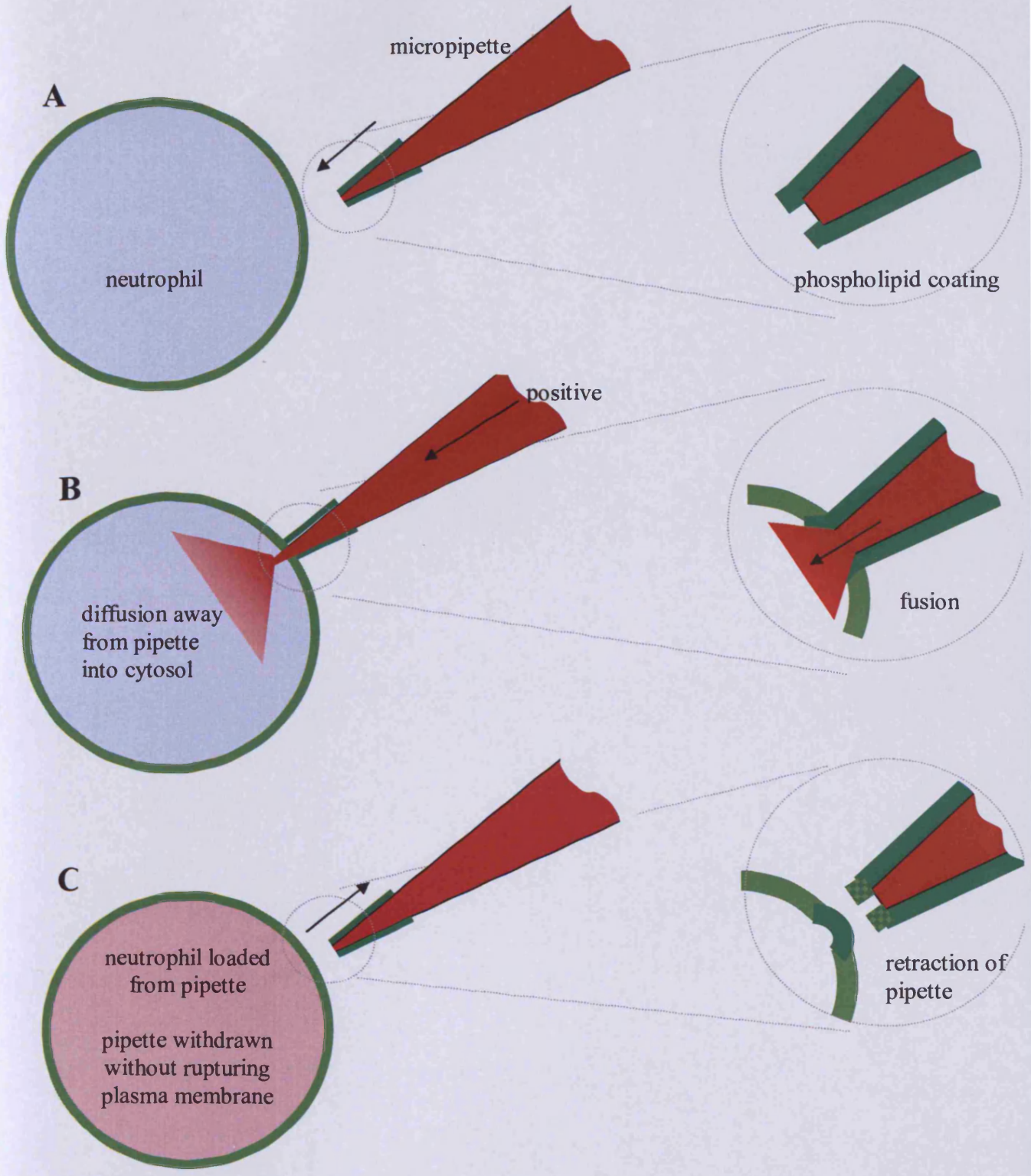

Fig 2.3.3.1 Soft Lipid Assisted Microinjection (SLAM)

This schematic representation of SLAM shows the phospholipid-coated micropipette (A), which is loaded with a high concentration stock of what is to be injected. Surface tension prevents leaking. The micropipette is brought into close contact with the neutrophil membrane. Fusion occurs (B) and the medium enters the cytosol. This requires positive pressure to overcome the capillary action acting in the opposite direction. Once sufficient medium has been injected into the neutrophil, the pipette is gently retracted (C). This allows the plasma membrane to reform on the neutrophil and leaves the micropipette coated ready to microinject another cell.

Micropipette tips were pulled in-house to approximately 0.1 μm diameter. The micropipette was loaded with 1-2 μl of the highly concentrated stock of the molecule to be injected. The micropipette was then attached to the pressure controller (Eppendorf Femtojet pressure controller) and a motorised manipulator for fine control. No pressure was applied at this stage. The tip of the microinjector was carefully aligned with the illumination field of the objective by eye and then more accurately positioned by fine movement viewed through the objective. This had to be done carefully to ensure the pipette tip did not crash into the glass coverslip, otherwise it would shatter. The objective was then refocused onto the plane where the neutrophils had adhered to the glass coverslip. The microinjector was slowly brought down into that focal plane and brought into contact with the surface of the neutrophil selected to be injected. The process was concurrently monitored by fluorescence of fluorescein. This revealed whether the contents of the microinjector were able to flow freely or whether it had become blocked. It also showed when fusion of the lipid coating on the SLAM pipette and the neutrophil plasma membrane occurred, as the fluorescein diffused into the cell. The pipette was then immediately withdrawn to prevent overloading or rupturing the neutrophil.

When the pipette became blocked it was withdrawn from the Krebs (+BSA) medium and cleaned by sending a pulse of positive pressure down the pipette, forcing some of the contents and the blockage out of the tip. To encourage close contact between the lipids on the SLAM pipette and the plasma membrane, negative pressure could be applied through the pipette. However, in most cases the inherent capillary action of the micropipette was sufficient to bring the plasma membrane into close contact with the micropipette. These changes in pressure had to be carefully controlled since too much

positive pressure would blow everything out of the field of view and, conversely, too much negative pressure would suck everything towards or into the pipette.

Experimental conditions were optimised to ensure a significant proportion of the neutrophils were adherent but not fully spread out, as spread out neutrophils become very thin and are nearly impossible to microinject without breaking either the neutrophil or the micropipette. Reducing spreading occasionally involved decreasing the temperature of the heated stage to 25 °C, or coating the glass coverslip with fibronectin. Spreading could be encouraged by treating the cells with a stimulant such as fMLP, however, most preparations of neutrophils would spontaneously spread if given sufficient time.

In experiments reported in this thesis, neutrophils were microinjected with caged-IP_3 (10 μM), Fluo-4 (1 μM), Nitra-5 (50 μM), and fluorescein. The fluorescein was added to the mixture when not microinjecting a fluophore because it fluoresces strongly even at low concentrations. This allows visualisation of successful microinjection and gives an indication of when the lipids on the surface of the SLAM pipette fuse with the plasma membrane. This helps prevent injection of large volumes or of assumption of successful microinjection when fusion has not actually occurred. However, fluorescein fluoresces most strongly at an excitation wavelength of 488 nm, which is the same as the Fluo-4 that is used to monitor Ca^{2+} concentration. The other Ca^{2+} probe most commonly used is Fura-2. However, this is excited at 340 nm and 380 nm, which are within the range for uncaging the caged IP_3 and caged Ca^{2+}. When it was necessary to monitor both the Ca^{2+} and uncage IP_3 or Ca^{2+} the problem of uncertainty of microinjection success was overcome by injecting many cells and observing changes

in the Ca^{2+} on exposure to UV light (360 nm). Those which had been successfully microinjected would respond with an increase in Ca^{2+}. Those injected with too much solution usually showed obvious morphological changes, such as the development of membrane blebs. These cells were discounted from experiments.

2.3.4 Measurement of Cytosolic Free Ca^{2+} in Neutrophils

The two most commonly used Ca^{2+} probes are fura-2 and Fluo-4. However, others used in this thesis include Fluo-3 and Calcium Red. They are all fluorescent probes whose fluorescence is changed by the binding of Ca^{2+}. They were loaded into neutrophils by the methods described above. All of these molecules are available in both the ester-conjugated form for passive loading and salt form for microinjection. It is possible to use these probes in neutrophils because neutrophils have an inherently large capacity for buffering Ca^{2+}. Therefore, the additional buffering effect of the chelating properties of these probes does not significantly increase the cellular buffering.

Once loaded, the neutrophils were allowed to settle onto and adhere to the glass coverslips. The Krebs (+BSA) medium and coverslip were maintained at 37 °C by a temperature controlled stage heater. Once the cells had adhered any non-adherent cells and any extra probe were gently washed away with room temperature Krebs (+BSA), ultimately adding back 100 μL of Krebs (+BSA) to cover the cells. The cells were then observed under microscopes according to which probes were being used in the experiment.

Fura-2

Fura-2 loaded cells were monitored using an inverted Nikon microscope with a 100 x objective oil-immersion lens. The Nikon microscope (Eclipse) is attached to a rapid monochromator. This rapidly changes the excitation beam from the high power light source between different specified wavelengths. The set up is represented in Fig 2.3.4.1. The rapid monochromator is necessary for the monitoring of Ca^{2+} by fura-2 because fura-2 is a ratiometric dye. Fura-2 exists in two different states – the Ca^{2+} free and Ca^{2+} bound states. Both of these states are fluorescent. However, the Ca^{2+} free state is maximally fluorescent at 380 nm, whilst the Ca^{2+} bound state is maximally fluorescent at 340 nm. These wavelengths are either side of the isoemissive point for the probe (see Fig 2.3.4.2). Both states emit at a wavelength of 505 nm. When the Ca^{2+} concentration increases in the cell the amount of fura-2-Ca^{2+} increases. This causes a marked increase in the emission of fluorescence when exciting at 340 nm and concurrent decrease in emission with excitation at 380 nm.

The images of emitted fluorescence were captured by an intensified CCD camera. The images of excitation at 340 nm and 380 nm were each captured and recorded by the computer. The computer then took a ratio of the emitted fluorescence from the two images to quantify changes in the Ca^{2+} concentration in the cell. The ratio eliminated any artefacts that could be created by differences in amount of probe in the cell or fura-2 rich organelles. An increased amount of probe would not change the ratio of Ca^{2+} bound to Ca^{2+} free. Therefore, when the ratio changed it could be considered a "real" change in the Ca^{2+} concentration, because the 340 nm signal increased while the 380 nm signal decreased (see Fig 2.3.4.2). Images were recorded over a time course during which the rapid monochromator allowed switching between 340 nm and

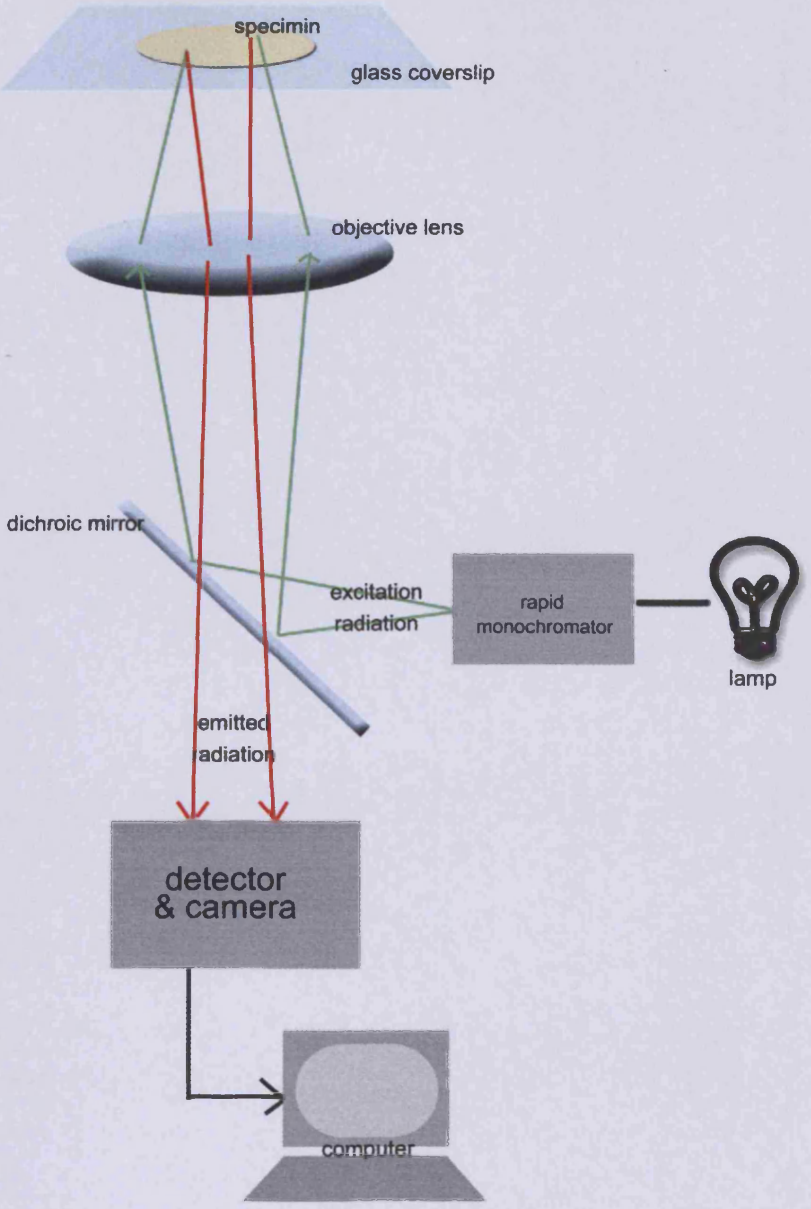

Fig 2.3.4.1 Set Up For Measuring Fura-2 on Nikon Eclipse Inverted Microscope

The cells are sedimented onto a glass coverslip. Light from the lamp passes through a rapid monochromator and a filter before being directed through the objective onto the sample by a dichroic mirror. Light emitted from the sample passes through the dichroic mirror to be detected by a high sensitivity camera. Light is collected from the whole wide field is detected by the detector. The signal from the camera is interpreted by the computer. A brightfield image is concurrently captured and recorded onto a VHS system.

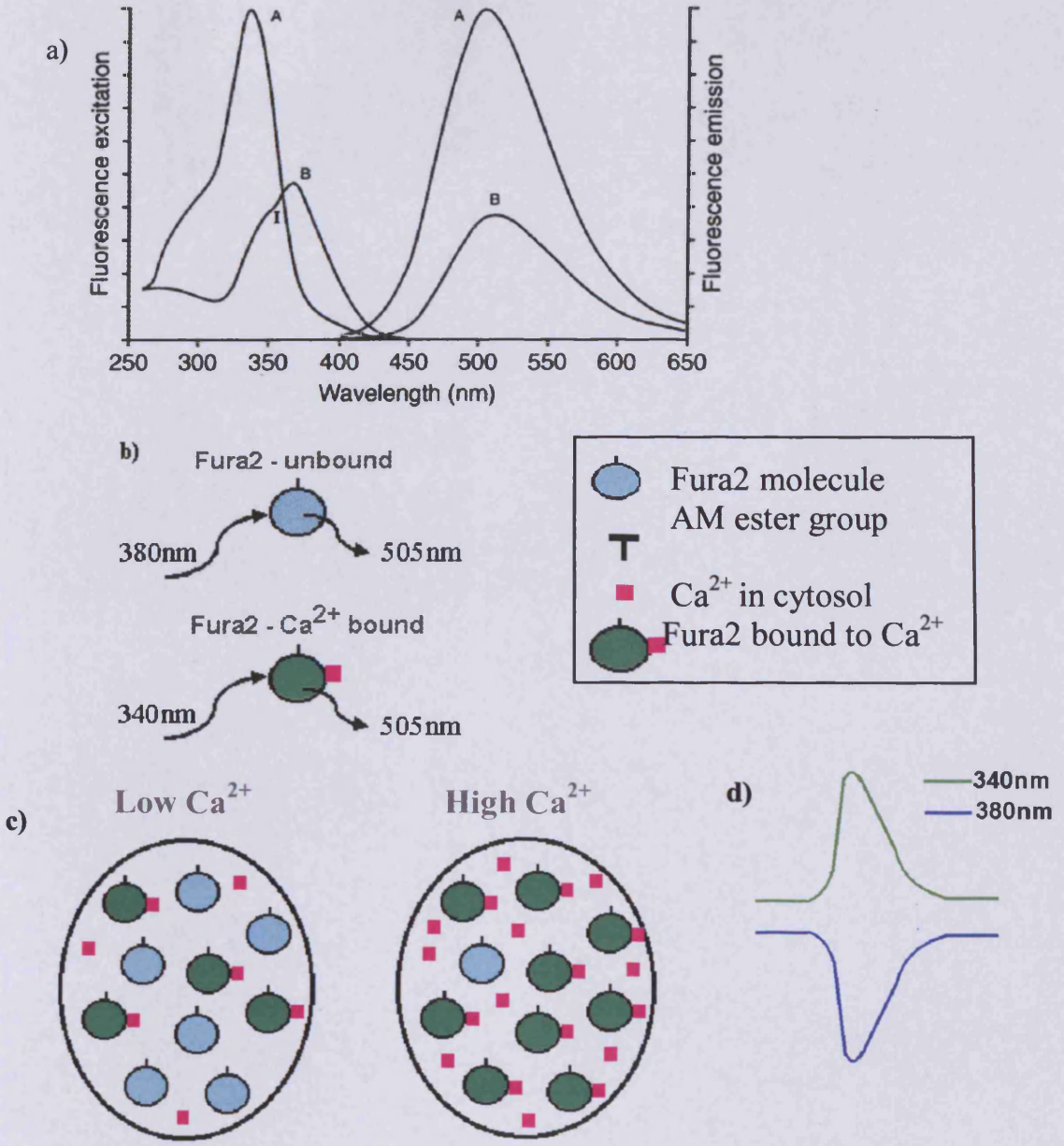

Fig 2.3.4.2 Fura-2 Functionality

Fura2 probe can be used to ratiometrically measure changes in the Ca^{2+} concentration in cells. (a) The excitation and emission spectra for Ca^{2+} bound fura2 (A) and Ca^{2+} free fura2 (B) is shown. The excitation spectrum for unbound fura2 displays a left shift when it binds to Ca^{2+}. Fluorescence of both states is detected at 505 nM. Two wavelengths are selected either side of the isoemissive point (I) to differentially excite the 2 states of the fura2 probe. (b) 380 nm is used to excite Ca^{2+}-free fura2 and 340 nm selected for Ca^{2+} saturated fura2. (c) Increasing Ca^{2+} results in an increase in the number of Ca^{2+}-bound-fura2 molecules at the expense of free fura2. (d) This causes a change in the detected fluorescence intensity for the 2 excitation wavelengths and can be measured as an increase in the ratio of 340/380 nm excitation.

380 nm. The computer calculated the ratio and gave a read-out of the bound:free (340/380) ratio as a single image.

Images were acquired with a 16-frame averaging and threshold background subtraction to reduce noise. This resulted in an acquisition rate of at least 0.6 frames/second (f/s). The ratiometric Ca^{2+} images were pseudo-coloured with an appropriate look up table (LUT). Changes in the ratio were observed and recorded during the application of stimuli to cells. In most cases a video was used to record the brightfield image at the same time, so as to observe any morphological changes or observe when microinjection/micromanipulation occurred.

Fluo-4

Fluo-4 loaded cells were observed on either the Nikon Eclipse (as for fura-2) or the inverted Leica confocal scanning microscope (LCSM) SP2. The LCSM used a 60 x oil immersion objective. The excitation radiation was provided by lasers with pre-specified wavelengths. The set up is represented in Fig 2.3.4.3. Unlike Fura-2, Fluo-4 is a single wavelength measurement for Ca^{2+} concentration. Fluo-4 with no Ca^{2+} bound is mildly fluorescent. When Ca^{2+} binds, the fluorescence markedly increases (see Fig 2.3.4.4). Fluo-4 is excited at 488 nm and emits at 550 nm. The emitted fluorescence is captured in a photo-multiplier tube (PMT). The PMT can be used to increase the gain from the signal, or the laser strength can be adjusted to increase or decrease the amount of exciting light the sample is exposed with. Fluo-4 is a relatively photo-stable molecule and did not significantly bleach during the course of the experiments undertaken. However, using a stronger laser beam and longer exposure times would break down the Fluo-4 resulting in decreased fluorescent signal.

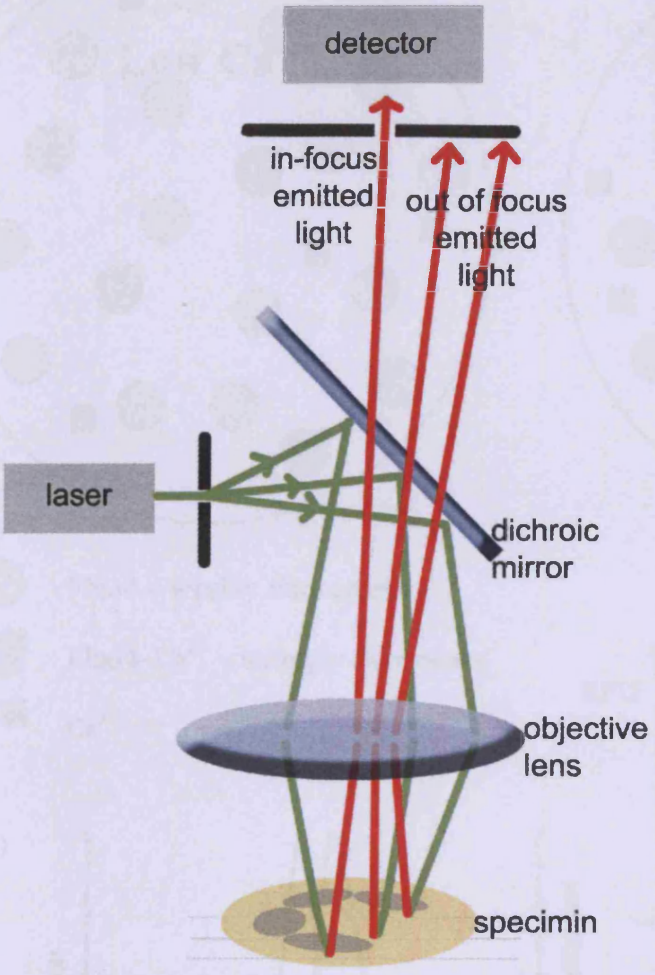

Fig 2.3.4.3 Set Up for Measuring Fluo-4 On Leica Resonance Scanning Laser Confocal Microscope, SP2

The SP2 is an inverted confocal microscope (inverse of what is shown above). A laser beam is passed through a resonant head that rapidly scans across the specimen from left to right (x-axis). The resonating head is mechanically moved up and down (y-axis) to pass the laser across the whole field of interest. The laser beam passes through a pinhole before a dichroic mirror reflects it through the objective onto the specimen. Emitted light passes through the dichroic mirror and encounters a second pinhole. Only light emitted from the focal plane passes through the pinhole, through a photo-multiplier tube to the detector. Out-of-focus light is not collected. Thus the term "confocal" since the light is effectively focused twice resulting in restriction of the depth of field.

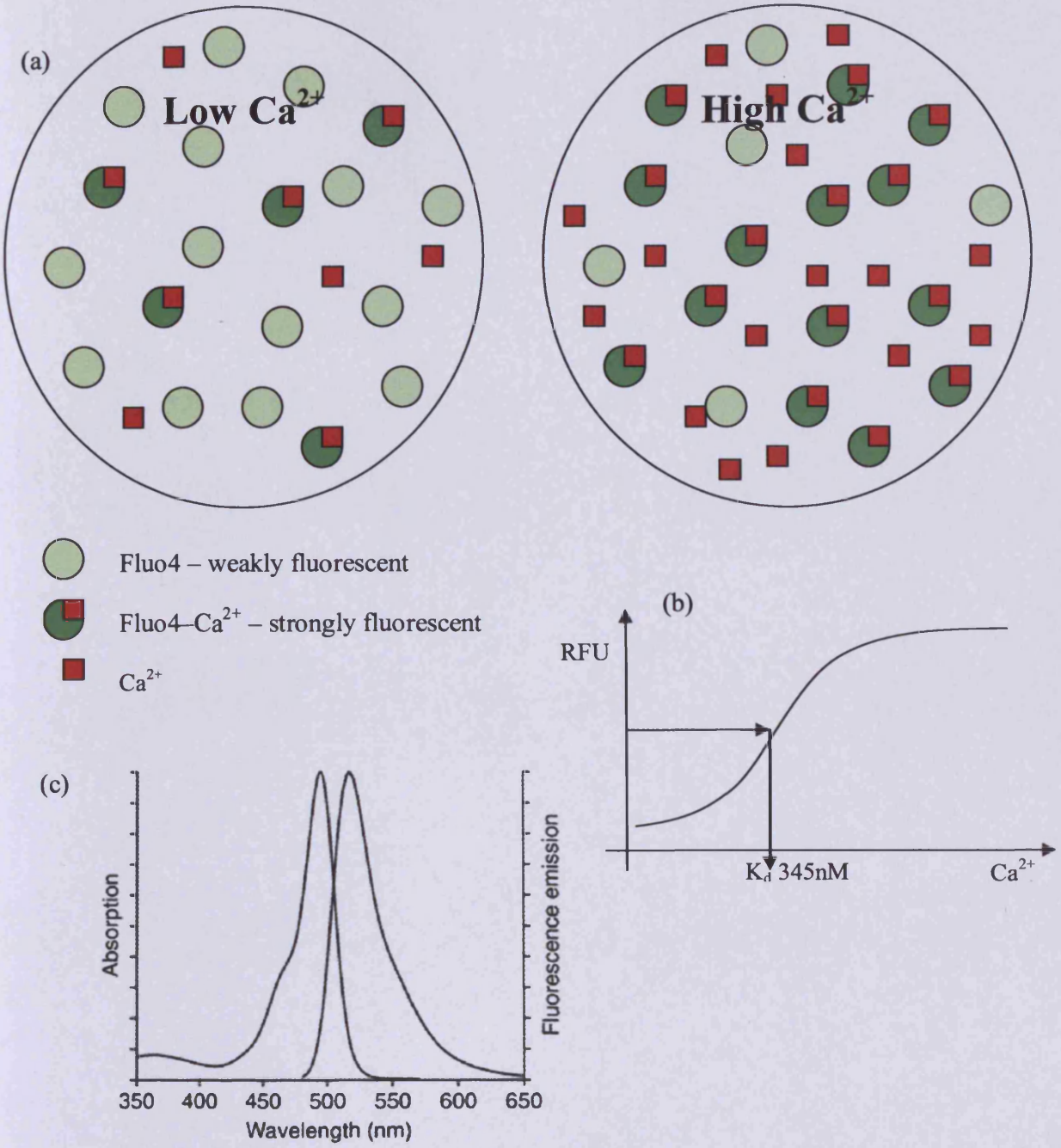

Fig 2.3.4.4 Functionality of Fluo-4

Fluorecence of Fluo4 increases when Ca^{2+} binds (a) with a Kd of 345 nM (b). The stokes shift from absorption to emission is sufficient for imaging (c).

The computer recorded the output from the PMT and the image was pseudo-coloured according to the intensity of the emitted light. Images were recorded over a time course during which the cells were stimulated. The LCSM allowed averaging to be used, but the resolution was much higher than on the Nikon. Therefore averaging of images was not normally applied. The acquisition time could also be greatly varied by many parameters as will be discussed in chapter 3. The speed usually used was 60 ms/frame giving approximately 15 frames/s. This allowed rapid subcellular Ca^{2+} events to be investigated in a level of detail that was not possible on the Nikon. Brightfield images were captured alongside the fluorescence images in a separate PMT. This allowed observation of changes in cell morphology due to the stimuli. The brightfield images were captured at the same rate as the fluorescent images.

2.3.5 Cell Culture

Most experiments were carried out with freshly isolated neutrophils from healthy volunteers. However, some experiments included the use of cultured cells. These included cells from the Chinese Hamster Ovary (CHO) line and ZR cells. 1 ml aliquots of frozen cells were rapidly thawed and reconstituted in 5 ml of warmed (37 °C) complete DMEM. They were allowed to grow to approximately 70 % confluence before being split. To split the cells the DMEM was aspirated and replaced with 1 ml of trypsin in EDTA for 5 minutes at 37 °C. Once the cells had detached from the flask, the trypsin was deactivated by adding back 5 ml of DMEM. Any remaining attached cells were washed off with repeated rinsing with the trypsin-DMEM mixture. The cell suspension was then centrifuged at 500 x g for 5 minutes to pellet the cells. The supernatant was removed and the cells were resuspended in DMEM. ZR cells can be split by scraping rather than using trypsin-EDTA. In this case the cells were gently

detached from the surface of the incubation flask with a cell scraper before being placed directly in a new flask. This method does not digest any of the cell surface proteins and is therefore preferred for any study including cell surface interactions. The cells were split at a ratio of 1:3 by area of the flask/wells and maintained in growth phase at a maximum of 80 % confluence.

2.3.6 Statistics

All experiments were carried out on at least three different occasions with neutrophils isolated from various different healthy blood donors by different members of the lab. Statistical significance is set at $p<0.05$ unless otherwise stated. All data shown is representative of at least three similar results.

CHAPTER 3

Optimisation of Rapid Optical Measurement of Cytosolic Free Calcium

3.1 Introduction

There have been many advances in microscopic techniques for investigating Ca^{2+} signalling in small cells such as neutrophils. These include the expansion of the family of fluorescent Ca^{2+} sensitive probes, with an increasing range of affinities for Ca^{2+} and excitation wavelengths (Tsien, 1989: Shaner et al, 2005). Advances in fluorescent microscopy have also increased both the temporal and spatial resolution of Ca^{2+} signalling detection, resulting in an increasing number of reports of subcellular Ca^{2+} events underlying larger Ca^{2+} waves and whole-cell concentration changes.

Despite increasing technical advances, it remains difficult to study Ca^{2+} signalling in smaller cells such as neutrophils. The small size of these cells (having a diameter of approximately 10 μm) dictates that sub-cellular signalling events are on the edge of the optical resolution cut-off. Despite this, there are reports of subcellular signalling events (Pettit & Hallett, 1996b) including the existence of an extremely localised zone of elevated Ca^{2+}, which travels around the neutrophil periphery (Kindzelskii & Petty, 2003). This travelling zone of high Ca^{2+} was reported to be present in unstimulated but polarised neutrophils, travelling in a "clockwise" direction around the cell at regular intervals of 20 seconds. This remains the only sub-cellular Ca^{2+} event reported in neutrophils to date. As these Ca^{2+} "z-waves" were detected only at very high speed imaging, progress in this area can only be made with both high spatial and temporal resolution. It was therefore necessary to optimise the existing imaging technology to permit high speed microscopy suitable for further study and characterisation of sub-cellular Ca^{2+} signalling events in neutrophils.

3.1.1 Confocal Microscopy

The traditional form of fluorescence microscopy, known as "wide-field" microscopy, excites and detects all fluorescent molecules within the cells. This allows visualisation of whole cells but necessarily results in blurring of objects not in the focal plane. These out-of-focus fluorescent objects can obscure the view of objects beneath them. This is especially significant when looking for very small objects, such as the sub-cellular Ca^{2+} events in small cells.

Confocal microscopy was developed as a solution to the "out of focus" problem by cutting out the light from objects outside of the focal plane. Since only light from a single optical plane is detected, confocal microscopy is a method of "optical sectioning". The microscope has two pinholes, one in front of the light source, usually a laser, and the other in front of the detector, usually a photomultiplier tube. Their position is such that only the excited and emitted light from the same focal point (the confocal point) is detected. The pinhole in front of the detector cuts out light emitted from anywhere except the defined focal plane in the sample, thus eliminating any out-of-focus objects or blurring that they induce (Fig 3.1.1).

3.1.2 Theory of Resonant Scanning Confocal Microscopy (RSCM)

Lasers are the preferred illumination source because they have well defined wavelengths and high power. The laser also produces a narrow beam, which can pass through the excitation pin hole. The laser beam must be scanned across the sample to illuminate the whole field. Most confocal microscopes use mirrors to steer the laser beam left and right, and up and down across the sample. The mirrors must be mechanically moved from left to right, and top to bottom to scan the laser beam across

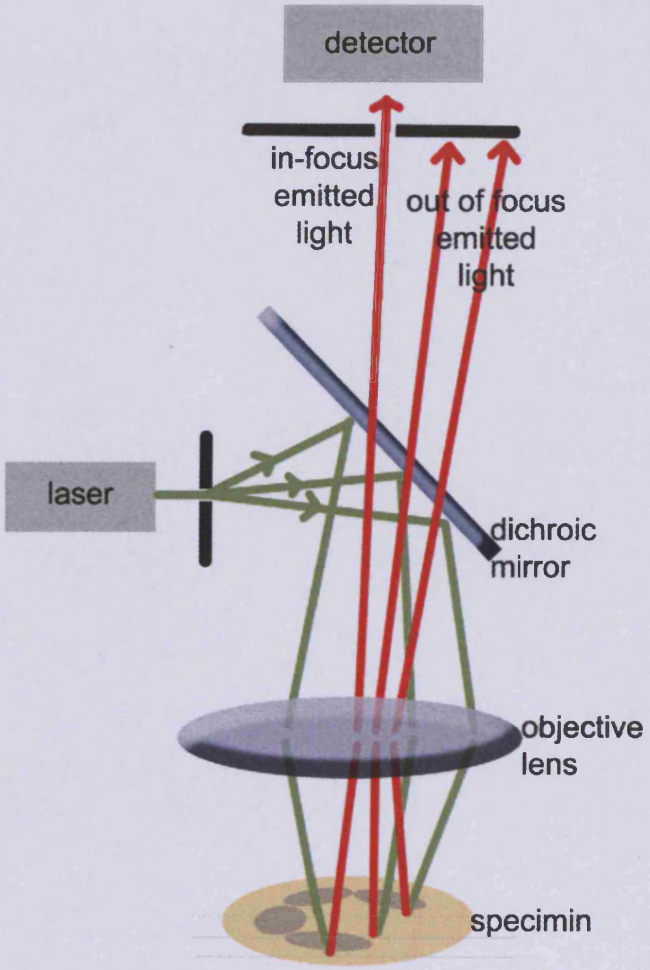

Fig 3.1.1 Ray Diagram of Confocal Microscope

Green lines represent excitable radiation from the laser. Red lines represent the emitted radiation from the specimen. Only light from the specified focal plane passes through the second pin-hole to the detector. (NB, the Leica SP2 system is an inverted version of this set up.)

the field of interest. This takes a significant amount of time, which limits the speed at which an image can be constructed. However, recent developments have included resonance scanners. The mirror is attached to a resonating mechanism, which causes the mirror to flip from side to side at a much higher speed. In the Leica SP2 confocal microscope used in this thesis, the mirror resonates left and right at 40 Hz. This resonating mirror is then mechanically moved down to pass the scanning laser over the field of view. Therefore, the acquisition time per frame is limited by the length of time it takes to move the mirror from the top of the field to the bottom and back again, rather than also being limited by the side-to-side action required in non-resonant scanning confocal microscopes.

The manufacturer's guidelines on estimated speeds indicate that it is possible to capture images at speeds of up to 29 frames per second (Table 3.1.1). However, it does not clarify whether these speeds produce usable images in experimental conditions suitable for measuring Ca^{2+} or other outputs that might be used.

3.1.3 Bidirectional Scanning Modes

The laser will excite molecules as it sweeps across the sample and these can be detected in the focal plane of the field of view. Conventionally, the signal is detected as the laser moves from left to right. However, the SP2 microscope also has the capacity to capture the fluorescence as the laser flicks back from right to left. If this data is recorded, this doubles the speed of acquisition as the mirror is only required to resonate half as many times to cover the same number of passes across the field. Leica indicate that it should be possible to capture twice the number of frames per second than with monodirectional scanning (Table 3.1.1). 29 frames per second in

Lines	512	256	128	64	32
Normal Scanning	4	5	9	16	29
x-bidirectional	7	9	19	32	58

Format	1024x1024	1024x512	1024x256	1024x128		
Normal Scanning	2	4	5	9		
x-bidirectional	5	7	9	19		

Format		512x512	512x256	512x128	512x64	512x32
Normal Scanning		4	5	9	16	29
x-bidirectional		7	9	19	32	58

Format			256x256	256x128	256x64	
Normal Scanning			5	9	16	
x-bidirectional			9	19	32	

Table 3.1.1 Leica Microsystems User Guidelines for TCS SP2 RS

Frame rate (frames acquired per second) depends on the number of lines scanned in the y-direction (see upper table "Lines"), and is independent of the distance covered in the x-direction as demonstrated in the lower "Format" tables, where there is no difference, for example, between 1024 x 256 and 256 x 256.

monodirectional mode becomes 58 frames per second in bidirectional mode. However, the speed that the beam moves forward and backwards is rarely the same, so the data collection in the two directions may not fully align. This is described as "out of phase". However, it is possible to manually adjust the phase of the images created.

3.1.4 Aims

The work reported in this chapter was a systematic investigation of the effect of software-controllable parameters on image acquisition rate. The aim was to establish the optimal settings for maximum usable imaging speeds.

3.2 Results

3.2.1 Optimisation of High Speed Scanning Using RSCM

As the Leica SP2 had many user-definable variables, it was necessary to establish the effect of each of these on the acquisition time per frame. Each variable was examined separately and the time required to acquire a series of images recorded. The time per frame was calculated and the effect of each variable thereby established. Neither the zoom function nor any parameter affecting the x-axis had any effect on image speed (Table 3.2.1). Presumably this was because the resonant scanning head moves the whole x direction regardless of the acquisition parameter set. However, there were profound effects when adjusting the size of the acquisition image in the y direction (Table 3.2.2). This was explained by the time required for the mechanical movement of the mirrors in the y direction being reduced when the distance to be covered was decreased. There was also a profound effect when using bidirectional acquisition rather than monodirectionality (Fig 3.2.1). With a minimum usable image size, the maximum acquisition rate was 17 ms/frame (Table 3.2.2). This is equivalent to the speeds given by Leica (Table 3.1.1) who state that it should be possible to achieve 58 frames per second, which would give a rate of 17.2 ms/frame in bidirectional mode.

It was important to establish whether these speeds would yield usable cytosolic free Ca^{2+} measurements. The effect of recording cytosolic free Ca^{2+} changes in response to a stimulus (fMLP) at different frame acquisition rates was therefore examined (Fig 3.2.2). It was possible to use the maximum rate for this and there was no obvious time distortion introduced. At frame rates from 1 frame/17 ms to 1 frame/100 ms, the recorded Ca^{2+} changes were similar and had identical rates of "up-phases" (Fig 3.2.2).

Variable	Does altering this variable affect acquisition time?	Comments
Zoom	No	
Pinhole size	No	
x-axis	No	
y-axis	***Yes***	***See table 3.2.2***
Line average	Yes	Increases time required for frame proportionally to the number of lines averaged
Frame average	Yes	Increases time required for frame proportionally to the number of frames averaged. (Can not be used in conjunction with frame stacking)
Stack	Yes	Increases time required for frame proportionally to the number of frames stacked. (Can not be used in conjunction with frame averaging)
Mono-/Bi-directional	***Yes***	***See table 3.2.2***

Table 3.2.1 Effect of User-Definable Variables on Leica SP2 Confocal Microscope

x (pixels)	y (pixels)	Mono- or Bi-directional scanning	Time (milliseconds per frame)
512	512	Mono	282
		Bi	141
512	256	Mono	215
		Bi	107
512	128	Mono	107
		Bi	53
512	64	Mono	62
		Bi	31
512	32	Mono	34
		Bi	17

Table 3.2.2 Effect of Y-Axis Size and Scanning Mode on Acquisition Speed

The table shows the time (milliseconds) required to record each frame as it varies according to the value of the y-axis and whether the laser scans mono- or bi-directionally.

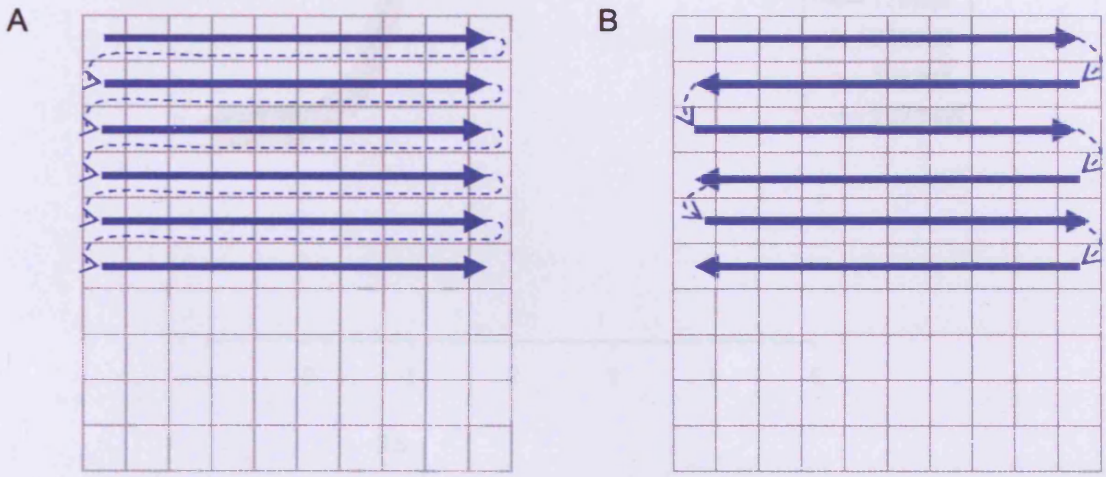

Fig 3.2.1 Confocal Scanning Methods

Schematic representations of monodirectional (A) and bidirectional (B) data acquisition modes. It is seen that the bidirectional mode acquires data on both the forward and backward sweeps of the laser. This halves the number of times the laser must scan the field of view to capture the same number of pixels and therefore increases the speed at which images can be acquired.

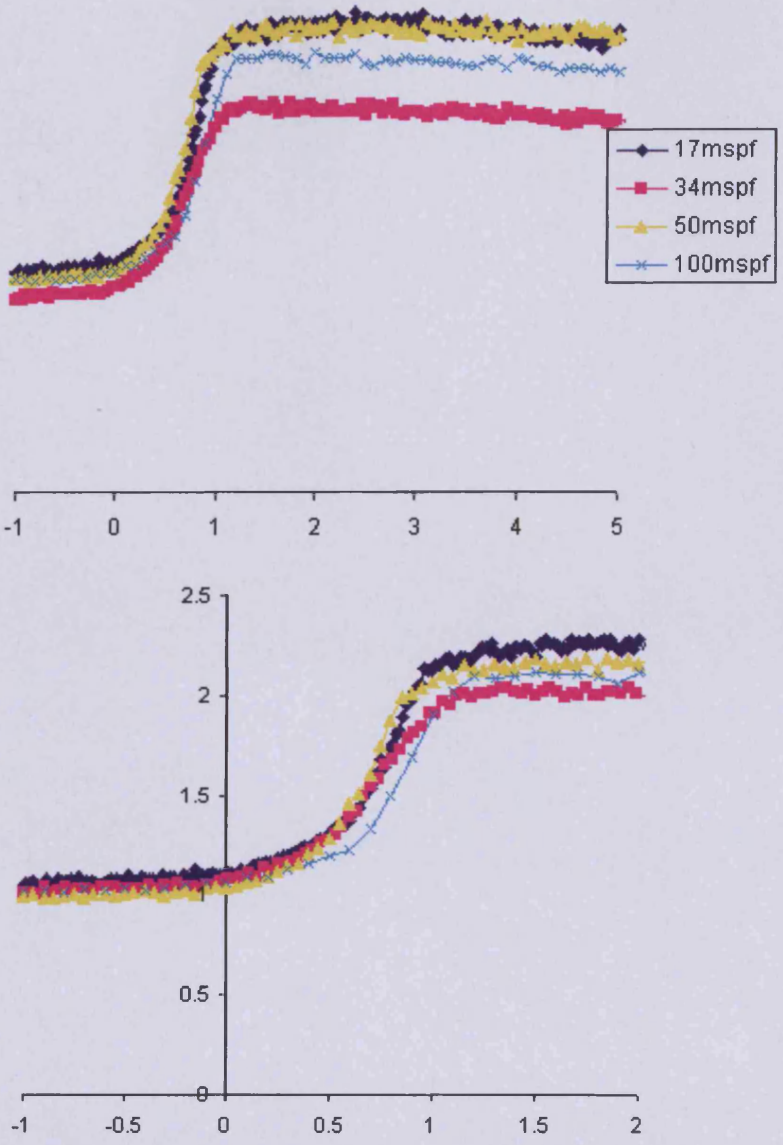

Fig 3.2.2 Increasing Acquisition Rate Does Not Reduce Quality of Data Set

The graphs show the increases in Fluo-4 fluorescence as an indicator of cytosolic free Ca^{2+} in neutrophils stimulated at time zero with fMLP using different acquisition rates. Each data set is from a different neutrophil representative of at least 5 others measured. The upper set of data shows the raw intensity increase over 6 seconds, whereas the lower graph shows the data as a fraction of the stimulation level. There are significantly fewer data points in the trace with the slower acquisition speed of 100 ms/frame compared to 17 ms/frame. Therefore rapid changes can be more clearly dissected out by using faster acquisition times without significantly compromising the quality of the data collected. (x axis time, y axis Ca^{2+} in RFU)

It was therefore concluded that the higher frame rates could provide Ca^{2+} data that was similar to those reported at slower frame rates and so would be capable of capturing cellular events faster than previously recorded.

It was also necessary to determine whether the quality of images acquired at these high speeds was too severely compromised to detect Ca^{2+} events that occur on a subcellular level, i.e., less than the whole cytoplasm involved. Images acquired at different speeds on the same cells are shown in Fig 3.2.4. It is clear that increasing the acquisition rate results in deterioration of the image. This higher level of background noise must be taken into account when interpreting experimental data and defining parameters of subcellular events, as it may be difficult to dissect real signal from experimental noise.

3.2.2 Is Rapid Scanning Confocal Imaging Fast Enough?

The scanner head resonator frequency is 4000 MHz, equivalent to 250 μs/cycle or 8000 bidirectional lines/s. So the theoretical minimum for one line is 125 μs of bidirectional scanning. However, in practice this could not be achieved. With an object size of 160 μm across x 10 μm down presented as an image size of 512 x 32 pixels, each pixel represents 0.3125 x 0.3125 μm. From the work presented earlier, the minimum time to capture a bidirectional image was 17 ms. Each laser line must therefore take 531 μs. Thus for each scan line there is 406 μs of dead time, which includes the computer time required to write the data to memory and mechanical effects relating to the mirror positioning. The maximum speed for "up-down imaging" is 10 μm per 17 ms, i.e., 588 μm/s. The maximum speed for "left-right imaging" is 2 x 160 μm per 530 μs, i.e., 0.6 μm/μs (1 μm /1.67 μs).

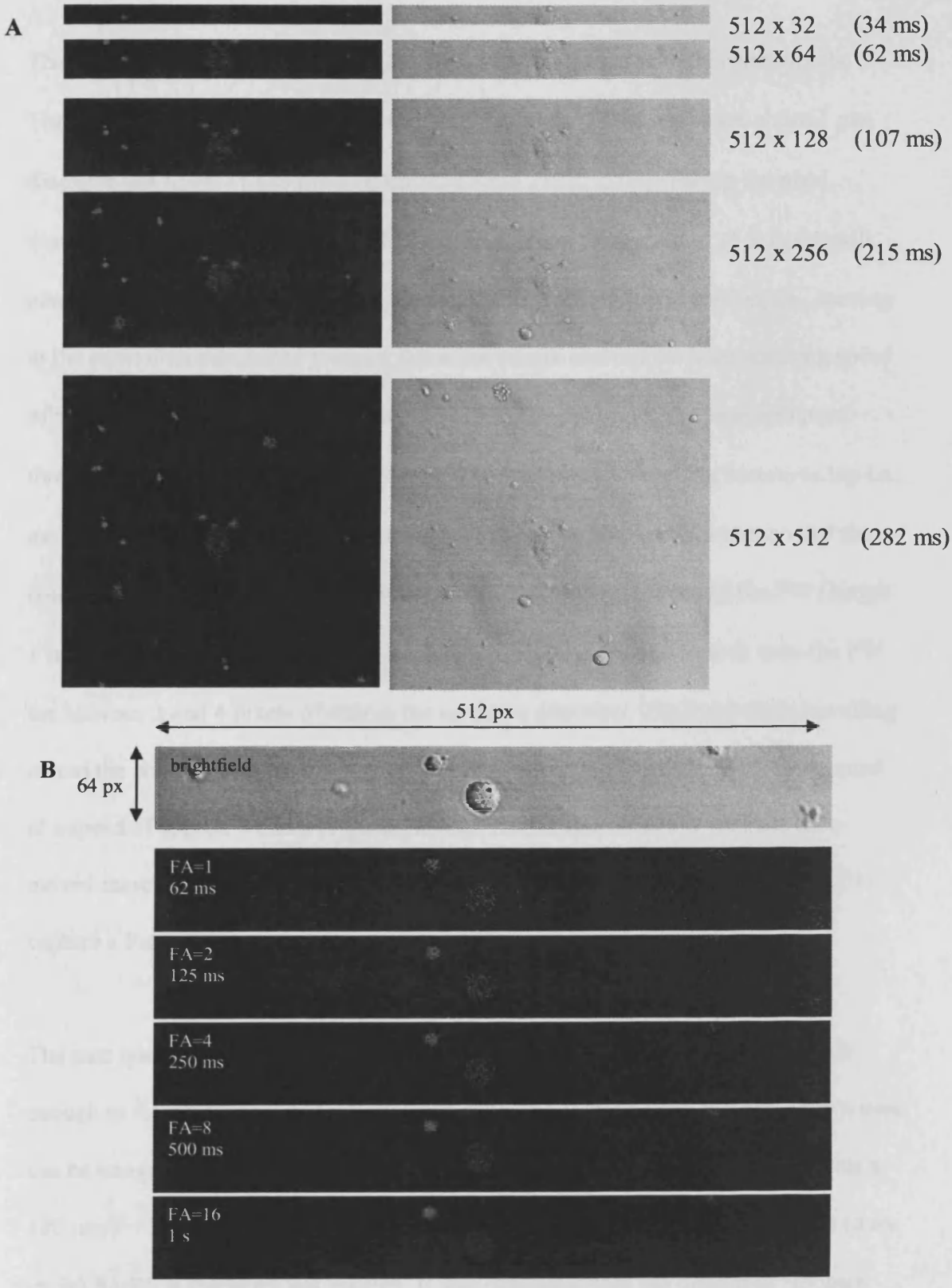

Fig 3.2.3 Increasing Acquisition Speed Decreases Image Quality and Resolution

Images were acquired from the same cells at different speeds determined by (A) frame size and (B) frame averaging (FA) as indicated.

These speeds must be compared to the fastest Ca^{2+} events reported in neutrophils. These are the "Ca^{2+} waves" reported by Petty's group. These waves are about 1 μm diameter and travel at 180 μm/s (Kindzelskii and Petty, 2003). Taking the pixel dimension calculated earlier as 0.3125 x 0.3125 μm, a "Petty wave" (1 x 1 μm) will occupy about 3 x 3 pixels. The Petty wave (PW) travelling top to bottom, i.e., moving in the same direction as the scanner, therefore cannot out-run the laser scanning speed of 588 μm/s. With a combined speed of 588 - 180 = 408 μm/s, the laser will pass through the PW (length 1 μm) in 2.45 ms. The Petty wave travelling bottom to top i.e., moving in the opposite direction to the scanner, crosses the laser scanner so that the combined speed is 588 + 180 = 768 μm/s. The laser will pass through the PW (length 1 μm) in 1.3 ms. As each laser line takes 530 μs there is enough time to scan the PW for between 2 and 4 pixels of data in the up-down direction. The Petty wave travelling across the cell in either the direction of the laser scanner or against it will be scanned at a speed of approx 0.6 m/s (1 pixel/500 ns). At this speed the PW will not have moved more than 1 pixel, i.e., $4x10^{-12}$ m. So the imaging speed is sufficiently fast to capture a Petty wave.

The next question is whether the resonance scanning (RS) image frequency is fast enough to follow a wave as it moves around the cell. It is reported that the Petty waves can be imaged at 20-30 ms frequency (duty cycle) when the wave moves by 20 ms x 180 μm/s = 3.6 μm (at exposures of less than 200 μs). The time between images (duty cycle) for RS is therefore fast enough. It was concluded that the optimised resonant scanning system would be fast enough to capture and faithfully record the fastest events known.

3.3 Discussion

The conditions for fast data acquisition have been defined. However, the speed at which the images are acquired necessarily reduces the image quality. At very high speeds the laser illuminates any given area for a very short period of time. Therefore, fewer photons of light are shone on the fluorescent sample, and fewer are emitted. This can decrease the resolution, resulting in a "dottier" image. This can later be compensated for *in silico* with blurring and smoothing to produce more satisfying images when looking at a larger scale. However, when looking for small Ca^{2+} events it is confusing to have a pixelated image where bright dots may be mistaken for Ca^{2+} puffs. Therefore, a lot of time was put into getting the balance between speed, image size (to encompass the whole cell in the field of acquisition), and resolution. This was achieved by using a slightly stronger laser beam than usually used, resulting in more excitation photons. The frame size was 125 x 512 pixels, giving an acquisition time of 63 ms per frame in monodirectional mode.

In the experiments performed by Petty et al (Kindzelskii & Petty, 2003), wide field illumination was used. There are some differences between this and laser scanning. For example, (i) only the area of cell under the laser point is interrogated so "exposure time" is always short; and (ii) fluorescence in other areas of cells (away from laser beam) cannot contribute to the signal.

As the fluorescence lifetime of Fluo-4 is about 1-10 ns, this represents an ultimate limit to imaging speed. In other words at 10 ns half time, a single molecule can emit only 100 photons in a μs. At this emission rate the image quality would be extremely poor and unlikely to yield usable images.

Since there is a link between speed and spatial resolution, we should consider whether "exposure times" will be fast enough to resolve those Ca^{2+} events which are small in size. The region of the Petty wave (Kindzelskii and Petty, 2003) i.e. 1 μm from the cell "edge" and about 1 μm long, will be interrogated (i) by the left-right sweep of the laser in 1.67 μsec, and (ii) by the up-down sweep in 1.7 ms. This is equivalent to a left-right "exposure time" of 1,670 ns for a section through the Petty waves and the next time the section is interrogated is 34 (or 17) ms later (duty cycle). Thus the left-right exposure time is fast enough.

3.4 Conclusion

In this chapter the conditions needed for maximum image acquisition have been defined. The fully optimised resonant scanning confocal microscopy system has a maximum usable speed of 17 ms/image. In order to achieve this speed image quality is compromised. The important variables for optimising speed and image quality were the frame size and the line averaging. With these optimised this system has sufficient temporal and spatial resolution to detect the sub-cellular Ca^{2+} events such as the z-waves reported by Petty *et al.* (Kindzelskii & Petty, 2003). In subsequent chapters the optimised resonant scanning system will therefore be used as the primary technique for further study of these events.

CHAPTER 4

Rapid and Localised Ca^{2+} Microevents in Neutrophils

4.1 Introduction

In a number of cell types, it has been established that there are elemental events that underlie many Ca^{2+} signals. These include localised Ca^{2+} events which are restricted to broad regions of the cell, such as the granular cytoplasm of pancreatic acinar cells (Petersen, 2005: Osipchuk, 1990: Thorn, 1993) and those restricted to subdomains within the cells, such as Ca^{2+} sparks and puffs (Niggli, 1999). The latter can be best visualised when Ca^{2+} is released from storage sites in muscle cells and oocytes (Parker, 1996) and there are surprisingly few reports of similar micro-events in small and non-excitable cells. The best characterised Ca^{2+} puff events in small cells are probably in HeLa cells (Bootman et al, 1997: Thomas et al, 2000: Tovey, 2001) and in a rat basophilic cell line (Horne et al, 1997).

The scarcity of reported Ca^{2+} puff events in smaller non-excitable cells may be due to (i) the technical difficulties in rapid Ca^{2+} imaging in small cells or (ii) the absence or attenuation of such signals resulting from the higher density or closer proximity of organelles, which release, sequester or impede diffusion of Ca^{2+} ions. Human neutrophils, however, have a "simplified" microanatomy with few mitochondria and only a single "vestigial" ER/Golgi organelle near the multi-lobed nucleus (Bessis, 1973: Schmid-Schonbein et al, 1980) should be beneficial in detecting these localised Ca^{2+} micro-events. It is therefore intriguing that conventional Ca^{2+} release "puffs" were reportedly absent in this cell type (Kindzelskii and Petty, 2003:2005a,b: Kindzelskii et al, 2004) and replaced by extremely localised and circularly mobile zones of elevated Ca^{2+} (called here zonal or z-waves). Using ultrafast non-confocal fluorescent imaging of indo-1 loaded neutrophils with acquisition times of 50 nsec, Petty's group reported that there is an extremely localised zone of elevated Ca^{2+},

which travels around the periphery of unstimulated, polarised neutrophils in a "clockwise" direction at regular intervals of 20 seconds (Kindzelskii and Petty, 2003, 2005: Kindzelskii et al, 2004). When stimulated with the IP_3-generating, G-protein linked receptor agonist, formylated-methyl-leucyl-phenylalanine (fMLP), the "z-wave" is reported to split into two opposite travelling zones. This group found no other Ca^{2+} signals in neutrophils, such as conventional stationary Ca^{2+} puffs or global cytosolic changes. The group have also reported that Ca^{2+} z-waves underlie regular Ca^{2+} spiking in a number of cell types with different micro-anatomical layouts, including CHO cells (Worth et al, 2003) and HT1080 fibrosarcoma cells (Huang et al, 2004).

4.1.1 Aims

These data obviously present a major challenge to the conventional views of Ca^{2+} signal generation. Since neutrophils are the cell-type in which Ca^{2+} z-waves but not conventional Ca^{2+} signalling have been most commonly reported by this group (Kindzelskii & Petty, 2003, 2005: Kindzelskii et al, 2004), it is possible that the neutrophil micro-anatomy may play a part in this type of Ca^{2+} signalling. The initial aim of the work presented in this chapter was therefore to extend the characterisation of the reported Ca^{2+} z-waves in neutrophils and to correlate them with the location of organelles within the cell. However, in contrast to the reports from Petty's group, "conventional" stationary Ca^{2+} "puffs" and global Ca^{2+} signals in neutrophils were discovered but there was no evidence for Ca^{2+} z-waves.

4.2 Methods

4.2.1 Uncaging IP_3 In Neutrophils, Adherent and In Suspension

It is important to understand the theoretical basis for the photolytic uncaging molecules, and more specifically IP_3.

4.2.1.1 Theory of IP_3 Uncaging

IP_3 forms a central part of the Ca^{2+} signalling cascade in neutrophils. Many of the extracellular stimuli result in the activation of phospholipase C, either β or γ isoforms. Both enzymes cleave $PI(4,5)P_2$ to produce IP_3 and diacylglycerol (DAG). The IP_3 is thus liberated from the PIP_2 in the plasma membrane and is free to diffuse into the cytoplasm and bind with the IP_3 receptor (IP_3R) on the surface of the intracellular Ca^{2+} store, inducing the release of Ca^{2+} from the store. As this store empties it induced Ca^{2+} channels to open in the plasma membrane and Ca^{2+} from the extracellular medium flows in. Thus inducing changes in IP_3 concentration will produce physiologically relevant Ca^{2+} events. Also, this initial release of Ca^{2+} from the store is amplified by the store-operated Ca^{2+} influx route so that a small change in the cytosolic IP_3 concentration will induce large changes in the concentration of Ca^{2+}.

IP_3 has a very short half life inside cells as the three phosphate groups make it a highly reactive molecule. Therefore, introducing IP_3 into the cells requires masking the reactivity of these groups. This is achieved with a molecular cage on each of the three phosphate groups. This caged molecule is introduced into neutrophils in an ester-linked propyl-methoxyl form, which allows passive diffusion of the molecule into the cells across the lipid rich plasma membrane. Once inside the cells, non-specific esterases cleave off the ester-linked groups. This traps the molecule inside the cell and

means it no longer acts on the diffusion gradient, resulting in accumulation of the caged molecule within the cell. The bonds attaching the cage are UV sensitive. Previous photolytic uncaging of fluorescein by UV irradiation indicated that there is no significant delay in uncaging and that uncaging is not hindered by the intracellular structure but appears to occur uniformly across the cell.

The changes in the molecular structure from the caged IP_3 PM result in the generation of biologically active IP_3 molecule, which is free to bind to IP_3 receptors (IP_3R) and cause physiological responses.

4.2.1.2 Practice of IP_3 Uncaging

Neutrophils were loaded with caged-IP_3-PM in suspension for 30 mins. This allowed sufficient accumulation within the neutrophil for uncaging to release enough IP_3 to induce Ca^{2+} signalling events.

Caged-IP_3 loaded neutrophils were allowed to settle onto a glass coverslip on a temperature controlled microscope stage, maintained at 37 °C. These experiments were carried out on the Leica Confocal Scanning Microscope (LCSM). Confocal microscopy optically slices through the sample. This allowed imaging of all stages of neutrophil adhesion, from neutrophils in suspension, during adhesion, and to fully adherent neutrophils. At each of these stages it was possible to expose the sample to UV light (360 nm) provided by ozone free xenon light source (HBO 100W), through a UV filter (350-370 nm band pass). The beam was focussed through the same objective lens as the laser beam used for the fluorescence and brightfield images. Therefore the UV beam was focussed at the same focal plane in the sample as the images were being

taken. However, it is worth noting that the UV beam was slightly scattered by the glass and Krebs (+BSA) medium that the neutrophils were in. The UV beam was still sufficiently strong to uncage the IP_3, but also uncaged IP_3 in cells around the field of view. Therefore, repeated exposures on a single coverslip had to be carried out at distal sites from one another.

To uncage IP_3 in neutrophils in suspension it was necessary to act quickly. Once the suspension of cells was put onto the coverslip, the neutrophils rapidly sedimented onto the surface of the coverslip and began to engage with the glass. Therefore, once a cell was in the focal plane in contact with the coverslip, the UV exposure was carried out. Then the cell was monitored for morphological changes, Ca^{2+} events, or any other markers of choice.

To uncage IP_3 in adherent neutrophils, the loaded cells were allowed to settle onto the glass coverslip for 3-5 mins. Any non-adherent cells were gently washed away with Krebs (+BSA). It was important to wash gently so no morphological changes were induced by the flow forces exerted by strong pipetting of Krebs (+BSA) over the cells. The focal plane of the LCSM was put through the adherent cells. The cells were then exposed to UV light and any morphological changes, Ca^{2+} events or other markers were observed before, during and after the exposure.

It was also possible to uncage IP_3 in cells on a conventional wide-field fluorescence microscope (Nikon Eclipse microscope) coupled to an rapid monochromator to generate monochromatic light at 360 nm. This allowed rapid switching between a non-uncaging (480 nm) and uncaging (360 nm) wavelength illuminating the

neutrophils through the objective. However, it was not possible to concurrently record Ca^{2+} changes using fura2 as the Ca^{2+} indicator because its excitation wavelengths (340 nm and 380 nm) would also induce uncaging. This method was used to observe changes in morphology of the neutrophils. This microscope is non-confocal and therefore the whole field of view was exposed to the UV radiation. This meant fewer exposures could be carried out per coverslip as compared to the LCSM. During uncaging a video was recorded to capture any morphological changes occurring in the cells. UV exposure was marked by rapidly putting the shutter across, thus marking the time on the film for future cross-correlation.

Controls were carried out on both microscopes, as described in Section 3.1.2. This ensured that there was no lag in uncaging and that sufficient IP_3 was being uncaged to trigger signalling pathways within the neutrophils.

4.2.2 3D Reconstruction

Neutrophils were loaded with organelle specific dyes in suspension, including mitotracker red and lysotracker green. The loaded neutrophils were allowed to adhere to a glass coverslip. The non-adherent cells and any excess dye were washed away with Krebs (+BSA). If acridine orange was used, it was added to the adherent cells on the coverslip, allowed to integrate into the DNA and then excess was washed away with copious amounts of Krebs (+BSA). The LCSM was then used to image sections through the vertical plane of the field of neutrophils. The sequence of images was then imported into Imaris software, which integrated between the images to produce a 3D reconstructed image of the neutrophil (Fig 4.2.2). It was possible to manually define the thickness of the slices taken. The more slices taken, the higher the resolution.

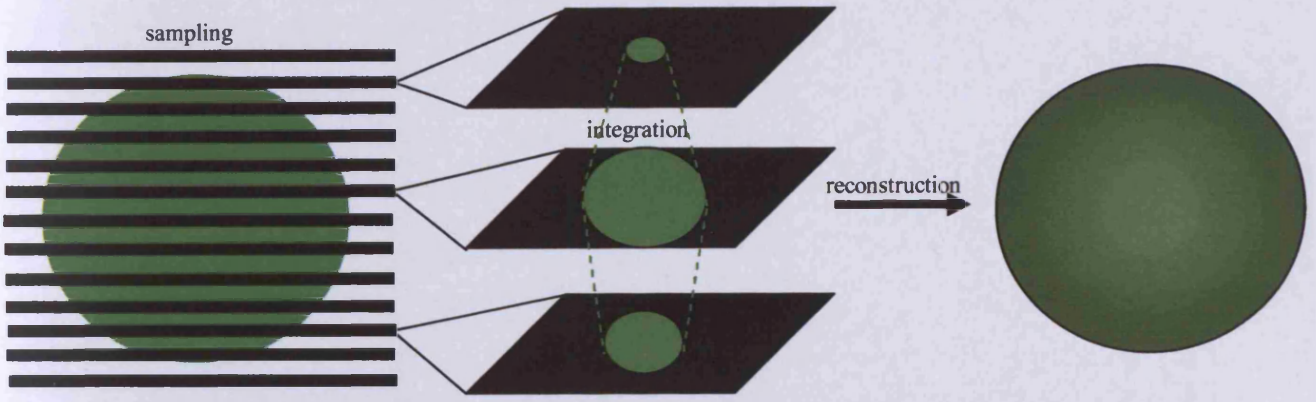

Fig 4.2.2 Three-Dimensional Reconstruction of Images Acquired by Confocal Microscopy

Slices are taken of x-y plane images through the z-plane and then integrated by Imaris software to produce a 3D reconstruction of the imaged object.

This was particularly important when using mitotracker as there is some controversy surrounding the number of neutrophil mitochondria.

It was possible to load neutrophils with two dyes at a time and therefore visualise the relative positions of different organelles. The most commonly used combinations were acridine orange with one of either lysotracker or mitotracker. When lysotracker was present in a concentration in excess of that required to label the lysosomes it began to stain the inner surface of the plasma membrane. This proved a good marker for the edge of the cytosol and the cell shape. The Imaris software also allowed "fly-through" movies to be made of the 3D reconstruction. This gives a better feel for the relative positions of organelles compared to a static, albeit 3D, image.

4.3 Results

4.3.1 Ca^{2+} Puffs Induced by GPN in Adherent Neutrophils

In order to establish whether the techniques established in Chapter 3 were capable of detecting Ca^{2+} microevents that were severely spatially and temporally restricted, in the way reported by Petty's group, artificially generated Ca^{2+} microevents were produced using glycylphenylalanine B-naphthalamide (GPN). This agent acts by osmotically lysing neutrophil granules containing lysosomal cathepsin C, for which it is a substrate. It has been reported to cause the release of intra-lysosomal Ca^{2+} into the neutrophil cytosol (Styrt and Klempner, 1998). As simple lysis of granules would not be expected to trigger Ca^{2+} z-waves in neutrophils, this provided a test situation with stationary Ca^{2+} microevents. Neutrophils were loaded with Fluo4 to detect Ca^{2+} and lysotracker red to monitor lysosome (granule) lysis. Although GPN caused neutrophil lysis after 100-200 seconds (presumably as a result of the release of proteolytic and degradative lysosomal enzymes into the cytosol), the release of lysotracker red occurred earlier than this and localised Ca^{2+} release events were detectable within neutrophils. These were equivalent to conventional Ca^{2+} puffs. There was decrease in lysotracker intensity within lysosomes after the addition of GPN (as expected for granule lysis) and a Ca^{2+} spike indicative of a Ca^{2+} puff in the chosen region of interest observed (Fig 4.3.1). Therefore it can be concluded that neutrophils can produce Ca^{2+} puffs and that the rapid resonant scanner technique had sufficient speed and resolution to detect them above the background noise.

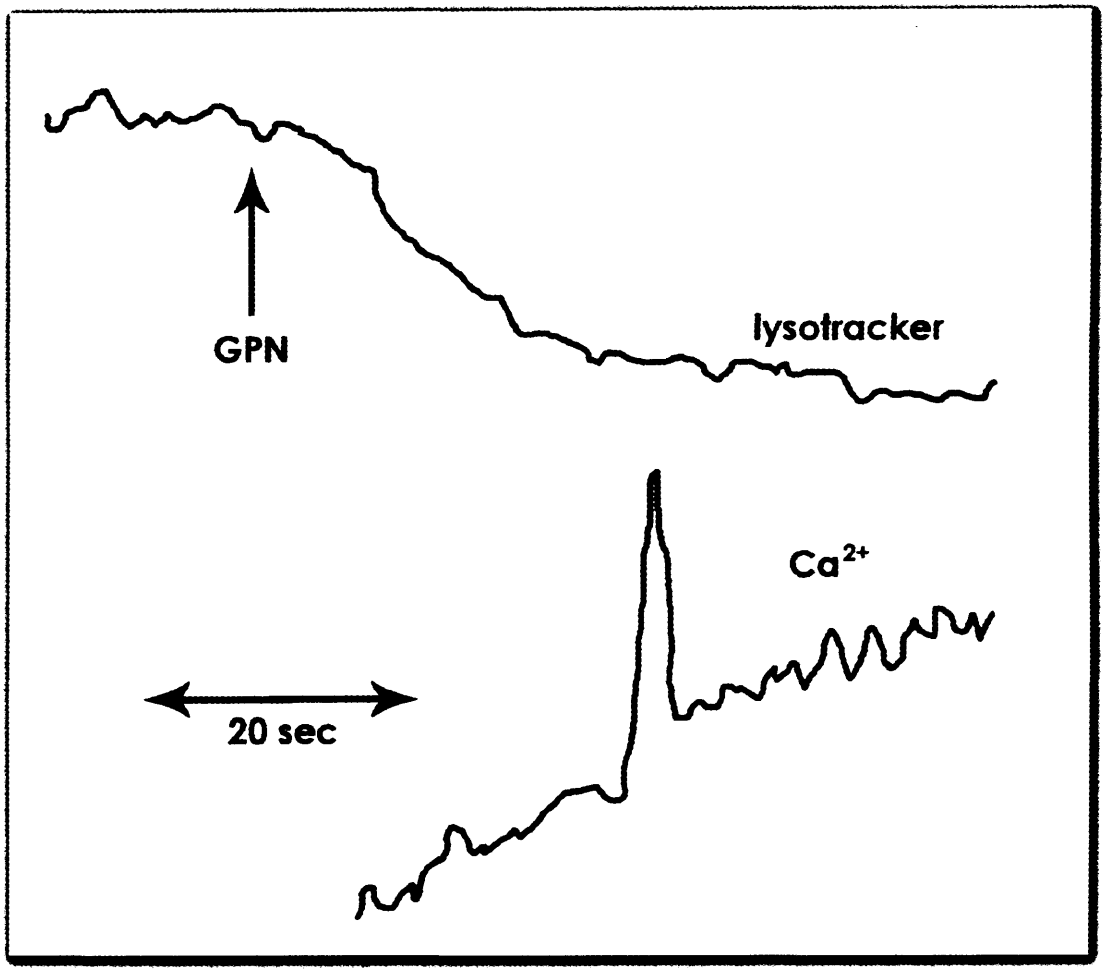

Fig 4.3.1 GPN Induced Experimental Ca^{2+} Puffs in Neutrophils

The upper trace shows the decrease in lysotracker red fluorescence following the addition of GPN. The lower trace shows the Fluo4 fluorescence, indicative of Ca^{2+} concentration in a defined region of interest in the same neutrophil. The spike is a distinct Ca^{2+} release event within that region. (x axis represents lysotracker and Ca^{2+} concentration respectively against y axis of time)

4.3.2 Multiple Ca^{2+} Release Sites in Neutrophils

Addition of GPN to neutrophils caused lysis of any granule that contained cathepsin C, resulting in the release of any Ca^{2+} stored in that granule. There were often multiple Ca^{2+} release events within an individual neutrophil (Fig 4.3.2). It was possible to detect between 1-6 localised Ca^{2+} release events within a single neutrophil. The Ca^{2+} release events did not all occur at exactly the same time, as seen in the time sequence of images (Fig 4.3 2). The 3D plot demonstrates the distribution of Ca^{2+} in the neutrophil, revealing that multiple release sites were detectible and distinguishable from one another. These multiple releases are due to Ca^{2+} being freed from cathepsin containing azurophilic granules, and not necessarily from conventional Ca^{2+} stores. However, they do reveal that it is possible to detect and distinguish subcellular Ca^{2+} events.

4.3.3 Experimentally Induced Ca^{2+} Puffs Fit Theoretical Diffusion Model

Ca^{2+} diffusion equations were used to predict the detectbility of Ca^{2+} puffs under the experimental conditions used. This determined the theoretical spread of Ca^{2+} from the site of initial release and the peak height at a given distance from the release site. The profile through a Ca^{2+} puff induced by GPN (black) was compared against the theoretical graph (yellow) in Fig 4.3.3a. It can be seen that the two almost exactly line up. This allowed us to extrapolate theoretical limitations and optima for detecting Ca^{2+} puffs in neutrophils and to translate these theories into practice during experiments. The level of background noise is also worth noting in Fig 4.3.3a as it is relatively high. This statistical noise produces uncertainty in establishing the exact parameters of the puff event, and must therefore be given consideration in further experiments. The Ca^{2+} puffs induced by GPN are shown in Fig 4.3.3b. The third puff

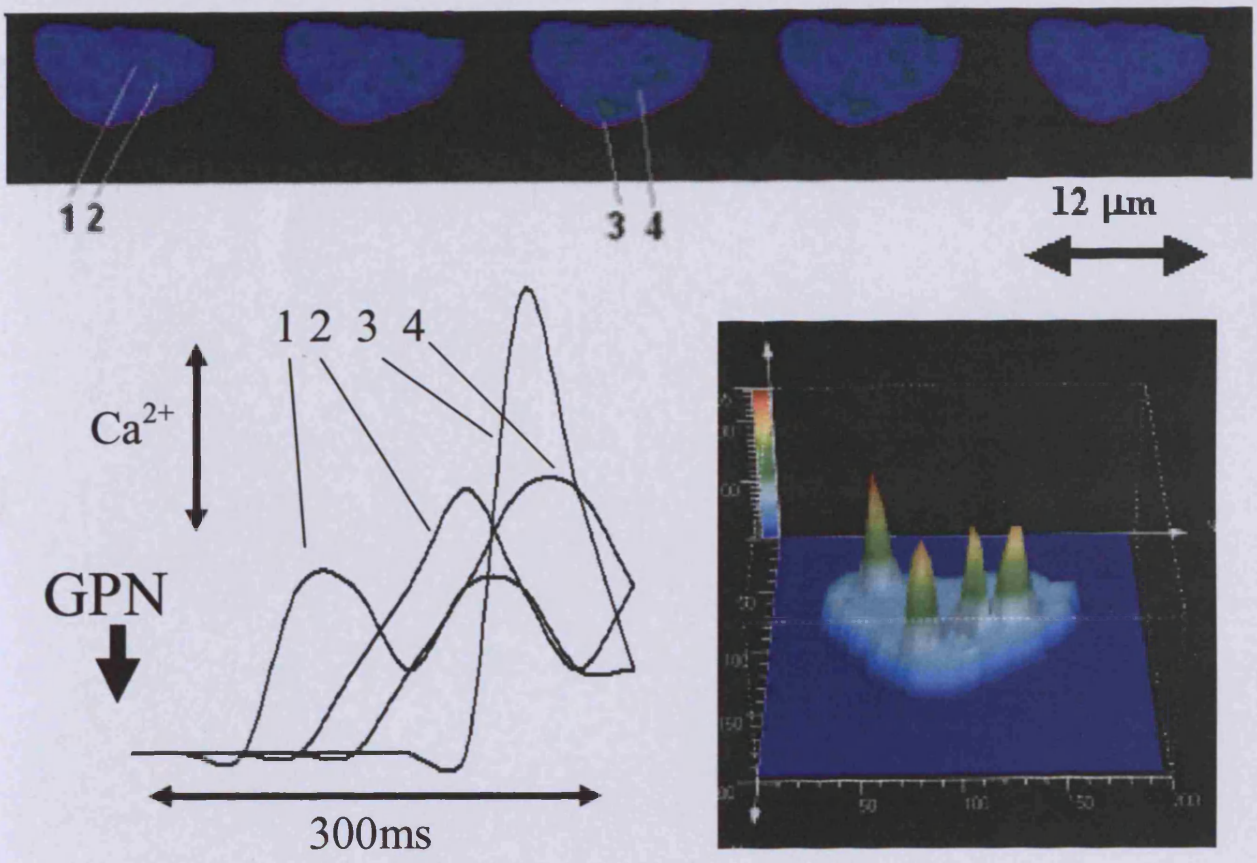

Fig 4.3.2 GPN Experimentally Induced Multiple Ca^{2+} Release Events

The sequence of images is pseudocoloured Fluo4 frames representing Ca^{2+} distribution. The images are taken at 33 msec apart. Four distinct Ca^{2+} release events are indicated. The trace shows each of these release events with time, revealing that they have different start times and variable peak characteristics, but are each detectable and distinguishable. The 3D plot demonstrates the distribution of Ca^{2+} (z-axis) through the neutrophil, revealing multiple release events.

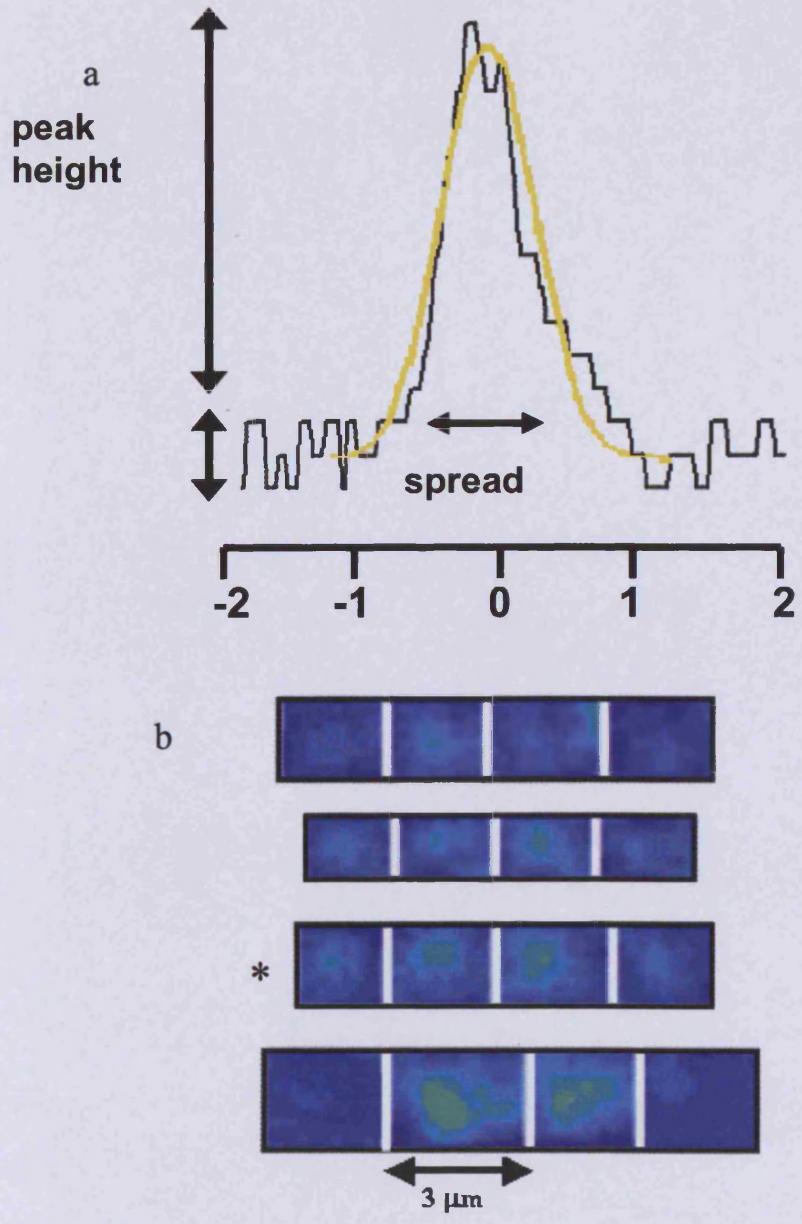

Fig 4.3.3 Experimentally Induced Puffs Correspond To Theoretical Diffusion Models
(a) The profile of a GPN-induced Ca^{2+} puff (black) was compared to the theoretical graph (yellow). Point 0 represents the point of initiation that the Ca^{2+} diffuses away from. Note there is a relatively high level of background noise, which must be taken into account in characterising parameters of Ca^{2+} events. (b) Sequential images of each of the 4 GPN-induced Ca^{2+} release events from Fig 4.3.2. None of the puffs exceeded 3µm in diameter nor did the central point move significantly. The third puff (*) is represented in the trace in (a). Each sequence of images covers 550 msec.

was used for comparison with the theoretical Ca^{2+} spread graph. The puffs persisted for a number of capture frames with each sequence covering 550 ms. None of the puffs was captured at larger than 3 μm in diameter. The variation between the puffs could be accounted for by variability in their positioning within the neutrophil in the z-plane. If the point of origin of the puff is slightly out of the field of view, the area with the high Ca^{2+} concentration will be smaller by the time it has diffused into the confocal plane.

4.3.4 Theory of Ca^{2+} Puff Detection Limit

There are a number of factors contributing to the detectability of small changes in molecular probes by confocal microscopy. Four of these are discussed below, namely statistical effects (A), z-plane location (B), apparent size at remote imaging locations (C), and detectability at remote imaging planes (D).

A. Detection Limitations Due to Statistical Effects

The ability to detect a localised Ca^{2+} event depends on both the magnitude of the event (peak height) and spread of the event (see Fig 4.3.3a).

If two regions were selected on the Fluo4 image, one bounded by the Ca^{2+} puff and the other outside the Ca^{2+} puff, a significant difference between the two would arise when the actual difference in Fluo4 intensity (related to cytosolic free Ca^{2+} concentration) was greater than δ, where:

$$\delta > [\sqrt{(2/n)}][\sigma(Z_{2\alpha}+Z_{2\beta})]$$

and n is the number of pixels occupied by the elevated intensity, σ is the standard deviation of the distribution of intensity values, Zx is the standard normal deviate exceeded with probability x, α is the significance level for the test and $(1-\beta)$ is the power of the test. Areas of interest in which the number of pixels exceed n would detect a statistical intensity δ, where:

$$n > 2[\sigma(Z_{2\alpha}+Z_{2\beta}./\delta]^2$$

Thus the "detectabilty" of the Ca^{2+} puff in the imaging plane is proportional to $n\delta^2$ (Fig 4.3.4iii).

B. Detection Limitation Due to z-Plane Confocal Imaging Location

The magnitude of the imaged event will depend on how distant the imaging plane is from the release event. If the release of Ca^{2+} occurs over a short time relative to the diffusion time (t_0) at a rate of i from a site, which is small compared to diffusion distance, the boundary condition give the following equation:-

$$C(r,t)= it_0/ (4 \pi Dt)^{3/2} e^{(-r2/4Dt)}$$

where r is the distance from the release site, t is the time after release and D is the diffusion constant for Ca^{2+} (or Fluo4-Ca^{2+}).

With the z-confocal plane at a position z distant from the release site, the release event would appear to have a maximum peak of

$C_{(peak)}= 0.0736it_0/z^3$ and occur at $t_{(peak)}= z^2/6D$.

(see Berg HC (1993)).

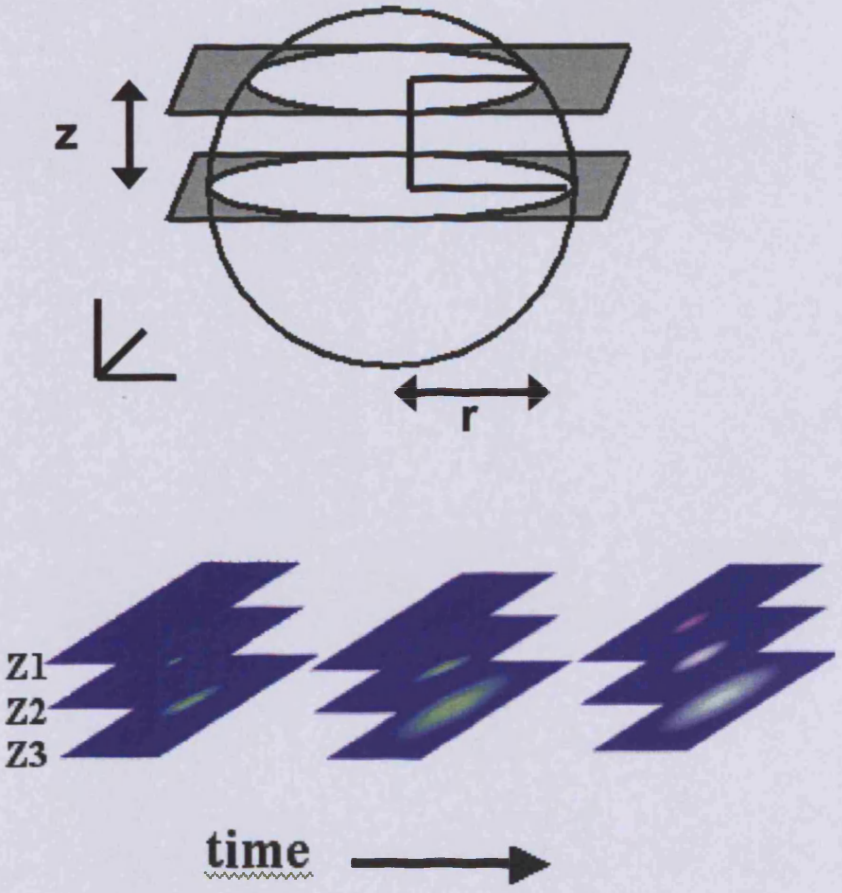

Fig 4.3.4 Apparent Size Of Ca^{2+} Event At Remote Imaging Plane

Representation of the change in the apparent size of a Ca^{2+} event dependent upon distance (z) from the point of initiation. The top diagram illustrates a spherical Ca^{2+} puff and its visible size in two imaging planes separated by distance z. The radius (r) of the observed puff is varied according to z. The bottom diagram illustrates three different imaging planes z1,2,3 at three progressive time points. Over time the Ca^{2+} diffuses away from the point of initiation resulting in a bigger, but dimmer appearance. If the event occurs in z3, it would not be seen in z1 until a later time point and would look smaller and less bright.

The peak concentration reached does not depend on the diffusion constant and is simply inversely related to the volume of the Ca^{2+} puff in reaching the observing plane. Thus the difference to be detected, δ, at the signal at the peak above is related to z-distance of the imaging plane by $\delta \propto 1/z^3$ (Fig 4.3.4i).

C. Apparent Size of Ca^{2+} Event at a Remote Imaging Plane

The area, or number of pixels, n, occupied by the boundary of detectably increased Fluo4 intensity pixels (Fig 4.3.5) resulting from a spherical Ca^{2+} puff on an imaging plane distant from the release event is simply $\pi(r^2-Z^2)$. So the number of pixels (n, expressed as a proportion to the actual Fluo4 intensity and area) occupied by the puff in plane z remote is $N= 1- z^2$ (see Fig 4.3.4ii) where z is the z distance (expressed in proportion to the Ca^{2+} puff radius, r).

D. Detectability of Ca^{2+} Event at Remote z-Planes

From the above, it is seen that n (the number of pixels occupied by the Ca^{2+} event) and δ (the increase in signal for detection) are both reduced by the distance of the imaging plane from the event.

So the event will be detectable only when $n\delta^2$ exceeds the $2[\sigma(Z_{2\alpha}+Z_{2\beta.}]^2$. This set the limit of detection (power = 80 %) in our experiments to about 50 nM above resting Ca^{2+} concentration in an area of at least 0.8 μm^2 (radius = 0.5 μm) and so localised Ca^{2+} events of this magnitude would be undetectable at z-planes more than 0.5 μm distant.

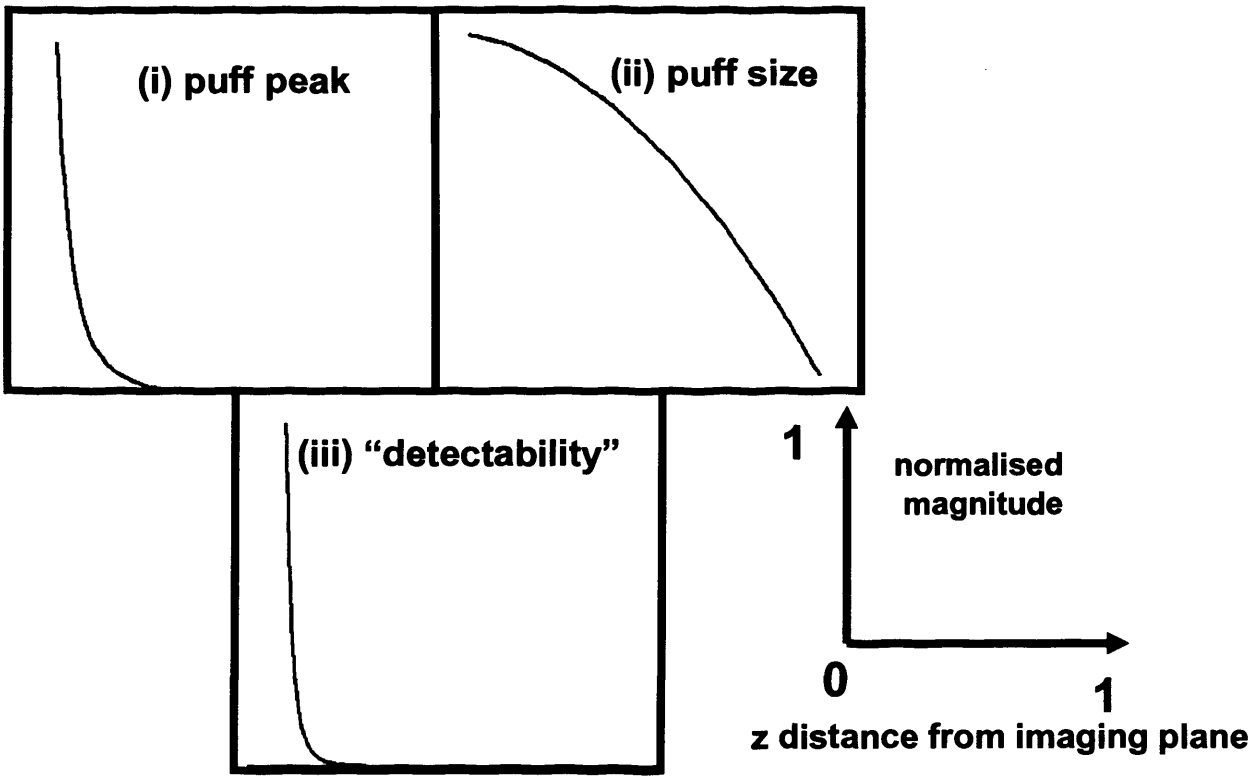

Fig 4.3.5 Detectability of Ca^{2+} Event At Remote Z-Plane

(i) As the distance between the Ca^{2+} event and the imaging plane increases, the apparent puff peak decreases very rapidly. (ii) As the distance increases, the apparent puff size, i.e. the number of pixels occupied decreases. These two parameters combined result in (iii) a sharp decline in the "detectability" of a Ca^{2+} event, leading to a limit of detection to be used in following experiments of approximately 50 nM above resting Ca^{2+} concentration in an area of at least 0.8 μm^2, and resulting in a limit of detection of 0.5 μm distant in the z-direction.

4.3.5 Failure to Capture Ca^{2+} z-waves Not Due to Inadequate Spatial Resolution

The above experiments with GPN induced Ca^{2+} events indicate that the method is sufficient to capture Ca^{2+} puffs within 1 μm of the confocal plane. However, the z-wave was reported to have a lateral size of less than 1 μm, and may have a similar vertical dimension, and therefore only be detectable within a limited range of confocal z-planes. A detailed study was therefore undertaken to acquire Fluo4 confocal images at high frequency at different planes within the vertical direction from the base of adherent neutrophils (contact with the coverslip), through the widest circumference (where the z-waves have been reported) and through the cell apex at steps of 0.5 μm. However, in no imaging plane was evidence for Ca^{2+} z-waves found in neutrophils that were resting, polarized or adherent bit not polarized. Thus the failure to detect Ca^{2+} z-waves could not be attributed to inadequacies in either z-plane or xy plane resolution.

4.3.6 Ca^{2+}-Microevents Accompany Neutrophil Stimulation

Since no spontaneous Ca^{2+} z-waves were captured, we sought to establish whether fMLP could generate experimental z-waves or other localised micro-events. This stimulus (0.01-1 μM) caused a transient global Ca^{2+} elevation with variable times of onset and lasting approximately 100 sec, similar to those reported previously (Davies et al, 1991: Scharff et al, 1993) without any evidence of z-waves. Examination of high frequency image sets of the initial 1-2 secs after addition of the stimulus showed that in some cells (1/15; $n \approx 300$) a localised Ca^{2+} elevation (puff) preceded the global Ca^{2+} signal (Figs 4.3.6 and 7). In no case did the centre of localised Ca^{2+} puff move significantly, and in no cell was more than one localised Ca^{2+} elevation site identified. In some cells, there was a double Ca^{2+} puff before the global rise in Ca^{2+}.

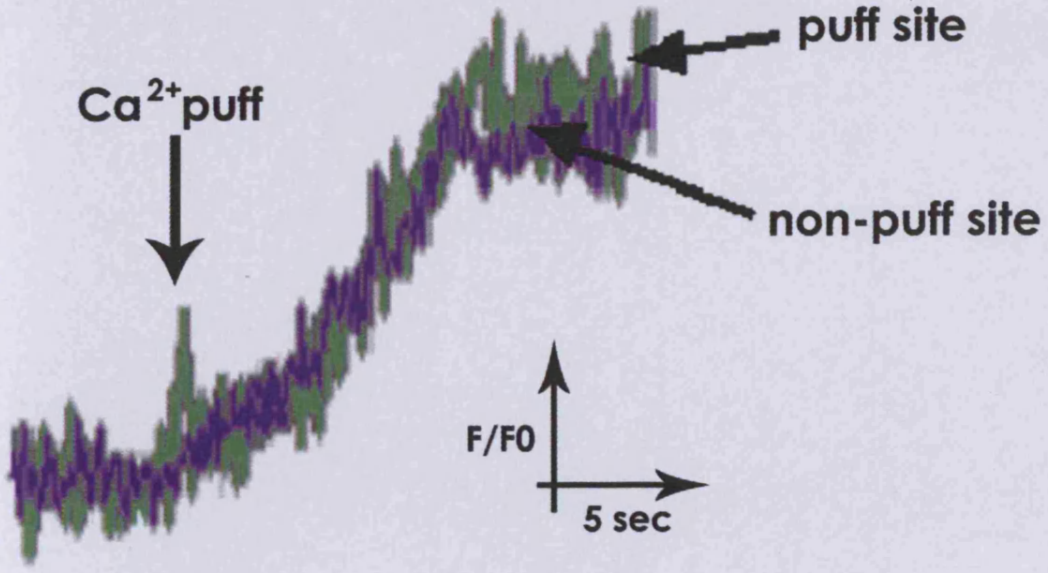

Fig 4.3.6 Ca^{2+} Puff Induced By fMLP

The trace shows the Ca^{2+} concentration as a ratio of the Fluo4 fluorescence / Fluo4 at time 0. The green trace is readings from a site where a Ca^{2+} puff was observed. The purple trace is from a non-puff site of equivalent size within the same neutrophil. The Ca^{2+} puff is seen as a spike in the green trace above the background noise. The trace then rises as Ca^{2+} influx occurs.

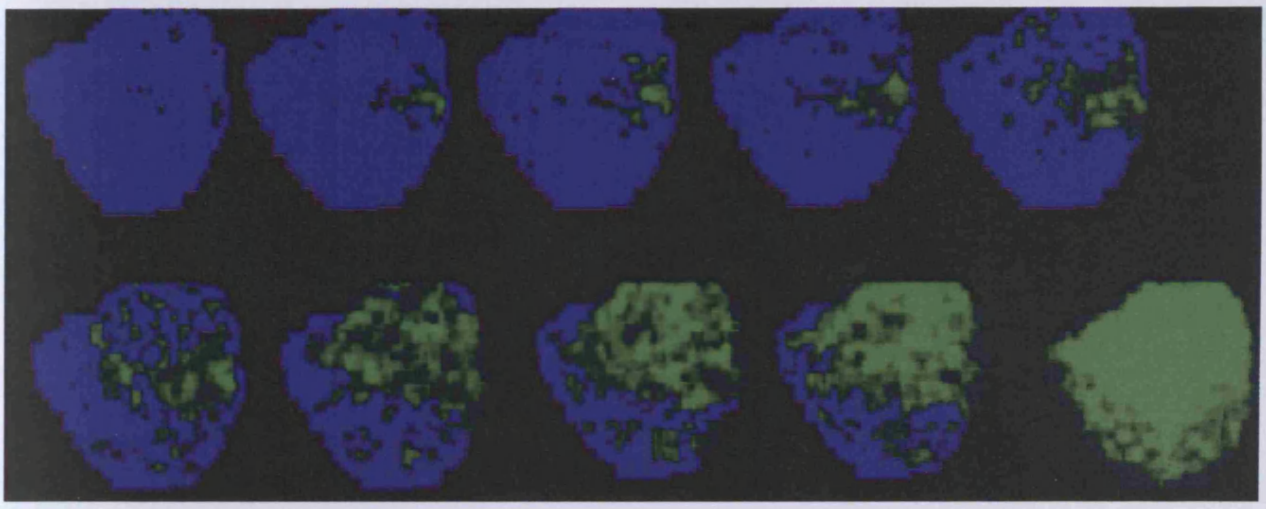

Fig 4.3.7 Ca^{2+} Puff Followed By Ca^{2+} Influx Wave

A series of images taken at 33 msec apart pseudocoloured for Ca^{2+} with blue representing low and green representing elevated Ca^{2+}. In the top row a Ca^{2+} puff can be seen persisting for at least 4 frames (> 200 msec) before a Ca^{2+} influx wave is triggered, adjacent to the puff site, which sweeps across the cell from the top right corner to the bottom left, resulting in a global transient increase in Ca^{2+} as seen in the last image.

The second puff always occurred from the same site as the first (Fig 4.3.9). This low frequency of observation of Ca^{2+} micro-events (1/15) was never exceeded at any pre-selected z-position imaging plane. In a series of experiments in which the imaging plane was set at different z-positions within the neutrophil, fMLP induced Ca^{2+} puffs and global changes but no Ca^{2+} z-waves were detected. These observations suggest that the stationary Ca^{2+} puffs were randomly located relative to the z-plane of the cell. From the maximum magnitude of the signal, it was estimated that they would be detectable at confocal planes within 0.5 μm. Thus the probability of observing a single physiological Ca^{2+} micro-event triggered within the neutrophil (z dimension = 8 μm) would be about 1/8. This is a higher frequency than we observed and suggested that either Ca^{2+} release events in neutrophils were less than 1 puff/cell or that approximately half of them were of undetectable for another reason. One reason may be because they were often swamped by the large global Ca^{2+} signal that always followed. This global Ca^{2+} signal was observed as a wave sweeping across the cytosol from near the initial Ca^{2+} release site (Fig 4.3.7 images at 33 msec intervals). This was more clearly visualised with 3D plots in Fig 4.3.8 revealing the location of the Ca^{2+} puff as well above the background level of Ca^{2+} occurring distinctly before the influx wave, which initiated near the site of the Ca^{2+} puff.

4.3.7 Ca^{2+} Puffs Attributed to Store Release

Ca^{2+} signals in neutrophils occur either by release from intracellular stores or by influx through Ca^{2+} channels in the plasma membrane. However, it was difficult to distinguish between them since any Ca^{2+} puff could have been swamped by the Ca^{2+} influx wave. The Ca^{2+} puffs observed were attributed to Ca^{2+} release from an intracellular Ca^{2+} storage site because they persisted in the absence of extracellular

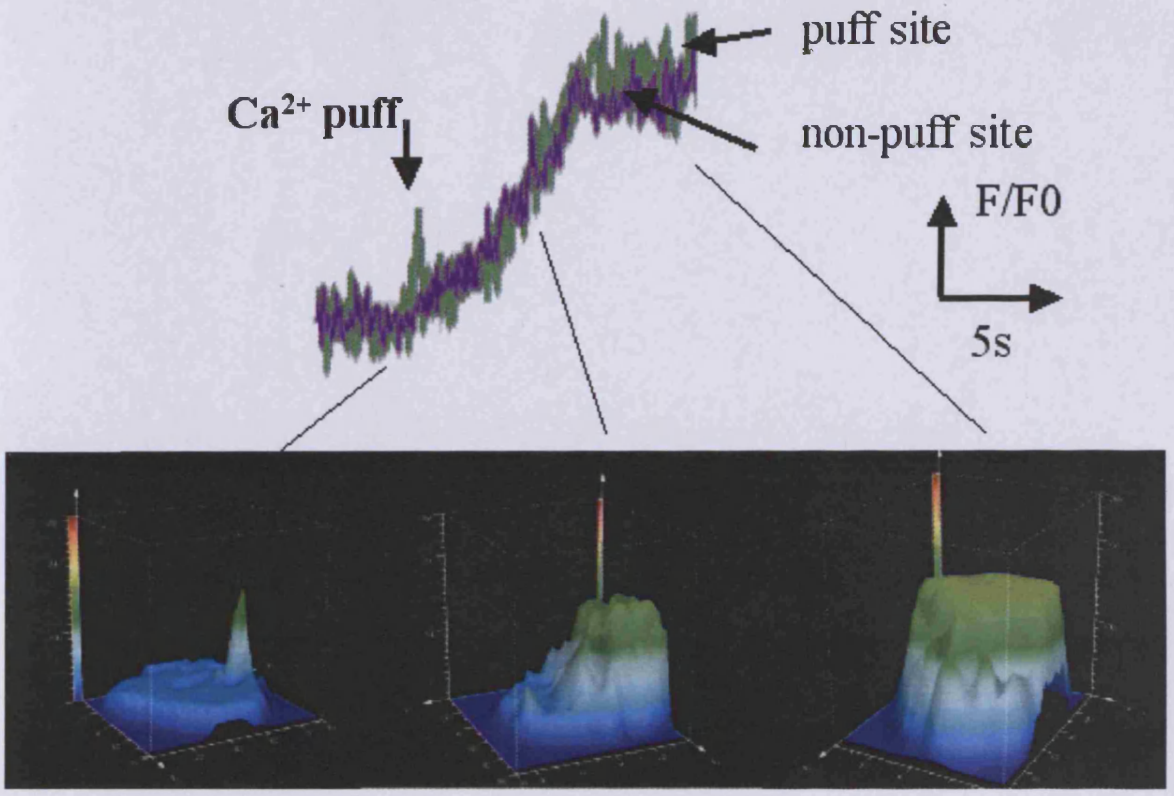

Fig 4.3.8 Ca^{2+} Puff Distinct From Influx Wave

The trace shows the Ca^{2+} concentration at two regions of interest in the same neutrophil. In the region plotted as a green line, a Ca^{2+} puff occurred, but not in the purple. The 3D plots have Ca^{2+} concentration in the vertical axis and clearly show the Ca^{2+} puff as well above the background level in the cell and distinguishable from the influx wave that sweeps from the right to the left of the cell.

Ca^{2+} and during Ca^{2+} channel blockade. Fig 4.3.9 compared a Ca^{2+} puff with and without blockade of the Ni^{2+} sensitive Ca^{2+} channels. The Ca^{2+} puffs were of comparable magnitude and duration. Both were the result of stimulation with fMLP. It was thought that Ca^{2+} puffs might be easier to visualise without Ca^{2+} influx potentially swamping them.

Ni^{2+} was used to block Ca^{2+} influx and the neutrophil was stimulated with fMLP as before. The resulting Ca^{2+} signal was imaged at high speed. This revealed Ca^{2+} puffs at a slightly higher frequency of observation (1/12 compared to 1/15 without Ni^{2+} blockade). Fig 4.3.10 is a series of images at ~100 msec intervals with a Ca^{2+} puff. The puff was reconstructed in 3-dimensions in Fig 4.3.10b. The Ca^{2+} influx was totally absent in these experiments. Therefore, the global Ca^{2+} signal was driven by Ca^{2+} influx through Ni^{2+}-senstive Ca^{2+} channels. This was consistent with the production of IP_3 by activation of the receptor for fMLP (Scharff et al, 1993), release of stored Ca^{2+} and the induction of store-operated Ca^{2+} influx (Davies-Cox et al, 2001).

4.3.8 Uncaging IP_3 Induced Ca^{2+} Signals in Neutrophils

In order to test whether IP_3 was able to generate Ca^{2+} puffs (or z-waves), photolytic uncaging of caged IP_3 was used. The use of uncaging IP_3 was considered to reproduce physiologically relevant signalling cascades in these cell types. There are only a finite number of IP_3R in each cell. Once there is sufficient IP_3 produced to saturate these receptors, no further signalling can be induced.

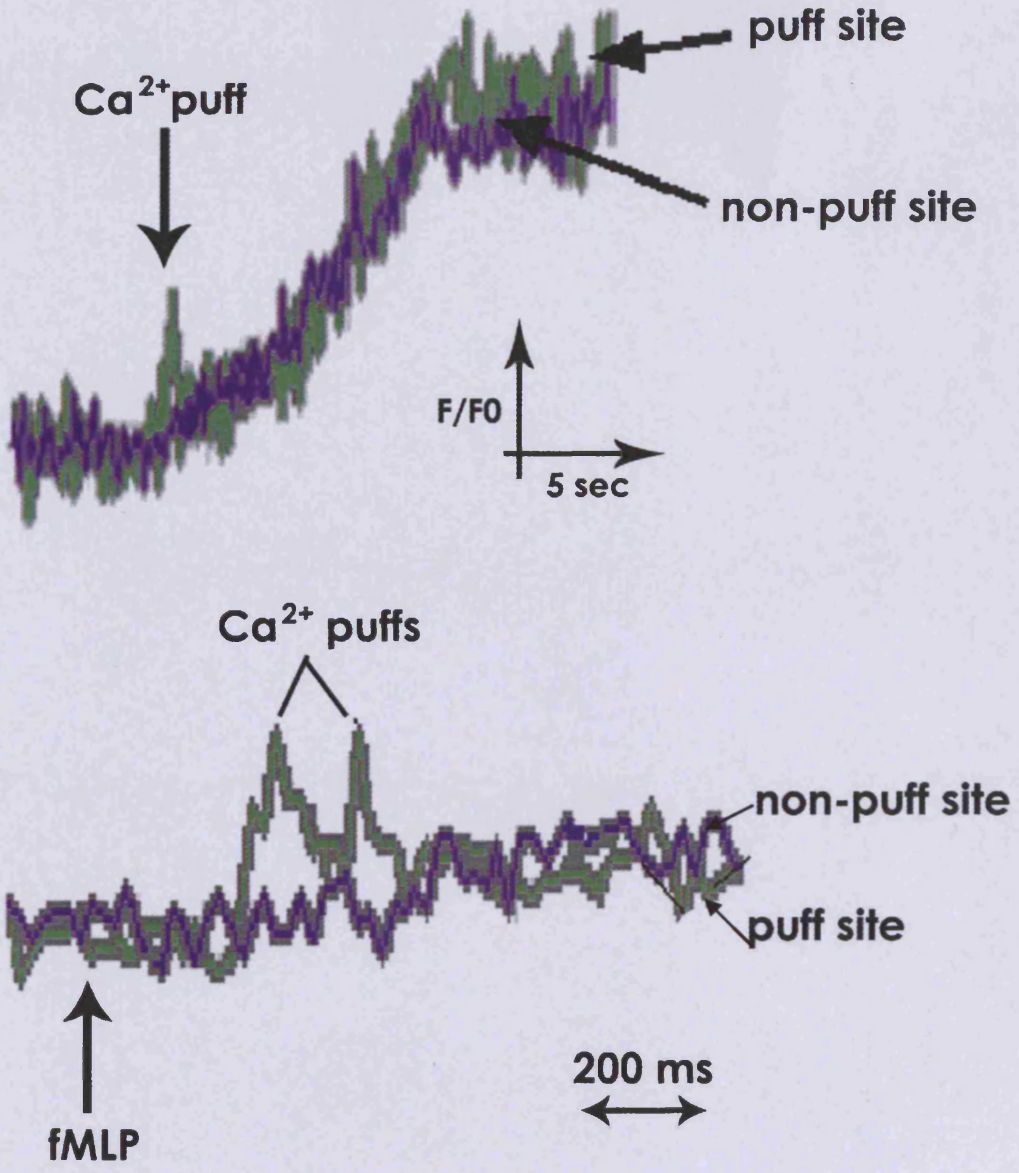

Fig 4.3.9 Ca^{2+} Puffs Occur Independently Of Ca^{2+} Influx

The upper trace shows a Ca^{2+} puff following stimulation with fMLP (1 μM). The puff is a distinct spike above the background trace. Ca^{2+} influx occurs shortly afterwards. The lower trace shows a similar experiment, but the Ca^{2+} channels have been blocked with Ni^{2+} (1 mM) so no Ca^{2+} influx will occur. It can bee seen that Ca^{2+} puffs did still occur in these cells. In this case there were two release events from the same location within 200 ms of each other. In both traces the green line represents the region of interest in which the puff occurred, the purple represents a region of similar size in the same neutrophil without a puff.

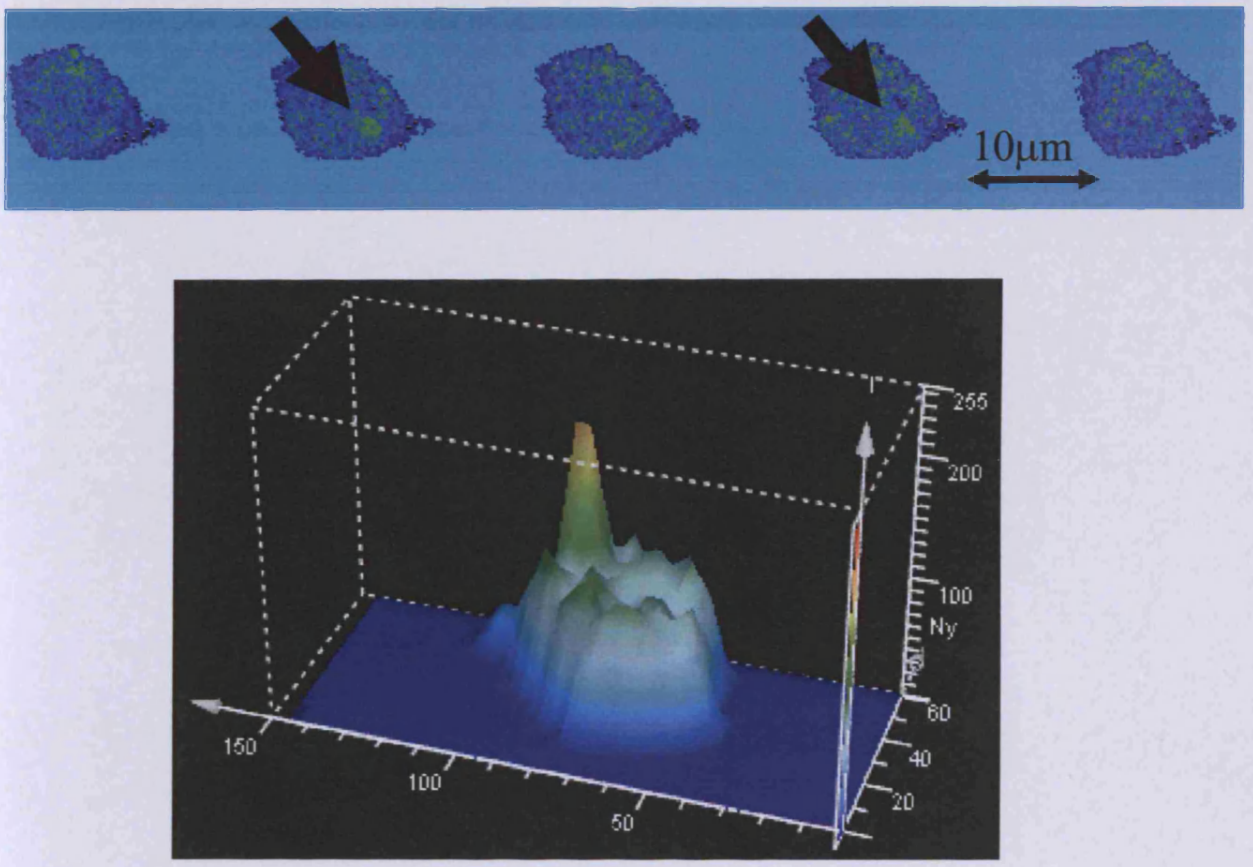

Fig 4.3.10 Ni^{2+} Blockade Of Ca^{2+} Influx Resulted In Detection Of fMLP Stimulated Ca^{2+} Puffs.

The series of images are taken at 100 msec intervals and pseudocoloured for Ca^{2+} with blue being basal level and green being elevated. The neutrophil was treated with Ni^{2+} (1 mM) to prevent Ca^{2+} influx and then stimulation with fMLP (1μM). This resulted in a Ca^{2+} puff at a distinct site. There were two releases seen in this cell, but both occurred from the same site. The 3D image reveals the puff as well above the background level.

To establish this technique using the set-up that allows concurrent monitoring of neutrophils, caged fluorescein was employed. The structure of caged-fluorescein can be seen in Fig 4.3.11, clearly indicating the caging bonds that are optimally photolytically cleaved at a wavelength of 360 nm. The cage masks the fluorescent moiety of fluorescein. Thus, when the cage is broken there should be a concurrent increase in the fluorescence. Fluorescein is excited at 488 nm and emits at a peak of 560 nm. This is equivalent to the wavelengths used to measure Ca^{2+} with Fluo4, thus providing an excellent control to show that exposure of the sample to UV light suitable for uncaging does not interfere with the signal created by stimulating a fluorophore at 488 nm.

The graph in Fig 4.3.11 shows the fluorescence of a slide coated with caged-fluorescein, exposed to UV light and monitored by excitation at 488 nm. There is a marked increase in fluorescence at the exact time the UV light is allowed onto the field of observation. There is no delay in the uncaging effect. There is a plateau as all the fluorescein in the field of observation is uncaged. This plateau is reached quickly. The evidence indicating no lag in uncaging relative to the start of UV exposure proves this method as viable for uncaging biologically active molecules.

Initially it was necessary to test whether it was possible to uncage molecules on the confocal microscope set up. A coverslip was coated with caged-fluorescein, which has the same uncaging wavelength sensitivity to caged-IP_3 and similar emission spectra to Fluo4. This was illuminated at 360 nm and the increase in fluorescence monitored. There was no lag time in the increase in fluorescence and maximal fluorescence was

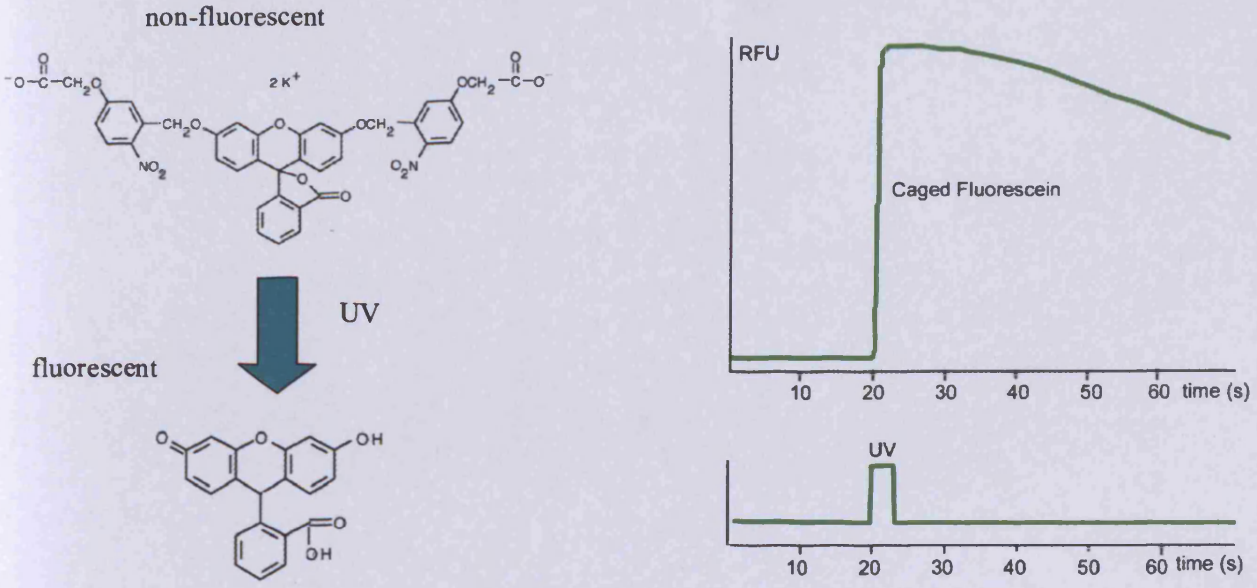

Fig 4.3.11 Irradiation Of Sample With UV Is Sufficient To Uncage Fluorescein

The structures on the right are caged (top) and uncaged (bottom) fluorescein. The UV light breaks the bonds sensitive to those wavelengths, releasing the fluorescein molecule. The caging moieties act to prevent fluorescence, this when the cage is broke then fluorescent fluorescein is released. The trace shows experimental data of UV irradiation of a caged-fluorescein coated coverslip resulting in an increase in the fluorescence (excitation 488 nm, emission 560 nm, similar to Fluo4). The increase occurs without significant lag and reaches a maximum very rapidly. The signal is not disrupted by the 360 nm UV irradiation either.

reached very rapidly. This indicated that uncaging was a suitable technique to be used on this microscope setup.

Neutrophils were loaded with Fluo4 and caged-IP_3, either by SLAM injection or from an acetoxy-methyl ester precursor. Once they had adhered to the coverslip the excess IP_3 was washed away with Krebs buffer. The cells in were then exposed to UV light to photolyse the cage and release the IP_3 while the Ca^{2+} was being monitored. Some neutrophils showed an increase in Ca^{2+} almost immediately, while others demonstrated a variable lag (Fig 4.3.12). All Ca^{2+} transients were comparable to those seen in the literature and in other experiments in this report. It was worth noting that platelets consistently responded more rapidly than neutrophils. Fig 4.3.13 shows how there is almost no lag time between UV illumination and a sharp rise in Ca^{2+} in a platelet. This is thought to be because platelets have a smaller volume and therefore reach a critical concentration of IP_3 to trigger Ca^{2+} events faster than a neutrophil within the same field. Therefore, platelets were used as an internal control for uncaging efficiency.

The similarities in Ca^{2+} events induced by uncaging IP_3 implied that uncaging was also likely to induce Ca^{2+} puffs. Indeed, close scrutiny of images acquired at high speed during photolysis of caged-IP_3 revealed localised Ca^{2+} puffs and global signals (Fig 4.3.14) that closely resembled Ca^{2+} puffs seen with fMLP stimulation.

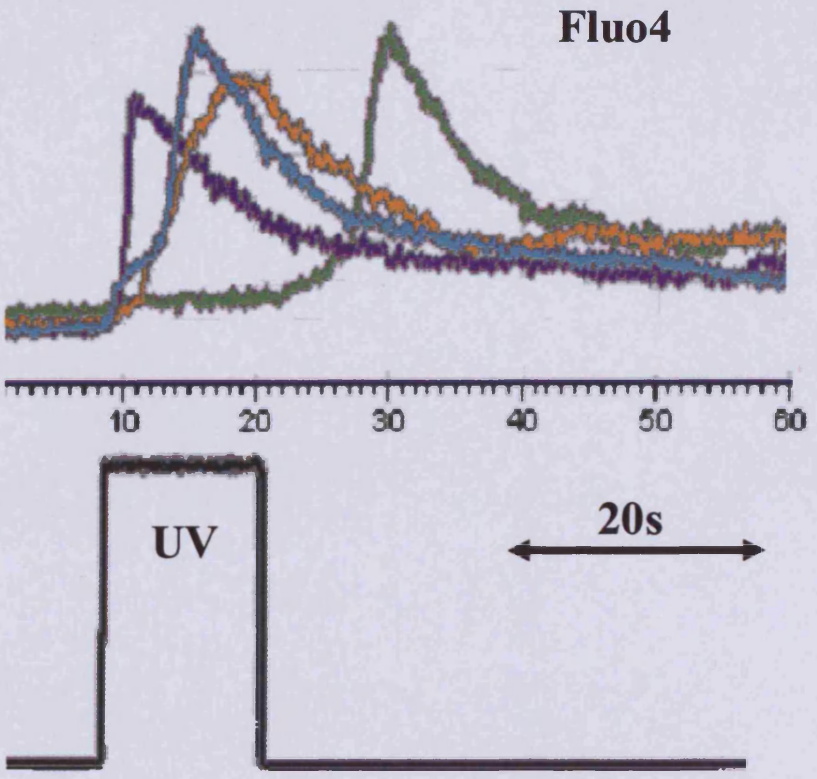

Fig 4.3.12 Global Ca^{2+} Signals Induced By Photolytically Uncaging IP_3

UV illumination (360 nm) of neutrophils loaded with caged IP_3 and Fluo4 induced global Ca^{2+} signals with variable onset. The period of UV is seen in the bottom trace. The upper trace shows Ca^{2+} signals for 4 different neutrophils with variable onset. Each curve has the typical 'fast up, slow down' rates of Ca^{2+} signals seen with other stimuli.

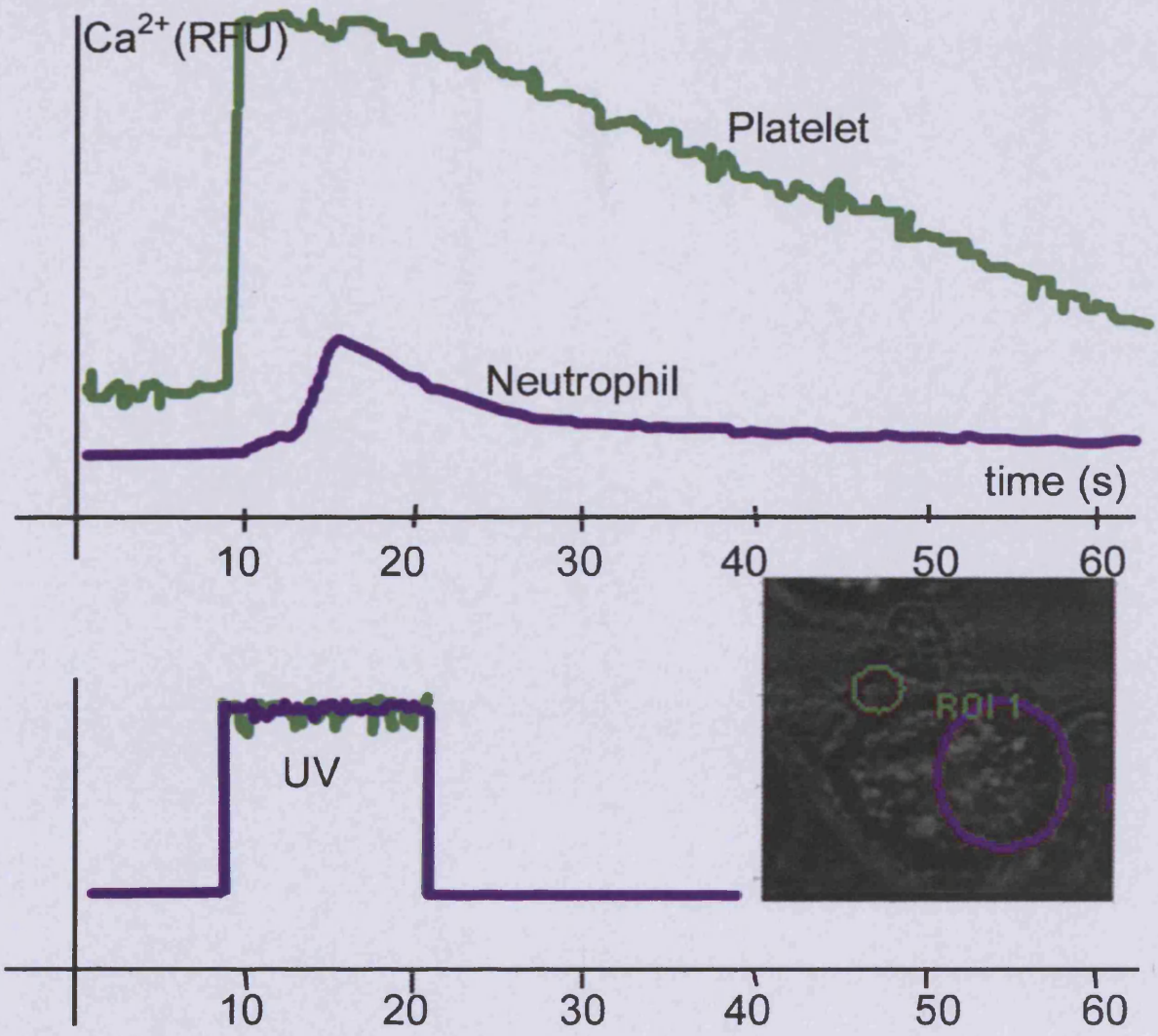

Fig 4.3.13 IP_3 Release Induced Ca^{2+} Changes In Platelets Almost Immediately

The lower trace shows the UV illumination of a sample of neutrophils and platelets. The upper trace shows the Ca^{2+} (Fluo4) response to UV photolytic uncaging of IP_3 in both a platelet (green) and a neutrophil (purple). The platelet response is almost immediate whilst the neutrophil shows a delay. The regions of interest around the platelet and neutrophil are shown on the phase contrast image.

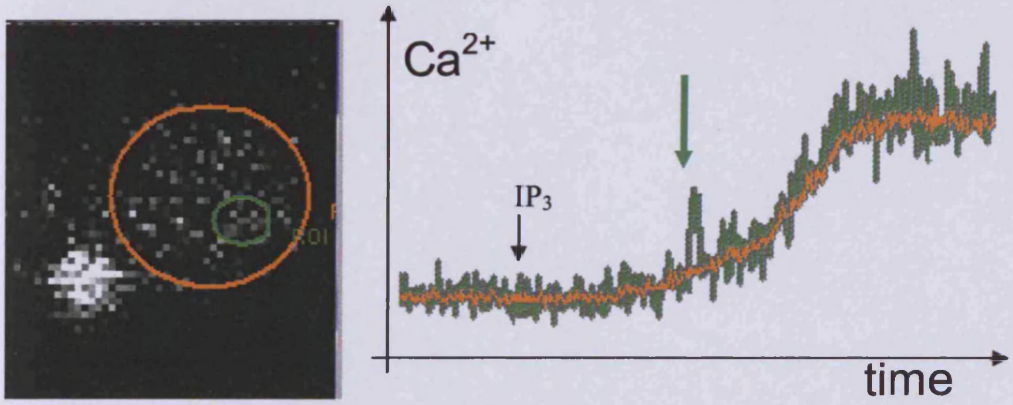

Fig 4.3.14 Ca^{2+} Puffs Generated By Uncaging IP_3.

Photolysis of caged IP_3 (indicated by first arrow) induced localised Ca^{2+} puffs and global Ca^{2+} events as seen in the trace. The orange region of interest encompasses most of the neutrophil and the green region is where the Ca^{2+} puff occurred. The Ca^{2+} puff is indicated on the trace by a green arrow.

4.3.9 Characteristics of Ca^{2+} Puffs in Neutrophils

Since the "distant observer" effect of the confocal imaging plane would report puffs with smaller magnitudes, spreads and distorted time courses (as discussed earlier), the largest ten events in a series of experiments was used to estimate the actual Ca^{2+} characteristics of the release event. Examples of these are shown in Fig 4.3.15 showing puffs without Ca^{2+} influx, before Ca^{2+} influx and during Ca^{2+} influx. The peak Ca^{2+} of the release event was estimated to be 246 ± 131 nM and a maximum detectable spread area of 6.57 ± 2.43 μm^2 (approx. diameter = 2.8 μm) with duration 235 ± 183 ms (n=10). As these are within the range of Ca^{2+} puffs reported in other cell types, it was concluded that these were conventional Ca^{2+} signals generated by the release of Ca^{2+} from a single stationary Ca^{2+} release site, and no evidence for Ca^{2+} z-waves was found.

4.3.10 The Anatomical Basis for Ca^{2+} Micro-events Within the Neutrophil

Since Ca^{2+} z-waves are reported to travel only around the periphery of the neutrophil (in the equatorial plane relative to the observer), it was important to establish whether the distribution of organelles could contribute to the Ca^{2+} micro-event distribution. The Ca^{2+} release events reported in this thesis in response to fMLP or IP_3 uncaging were always detected on or within 2 μm of the nuclear boundary, as located in the phase contrast image (Fig 4.3.16). The multi-lobed nucleus in the neutrophil, however, occupied a large fraction of the cytosol and consequently demarcated a zone of peripheral cytosol in which the Ca^{2+} z-wave may travel. It is, however, unlikely that this organelle can have such a role because the nuclear boundary does not present a significant barrier to diffusion of either Ca^{2+} or Fluo4.

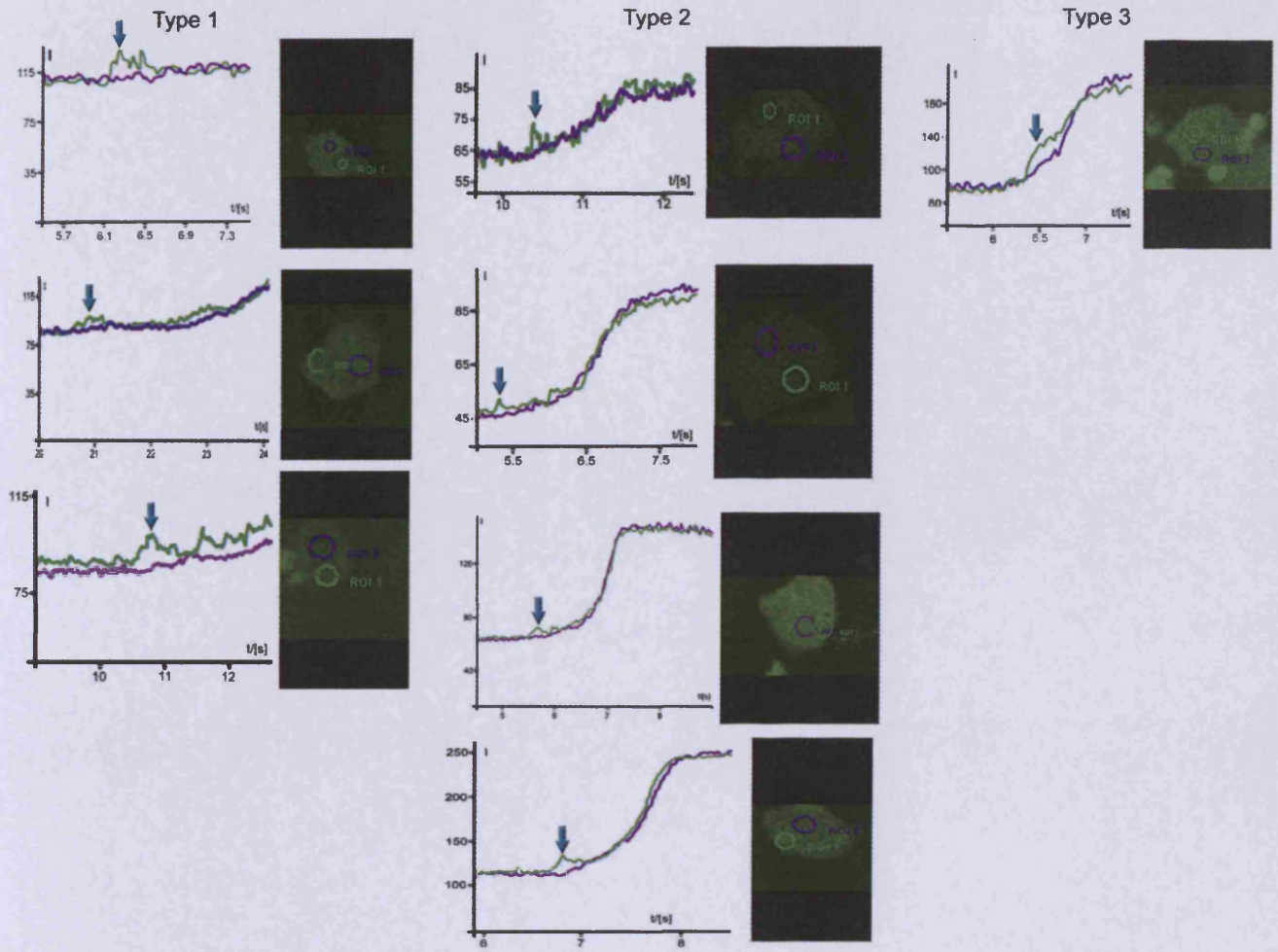

Fig 4.3.15 Examples of Ca^{2+} Puffs

Ca^{2+} puffs are crudely divided into three types. Type 1 occur without Ca^{2+} influx, where influx has been blocked by Ni^{2+} or in cells with no extracellular Ca^{2+} (chelated by EDTA). Type 2 are Ca^{2+} puffs distinguishable from Ca^{2+} influx. Type 3 are Ca^{2+} puffs that are seen during the Ca^{2+} influx wave as a region that appears to have a locally larger increase in Ca^{2+}.

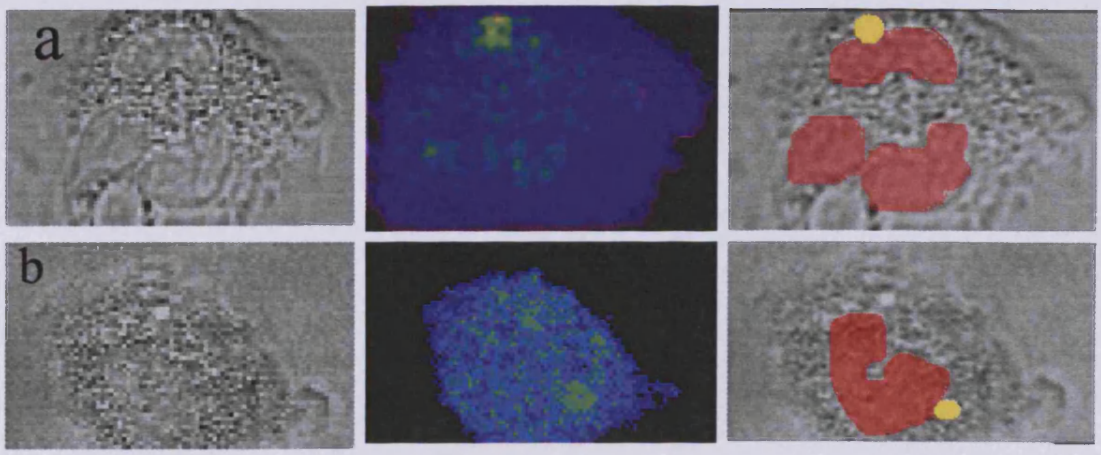

Fig 4.3.16 Ca^{2+} Puffs Located Near the Nuclear Boundary

Both examples show a phase contrast image of a neutrophil, the pseudocoloured Ca^{2+} distribution and an overlay of the nuclear lobes as located on the phase contrast and the location of the Ca^{2+} puff. The Ca^{2+} images each reveal a Ca^{2+} puff as a distinct region of locally elevated Ca^{2+}. The blue is background and green is elevated Ca^{2+}. In both cases here the Ca^{2+} puff was located adjacent to the nuclear lobes.

The distribution of cytosol relative to the multi-lobed nucleus was visualised in 3D by taking optical slices through a neutrophil loaded with a combination of mitotracker-red, lysotracker-red or acridine orange, which binds DNA and emits in the green spectrum. The optical slices were then integrated by Imaris software to produce the 3D reconstructions in Fig 4.3.17, illustrating the large nucleus occupying a significant proportion of the cell. Mitochondria, which may act as a Ca^{2+} diffusion "firewall" in some cells (Park et al, 2001), are few in neutrophils and mitotracker staining in living neutrophils showed that they are not placed appropriately to act in this way (Fig 4.3.18). Most mitochondria were imaged towards the centre of the neutrophil and could not act as a diffusion barrier that would restrict z-waves to the neutrophil edge.

4.3.11 Peri-Nuclear Ca^{2+} Events in Neutrophils

Despite the fact that the nuclear envelope is not a significant barrier to either Ca^{2+} or Fluo4, a hydrophobic Ca^{2+} indicator that partitioned into the nuclear envelope of neutrophils, MOMO, (Fig 4.3.19) was used to search for the cytosolic free Ca^{2+} z-wave. As the indicator was anchored at the nuclear envelope it was suitably placed to record Ca^{2+} towards the periphery of the neutrophil, and would provide an opportunity to capture the Ca^{2+} z-wave as it passed without significant diffusion of the indicator. However, as with the cytosolic Ca^{2+} probes, this indicator also failed to detect Ca^{2+} z-waves in either unstimulated polarised or stimulated neutrophils. However, this probe did record global and local changes in cytosolic free Ca^{2+} in response to fMLP (Fig 4.3.20). Uncaging IP_3 globally generated initial localised Ca^{2+} puffs, which were detected by MOMO in the nuclear clefts in a similar manner to fMLP. Therefore the nuclear location or shape did not provide an explanation for the reported peripheral location of Ca^{2+} z-waves.

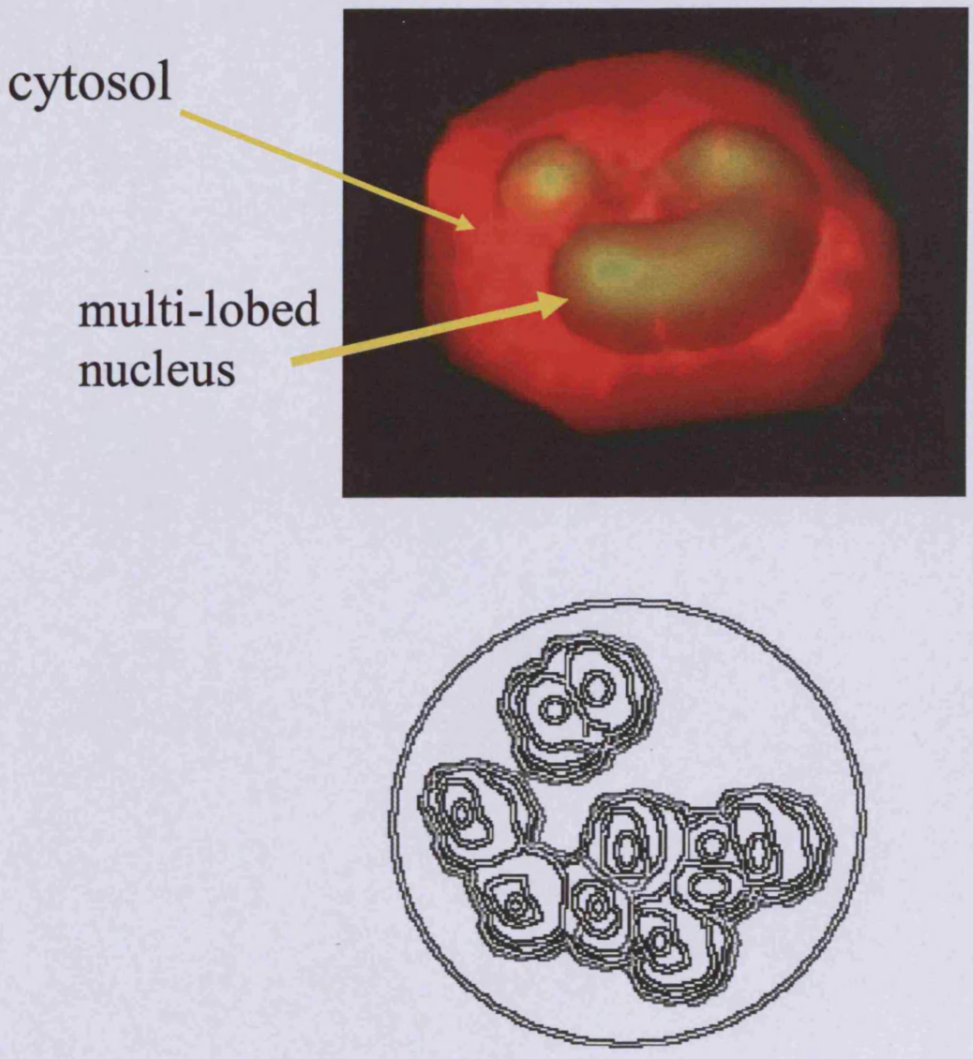

Fig 4.3.17 3D Reconstruction of The Neutrophil Nuclear Lobes Resembled By The Distribution Map For Ca^{2+} Puffs

Imaris software produced a 3D reconstructed image from confocal slices through a neutrophil to reveal the 3D shape and cytosolic position and volume of the nuclear lobes. The nuclear lobes are pseudocoloured green and the cytosol and plasma membrane are red. A topographical distribution map of Ca^{2+} puffs closely resembles the distribution of the nuclear lobes of mature neutrophils.

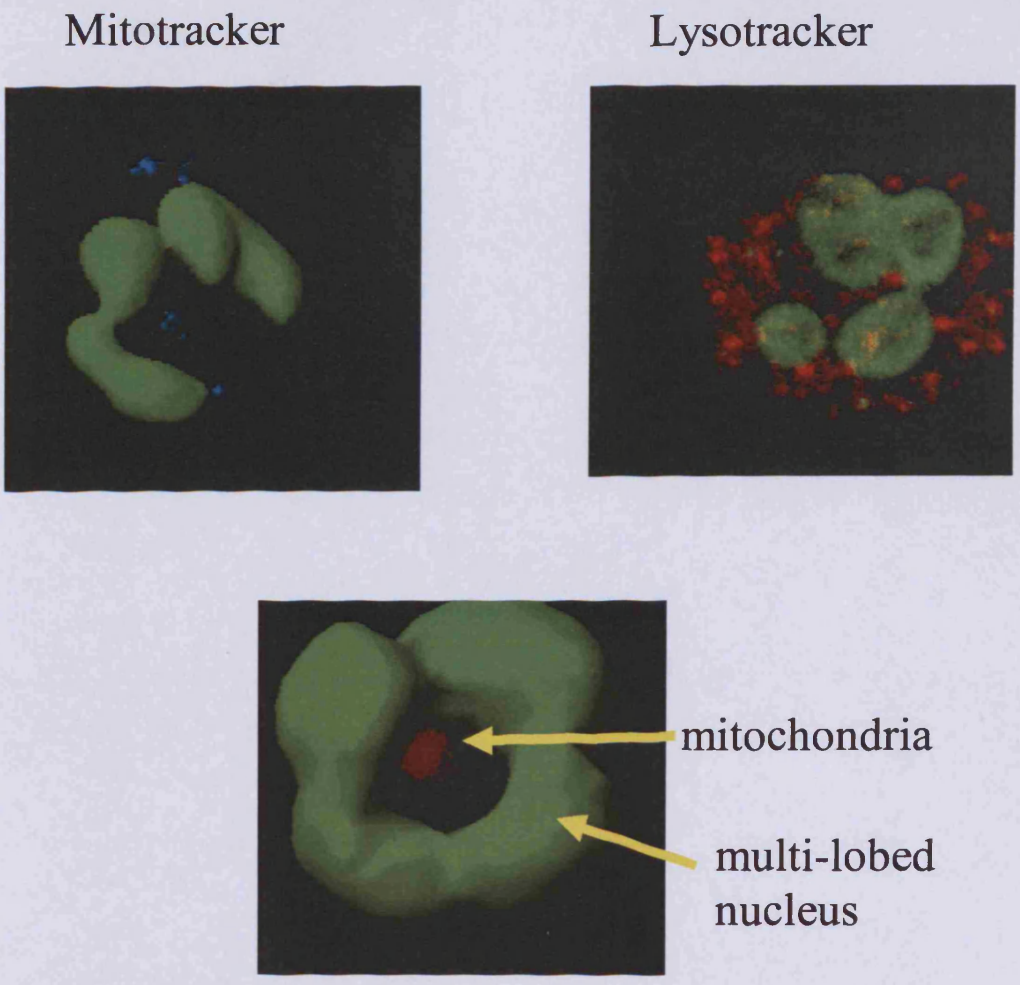

Fig 4.3.18 3D Reconstruction of Nuclear Lobes With Mitochondria And Lysosomes
The nucleus occupies a significant proportion of the cytosol of neutrophils. Mitotracker revealed just one or two regions of staining, indicating just one or two mitochondria per neutrophil, consistent with EM images. Lysotracker reveals ubiquitous distribution of lysosomes throughout the cytosol.

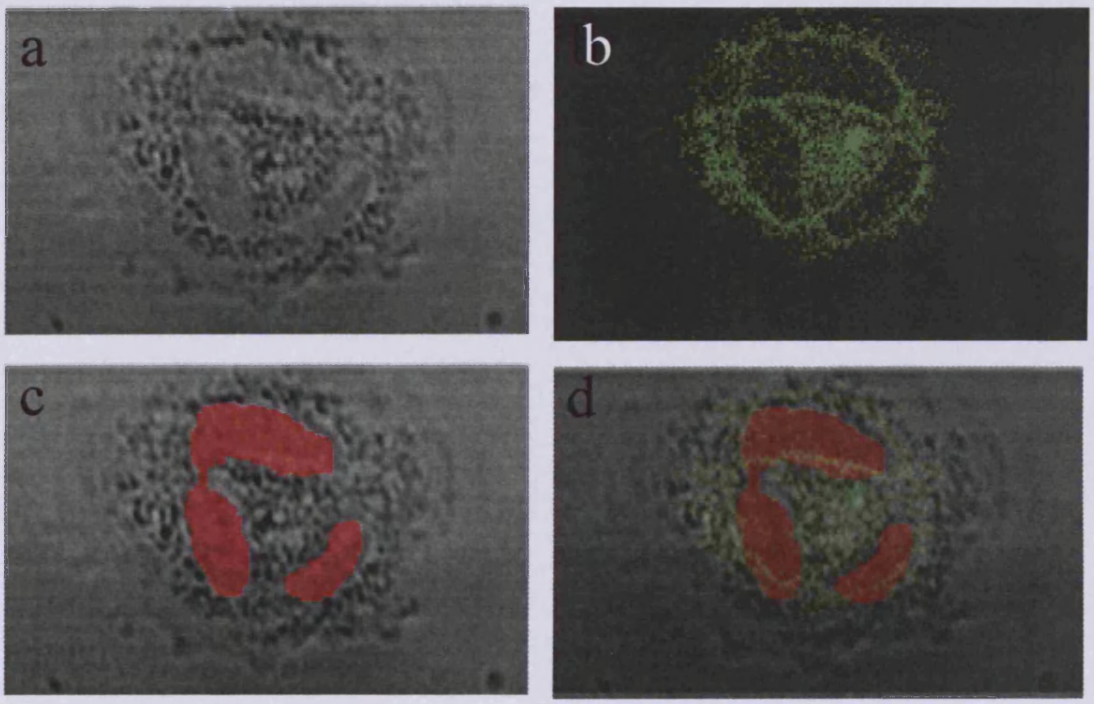

Fig 4.3.19 MOMO Localised To The Nuclear Envelope

(a) A phase contrast image of a neutrophil spread on a glass coverslip. (b) Confocal section of MOMO distribution. (c) Nuclear lobes as located from the phase contrast image. (d) Overlay of the nuclear lobes and MOMO. It can be clearly seen that MOMO localises to the nuclear envelope as well as other membrane rich organelles within the cytosol.

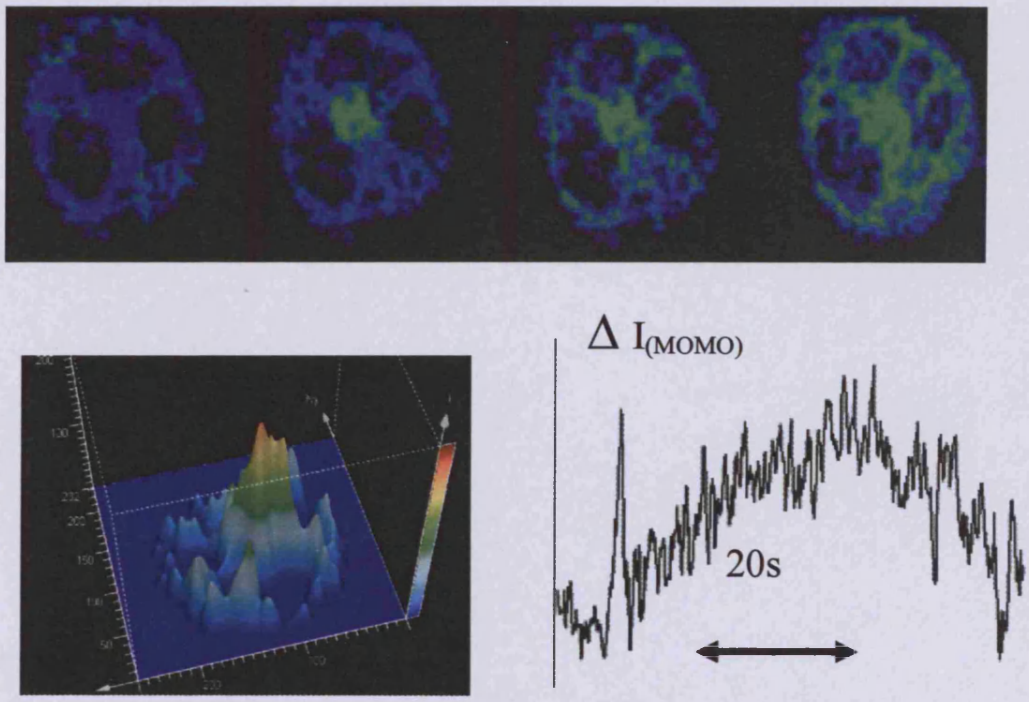

Fig 4.3.20 Perinuclear Ca^{2+} Events Detected By MOMO

The series of images following stimulation with fMLP revealed a Ca^{2+} event starting in a cleft between nuclear lobes. The images were pseudocoloured such that blue is the basal Ca^{2+} concentration and blue is elevated. MOMO did not enter the nuclear lobes and therefore they appear black. The Ca^{2+} event started in the nuclear cleft and spreads out towards the edge of the neutrophils until there was a global increase in the Ca^{2+} concentration. The Ca^{2+} puff is more clearly seen in the 3D plot illustrating it as having a concentration well above background. The trace shows the raw data for the change in MOMO fluorescence during the stimulation.

4.3.12 Ca^{2+} Storage Sites in Neutrophils

The single locus for the Ca^{2+} release site suggested that neutrophils may have only a small number (or one) Ca^{2+} storage location. This was suggestive of the single vestigial Golgi structure identifiable by electron microscopy (Bessis, 1973), which is associated with the nucleus. In order to test this, chlortetracycline (CTC) was used as a marker of a region of high Ca^{2+} concentration such as that expected to be within Ca^{2+} stores. Free CTC diffuses readily across membranes, but becomes unable to diffuse once bound to Ca^{2+} and so is a useful probe for Ca^{2+} stores. It has a low affinity for Ca^{2+} (Kd about 400 μM), and consequently accumulates at sites of very high Ca^{2+}, marking the locations of membrane enclosed high Ca^{2+} sites within the cell. In neutrophils, CTC accumulates into only one or two discrete organelles (Fig 4.3.21). The location of this organelle is similar to that expected for the vestigial Golgi structure, which can be stained by DiI (Fig 4.3.21e). There was no dramatic difference in the location of these sites in the "polarised" neutrophils (Fig 4.3.21a, d, e). The sites of the high Ca^{2+} storage organelles may correlate with the location of Ca^{2+} release sites (Pettit and Hallett, 1998).

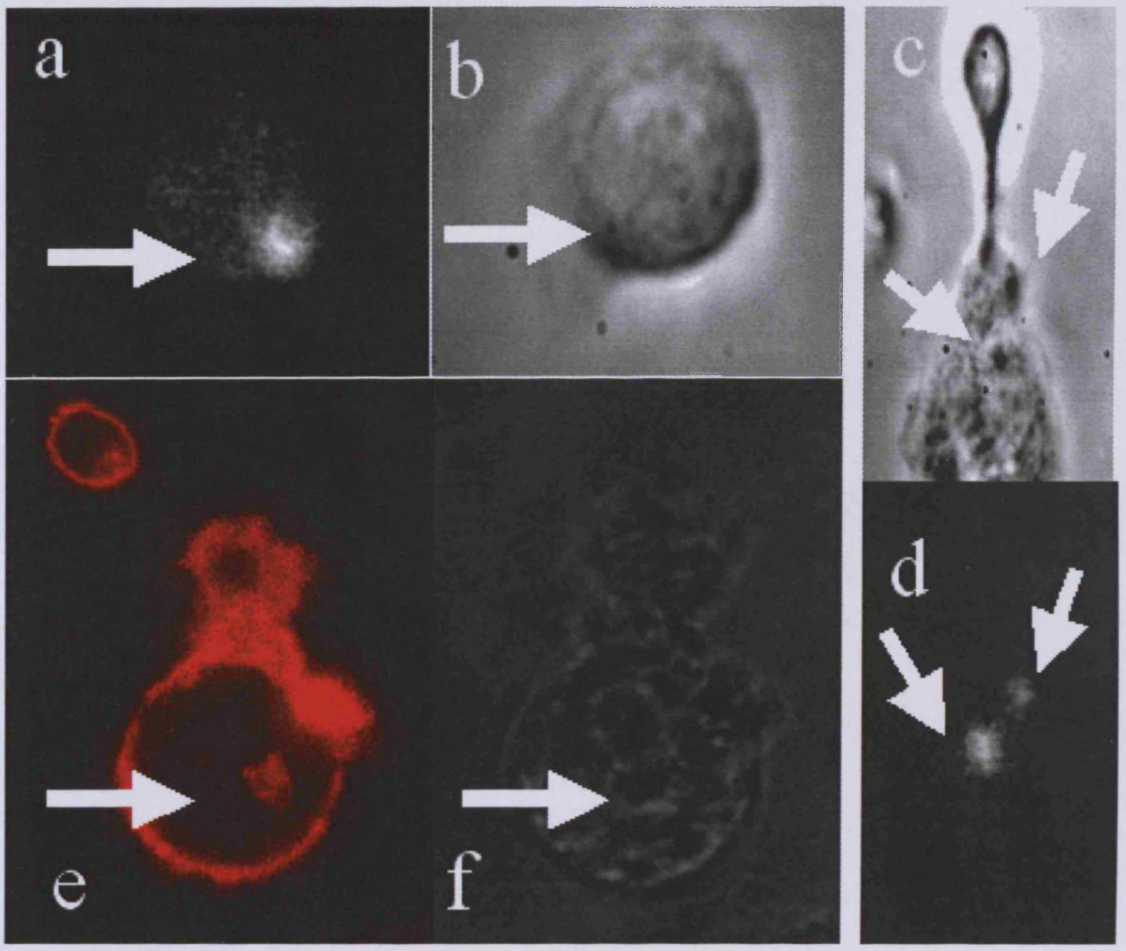

Fig 4.3.21 Few High Concentration Ca^{2+} Storage Sites Within Each Neutrophil
Chlortetracycline (CTC) has a low affinity for Ca^{2+} and cannot diffuse once bound to Ca^{2+}. Therefore it accumulated at sites of high $[Ca^{2+}]$. (a) reveals a distinct puncta of CTC in a non-polarised neutrophil as seen in the brightfield image (b). (c) shows the brightfield image of a motile, polarised neutrophil. (d) two distinct puncta of CTC were revealed within this neutrophil. (e) is a confocal image of a DiI loaded polarised neutrophil, pseudocoloured, revealing one distinct region of equivalent to the CTC accumulation. The region is marked on the corresponding phase contrast image (f). The brightfield and phase contrast images indicate that the CTC accumulation occurs near the nuclear lobes of the neutrophil.

4.4 Discussion

The Ca^{2+} toolkit contains many different components as detailed in Chapter 1. Neutrophils utilise many of these tools to make up their Ca^{2+} signalling events. Petty et al had reported a small, elevated travelling zone of elevated Ca^{2+} in neutrophils, referred to here as the "z-wave". These Ca^{2+} "z-waves" were not seen throughout the course of these experiments, despite numerous attempts to stimulate and visualise them. It was determined that the lack of recorded "z-waves" was not due to deficiencies in the technology, nor the experimental parameters used.

Despite the lack of the "z-wave", more conventional Ca^{2+} signalling events were recorded and characterised at high speed. The most notable of these is the Ca^{2+} puff, which has been characterised for the first time here in chapter 4. The Ca^{2+} puffs were induced by extracellular stimulus with fMLP. The fMLP binds to the g-protein coupled transmembrane receptor. The receptor then triggers a number of signalling cascades, culminating in the central point of the production of IP_3. IP_3 binds to the IP_3R in the membrane of the intracellular Ca^{2+} store. In most cells this is the endoplasmic reticulum (ER). However, during the differentiation of myeloid cells to produce neutrophils, the ER is lost. Electron microscopy (EM) images have indicated a potential 'vestigial ER', which could be the neutrophilic Ca^{2+} store. This vestigial ER appears to be continuous with the nuclear envelope. Binding of IP_3 to the IP_3R causes release of Ca^{2+} from the store. This is referred to as the Ca^{2+} puff many cell types, such as pancreatic acinar cells, cardiac myocytes, rat basophils (Bootman et al, 1997: Thomas et al, 2000: Tovey, 2001). Studies were undertaken to try to identify the source of these Ca^{2+} puffs in neutrophils. The microanatomy was reconstructed in 3D, but the most likely culprit remains a peri-nuclear high Ca^{2+} store as revealed by CTC

staining. The 3D reconstructions also failed to identify any likely cause of a "z-wave". It is possible that the reported "z-wave" was an artefact of the experimental conditions, such as changes in pH near the plasma membrane affecting the fluorescence of the probe, but it is deemed unlikely to be the result of changes in Ca^{2+}.

Similar Ca^{2+} events were also induced by photolytically uncaging IP_3 inside the neutrophils. This also resulted in conventional Ca^{2+} puffs and waves. This technique allowed the specific IP_3 pathway to be stimulated, reducing the chances of potential cross talk that can occur with fMLP stimulation, which results in other second messengers being produced down the g-protein linked receptor pathways. This highly controllable, specific technique is suitable for further studies into the effects of IP_3-mediated Ca^{2+} signals.

In many cell types, the emptying of the Ca^{2+} store induces opening of the Ca^{2+} channels in the plasma membrane. The Ca^{2+} floods into the cytoplasm of the cell down its concentration gradient that is maintained between the extracellular and intracellular medium by ATPases. For a long time it was not known how the emptying of intracellular Ca^{2+} stores resulted in the opening of Ca^{2+} channels in the plasma membrane. However, research by two different groups led to the report of a small molecular weight protein. This was dubbed Orai1 and STIM1 by the two groups. It was thought that these two proteins are one and the same, although recent research has indicated that they work in co-ordination to bring about Ca^{2+} influx as a result of store depletion. The mechanism of action of STIM1 and Orai are still debatable. However, in a recent review Parekh (2007) proposed three possible mechanisms of action as illustrated in Fig 4.5.1. Briefly, as Ca^{2+} is released from stores, Orai1 may be

stimulated to cause Ca^{2+} influx, but more likely is that as the concentration decreases, and Ca^{2+} dissociates from the EF-hand binding sites on STIM1. This causes the STIM1 to aggregate and translocate to distinct puncta in the store membrane. These puncta then interact with the CRACM1 protein in the plasma membrane to form a Ca^{2+} pore that directly channels Ca^{2+} from the extracellular milieu into the store, thus replenishing the depleted Ca^{2+} store. This would account for the time delay between Ca^{2+} release events in cells. Research is ongoing in this area and it remains uncertain whether this system plays a role in neutrophil Ca^{2+} signalling. However, this work has shown that IP_3 mediated Ca^{2+} store release plays a significant role in Ca^{2+} puffs and further Ca^{2+} signals in neutrophils.

4.5 Conclusion

The Ca^{2+} puffs we have found were similar in magnitude and duration to those reported in HeLa and basophilic cells (Bootman et al, 1997: Thomas et al, 2000: Tovey, 2001). We were, however, unable to detect any evidence for the reported Ca^{2+} z-waves using either cytosolic mobile or membrane immobilised Ca^{2+} indicators.

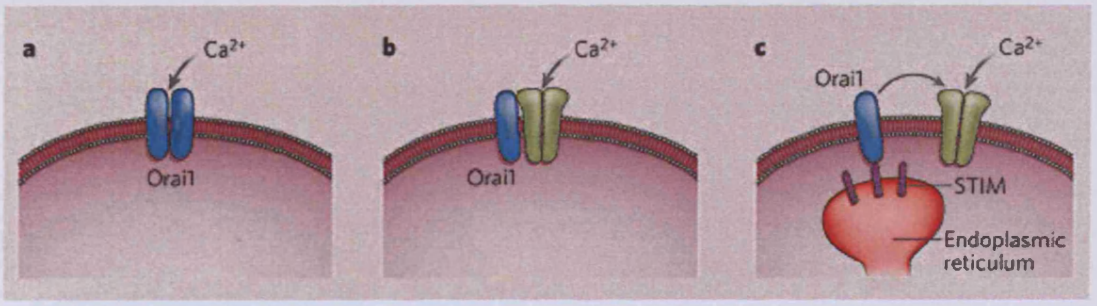

Fig 4.5.1 Three Potential Mechanisms of Action for STIM1

(a) Orai1 acts as the actual Ca^{2+} influx channel. (b) Orai1 activates an endogenous Ca^{2+} channels or (c) Orai1 activates an endogenous Ca^{2+} channel after interaction with STIM1 on the Ca^{2+} depleted ER. (Taken from Parekh, 2007)

CHAPTER 5

Morphology Alteration in Neutrophils During Cytosolic Ca^{2+} Changes

5.1 Introduction

The development and progression of inflammation is driven by the infiltration of leukocytes, especially neutrophils, into inflamed tissues from the circulation. This process is initially signalled by an array of cytokines that upregulate adhesion molecules such as ICAM-1 on vascular endothelial cells. This increases the adhesion of rolling neutrophils to the area of the blood vessel adjacent to the inflammed tissue and drives the extravasation mechanisms. These "inflammatory cytokines" have already become targets for therapeutic intervention in chronic inflammation, for example anti-TNFα therapy. However, the primary and common step in all inflammation is the adhesion and spreading of the neutrophil onto the endothelial surface. The dramatic morphological change of the neutrophil spreading reduces the surface area exposed to the flow forces of the circulating blood and leaves the cell in a suitable morphological condition to be able to extravasate either between endothelial cells or through an individual cell (see Chapter 1). The cellular machinery for this "neutrophil spreading" response remains poorly understood and therefore not suitable as a therapy target.

The pioneering work of Maxfield showed that neutrophils and macrophages spreading onto surfaces is preceded by large global increases in cytosolic free Ca^{2+} (Krusal et al, 1986: Krusal and Maxfield, 1987). These Ca^{2+} signals are clearly caused by adhesive signals from the surface to the cell. It has subsequently been shown that the immobilisation of cellular receptors such as the β2-integrin by surfaces or cross-linking of anti-integrin antibodies triggers similar Ca^{2+} signals to those discovered by Maxfield (Ng-Sikorski et al, 1991: Petersen et al, 1993). However, there is a fundamental problem in

experimentally investigating the relationship between Ca^{2+} signalling and the cell spreading event. Namely, the event (cell spreading) cannot occur without a surface for the cell to spread onto. Yet, the stimulus for the Ca^{2+} is provided by this same contact with a surface. In an early attempt to overcome this problem, cytosolic free Ca^{2+} was experimentally elevated by loading neutrophils with caged Ca^{2+} and uncaging the Ca^{2+} before the spontaneous or surface-induced spreading had occurred (Petitt and Hallett, 1998). This method established that elevating cytosolic free Ca^{2+} in this way could induce neutrophil spreading; it was found that the global concentration of cytosolic free Ca^{2+} required was much higher than physiologically occurred across the whole cell. This left uncertainty as to the physiological relevance of this data.

As described in previous chapters, work was carried out to establish that uncaging IP_3 elevates cytosolic free Ca^{2+} in neutrophils. This allowed another opportunity to study the relationship between Ca^{2+} and neutrophil spreading. The physiological route of elevating cytosolic free Ca^{2+} involves IP_3 generation, triggering Ca^{2+} release from intracellular IP_3-sensitive stores and influx of extracellular Ca^{2+}. Thus elevating IP_3 provides a trigger for "physiological" Ca^{2+} elevations. This experimental strategy would therefore be more likely to provide physiologically relevant insight into the Ca^{2+} related mechanism of neutrophil spreading.

5.1.1 Aims

The aim of the work presented in this chapter was to employ the experimental strategy of uncaging IP_3 to trigger cytosolic free Ca^{2+} signals within the physiological range, and

establish the effect on subsequent neutrophil morphological changes, specifically spreading. As IP_3 production causes release from Ca^{2+} stores as well as Ca^{2+} influx, it was necessary to dissect out these two components to establish which is vital to the cell spreading phenomenon. In an attempt also to establish down stream effects of elevated Ca^{2+} in the cell spreading response, a known target for Ca^{2+} was inhibited: the Ca^{2+}-activated protease calpain.

5.2 Methods and Materials

5.2.1 Ca^{2+} Measurement and Manipulation

Cytosolic free Ca^{2+} was measured as described in detail elsewhere (Section 2.3.4) using the resonant scanning head of the Leica RS confocal microscope, which had a frequency of approximately 40 MHz and was restricted to a field size of 32 x 512 pixels. Bi-directional data acquisition was used after manual adjustment of the phase to ensure synchronised data alignment in both directions. Neutrophils were allowed to adhere to the glass coverslip mounted onto a thermostatically control stage ($37 \pm 0.1\ ^{0}C$) in Krebs medium and soluble stimuli such as fMLP were added to them during a data acquisition run. During image acquisition, uncaging was achieved by positioning of an additional dichroic mirror and band pass filter to illuminate the microscopic field with UV (330 - 360 nm) light (430 DCLPO2 dichroic; Omega Optics) from a 100 W mercury arc lamp. It was shown, using caged fluorescein as a surrogate read-out, that this procedure generated photolytic product linearly with no initial time delay.

5.2.2 Quantification of Ca^{2+} and Morphological Changes

Adjustments to gain and offset were applied to whole time series data sets to allow genuine comparisons within a time sequence. Ratio images (F/Fo) were taken to negate differences in Ca^{2+} probe loading, but this never revealed Ca^{2+} signals that were not evident in the raw fluorescent intensity data set. Cytosolic free Ca^{2+} was calculated using the following equation, with the Kd for Fluo4 taken as 600 nM. Ca^{2+}=Kd[F-Fmin]/[Fmax-F]. Fmin and Fmax were found for Ca^{2+}-free and Ca^{2+} saturating probe as described earlier. Localised Ca^{2+} puffs were identified visually and confirmed by

statistical comparison of the "noise" in different locations in the cell (as described in Chapters 2 and 3). The cell morphology change during neutrophil spreading was dramatic and easily quantified by counting individual cells. For time relationships, the cell area or periphery was measured frame-by-frame or on specific frames at timed intervals using ImageJ software (NIH) and ImageMaster (PTI). All data shown were representative of a number of different experimental runs from at least three different blood donors as the source of neutrophils.

5.2.3. ECIS Quantification of Neutrophil Spreading

The kinetics of cell spreading was also quantified using Electric Cell–Substrate Impedance Sensing (ECIS), which is a non-invasive means of monitoring the kinetics of spreading of very small populations of neutrophils (about 5 cells / electrode) onto a 250 μm diameter gold electrode coated with fibronectin. As the neutrophils spread they reduce the effective area of electrode and the impedance signal rises (Wegener, et al, 2000). All measurements were performed at 37 °C and the final outcome confirmed by microscopic inspection of the electrodes.

5.3 Results

5.3.1 Elevation of Cytosolic Free Ca^{2+} Induces Neutrophil Spreading

Having established the characteristics of the Ca^{2+} signal induced by uncaging IP_3 in Chapter 4, it was possible to use this approach to investigate the effect of physiological Ca^{2+} signalling on neutrophil morphology. It was found that loosely adherent but spherical neutrophils underwent a rapid transformation into a flattened, "spread" morphology following IP_3 uncaging (Fig 5.3.1). In the control cells, the absence of photolysis of loaded cells, or photolysis of non-loaded cells the spreading rates were comparable and similar to the rate in the experimental cells before photolysis. However during photolysis of caged IP_3 there was an abrupt increase in the rate of spreading (Fig 5.3.1). Neutrophils also spread spontaneously on integrin engaging surfaces (such as fibronectin). On this surface, it was still possible to demonstrate an effect of IP_3 uncaging, by choosing cells that had not begun to spread (Fig 5.3.2). Under these conditions, the Ca^{2+} signal induced by IP_3 uncaging was not a simple response, but often had additional oscillations (e.g. Fig 5.3.2). It should be noted that in the absence of IP_3 uncaging, neutrophils on integrin engaging surface will both spontaneously signal Ca^{2+} and spread. The complex Ca^{2+} signal triggered by IP_3 uncaging in neutrophils in contact with the integrin-engaging surface was reminiscent of the multi-peak Ca^{2+} signals that occur during integrin-mediate phagocytosis (Dewitt & Hallett, 2002: Dewitt et al, 2003). The complexity of the Ca^{2+} signal has been attributed to cycles of Ca^{2+}-induced integrin untethering and mobilisation followed by further integrin induced Ca^{2+} signalling (Dewitt & Hallett, 2002: Dewitt et al, 2006).

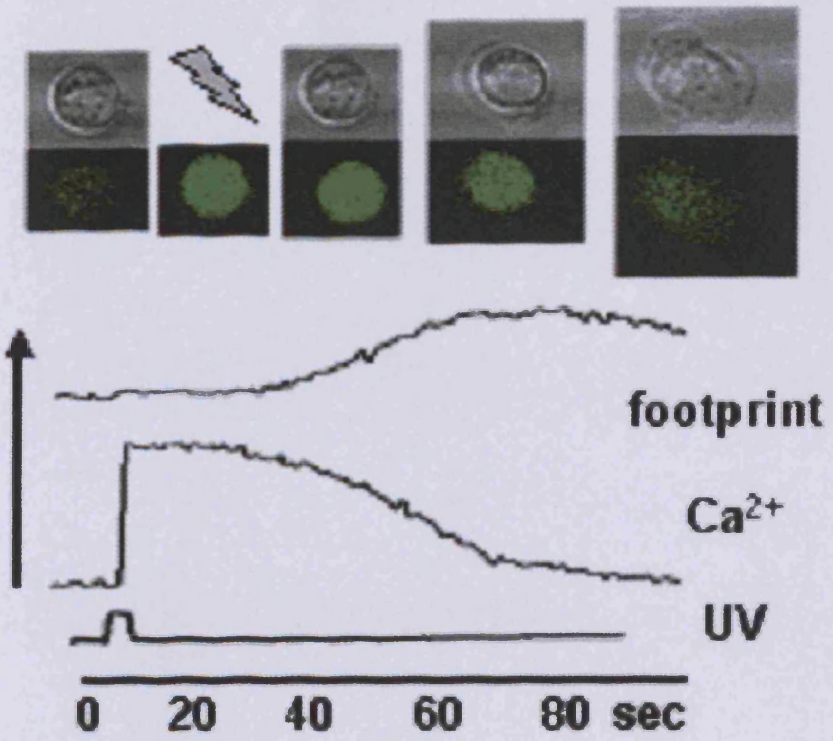

Fig 5.3.1 IP_3 Induced Neutrophil Spreading

The neutrophil shown has been loaded with Fluo4 (as an indicator of cytosolic free Ca^{2+}) and caged IP_3 from their membrane permeable esters. The upper panel shows images from a time sequence in which the top series are phase contrast images and the bottom series are the corresponding Fluo4 intensity images. At the image marked by the "lightning bolt", the uncaging wavelength (360 nm) was used. In the lower panel, the data is quantified. The graph marked "UV" show the 360 nm intensity. The graph marked "Ca^{2+}" shows the cytosolic free Ca^{2+} concentration and the graph marked "footprint" shows the area occupied by the cell (as a measure of spreading). (x axis are size of footprint, Ca^{2+} concentration and UV exposure respectively as labelled). This result was typical of at least 30 other experiments.

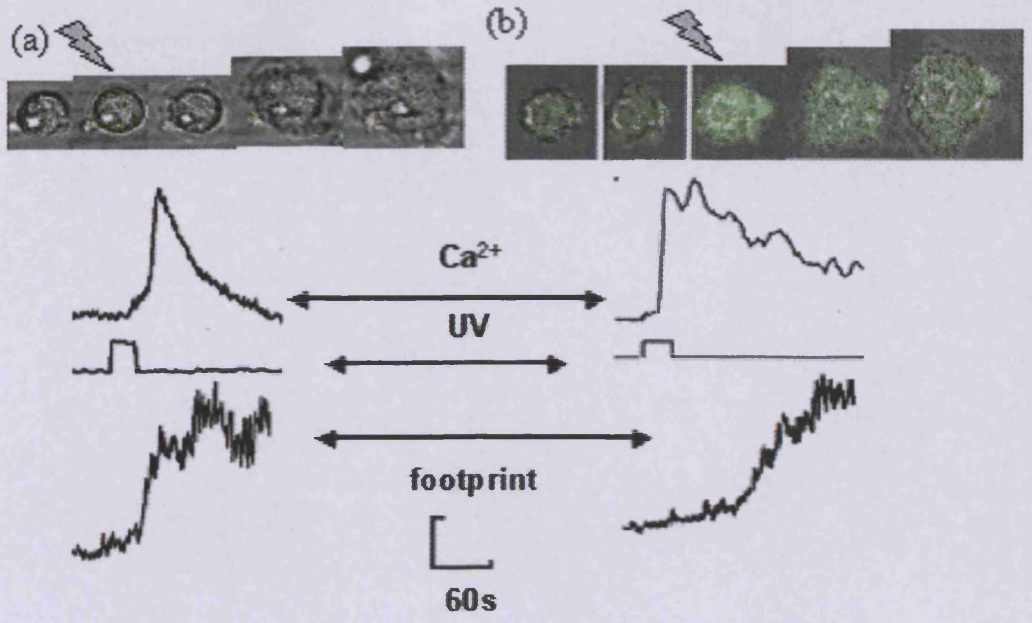

Fig 5.3.2 Comparison of IP_3 Induced Ca^{2+} Signal and Spreading Response on Glass or Integrin-Engaging Fibronectin

The neutrophils shown have been loaded with Fluo4 (as an indicator of cytosolic free Ca^{2+}) and caged IP_3 from their membrane permeable esters. The upper panel shows images from a time sequence in which the Fluo4 intensity has been superimposed on the phase contrast images. At the image marked by the "lightning bolt", the uncaging wavelength (360 nm) was used. In the lower panel, the data is quantified. The graph marked "UV" show the 360 nm intensity. The graph marked "Ca^{2+}" shows the cytosolic free Ca^{2+} concentration and the graph marked "footprint" shows the area occupied by the cell (as a measure of spreading). (a) A typical response of neutrophil Ca^{2+} signalling and spreading onto untreated glass and (b) a typical response of Ca^{2+} signalling and spreading onto fibronectin coated glass. This result was typical of five other experiments.

The onset of the rapid phase of spreading on glass coincided with the large Ca^{2+} signal rather than IP_3 induced trickle (shoulder) in 15 out of 16 cells in which the shoulder was clearly discernible. As the shoulder was associated with the Ca^{2+} release event rather than the Ca^{2+} influx event (Chapter 4), this suggested that Ca^{2+} influx may be the important Ca^{2+} signal.

5.3.2 Neutrophil Spreading Requires Ca^{2+} Influx

In order to establish whether the critical Ca^{2+} component temporally associated with the large Ca^{2+} signal was by Ca^{2+} influx, Ni^{2+} ions, were used to block the Ca^{2+} influx component. This strategy was shown to inhibit the large Ca^{2+} influx signal but not the Ca^{2+} release event visualised as a Ca^{2+} puff (Chapter 4). When Ca^{2+} influx was abolished by this route, neutrophils failed to spread in response to IP_3 uncaging (Fig 5.3.3). It was therefore concluded that IP_3 itself was not the crucial component, but that it was Ca^{2+} influx, through Ca^{2+} channels opened as a result of IP_3 mediated Ca^{2+} store release. This conclusion was consistent with the concept of high sub-plasma membrane Ca^{2+} associated with Ca^{2+} influx as the crucial signal. Ca^{2+} influx can generate concentrations of sub-plasma membrane Ca^{2+} in neutrophils in excess of 30-50 μM (Davies & Hallett, 1996, 1998). This localised high Ca^{2+} may activate sub-plasma membrane calpain-1, whose Kd is about 30 μM (Michetti et al, 1997). The sub-plasma membrane domain thus may be key for controlling neutrophil shape (Hallett & Dewitt, 2007: Dewitt & Hallett, 2007: Hallett et al, 2008). It also provides an explanation for the need for very high free Ca^{2+} when uncaging global Ca^{2+} rather than, as here, IP_3.

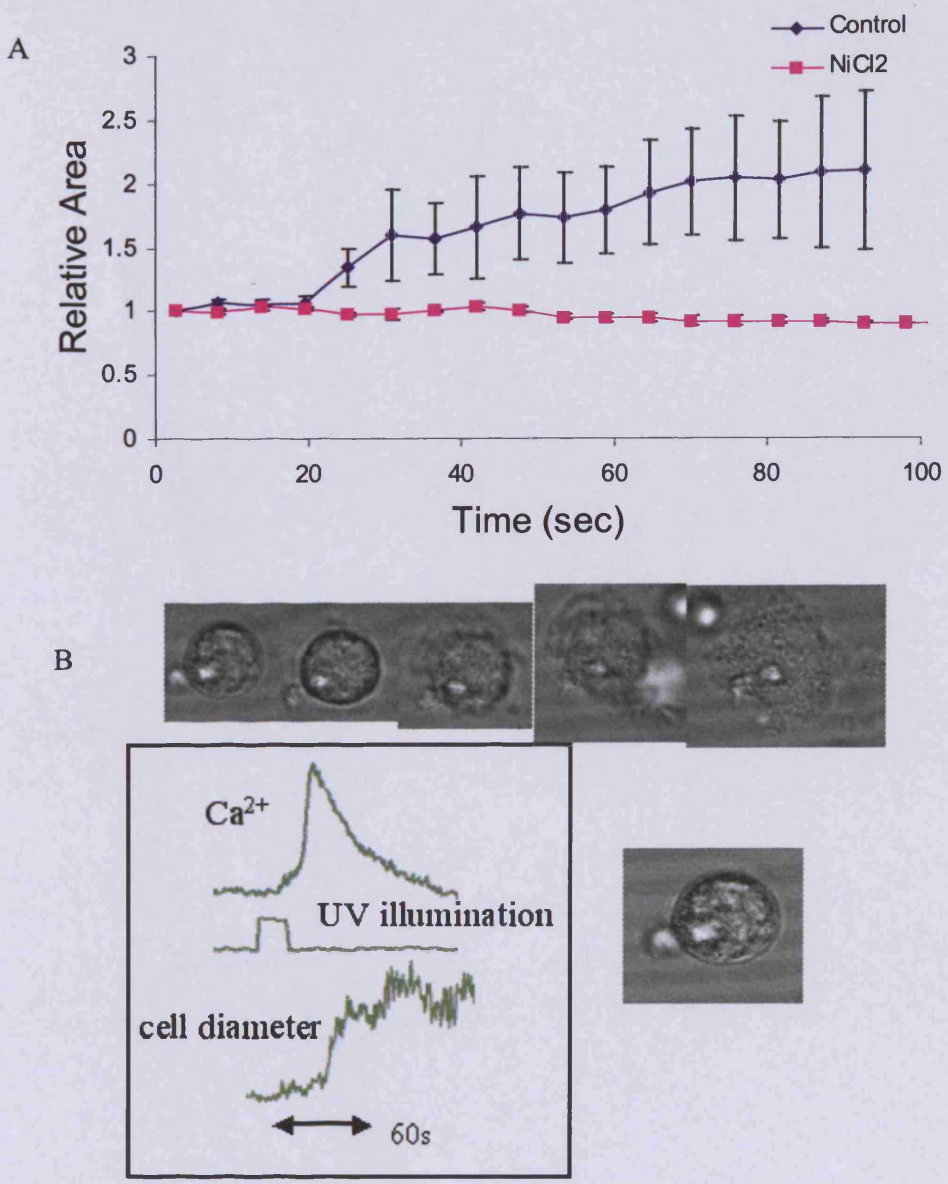

Fig 5.3.3 Inhibition of IP_3 Induced Spreading Response

Neutrophils were loaded with the Ca^{2+} probe Fluo4 and caged IP_3 via ester derivatives. The IP_3 was released by exposure to UV (360 nm) irradiation. (A) The area occupied by the neutrophil in the brightfield image was plotted for normal cells and those treated with Ni^{2+} (50 μM) to block Ca^{2+} influx. Shown as n=4 ± SD. (B) Series of images showing a spreading neutrophil in response to the Ca^{2+} influx that results from UV uncaging of IP_3. The trace shows sequence of UV then Ca^{2+} increase then increase in cell diameter.

5.3.3 Inhibition of Morphological Neutrophil Spreading by Calpain Activation Blockade

Two calpain inhibitors were used, which have separate modes of action. The calpain inhibitors PD150606 acts on calpain by binding to a non-EF Ca^{2+} binding site on calpain (Lin et al, 1997). It thus prevents the activation of calpain by Ca^{2+}. The calpain inhibitor, calpeptin inhibits the proteolytic site of the enzyme (Fig 5.3.4). It thus will inhibit proteolytic activity. The two molecules are also distinct in structure (Fig 5.3.4). Each inhibitor had no effect of Ca^{2+} signalling, but did significantly inhibited IP_3-induced spreading (Fig 5.3.5). The number of neutrophils adherent and spreading on integrin engaging surfaces as determined microscopically was also inhibited (Fig 5.3.6). This provided evidence that calpain was involved in the Ca^{2+} mediated spreading process.

5.3.4 Inhibition of Impedance Related Spreading by Calpain Activation Blockade

In the previous sections, neutrophil spreading was determined by microscopic observation alone. There are two potential problems with this approach. The first is that of observer bias. Although there was no selection of field to count cells, judgement was required to establish whether the cells were "spread" or not. Secondly, non-adherent cells tend to move around by refloating. This acts as bias as experiments on uncaging, for example, can only be performed if the cell remains in the same location. A non-subjective method that would not be biased by non-adherent cells was therefore sought.

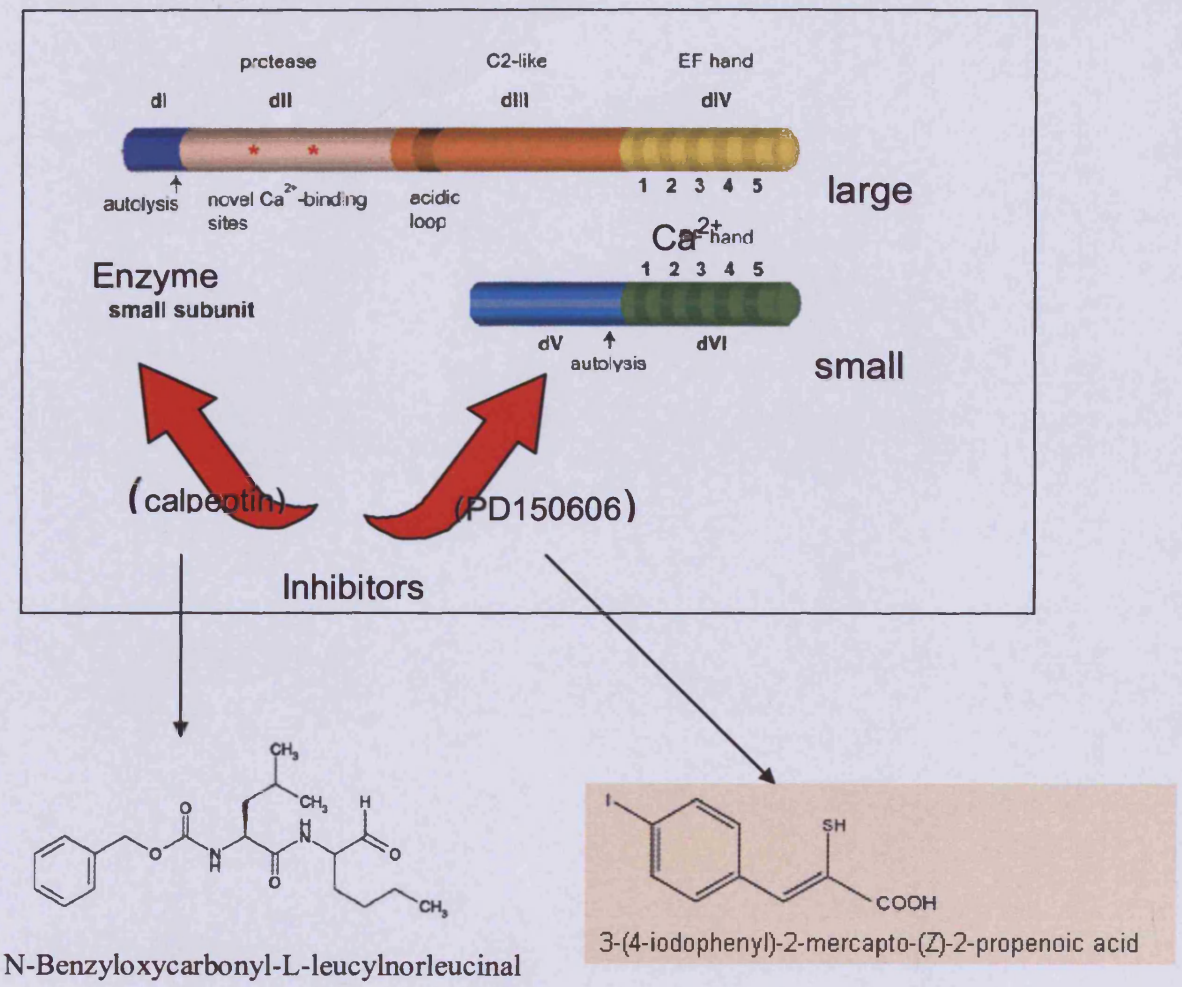

Fig 5.3.4 Calpain Inhibitors

A schematic of the calpain protein is shown with both subunits. The two commonly used calpain inhibitors work on different regions of the peptide. PD150606 binds a non-EF Ca^{2+} binding site preventing Ca^{2+} activation of calpain. Calpeptin inhibits the proteolytic site of the enzyme, thus preventing its functionality. These two inhibitors are distinct in structure.

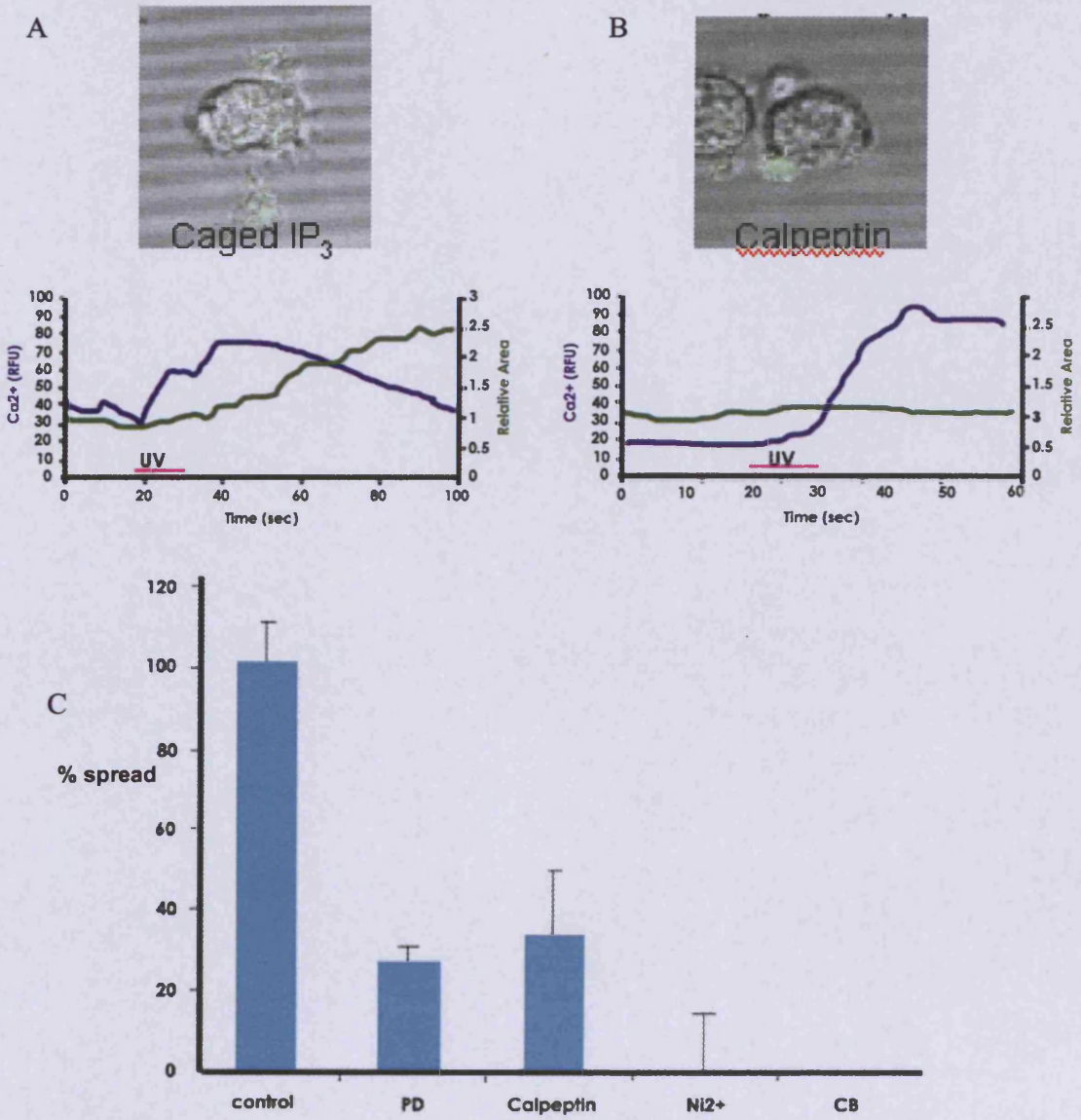

Fig 5.3.5 Inhibiting Calpain Activity Prevents Cell Spreading but not Ca^{2+} Influx

Neutrophils were loaded with caged IP_3 and Fluo4 (Ca^{2+} indicator). UV light was used to uncage IP_3 and trigger Ca^{2+} signals as shown in both traces above. In the left panel (A) the neutrophil spread out (green) as a result of the Ca^{2+} influx (blue). However in the right panel (B) the Ca^{2+} signal was normal but spreading was inhibited by the calpain inhibitor calpeptin (50 μM). The same effect was true of PD160505 (50 μM) as shown in the graph (C). Ni^{2+} blockade (1 mM) of influx completely inhibited spreading as did treatment with cytochalasinB. All the treatments are significantly different from the control ($p<0.05$, t-test), but not each other.

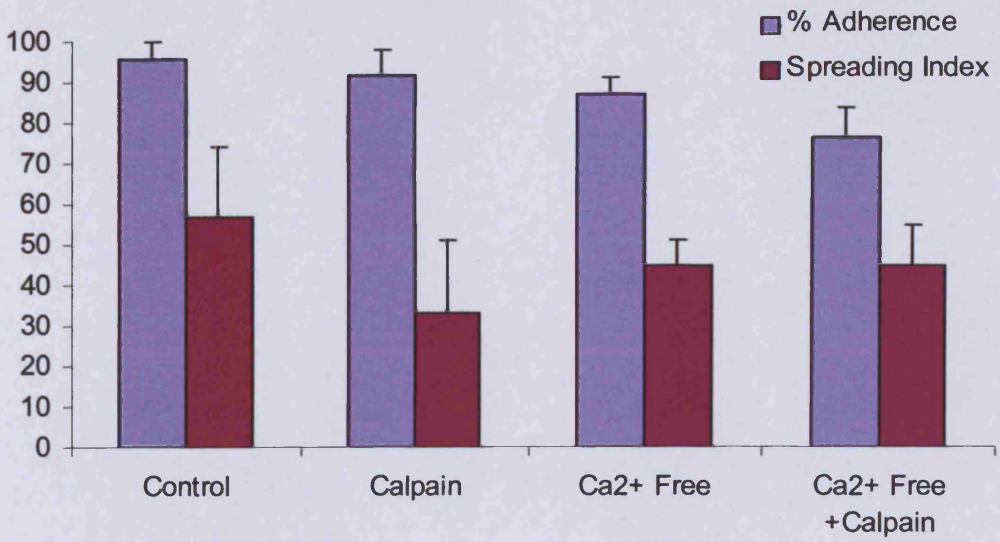

Fig 5.3.6 Calpain Inhibition Decreases Spreading without Impeding Adhesion

Neutrophils were put in conditions of either calpain inhibition (calpeptin, 50 μM) or Ca^{2+} free medium containing EDTA or both. They were then allowed to settle onto a glass coverslip and the % adherence calculated as cells remaining after washing / total cells settled onto coverslip. A combination of Ca^{2+} free medium and calpain inhibition significantly reduced adherence ($p<0.05$). A spreading index was also calculated. Calpain inhibition significantly prevented spreading $p<0.05$) and Ca^{2+} free medium had a similar effect, although not significant in this experiment. A combination of the two did not make a further difference. N=5 (± SD).

Firm adherence of cells to electrically conducting substrates (electrode) reduces the area of the electrode available. The more cells attached or the larger area occupied by the same cells (spreading) the greater the reduction in apparent electrode area. This effect has been exploited in systems that measure the electrical impedence of the electrode/substrate as cells attached (ECIS). Although it is a non-imaging approach, the gold electrode is thin enough to allow low resolution imaging of the area from which the electrical measurements are taken. A non-imaging approach, measuring the electrical impedance resulting from neutrophils adherence was very sensitive and could distinguish small numbers of spread neutrophils (Fig 5.3.7a). However, extreme care must be taken as solvents such as DMSO also affect the impedance measurement at this sensitivity. Also the measurement is sensitive to changes in temperature and proteins. It was also found the signal unexpectedly decreased rather than increased with some protein coatings. Despite this, with care, measurements could be taken. In Fig 5.3.7b, a comparison between the signal from medium alone and medium containing cells is shown. On addition of cells, the signal (unexpectedly) decreases relative to medium alone. It is not known why this occurs but it was reproducible. The addition of DMSO (0.01 %) elicits an increase in signal in both the medium alone and the medium containing cells experiment. Clearly this is an artefact unrelated to cell spreading behaviour. However, while the addition of fMLP (dissolved in DMSO) elicits a similar artefact in the medium only control, the cells show a clear impedance signal. Separate experiments showed that as with glass substrate, the addition of fMLP induced rapid neutrophil spreading. The second addition of fMLP produced only the DMSO artefact signal in both cell containing and cell absent conditions. Thus while there are clear artefacts, it is possible to interpret the signals.

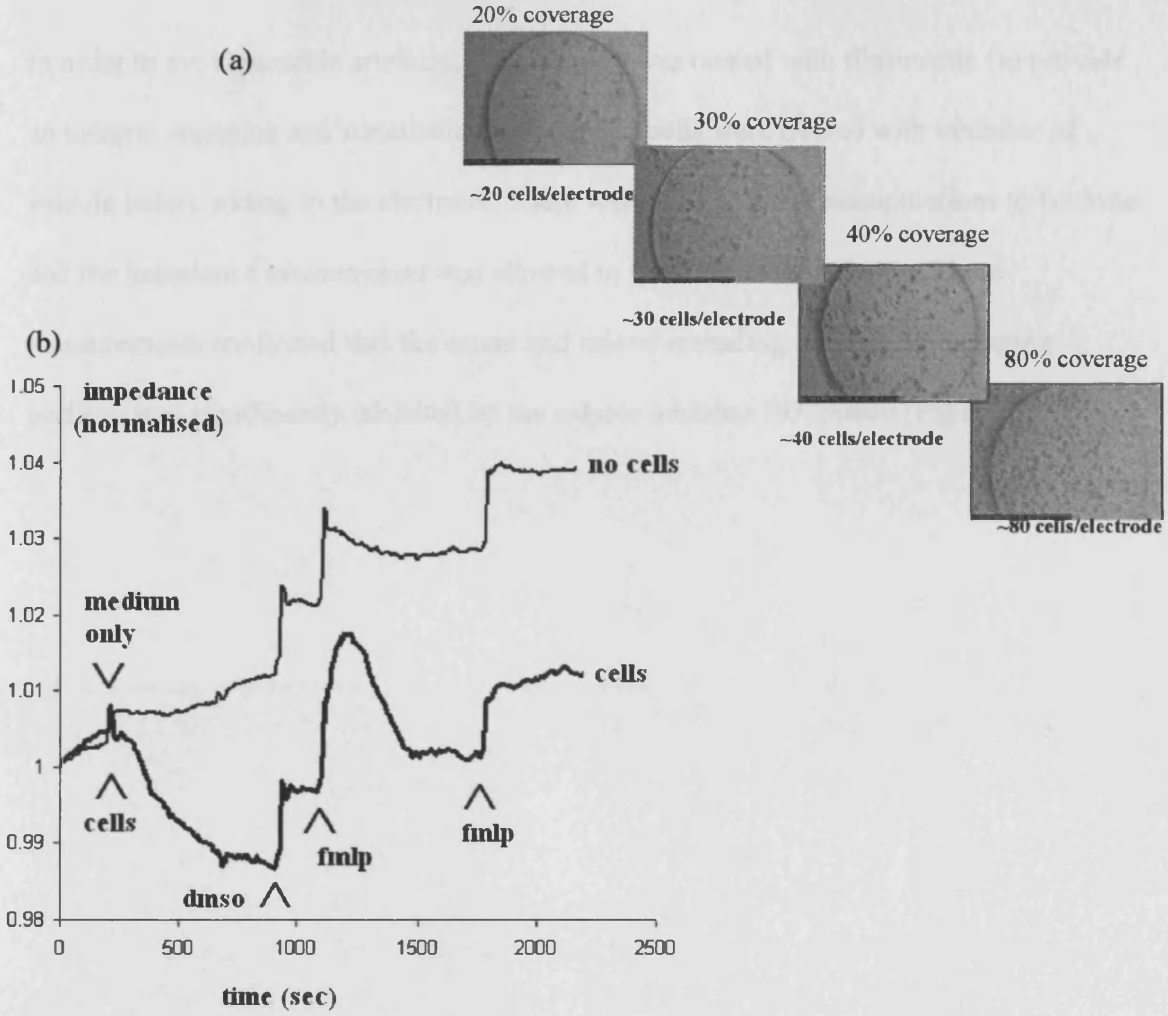

Fig 5.3.7 ECIS Impedance Measurements

(a) Low resolution images of the gold electrode (250 μm) with varying numbers of neutrophils attached. Impedance signal from each electrode was portioned to the number of neutrophils observed.

(b) A typical ECIS experiment, showing both cell-specific and artefactual changes in impedance signal. The method proceeded as follows:

Initially: 300 μl of medium (Krebs, pH 7.4, 37 ^{0}C. 0.1 % BSA)

At first arrow: 100 μl of medium or medium + neutrophils was added

At second arrow: 100 μl was withdrawn and replaced with 100 μl of medium (DMSO 0. 1%)

At third arrow: 100 μl was withdrawn and replaced with 100 μl of medium containing fMLP dissolved in DMSO to give final concentration of 1 μM and DMSO 0.1 %.

At fourth arrow: 100 μl was withdrawn and replaced with 100 μl of medium containing fMLP dissolved in DMSO to give final concentration of 1 μM and DMSO 0.1 %.

In order to avoid possible artefacts, the electrode was coated with fibronectin (to provide an integrin engaging and stimulatory surface) and cells were treated with inhibitor of vehicle before adding to the electrode. There were thus no other manipulations to be done and the impedance measurement was allowed to continue to completion. These measurements confirmed that the extent and rate of spreading on integrin-engaging surfaces was significantly inhibited by the calpain inhibitor PD150606 (Fig 5.3.8).

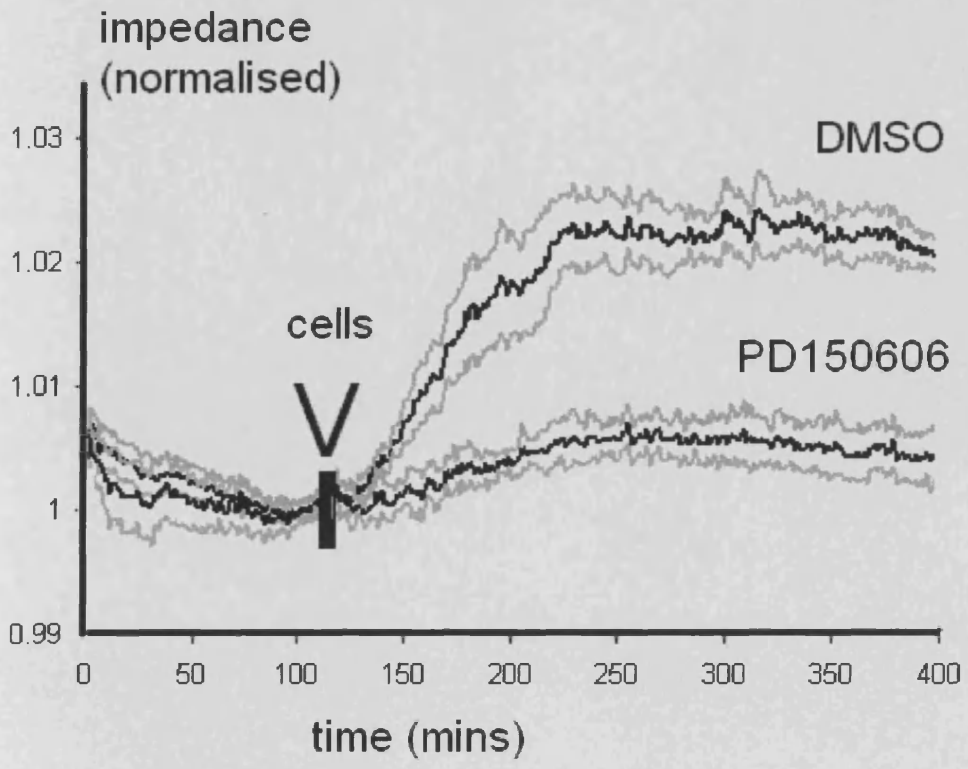

Fig 5.3.8 Inhibition of Neutrophil Spreading as Determined by ECIS

At the arrow, neutrophils, either treated with PD150606 (50 μM) or DMSO as indicated, were added to the ECIS electrode chamber. The heavy line shows the mean and lighter lines the standard deviation of three separate electrodes. The graph shows the data for experiments on the same donor. Similar results were obtained on three other donors on different days.

5.4 Discussion

Adhesion of neutrophils to the vascular endothelium is an essential prelude to the process of extravasation. The adhesion triggers the dramatic morphological change in the neutrophil, dubbed "spreading". It has been established that this event is preceded by a transient increase in cytosolic free Ca^{2+}. I have shown here that neutrophil spreading can be triggered by uncaging IP_3 in the cytosol. The IP_3 causes Ca^{2+} store release and subsequent Ni^{2+}-inhibitable Ca^{2+} influx into the neutrophil.

It was established that Ca^{2+} influx is the essential component for the rapid acceleration of neutrophil spreading. Uncaging Ca^{2+} to similar levels of cytosolic free Ca^{2+} concentration as that achieved by IP_3 induced release failed to trigger spreading. Inhibiting Ca^{2+} influx also prevented spreading. The Ca^{2+} influx that precedes neutrophil spreading was accompanied by the activation of cytosolic calpain, a Ca^{2+}-activated protease. Pharmacological inhibition of calpain activity reduced both the number of adherent neutrophils and the rate of spreading as determined by ECIS. These data were consistent with the dependence of cell spreading on Ca^{2+} influx, which generates localised high concentrations of Ca^{2+} just under the plasma membrane, causing local activation of calpain resulting in membrane remodelling and expansion.

The inhibition of calpain significantly reduced the neutrophil adherence and spreading. Both of these phenomena are required for the extravasation of neutrophils in response to inflammatory stimuli. The pharmacological inhibition of calpain could therefore offer a

suitable alternative therapy that would be common for many types of chronic inflammatory conditions.

It is important to note that the experimental conditions used for the majority of the experiments presented in this chapter were not aimed at replicating physiological conditions, but rather were intended to investigate the signalling pathways that occur within the neutrophil. Spreading of neutrophils on glass in response to IP_3 uncaging was used as an experimental system that allowed the temporal and causal relationship between Ca^{2+} signalling and cell spreading to be investigated robustly. This system also allowed the effects of inhibitors to be investigated without the complications of effects on other signalling systems. The work in this chapter therefore poses the question as to the physiological significance between Ca^{2+} influx and physiological neutrophil morphological changes. This is explored in the following chapter.

5.5 Conclusion

From the work presented in this chapter, it was concluded that physiological Ca^{2+} influx was the essential component for the rapid acceleration of neutrophil spreading. Accompanying the physiological Ca^{2+} influx that preceded neutrophil spreading, there was an activation of cytosolic calpain, a Ca^{2+} activated protease. Pharmacological inhibition of calpain activity reduced both the number of adherent neutrophils and the rate of spreading as determined by ECIS, and this could therefore be considered an alternative therapy for treatment of chronic inflammatory conditions.

CHAPTER 6

Physiological Cytosolic Free Ca^{2+} Signalling in Neutrophils Mediated by β2 Integrin

6.1 Introduction

In the previous chapters, the techniques established for monitoring fast Ca^{2+} events in neutrophils were used to visualise Ca^{2+} signalling events that accompany stimulation by formylated peptide and elevation of IP_3. Previous studies have shown that Ca^{2+} signalling stimulated by formylated peptide in human neutrophils is similar to those seen in other cell types and involves G-proteins, IP_3 generation and store operated Ca^{2+} influx (Taylor & Thorn 2001). The sequence of Ca^{2+} puff followed by Ca^{2+} wave, which were visualised, were thus the result of this well characterised Ca^{2+} signalling pathway. Physiologically, threshold effects in PLC activation mean there may be a rapid, step-wise increase in cytosolic IP_3 similar to that induced by uncaging IP_3. In the last chapter, I demonstrated that when cytosolic IP_3 is experimentally elevated from an inert caged-precursor, human neutrophils undergo a remarkable, rapid spreading response that may be related to a physiological outcome. However, there is rarely a sudden incremental rise in the concentration of an extracellular formylated peptide in physiological situations. Neutrophils sense low concentration of formylated peptide, which guides their chemotaxis towards higher concentrations. At no time, therefore, would they normally experience a sudden change in formylated peptide concentration. Furthermore, the concentration of formylated peptide required to induce the Ca^{2+} events observed is rarely reached physiologically. Care must therefore be taken in extrapolating to the physiological situation. However, rapid neutrophil shape change is a characteristic of responses involving β2 integrin, such as during phagocytosis of C3bi opsonised particles or adhesion to endothelial cells expressing ICAM-1. As engagement of β2 integrin is also known to trigger cytosolic free Ca^{2+} signals (Ng-Sikorski et al, 1991: Petersen et al, 1993), it is proposed that the link between elevation of cytosolic free Ca^{2+} and cell shape change are more relevant

to stimuli that involve this route. In this chapter, I will therefore present work aimed an investigating this linkage.

6.1.1 Aim

In this chapter methods that more closely resemble the physiological stimuli of neutrophils have been developed in order that Ca^{2+} signalling under these conditions can be studied. Two situations in which neutrophils are stimulated by binding to ligand immobilised on surfaces will be explored. The first is stimulation of phagocytosis in response to β2 integrin binding to iC3b immobilised on zymosan particles. The second situation is stimulation of neutrophil adhesion and spreading in response to β2 integrin binding to ICAM-1 expressed on cell surfaces.

6.2 Methods

6.2.1 Micromanipulation of Zymosan and Neutrophils

Micromanipulation involved the same pieces of equipment as those employed for microinjection as described in Section 2.3.3. However, the micropipette was not coated with the SLAM coating, nor loaded with anything. The tips were pulled in-house to 1 μm (rather than 0.1 μm used for microinjection). This allowed for manipulation rather than injection. These micropipettes were used to deliver opsonised zymosan particles to the neutrophil surface and so induce phagocytosis on demand.

The micropipette was attached to a pressure controller as in the injection experiments. This would allow control of particles, which could be held in the mouth of the pipette

for refined movement, and controlled release of the particle. The micropipette was held in a motorised manipulator for fine control.

Neutrophils were loaded with Ca^{2+} indicators appropriate for the imaging experiment. The cells were then allowed to settle and adhere to a glass coverslip. Conditions were optimised so that a significant population of the neutrophils were adherent but not fully spread out as previously described (Sect. 2.3.3). Fully spread neutrophils tend to be disinclined to either be microinjected or to phagocytose.

The micropipette was moved into the field of view (100 x objective) containing adherent neutrophils. A suspension of opsonised zymosan particles (3-5 μl, 1 mg/ml) was added to the Krebs (+ BSA) on the coverslip. The zymosan were allowed to settled and then an area was chosen where a single zymosan could be delivered to a neutrophil. The micropipette was moved next to the zymosan particle and a slightly negative pressure sent down the pipette, drawing the particle into the mouth of the pipette. The zymosan particle was then delivered to the neutrophil. Once firm contact had been established, the negative pressure through the micropipette was removed, releasing the particle. The micropipette was then moved away from the site and phagocytosis allowed to proceed. The morphology and Ca^{2+} signals were recorded over the time course of the phagocytosis event.

This technique was used with both conventional fluorescence (Nikon Eclipse) and confocal microscopy (Leica LCSM). The LCSM had the advantage of being able to focus on the plane of the phagocytic event. Any Ca^{2+} signals that occurred near the phagocytic cup would be more clearly resolved. The LCSM also has a higher capture

rate, resulting in more frames per second being recorded and therefore higher temporal resolution of any events.

6.2.2 Tissue Culture of CHO Cells

Chinese Hamster Ovary (CHO) cells were grown in tissue culture under standard culture conditions as described in Section 2.3.5. These are a carcinoma cell line and therefore survive for multiple passages. The cells were maintained in complete DMEM containing 10% FBS, which kept them in a state of replication and growth.

6.2.3 Transfection of CHO Cells With ICAM-1-GFP Plasmid

CHO cells were split with trypsin-EDTA and seeded at a relatively low density (c. 10^5 cells / ml) on glass coverslips in 6 well plates. To keep the cells in the centre of the coverslip a "well" was created with vacuum grease on the coverslip. Cells were allowed to grow to approximately 50 % confluence before being transfected.

The ICAM-1-GFP plasmid was a generous gift from Bill Luscinskas (Harvard Medical School, US). Plasmid (1 µl) was mixed with DMEM (50 µl) with no additives (no add.). Metafectine (2 µl or 4 µl) was mixed with DMEM (no add., 50 µl). The plasmid was then mixed with the metafectine. This mixture was allowed to incubate for 20 minutes at room temperature to allow plasmid DNA-metafectine complexes to form. The medium was aspirated from the CHO cells to be transfected and warm DMEM (no add. 200 µl) replaced. The plasmid-metafectine mixture was added to this DMEM and mixed gently. The CHO cells were incubated with the plasmid-metafectine complexes for 3-4 hours in the tissue culture incubator (37 °C,

5% CO_2). After this time the medium was aspirated and replaced with warm, complete DMEM (3 mls). The cells were left to recover and grow for 24 hours.

Experiments were then carried out on the CHO cells that had grown in the vacuum grease "well" on the coverslip. A successful transfection resulted in expression of the GFP tagged ICAM-1 molecule localised in the plasma membrane of the CHO cell. There were varying degrees of transfection efficiency, but it was decided that 4 μl of metafectine to 1 μl plasmid DNA gave the best results.

As with all transfection experiments, there was some variation in the final expression levels of the GFP-ICAM-1 as can be seen in Fig 6.2.3.1. This shows both under and over expression, with the latter resulting in back-log in the protein production machinery, for example the Golgi apparatus. It was decided that optimal expression was defined by localisation of the GFP-ICAM-1 to the plasma membrane without significant fluorescence build up in other organelles. Since experiments were carried out on single cells, it was possible to choose cells that had the optimal expression of the GFP-ICAM-1.

6.2.4 Fluorescence Recovery After Photobleaching (FRAP)

This technique was employed to estimate the motility of the GFP-ICAM-1 that had been transfected into CHO cells. The technique involved localised photobleaching of fluorescent molecules in a define area in order that the mobility of fluorescent molecules could be observed as they diffused back into the bleached area. Localised photobleaching was achieved by restricting the laser scanning area using the "zoom" control and turning the laser strength up to its maximum output, until the fluorescence

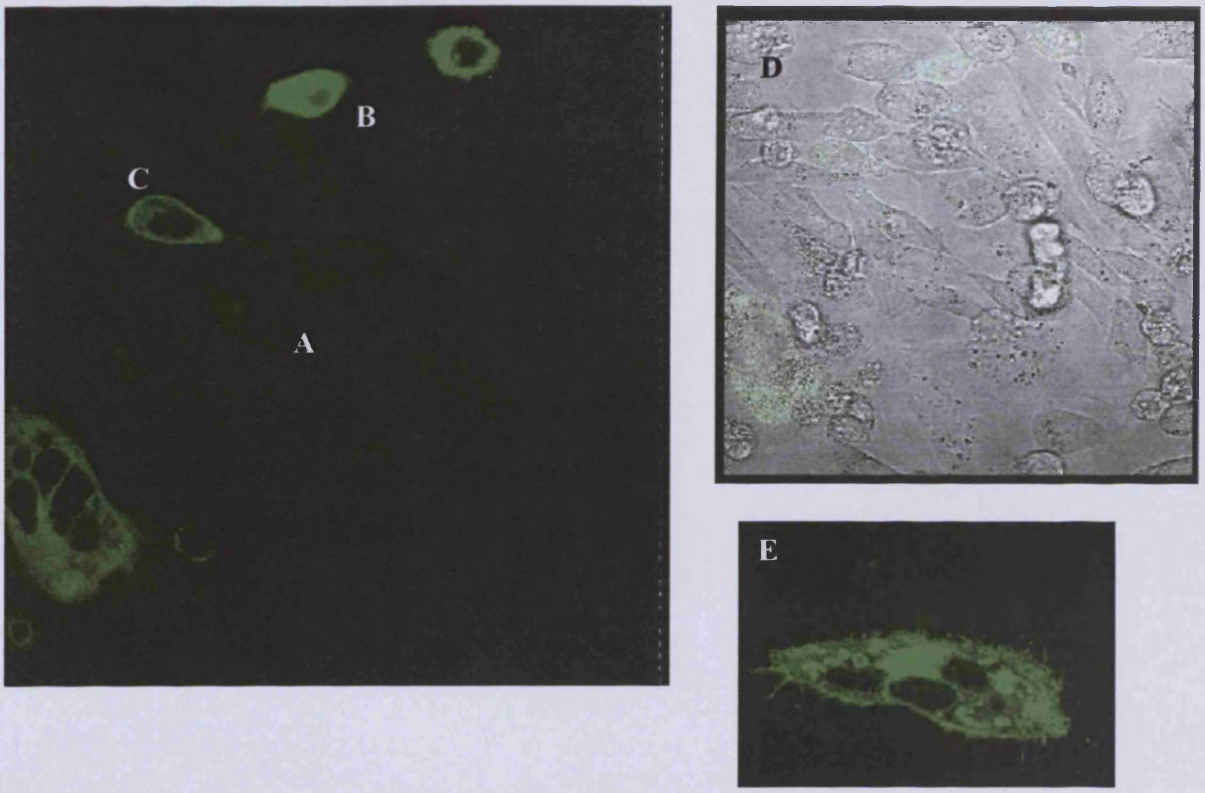

Fig 6.2.3.1 Variable Transfection Efficiencies of ICAM-1-GFP (tailless)

Images showing the variable transfection efficiences in the same field of view of transfected CHO cells. (A) underexpression leading to barely visible fluorescence, (B) overexpression resulting in the protein being backed up in the production machinery and thus incorrectly distributed, and (C) optimum levels with appropriate distribution of the fluorescence and distinct localisation to the plasma membrane. For reference, the overlay with the brightfield image is shown (D). It is worth noting that transfected CHO cells do not vary in their cellular morphology to non-transfected cells. (E) is a clear example of overexpression with the fluorescent protein in various organelles throughout the cytoplasm.

intensity of the defined area was significantly reduced (5-30 sec). The recovery of fluorescence in the photobleached area, if any, was observed over time using low intensity confocal imaging as usual. The fluorescence intensity was monitored in both the region of bleaching and an adjacent non-bleached region so that the proportional return of fluorescence and the speed gives an indicator of the motile fraction of the fluorescent molecule could be quantified. LCSM was especially useful for this technique when looking at membrane bound fluorescent probes as it allowed the membrane to be seen in a planar profile. It was expected that GFP-ICAM-1 would be localised in the membrane of the CHO cells. A cell was selected that showed good localisation. A region of the membrane was then zoomed in on and the fluorescence was bleached. The zoom was returned to 1 and imaging continued.

The GFP-ICAM-1 construct used was a tail-less version of ICAM-1 and therefore expected to be more motile than the complete ICAM-1. The intracellular domain of the complete ICAM-1 forms interactions with cytoskeletal proteins, which would prevent motility. The experiment required the GFP-ICAM-1 to be potentially motile, since it was attempting to decipher whether ICAM-1 accumulated at sites of interaction with neutrophils, and whether this interaction induces Ca^{2+} signalling events and subsequent changes in neutrophil behaviour or morphology. The latter was monitored by concurrently imaging the brightfield image of the cells through a separate photo-multiplier tube.

6.3 Results

6.3.1 Ca^{2+} Signals Induced by Phagocytosis

The major role of neutrophils is phagocytosis, hence their description as "professional" phagocytes. There is ample evidence to show that whole cell Ca^{2+} signalling occurs during phagocytosis (e.g. Dewitt & Hallett, 2002). There are also indications in the current literature that there may be more complex sub-cellular signalling events underlying the whole-cell Ca^{2+} events that are commonly seen. To mimic the physiological function of phagocytosis, zymosan particles that had been opsonised with serum (C3bi) were delivered to neutrophils. In this way, the Ca^{2+} events during the process of phagocytosis were observed and characterised using the confocal microscopy techniques established in Chapter 3. Non-confocal microscopy results in a dilution or blurring of micro-events because the fluorescence signal is collected as an average through the whole thickness of the cell. In contrast, confocal microscopy allows the positioning of the plane of observation to be aligned with the introduction of the zymosan particle to the neutrophil. Two methods were used to control the plane in which the zymosan was introduced to the neutrophil: (i) micromanipulation and (ii) adherent non-opsonised zymosan on a coverslip.

6.3.1a Ca^{2+} Signals Induced By Micromanipulated Phagocytosis

Although it has been well established that Ca^{2+} signals occur during phagocytosis, the rate at which Ca^{2+} data can be collected has been slow. In the experiments performed here, the data was collected at much higher acquisition rates sufficiently high to reveal any sub-cellular transient Ca^{2+} events. Neutrophils were loaded with the Ca^{2+} sensitive probe Fluo4, and phagocytosis was induced by micromanipulation of zymosan particles that had been opsonised with C3bi by incubation with normal human serum.

This approach triggered phagocytosis of micromanipulated zymosan and generated a typical Ca^{2+} signal (Fig 6.3.1.1). The responses generated were very similar to those reported in the literature (e.g. Dewitt & Hallett, 2002: Dewitt et al, 2003). In order to attempt to visualise sub-cellular transient Ca^{2+} signals, this process was repeated with various positions for the introduced zymosan particle and the confocal imaging plane. Using this approach, the location of the forming phagocytic cup and the beginning of the Ca^{2+} influx wave could be observed. The Ca^{2+} wave swept across the cell from the site of phagocytosis resulting in a global increase in Ca^{2+} (Fig 6.3.1.2). Although the origin of the global Ca^{2+} wave was clearly defined by the phagocytic cup region, no clearly defined Ca^{2+} puffs or smaller release events preceded this or were seen during the course of these experiments. However, it was difficult to pre-determine the optimal plane for observation of the Ca^{2+} signal because the neutrophil often underwent a dramatic morphological change during phagocytosis. For example, the cell sometimes flattens down as it stretches towards the presented zymosan particle, making the initially selected imaging plane too high. In other cases, the morphology change resulted in the whole phagocytic cup and zymosan being lifted up out of the confocal plane. Therefore, it was necessary to develop a technique that would limit the plane in which phagocytosis could occur.

6.3.1b Ca^{2+} Signals Induced by C5a Directed Phagocytosis

In this method, zymosan particles were immobilised on the glass surface. Whole serum was added to the immobilised zymosan particles, triggering the complement activation and cascade, which both coated the zymosan particles in C3bi fragments and produced concentration gradients of C5a from individual zymosan particles, up

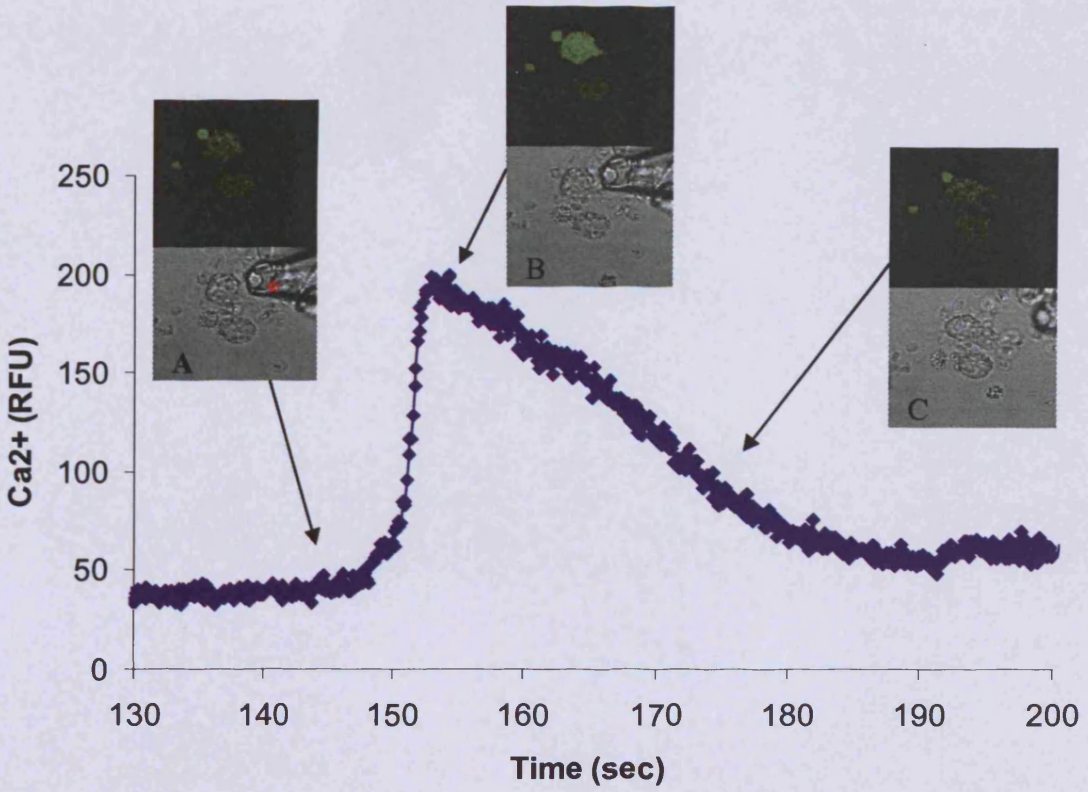

Fig 6.3.1.1 Typical Ca^{2+} Signal – Micromanipulated Phagocytosis

Trace of Ca^{2+} signal during phagocytosis of micromanipulated zymosan particles. Three stages are shown in both Fluo4 fluorescence and brightfield image are (A) contact before pseudopod extension, (B) extension of pseudopods triggering Ca^{2+} influx and (C) closure of the phagosome as Ca^{2+} returns towards basal levels. The micropipette can be seen in the brighfield images (labelled with *).

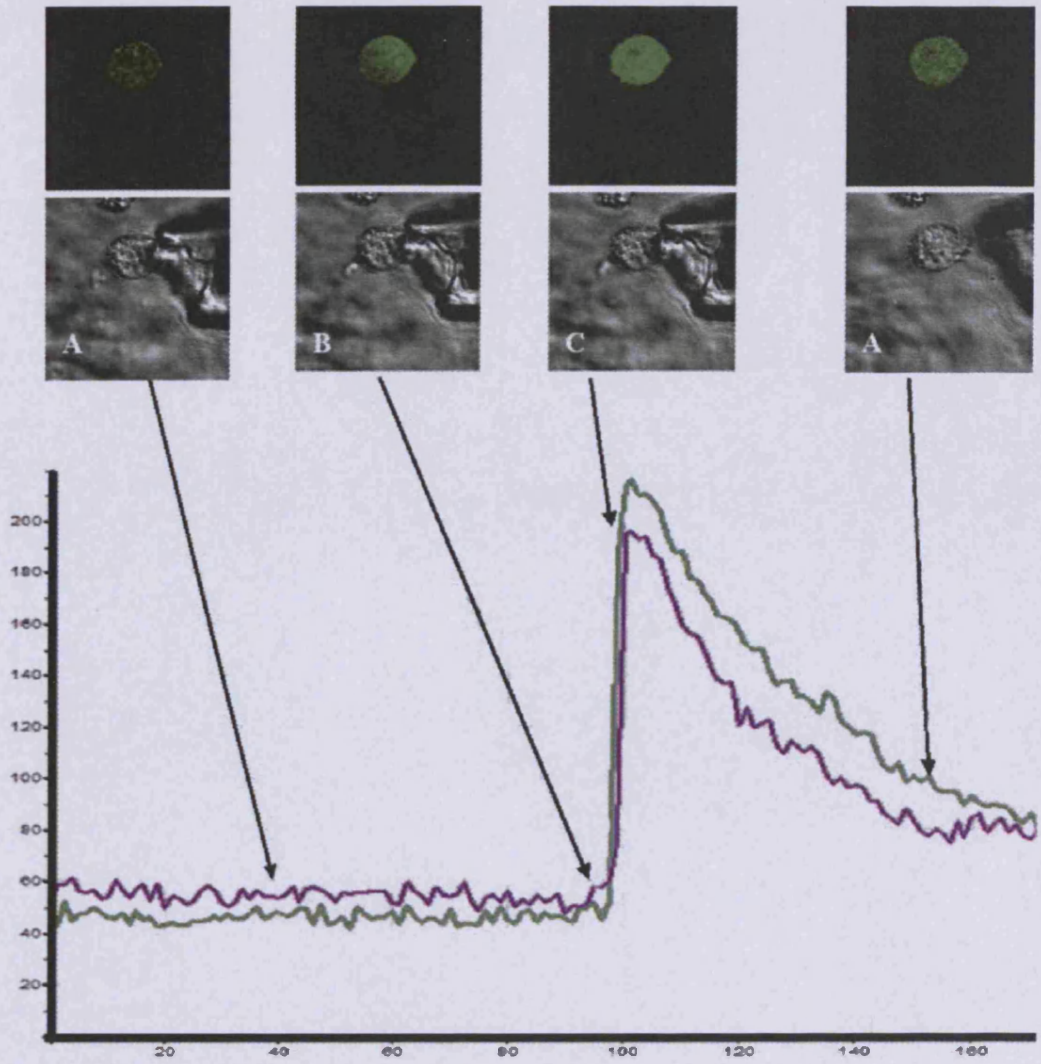

Fig 6.3.1.2 Ca^{2+} wave Initiate Near the Site of Phagocytosis

Ca^{2+} trace from two regions of interest (ROI). ROI 1 (green) at the site of phagocytosis, ROI 2 (purple) at a distal site. An initial lag time in onset of Ca^{2+} is clearly visible at the time point indicated by B. Corresponding fluorescence and brightfield images for 4 stages are indicated. (A) Before phagocytosis, (B) initiation of Ca^{2+} signal at site of phagocytosis seen as a wave sweeping from right-to-left (C) peak Ca^{2+} where whole cell has elevated Ca^{2+} level and (D) after phagosome closure and withdrawal of micropipette.

which the neutrophils are attracted. This sequence was a relevant physiological model since neutrophils migrate along concentration gradients of C5a and bacterial peptides to locate infected or damaged cells *in vivo*. Once the neutrophil located the opsonised zymosan, phagocytosis proceeded whilst Ca^{2+} changes could be monitored a high speed. This approach had the further advantage that, as the zymosan were adherent to the coverslip, the plane of phagocytosis was restricted. This should result in pseudopodia forming in a defined plane parallel with the confocal sectioning plane, thus increasing the possibility of observing micro-events of Ca^{2+} (see Chapter 4).

The technique developed involved (i) allowing a suspension of non-opsonised zymosan to dry onto the coverslip and removal of excess, non-adhered zymosan particles (ii) addition of neutrophils to the coverslip, to allow adherence before (iii) the addition of human serum, triggering the complement cascade. In these experiments, the neutrophils were relatively inactive until the serum is added. Then they suddenly begin to migrate with purpose towards the adherent zymosan. Once the neutrophil encounters the C3bi-opsonised zymosan particle, β2-integrins on the neutrophil are engaged and phagocytosis is induced. As the neutrophils encounters the adherent zymosan, a typical Ca^{2+} response was also observed (Fig 6.3.1.3). It can be seen that this Ca^{2+} response is similar to the Ca^{2+} signal triggered by micromanipulated presentation of the particle (Fig 6.3.1.1). This suggests that the presence of C5a and chemotaxis had not significantly altered the phagocytosis signal.

The advantage of this technique was that the phagocytic plane was pre-determined and guaranteed. However, the confocal imaging plane was 1 μm, whereas the zymosan particles used are approximately 2-3 μm in diameter. Therefore, it was necessary to

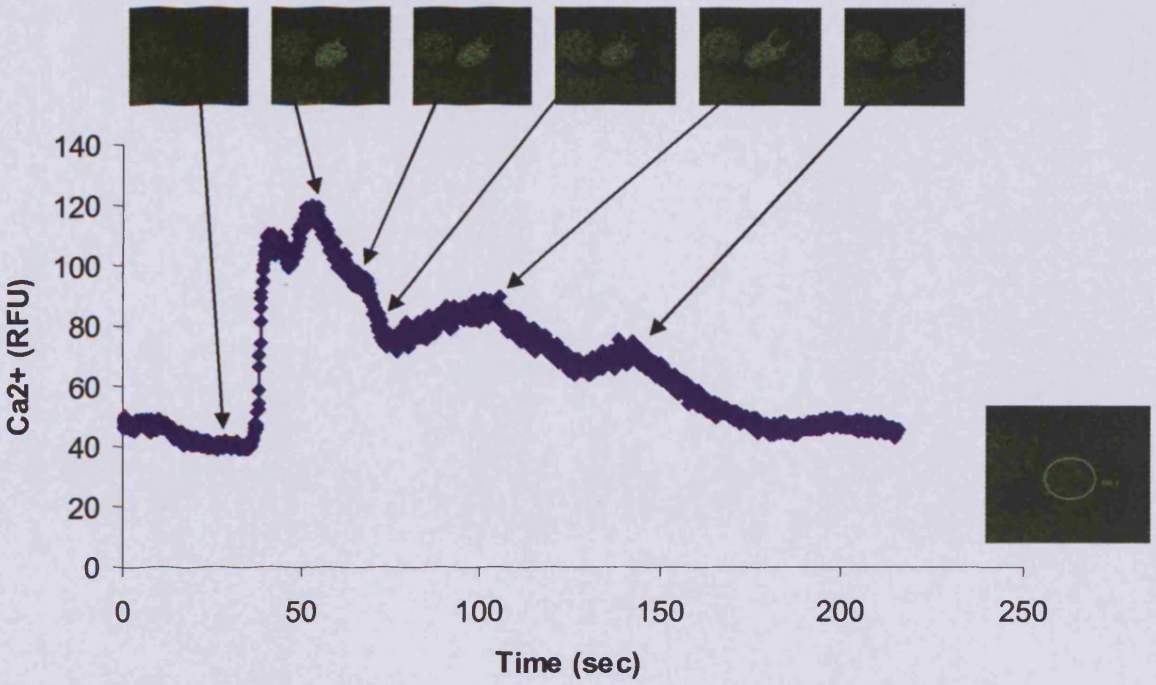

Fig 6.3.1.3 Typical Ca^{2+} Trace – Adherent Zymosan

Non-opsonised zymosan particles were allowed to dry onto a glass coverslip. Neutrophils were added and allowed to settle. Normalised human serum was then added and the complement cascade being triggered by the zymosan. This produced chemoattractant and opsonising complement fragments and the neutrophils phagocytosed the zymosan particles. The trace above shows the Ca^{2+} during this event.

visualise the Ca^{2+} signals at planes spanning the whole height of the zymosan particle to ensure optimum chances of catching a sub-cellular Ca^{2+} event. For most experiments, the focal plane was set half way through the phagocytic cup. Diffusion theory (see Section 4.3.3) dictates that a Ca^{2+} puff within 1 μm of the confocal plane should be within the limits of detection and distinguishable above the background noise. Therefore, if a Ca^{2+} puff occurred in the vicinity of the phagocytic cup it should be captured by the confocal microscope. Despite this, no Ca^{2+} puffs were observed under these conditions. Close examination of sequences of images of Ca^{2+} during phagocytosis of adherent zymosan particles did not reveal any Ca^{2+} puffs. Ca^{2+} waves, which were initiated near the site of phagocytosis, were observed to propagate across the neutrophil under these conditions (Fig 6.3.1.4). This Ca^{2+} wave propagation in the absence of an initiating Ca^{2+} puff was thus observed under all conditions of phagocytosis. The absence of an initiating Ca^{2+} puff suggested that the mechanism of Ca^{2+} signalling by this route may have differences from that induced by formylated peptide.

6.3.2 Ca^{2+} Signals Induced by ICAM-1 Engagement

During phagocytosis, the global Ca^{2+} signal was followed by rapid extension of pseudopodia around the particle. These morphological changes were reminiscent of the effect observed in previous experiments with formylated peptide. With this stimulus, it was observed that induction of Ca^{2+} signalling often resulted in changes in neutrophil morphology, such as spreading from its round, circulating form to a much thinner disc with a larger surface area (refer to Chapter 5 for further investigation). This mimics what is known to occur *in vivo* as a neutrophil encounters an area of vascular endothelium that has been stimulated to express adhesion molecules

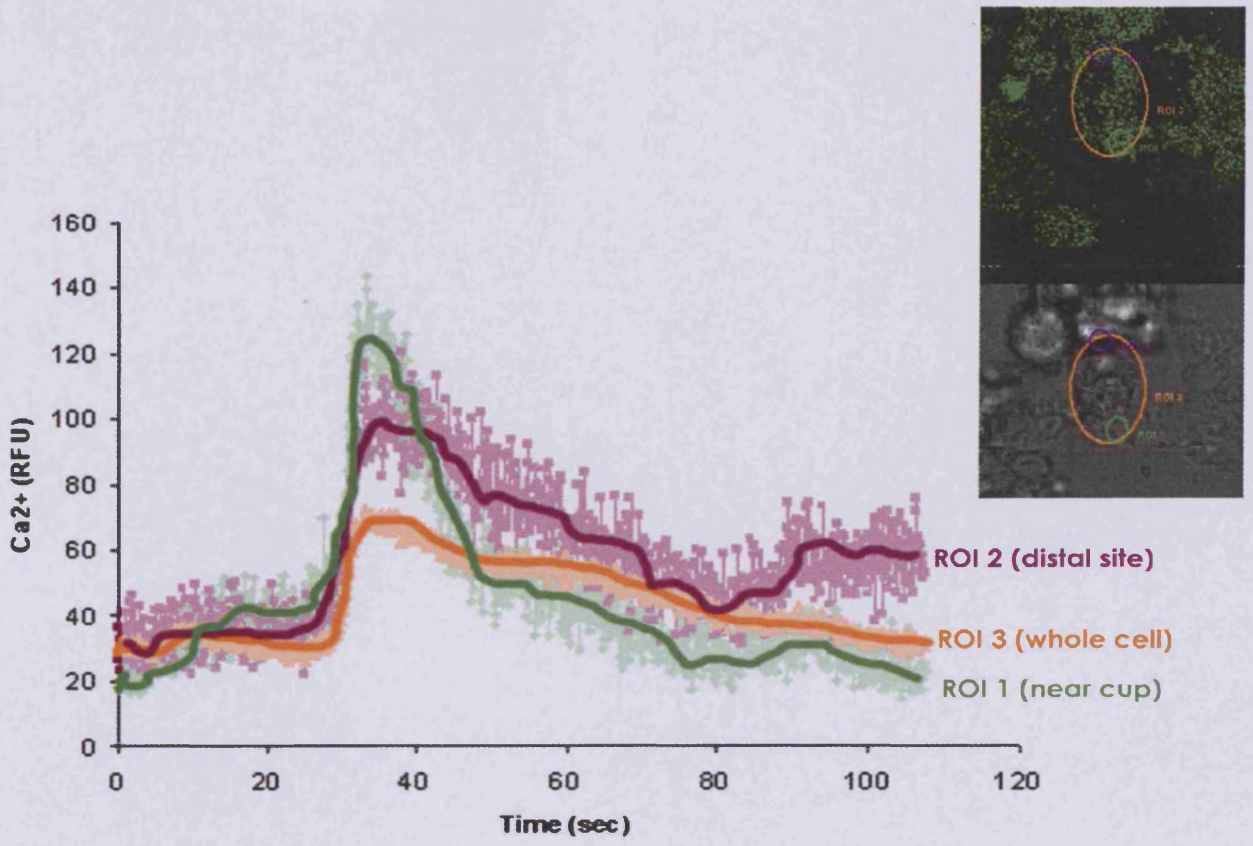

Fig 6.3.1.4 Ca^{2+} Wave Occurring in Neutrophils During Phagocytosis of Adherent Zymosan

Phagocytosis occurred at the cup adjacent to ROI 1(green). The trace indicates that the Ca^{2+} in the peri-phagocytic region (ROI 1) rises before the distal region (ROI 2, purple).

(ICAMs) on its luminal surface. Neutrophils roll along the surface of the blood vessel by loosely binding and disconnecting from selectins, until they encounter a region of cells expressing ICAM-1. This is the counter-ligand for β2 integrin. Binding between ICAM-1 and β2 integrin results in immobilisation of the neutrophil as it flattens down and firmly adheres to the endothelium. In order to study the rapid Ca^{2+} signals during this event, ICAM-1 was expressed on the surface of CHO cells, to provide a model for the physiological event. This approach also allowed the distribution of surface ICAM-1 to be observed using ICAM-1-GFP chimeric protein. Since ICAM-1-GFP binding partner is β2 integrin, the distribution of GFP on the cell beneath the attached neutrophil would reflect the distribution of β2 integrins. However, such an approach depends on the ability of the ICAM-1-GFP construct to move freely in the membrane. Since the cytosolic tail of ICAM-1 may interact with cytoskeletal components, a tailless variant of ICAM-1 was used in these experiments (Fig 6.3.2.1).

The transfection efficiency or protein expression varied between cells on the same coverslip (refer to Fig 6.2.3.1). This gave a useful control cell phenotype in the experiments (i.e. CHO not expressing ICAM-1). By comparing the phase contrast appearance of CHO cells, it was also concluded that ICAM-1 transfected cells were not morphologically different from those expressing ICAM-1 (refer to Fig 6.2.3.1). Thus transfection itself or expression of the protein had no obvious consequence to the cells morphology. Some CHO cells over-expressed the tailless-ICAM-1-GFP protein, which became backed up in the protein synthesis machinery. In these experiments, it was possible to exclude such cells and select cells with acceptable levels of ICAM-1 expression. Cells were chosen for experimental work in which ICAM-1-GFP was clearly localised to the plasma membrane (Fig 6.3.2.2). Since only the GFP domain of

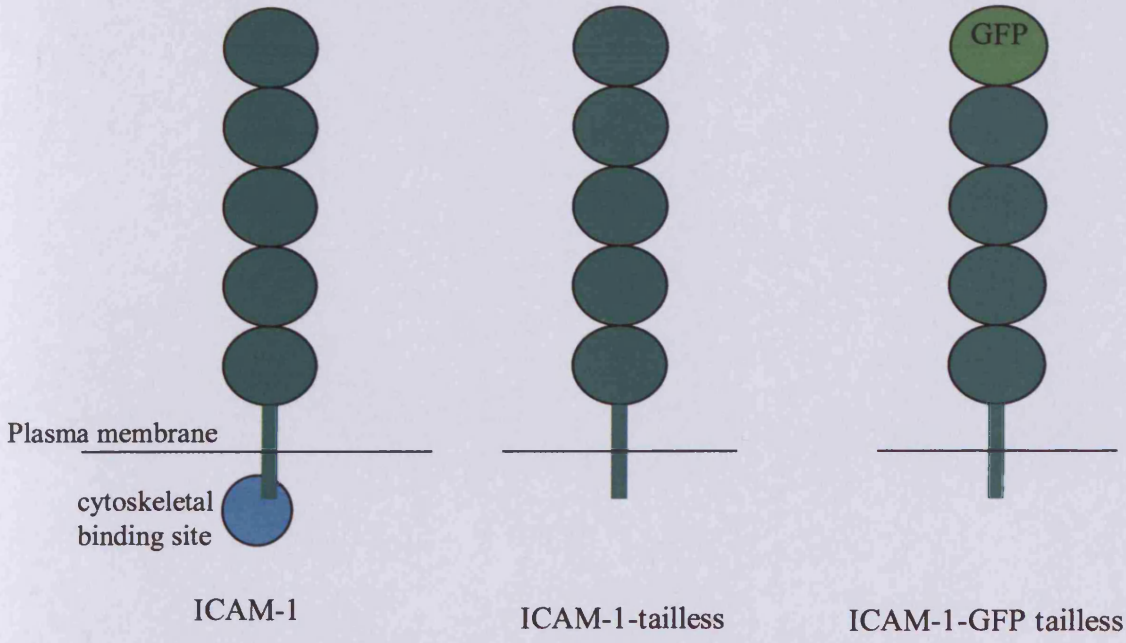

Fig 6.3.2.1 Schematic Representation of ICAM-1-GFP Tailless

Shown in comparison to complete ICAM-1 that would bind to the cytoskeleton and the tailless, non-GFP version, which would be more freely diffusible.

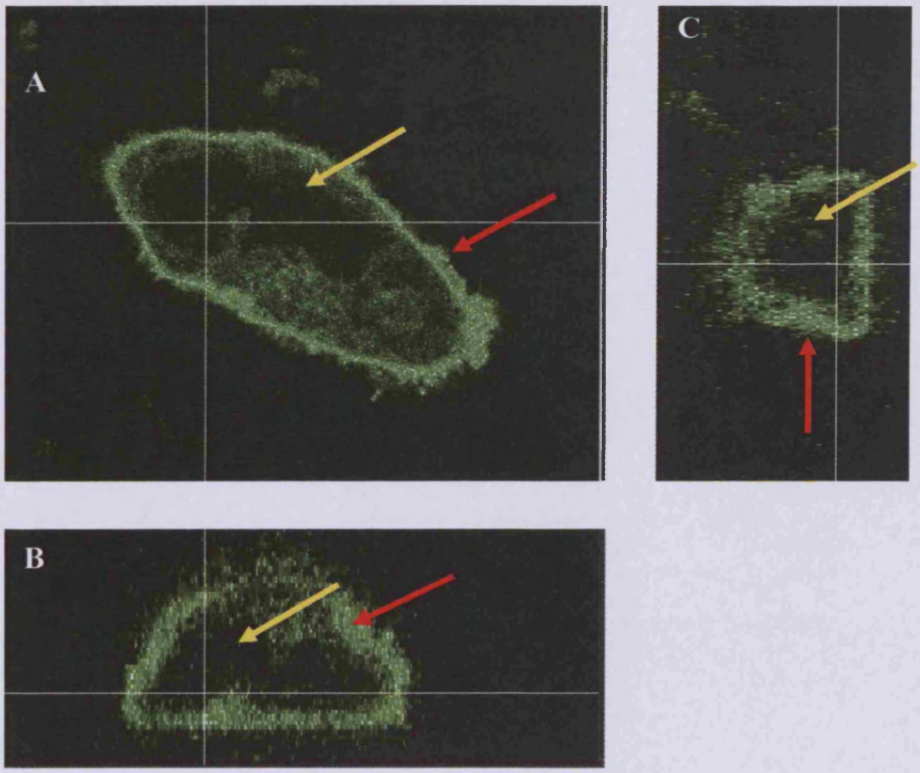

Fig 6.3.2.2 3-Dimensional Reconstruction of Confocal Sections Indicated Localisation for ICAM-1-GFP (tailless)

Confocal slices were collected at 0.5μm intervals and integrated to produce this image with slices taken in three planes (a) x-y, (b) y-z and (c) z-x. There is clear localisation to the plasma membrane (red arrow) and a notable lack of fluorescence in the nuclear lobes of the CHO cells (yellow arrow).

the chimeric protein could be imaged, the correct orientation of the ICAM-1-GFP in the plasma membrane was also established using a fluorescent-tagged antibody specific for the extracellular domain of ICAM-1. The presence of extracellular domain of ICAM-1 was detectable as a marked increase in fluorescence at the plasma membrane following addition of the antibody (Fig 6.3.2.3). It was thus concluded that the tailless GFP was inserted in the plasma membrane of CHO cells in the correct functional orientation.

6.3.2.1 FRAP Calculation of Tailless-ICAM-1-GFP Motile Fraction

In order to establish that the expressed tailless ICAM-1-GFP was free to diffuse in the plasma membrane, fluorescence recovery after photobleaching (FRAP) was used to determine the motile fraction of the tailless ICAM-1-GFP. Cells were chosen that had the optimal distribution of the GFP, namely localised to the plasma membrane. A section of the membrane was selected and the fluorescence distribution imaged. The selected plasma membrane segment was exposed to intense laser illumination for approximately 10 seconds to induce localised photobleaching of ICAM-1-GFP. The recovery of fluorescence into the bleached area was then monitored over a period of 10 minutes (Fig 6.3.2.4). The motile fraction for the tailless ICAM-1-GFP was estimated to be about 100 %, showing that all the GFP-construct was able to diffuse. These molecules diffused at a rate of about 0.5 μm^2 / s, which is similar to other freely diffusible proteins in the membrane. Thus, these data suggest that the GFP construct was free to diffusion of the protein and could act a probe for ICAM-1 clustering during neutrophils integrin engagement.

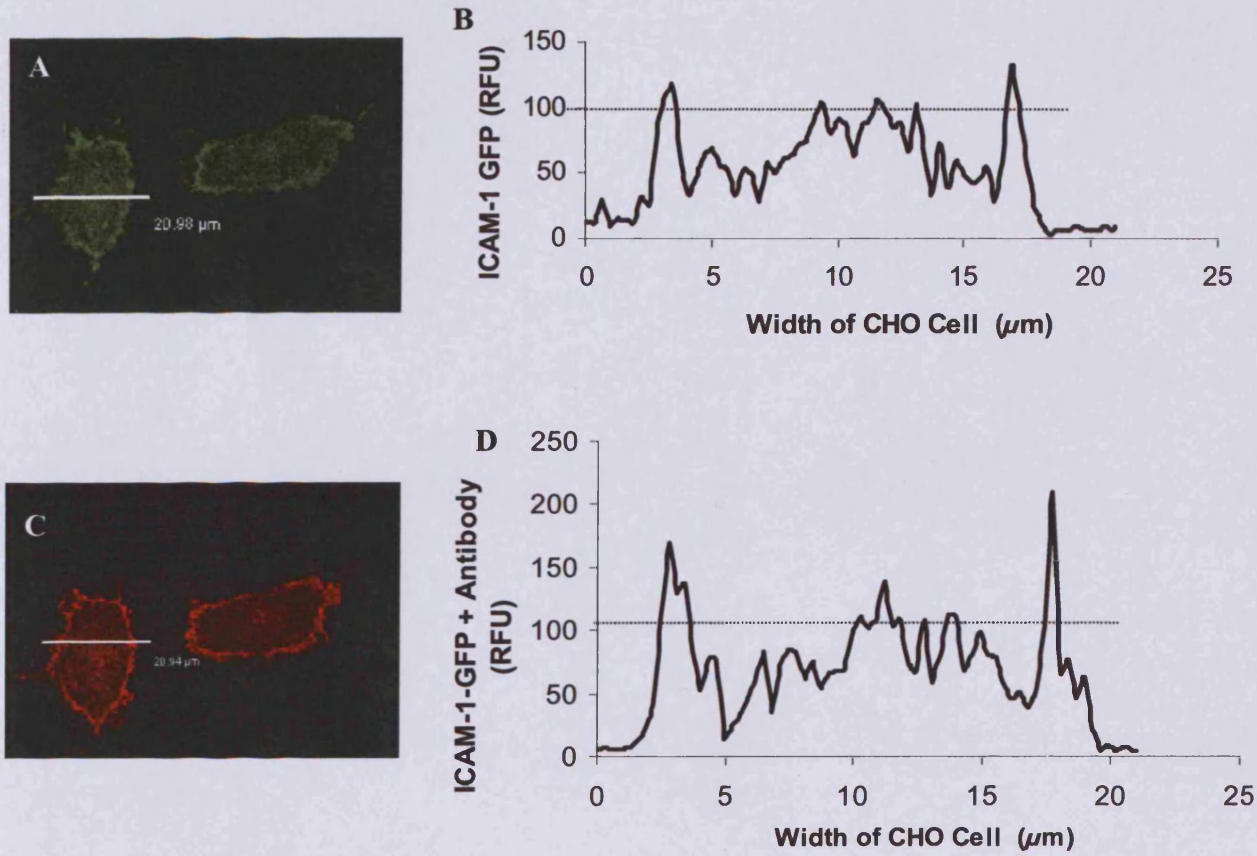

Fig 6.3.2.3 hICAM-1 antibody confirms localisation and orientation of ICAM-1-GFP (tailless) in plasma membrane

(A) Confocal fluorescence image of GFP localisation with cross-sectional line (white) along which the intensity was measured and plotted in (B). (C) Confocal fluorescence image after the addition of fluorescence tagged hICAM-1 antibody with cross-sectional line. (D) Fluorescence intensity along cross-sectional line showing marked increases at the plasma membrane regions.

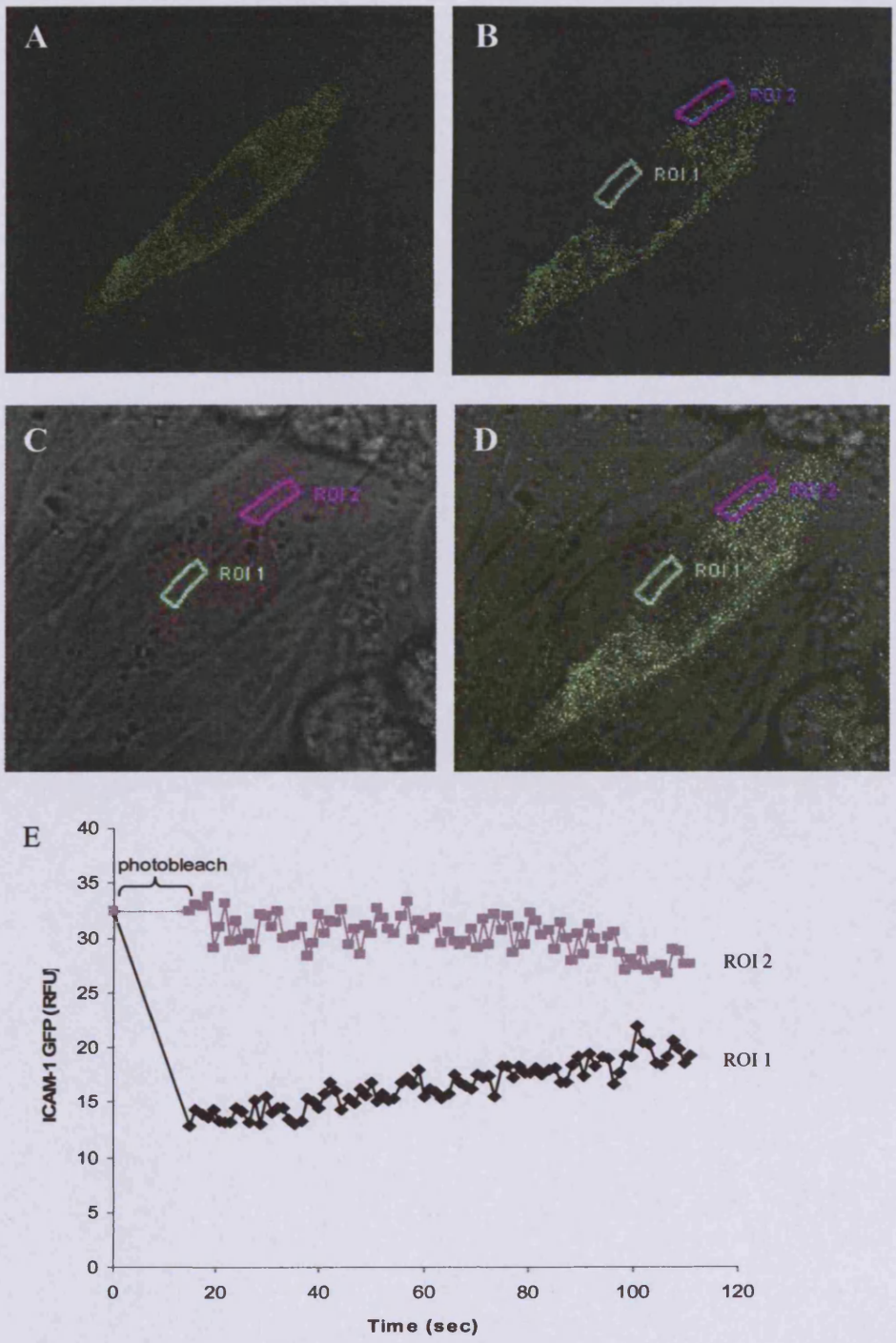

Fig 6.3.2.4 FRAP of ICAM-1-GFP (tail-less) in CHO cells

(A) Fluorescence of ICAM-1-GFP (tailless) transfected into CHO cell before photobleaching. (B) Fluorsecence after photobleaching marked with region of bleaching as ROI 1 and adjacent reference area as ROI 2. (C) Corresponding brightfield image with ROI marked. (D) Overlay of B and D. (E) Fluorescence recovery in the area after photobleaching (black) is compared to that of an adjacent, non-bleached area (grey).

6.3.3 ICAM-1-GFP and Ca^{2+} Changes in Neutrophils

In order to establish that this system would effectively trigger ICAM-1 mediated β2-integrin mediated Ca^{2+} signals, the Ca^{2+} indicator fura-2 was used. This indicator is excited at short wavelengths (340 and 380 nm), permitting the simultaneous imaging of ICAM-GFP (excitation 488 nm) distribution without cross-talk between the two fluorescent signals. The neutrophils were therefore loaded with the Ca^{2+} indicator fura-2 and added to CHO cells that had been transfected with tailless ICAM-1-GFP. The neutrophils that landed on CHO monolayers naturally migrated towards junctions between cells. However, neutrophils that landed onto areas of the naked coverslip that were not occupied with CHO cells remained relatively inactive. Therefore the micromanipulator was employed to move selected neutrophils into close contact with the CHO cells that were expressing the ICAM-1-GFP construct before they adhered to the coverslip. Once the neutrophil had firmly adhered to the CHO cell, the micromanipulator was retracted. The Ca^{2+} and GFP distribution were monitored by capturing images during this process using a rapid wavelength changing monochromator to illuminate the field with 340 nm, 380 nm to excite fura2 (at Ca^{2+} sensitive wavelengths) and 488 nm for GFP. The emitted images were captured using an intensified CCD camera attached to the Nikon wide-field microscope. There were no detectable cytosolic free Ca^{2+} in neutrophils during encounter with ICAM-1 on the CHO cell surface (Fig 6.3.3.1), even after forcing the cell to make an indentation into the CHO by micromanipulation (Fig 6.3.3.1b). In order to demonstrate that it was possible to record Ca^{2+} signals in this system, fMLP was used as a positive control (Fig 6.3.3.1). The changes in the distribution of ICAM-1-GFP were also imaged simultaneously. Despite the close contact between the neutrophil and the ICAM-1 expressing cell induced by forcing the neutrophil to deform the CHO cell membrane

(Fig 6.3.3.1c), there was no indication that the ICAM-1-GFP accumulated into distinct puncta at the site of neutrophil binding (Fig 6.3.3.1c). There were thus no obvious focal clusters formed that might be the sites of individual initiation loci for Ca^{2+} signals. It was not clear why Ca^{2+} signalling was not observed under these conditions, but as fura2 ratio imaging is considerably slower than fast laser scanning rapid confocal microscopy and higher image capture rates was also employed. For confocal imaging, Fluo4 was used as the Ca^{2+} probe. The drawback of this probe is that it is excited and emits light in the same range as the GFP emits making it difficult to distinguish between the Ca^{2+} and the GFP signals. Rapid confocal microscopy was used to capture images to be acquired at a high speed through the whole process of micromanipulation, firm binding and any subsequent changes in morphology and activity of the neutrophil. Using this technique, Ca^{2+} signals from the neutrophil were recorded at high speed and generated time courses of the cytosolic free Ca^{2+} change which were similar to those observed previously (Fig 6.3.3.2). The Fluo4 images at the start of the Ca^{2+} signalling event were extracted from the time sequence and examined closely for evidence of sub-cellular Ca^{2+} signalling events. However, none were detected during the time course of these experiments. The accumulation of tailless ICAM-1-GFP was clearly seen at the site of neutrophil adherence in these experiments (Fig 6.3.3.3), yet again without any distinct puncta of ICAM-1 localisation.

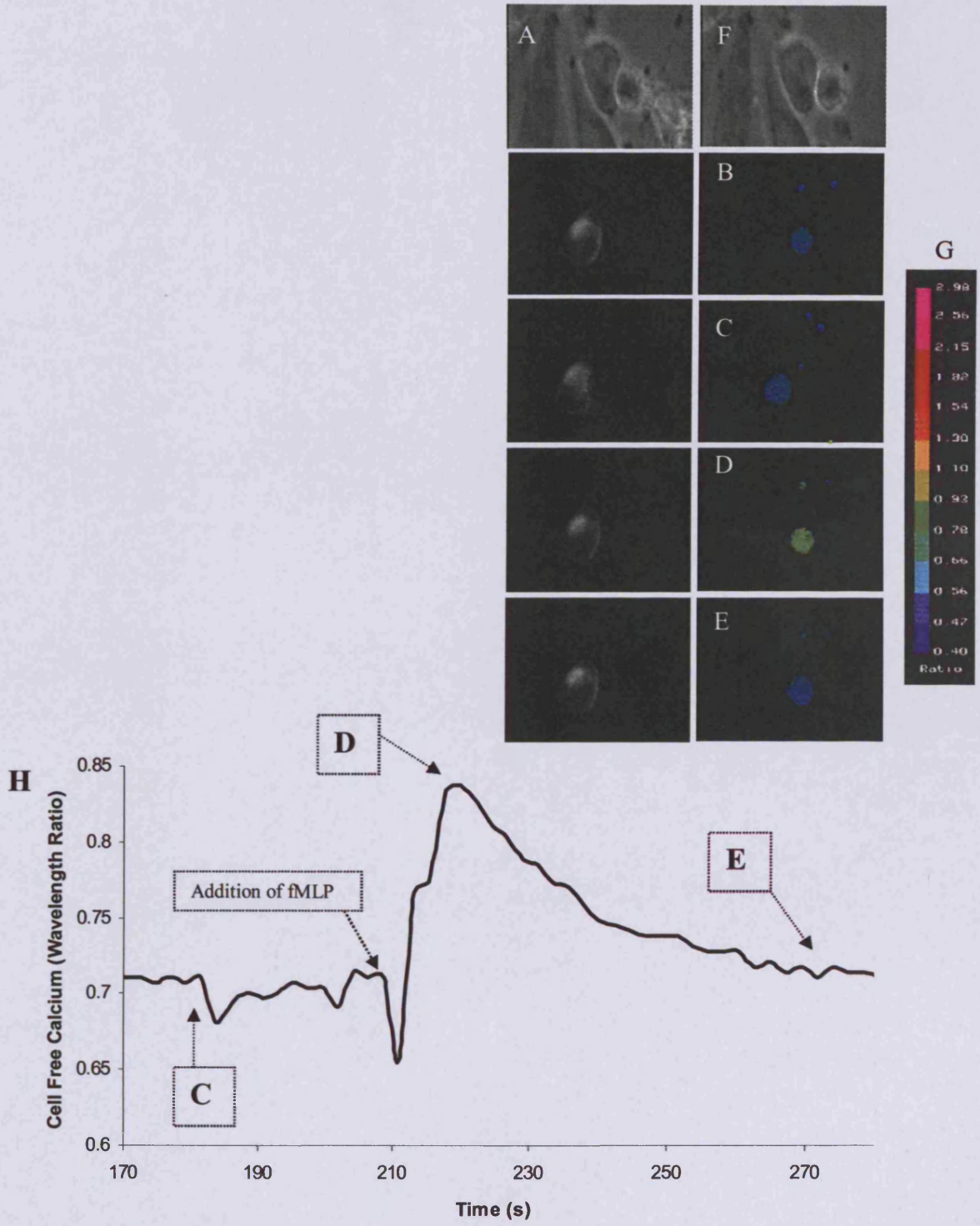

Fig 6.3.3.1 Typical Ca^{2+} signal achieved with neutrophil binding to ICAM-1-GFP (tailless) (A) Brightfield image of CHO cell and neutrophil (B) Before micromanipulation of neutrophil to aid adherence (C) Adhered neutrophil without Ca^{2+} signal induction (D) Ca^{2+} peak resulting from fMLP stimulation. (E) Image after recovery from Ca^{2+} signal. (F) Brightfield image after addition of fMLP. (G) Wavelength ratio colour scale (H) Trace of fMLP induced calcium signal with arrows to demonstrate location of images C, D and E as well as the addition of fMLP. Images on left are GFP in CHO, right are fura2 in neutrophil. Typical experiment n=4

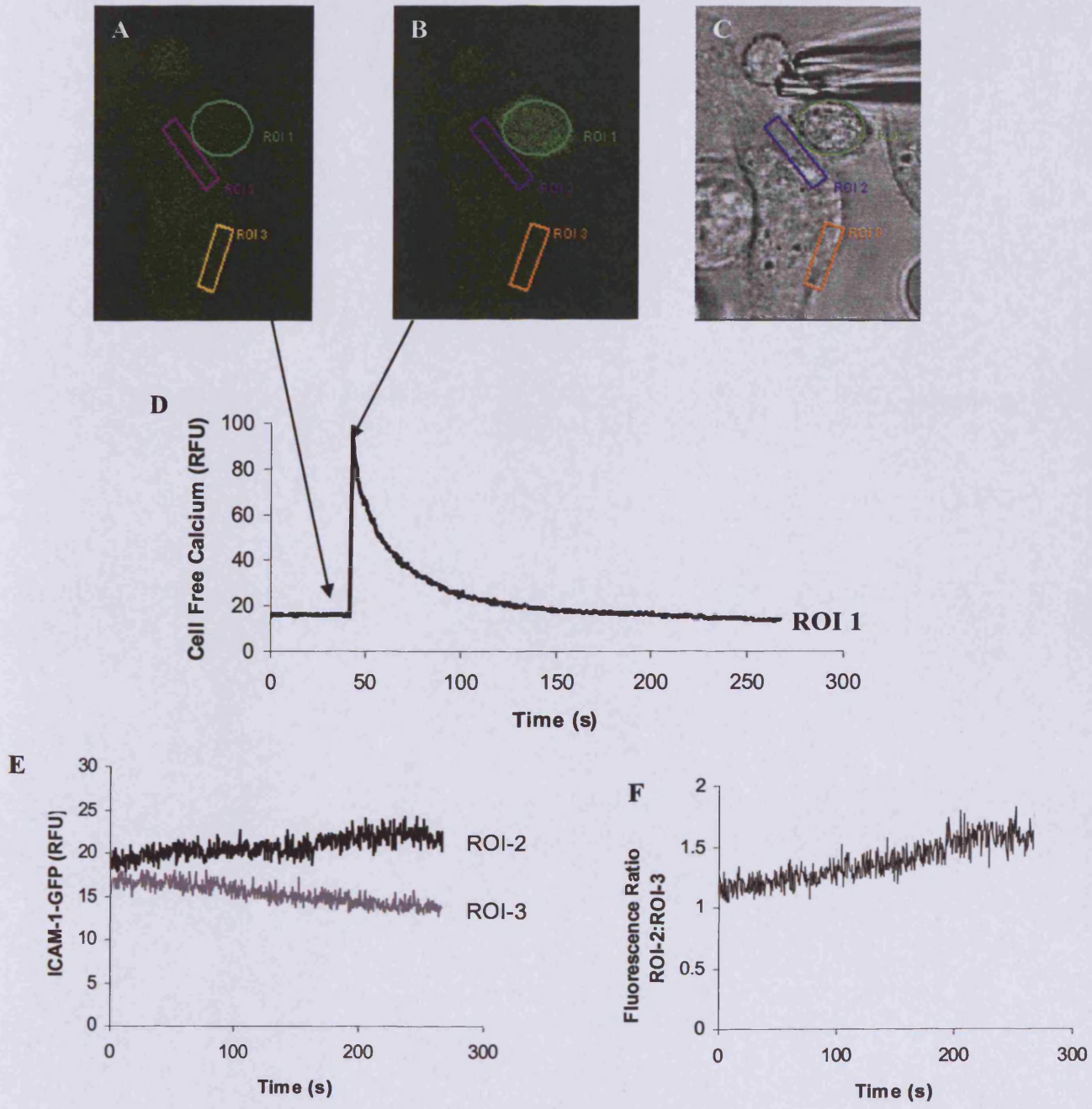

Fig 6.3.3.2 Ca^{2+} Transient in Neutrophil That Encounters ICAM-1 on CHO Cell

(A) Ca^{2+} level before firm contact between the neutrophil and transfected CHO cell (B) Shows the neutrophil firmly adhered to the transfected CHO cell at the time of calcium signal (C) Is the bright field image of A and B (D) Overlay of B and C (E) Trace of ICAM-1-induced calcium signal in the neutrophil (ROI-1, Green) (F) Graph comparing the ICAM-1-GFP intensity at the region of neutrophil contact (ROI-2, purple) and non-contact area (ROI-3, orange). (G) Graph of ICAM-1-GFP fluorescence ratio ROI-2:ROI-3 demonstrating the localisation of the receptor to ROI-2 (purple). Typical experiment n=3

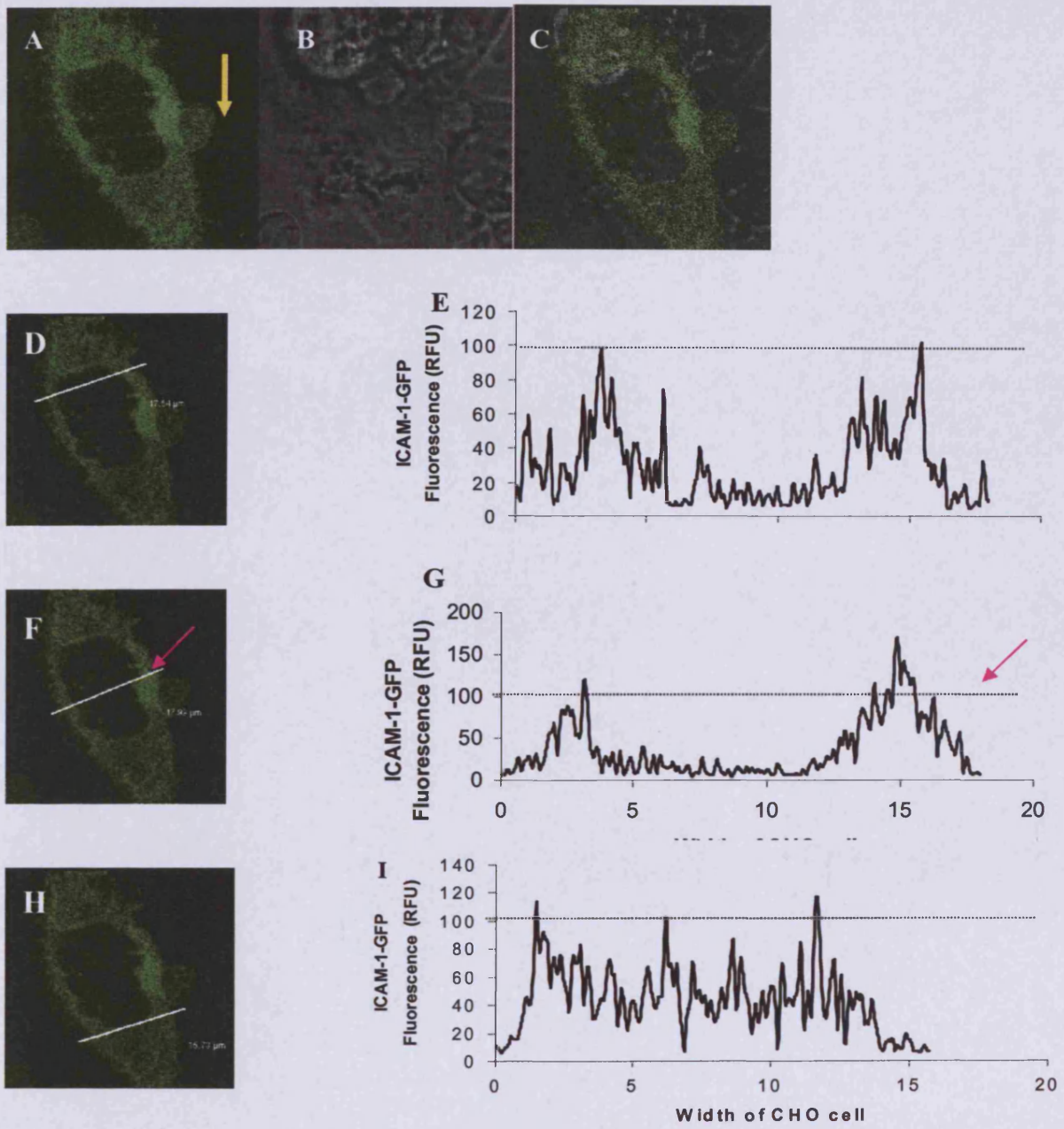

Fig 6.3.3.3 Accumulation of ICAM-1 at Neutrophil Binding Site

Comparison of fluorescence at different sites through the CHO cell expressing ICAM-1-GFP (tailless) with a neutrophil bound. (A) Neutrophil binding indicated by yellow arrow with corresponding brightfield image (B) and overlay (C). (D), (F) and (H) indicate the line of fluorescence intensity shown on graphs (E), (G) and (I) respectively. There is a marked increase in GFP fluorescence near the site of neutrophil binding (purple arrow).

As a control, the micromanipulator was also employed to attempt to adhere neutrophils to CHO cells that did not have ICAM-1-GFP expressed on the plasma membrane. In these experiments there were no detectable changes in the Ca^{2+} in the neutrophils (Fig 6.3.3.4).

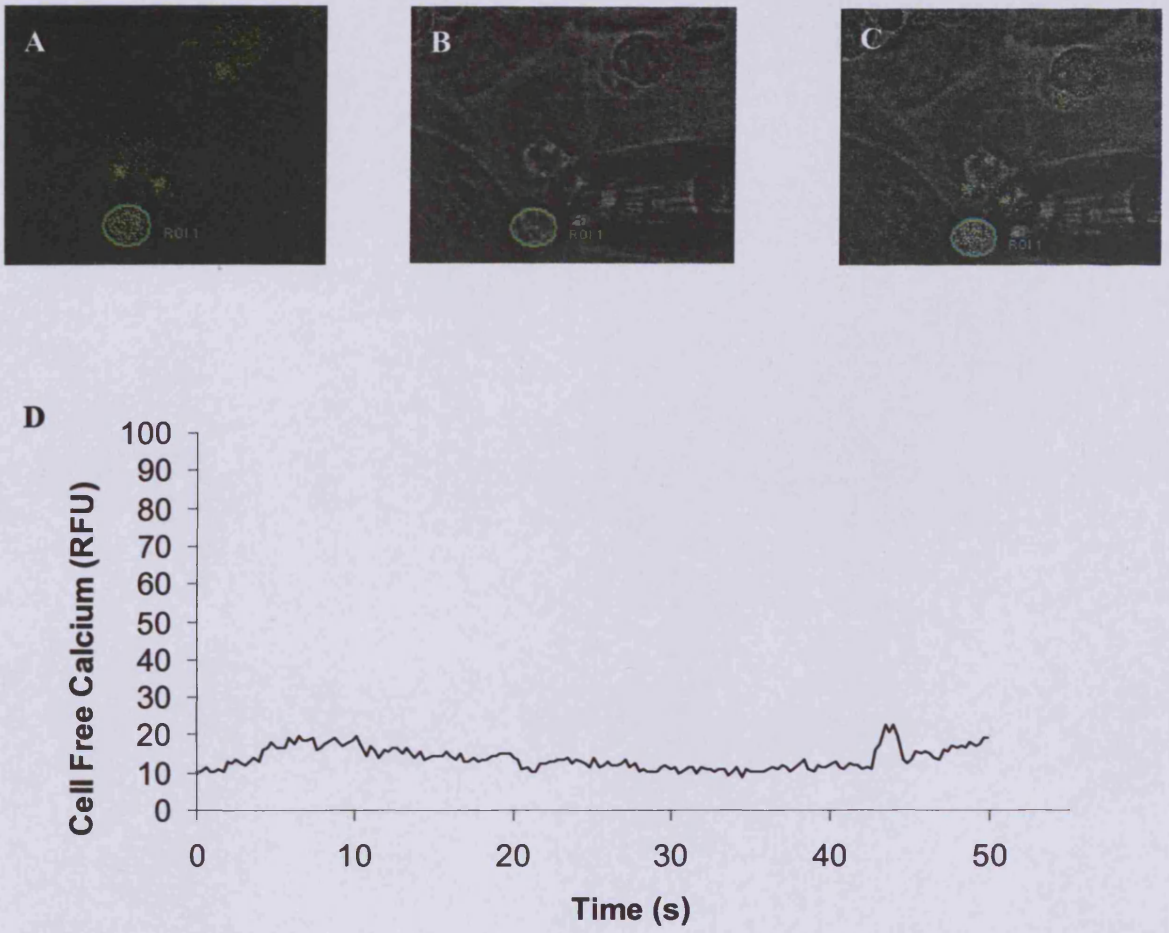

Fig 6.3.3.4 No Ca^{2+} Signal Induced by Non-Transfected CHO Cells

(A) Fluorescence image of neutrophil during forced contact with non-ICAM-1-GFP expressing CHO cell (not visible due to lack of fluorescence) (B) Corresponding brightfield image showing CHO cell, neutrophil and micropipette (C) Overlay of A on B, demonstrating the contact of the fluorescing neutrophil to the non-fluorescing CHO cell. (D) Trace of the cell free calcium level within the shown neutrophil (no calcium signal induced). Typical experiment n=3

6.4 Discussion

The Ca^{2+} signalling toolkit of neutrophils is beginning to be unravelled. The small-size and predisposition to apoptosis make these cells difficult to study. Many studies have resorted to using 'neutrophil-like' cell lines, which can be more easily controlled and manipulated. However, to truly investigate neutrophil behaviours it was deemed necessary to focus on studying human neutrophils and closely mimicking their natural behaviour *in vitro*. In Chapter 4 the subcellular Ca^{2+} signalling events, dubbed Ca^{2+} puffs, were characterised in neutrophils. Ca^{2+} puffs had previously been characterised in only a few other cell types. This was the first report of such Ca^{2+} events in neutrophils. However, the Ca^{2+} puffs were the result of experimental stimulation with supramaximal concentrations of the bacterial tripeptide formyl-met-leu-phe (fMLP) or uncaging the mediator IP_3 inside the neutrophil. This chapter aimed to investigate the Ca^{2+} signalling with more physiologically relevant stimuli. Thus, phagocytosis and binding to ICAM-1 were used as stimuli.

Phagocytosis is a fundamental function of the neutrophil. They have been dubbed "professional phagocytes" by many who study this aspect of their behaviour due to their incredible ability to undergo multiple phagocytic events within a relatively short timeframe. Indeed, in the course of these experiments, neutrophils were observed with more of their total volume being occupied by ingested zymosan particles than by normal cytosolic components. It has been well established that neutrophils undergo a large change in their cytosolic Ca^{2+} concentration during phagocytosis. This appears to be necessary for the closing of the phagocytic cup. To date there had not been a high speed study to dissect the whole-cell Ca^{2+} changes and investigate whether there are contributing subcellular elements.

This study asked whether there were Ca^{2+} puffs or other Ca^{2+} signalling events stimulated by the process of phagocytosis. Two techniques were employed in triggering phagocytosis in a controllable way. Unlike stimulation by formylated peptide, Ca^{2+} waves initiating near the β2-integrin binding site were discovered but no evidence for Ca^{2+} puffs was found.

The situation was similar in experiments designed to isolate the β2-integrin binding pathway. ICAM-1-GFP was transfected into CHO cells that do not normally express ICAM-1 on their cell surface. Neutrophils were then introduced to monolayers of these cells. Where the neutrophils encountered a monolayer of ICAM-1 expressing cells they naturally migrated to junctions between the cells. However, cells that landed in areas of the coverslip with no CHO cells were micromanipulated into contact with ICAM-1-GFP expressing cells. The Ca^{2+} was then monitored at both low and high temporal resolution, which both revealed global Ca^{2+} changes. Again, there was clustering of the ICAM-1-GFP seen at the site of contact, suggesting that it was being accumulated by the β2-integrin binding. However, there were no distinct puncta of ICAM-1-GFP. As with the phagocytosis experiments, and unlike the experiments with fMLP, global Ca^{2+} changes were seen, but rapid confocal imaging failed to reveal any Ca^{2+} puffs.

Presumably, if the Ca^{2+} puff sites are related to the nuclear envelope as discovered in Chapter 4, these may not be close enough to the cell periphery, where β2-integrin engagement was occurring to be activated. It is also interesting to note that as the Ca^{2+} release from the juxta- nuclear zone was "diagnostic" of IP_3 generation (Chapter 4), the lack of release from that site suggests that insufficient IP_3 was generated by β2-

integrin engagement to trigger it. In biochemical experiments where IP_3 levels have been measured, cross linking of β2-integrin molecules has been reported to either produce no IP_3 or at a level approximately $1/10^{th}$ that generated by formylated peptide (Fallman et al, 1993: Hellberg et al, 1996). It is thus suggested that the global Ca^{2+} signals could be the result of an alternative trigger of Ca^{2+} influx other than the IP_3 pathway.

6.5 Conclusion

Physiological, non-soluble stimuli induced Ca^{2+} signalling events in neutrophils. It was not possible to detect Ca^{2+} puffs under these conditions. However, both phagocytosis and binding to ICAM-1 induced Ca^{2+} signals were observed to be accompanied by dramatic morphological changes. This was consistent with the Ca^{2+} influx mediated cell spreading which is driven by elevation of IP_3.

CHAPTER 7

General Discussion

7.1 Introduction

The aim of the work presented in this thesis was to investigate the roles of global and sub-cellular Ca^{2+} events in neutrophil shape change during cell spreading and phagocytosis. This necessitated developing the methodology to visualise and quantify transient sub-cellular Ca^{2+} events. This involved exploiting a relatively recent advance in confocal microscopy technology, namely the resonant scanning head. This scanning mode allows the laser beam to be moved across the sample more rapidly than with conventional scanning confocal microscopes, as the scanning mirror which directs the laser beam resonates back and forth. Significant time was therefore spent in developing the Leica SP2 resonant scanning confocal microscope specifically to hunt for very rapid changes in Ca^{2+}. The confocal microscope also allowed for observations of more spatially restricted Ca^{2+} events than wide-field microscopes. Any event that was localised to a specific region of the cell could be detected in the confocal slice without the signal being diluted or distorted by the signal from the rest of the cell. As outlined in Chapter 3, the Leica SP2 enabled a high level of both temporal and spatial resolution that would allow the detection and subsequent characterisation of any subcellular Ca^{2+} events.

7.2 Petty Ca^{2+} "z-waves" – The Epilogue

The resonant scanning approach was employed in the attempt to visualise the Petty "z-waves" since it was calculated to have sufficient temporal and spatial resolution to detect these. As laid out in Chapter 4, Petty "z-waves" were not detected either in unstimulated, polarised neutrophils, or in cells stimulated with fMLP. The conclusion was therefore drawn that caution should be used when attributing any weight to the reported "z-waves". Subsequent to the completion of this work, correspondence with

other research groups revealed that they also had problems replicating the Petty results. Our results were presented at a conference in March 2008, at which Dr Howard Petty acknowledged problems with the reported "z-waves" and stated that his data would be withdrawn from the public domain, in response both to our results and correspondence he had received from other leading researchers. Our group was the first to publish data showing a lack of "z-waves", and it is thought that this may have encouraged others to openly share similar findings.

7.3 Ca^{2+} Microevents

A significant amount of time during the period of this PhD research was dedicated to the hunt for Ca^{2+} "z-waves", and this may have proved to be a distraction from the main goals. However, while searching for "z-waves", conventional Ca^{2+} signalling events were discovered in neutrophils, namely Ca^{2+} puffs. These were seen to occur before the Ca^{2+} influx wave swamped the cellular signal in neutrophils stimulated with fMLP. The puffs were releases of Ca^{2+} from IP_3 sensitive intracellular stores. There was only ever one Ca^{2+} release site, although multiple release events from a single site were occasionally seen. This corresponds with reports in the literature of a single region of vestigial ER near the nuclear lobes in the neutrophil that contain IP_3R. Indeed, mapping of the Ca^{2+} puffs formed a pattern resembling nuclear lobes of a neutrophil. These Ca^{2+} puffs could also be stimulated by uncaging IP_3 within the cell. IP_3 is downstream in the fMLP signalling pathway but is specific for IP_3 sensitive Ca^{2+} stores, since fMLP can also trigger other intracellular signalling pathways. The IP_3 triggered Ca^{2+} puffs, together with the pattern of release sites, led to the conclusion that Ca^{2+} puffs occur from peri-nuclear IP_3-sensitive Ca^{2+} stores.

7.4 Neutrophil Shape Change

It was observed during experiments to trigger Ca^{2+} signals that there was often a corresponding dramatic morphological shape change in the neutrophil. Since the neutrophil is known to undergo massive changes in its shape during physiological behaviours such as extravasation and phagocytosis, it was thought to be important to establish the role of Ca^{2+} in these events. Initially it was not known whether the Ca^{2+} signal was the cause or the result of shape change. The research presented in Chapter 5 clearly indicates that the Ca^{2+} signal occurs before dramatic shape change. This Ca^{2+} signal was important in accelerating neutrophil shape change. This research determined that the influx of Ca^{2+} provided a sufficiently high local concentration of Ca^{2+} just under the plasma membrane to activate calpain, which is a Ca^{2+} activated protease. Calpain cleaves the talin and ezrin proteins that connect the plasma membrane to the cellular cytoskeleton. This releases the plasma membrane for rapid shape change. It is interesting to note that there is a marked increase in the surface area of the cell during this phenomenon. Neutrophils have extensive folding of their plasma membrane when in their round state. Calpain activation and release of the membrane increases the overall surface area of the neutrophil. Inhibiting calpain caused a marked decrease in the adhesion of neutrophils to glass or fibronectin-coated coverslips, and it also reduced the rate of shape change induced by Ca^{2+} influx. This could be of pharmacological interest. Inhibiting calpain and therefore decreasing the neutrophil ability to extravasate into sites of chronic inflammation could provide a treatment for conditions such as rheumatoid arthritis.

The data shown in Chapter 4 established that conventional Ca^{2+} puffs and influx waves occur in response to soluble and non-physiological stimuli, fMLP and release of IP_3. The data in Chapter 5 further established that Ca^{2+} plays a vital role in activating Ca^{2+}

responsive signalling pathways, such as calpain, to cause the physiological behaviours including dramatic morphological changes that would accompany extravasation and phagocytosis. The next logic step was therefore to establish what forms of Ca^{2+} signalling were involved in these two processes. Ca^{2+} changes were therefore monitored at high speed in response to neutrophil adhesion to ICAM-1-GFP expressing CHO cells and in response to phagocytosis. Global Ca^{2+} changes were seen in both circumstances, although they were a rare occurrence with adhesion to ICAM-1. This may have been due to lack of sufficient ICAM-1 to cause crosslinking and activation of the β-integrin mediated signalling pathway. Phagocytosis was stimulated in two ways: with adherent zymosan and by micromanipulating a zymosan into contact with the neutrophil. There were hints of Ca^{2+} influx waves sweeping across the cells, although capturing clear examples was difficult in these small cells. However, there was a notable lack of Ca^{2+} puffs occurring during phagocytosis. It is therefore proposed that the global Ca^{2+} influx is triggered via a different signalling pathway than the IP_3-mediated Ca^{2+} release and Ca^{2+}-release -Ca^{2+}-influx route. The roles of PIP_3 have recently been established by Dewitt *et al* during phagocytosis and are likely to be the source of the Ca^{2+} influx trigger during phagocytosis and other β-integrin mediated signalling.

7.5 Future Work

The work reported in this thesis opens many interesting avenues for additional research. Future work could focus on developing calpain inhibitors, alongside high throughput techniques for measuring an output for the efficacy of these inhibitors, such as the ECIS machine described in Chapter 5. The current calpain inhibitors are not very efficient or selective for calpain isoforms, and there is therefore scope to improve these for potential

pharmacological use. They could also be tested on a cell model using monolayers of vascular endothelial cells such as HUVECs or HAECs (treated with TNFα to promote expression of ICAM-1), in order to explore how efficient the calpain inhibitors might be at diminishing extravasation. It is going to be important to firmly establish the source of Ca^{2+} signalling during phagocytosis. Understanding of this process would enable manipulation and modification of the pathways involved thereby potentially adapting the phagocytic capacity. This would allow tailoring of the capacity of an individual depending on whether their immune responses need to be enhanced or dampened. Rapid confocal laser scanning has opened the doorway to a plethora of research opportunities in small, active cells such as neutrophils. Future research could also include the study of the relationship and sequencing of signalling pathways, such as establishing whether Ca^{2+} signalling triggers or accompanies f-actin formation using dual dyed confocal microscopy. Since this research began, a new area of research in Ca^{2+} signalling has resulted from the discovery of STIM-1 and Orai. It is yet to be established whether these proteins play a significant role in neutrophils, or even whether they exist there. However, they have proved to be very important in other cell types. This could be an interesting area of further research, and development of inhibitors of this pathway could provide a novel, focussed alternative to thapsigargin.

7.6 The Ultimate Aim

Neutrophils are at the forefront of the immune system. They are notoriously difficult to study due to their short life spans and propensity towards apoptosis. There is a lack of suitable models, with both rodent "neutrophils" and HL60s only providing trends and indications as to what may happen in real human neutrophils. Therefore any research advance made directly in human neutrophils is valuable. However, the ultimate aim must be to understand the workings of these important cells with a view to being able to modify their behaviours and tailor them to individual needs. The work presented in this thesis provides an incremental increase in understanding, which it is hoped will eventually lead to achievement of these ultimate goals.

REFERENCES

Abbassi O, Kishimoto TK, McIntire LV. (1993) Neutrophil adhesion to endothelial cells. Blood Cells 19: 245-260

Abramson JS, Wheeler JG. (1993) The natural immune system: the neutrophil. Oxford University Press, New York, USA.

Alberts B, Bray D, Lewis J, et al. (1994) The Molecular Biology of the Cell. 3rd ed. New York: Garland Press

Allbritton NL, Meyer T, Stryer L (1991) Range of messenger action of calcium ion and inositol 1,4,5-trisphosphate. Science 258:1812-1814.

Al-Mohanna FA, Caddy KWT, Bolsover SR. (1994) The nucleus is insulated from large cytosolic calcium changes. Nature 367: 745-750.

Al-Mohanna FA, Hallett MB. (1988) The use of fura2 to determine the relationship between intracellular free Ca^{2+} and oxidase activation in rat neutrophils. Cell Calcium 8: 17-26.

Al-Mohanna FA, Hallett MB. (1991) Mechanisms of oxidase activation in neutrophils: importance of intracellular calcium and cytoskeletal interactions. In: Harris JR, ed. Blood Cell Biochemistry; Lymphocytes and Granulocytes. New York: Plenum Press, 289-334.

Al-Mohanna FA, Pettit EJ, Hallett MB. (1997) Does actin polymerization status modulate Ca2+ storage in human neutrophils? Release and coalescence of Ca^{2+} stores by cytochalasins. Exp Cell Res 1, 234, 379-87.

Anderson CL, Looney RJ. (1986) Human Ig Fc receptors. Immunol. Today 7: 264-266.

Anderson M, Dewald B, Baggiolini M. (1993) Neutrophil signal transduction and activation of the respiratory burst. Physiol Rev 73: 797-822.

Andersson T, Schlegel W, Monod A, et al. (1986) Leukotriene B4 stimulation of phagocytes results in the formation of inositol 1,4,5-trisphosphate: a second messenger for Ca^{2+} mobilization. Biochem J 240: 333-339.

Arif S, Mufti A. (1998) Immune, Blood, and Lymphatic System. Mosby's Crash Course. Mosby International Ltd, Barcelona, Spain.

Arnaout MA. (1990) Structure and function of the leukocyte adhesion molecule CD11/CD18. Blood 75: 1037-1050.

Babior BM. (1984) Oxidants from phagocytes: agents of defense and destruction. Blood 64: 959-966.

Baggiolini M, Wymann MP. (1990) Turning on the respiratory burst. Trends in Biochem Sci 15: 69-72.

Baker PF. (1972) Transport and metabolism of calcium ions in nerve. Prog Biophys Mol Biol 24:177-223.

Baker PF. (1976) The regulation of intracellular calcium. Symp Soc Exptl Biol 30: 67-88.

Becker EL, Kermode JC, Naccache PH, et al. (1985) The inhibition of neutrophil granule secretion and chemotaxis by pertussis toxin. J Cell Biol 100: 1641-1653.

Bell RM. (1986) Protein kinase C activation by diacylglycerol second messengers. Cell 45: 631-632.

Berg, HC. (1993) Random Walks in Biology. Princeton University Press. 22-23.

Berridge MJ, Irvine RK. (1984) Inosiol trisphosphate, a novel second messenger in cellular signal transduction. Nature 312: 315-317.

Berridge MJ, Lipp P, Bootman MD (2000) The Versatility and Universality of Calcium Signalling. Nature Reviews Molecular Cell Biology, 1, pp11-21

Berridge MJ. (1996) Sifting through the evidence. Biochem. J. 314: 1055-1056.

Bessis M. (1973) Cytologic diagnosis of leukemias by electron microscopy. Recent Results Cancer Res 43,63-70.

Bevilacqua M, Butcher E, Furie B, et al. (1991) Selectins: A family of adhesion receptors. Cell 67: 233-234.

Bootman, MD, Berridge MJ, Lipp P. (1997) Cooking with calcium: The recipes for composing global signals from elementary events. Cell 91; 367-373.

Borregard N, Cowland JB. (1997) Granules of the human neutrophilic polymorphonuclear leukocyte. Blood 15, 89: 3503-21

Borregard N, Herlin T. (1982) Energy metabolism in neutrophils during phagocytosis. J Clin Invest 70: 550-557.

Boulay F, Tardif M, Brouchon L, et al. (1990) The human N-formylpeptide receptor. Characteristation of two cDNA isolates and eveidence for a new subfamily of G-protein-coupled receptors. Biochemistry 29: 11123-11133.

Bradford PG, Rubin RP. (1985) Characterization of f-met-leu-phe stimulation of inositol trisphosphate accumulation in rabbit neutrophils. Mol Pharmacol 27: 74-79.

Brundage RA, Fogarty KE, Tuft RA, et al. (1993) Chemotaxis of newt eosinophils: calcium regulation of chemotactic response. Am J Physiol 265: C1527-C1543.

Burgess GM, McKinney JS, Irvine RF et al. (1985) Inositol 1,4,5-trisphosphate and inositol 1,3,4-trisphosphate formation in Ca^{2+} mobilising hormone activated cells. Biochem J 232:237-253.

Campbell AK, Hallett MB. (1983) Measurement of intracellular calcium ions and oxygen radicals in polymorphonuclear leukocyte-erythrocyte 'ghost' hybrids. J Physiol. 338, 537-50.

Case RM, Eisner D, Gurney A, et al. (2007) Evolution of Calcium Homeostasis: From birth of the first cell to an omnipresent signalling system. Cell Calcium 42 345-350

Caswell AH. (1979) Methods of measuring intracellular calcium. Int Rev Cytol. 56, 145-81

Cline MJ. (1975) The White Cell. Harvard: Harvard University Pres, pp4-16.

Cockcroft S. (1989) The role of inositol phospholipid metabolism and diacylglycerol production in neutrophil signal transduction. In: Hallett MB, ed. The Neutrophil; Cellular biochemistry and physiology. Boca Raton: CRC Press, 167-198.

Colnheim J. (1876a) Uber. Enteundung und Eitung. Virchow's Arch Pathol Anat 40, 1-25

Colnheim J. (1876b) Inflammation in Lectures in General Pathology. Syndenham, Society of London 1, 242-254

Cooke E, Al-Mohanna FA, Hallett MB. (1998) Ca^{2+}-dependent and Ca^{2+}-independent mechanisms in neutrophils. In: Hallett MB, ed. The neutrophil: Cellular Biochemistry and Physiology. Boca Raton: CRC Press.

Cornell-Bell AH, Finkbeiner SM, Cooper MS, et al. (1991) Glutamate induces calcium waves in cultured astrocytes. Science 247: 470-472.

Cramer EB, Gallin JI. (1979) Localisation of submembranous cations to the leading edge of human neutrophils during chemotaxis. J Cell Biol 82: 369-375.

Dace JV, Lewis SM. (1995) Practical Haematology. Churchill Livingstone. New York

Davies A, Lachmann PJ. (1993) Membrane defence against complement lysis: the structure and biological properties of CD59. Immunol. Rev 12:258-275.

Davies EV, Hallett MB, Campbell AK. (1991) Localised superoxide release by neutrophils can be provoked by a cytosolic calcium "cloud". Immunology 73:228-234.

Davies EV, Hallett MB. (1995a) A novel pathway for Ca^{2+} signalling in neutrophils by immune complexes. Immunology 85: 538-543.

Davies EV, Hallett MB. (1995b) A soluble factor directly stimulates Ca^{2+} entry in neutrophils. Biochem Biophys Res Commun 206: 348-354.

Davies EV, Hallett MB. (1996) Near membrane Ca^{2+} changes resulting from store release in neutrophils: detection by FFP-18. Cell Calcium 19: 355-362.

Davies EV, Hallett MB. (1998) High micromolar Ca^{2+} beneath the plasma membrane in stimulated neutrophils. Biochem Biophys Res Commun 30, 248, 679-83.

Davies-Cox EV, Laffafian I, Hallett MB. (2001) Control of Ca^{2+} influx in human neutrophils by IP_3 binding: differential effects of micro-injected IP_3 receptor antagonists. Biochem. J., 355, 139-143.

DeLisi C. (1980) The biophysics of ligand-receptor interactions. Quart Rev Biophys 13: 201-223.

Demaurex N, Lew DP, Krause K-H. (1992) Cyclopiazonic acid depletes intracellular Ca^{2+} storesand activates an influx pathway for divalent cations in HL-60 cells. J Biol Chem 267: 2318-2324.

Demaurex N, Monod A, Lew DP, et al. (1994) Characteristion of receptor-mediated and store-regulated Ca^{2+} influx in human neutrophils. Biochem. J. 297: 595-601.

Dewitt S, Hallett MB. (2002) Cytosolic free Ca^{2+} changes and calpain activation are required for ß2 integrin-accelerated phagocytosis by human neutrophils. J. Cell Biol. 159; 181-189

Dewitt S, Hallett MB. (2007) Leukocyte membrane "expansion": A central mechanism for leukocyte extravasation. J Leukocyte Biol 81: 1160–1164

Dewitt S, Laffafian I, Morris MR, Hallett MB. (2002) Measurement of cytosolic free Ca^{2+} in human neutrophils. Meth. Mol. Biol. 225 47- 60.

Dewitt S, Tian W, Hallett MB. (2003) Phagosomal oxidative activity during $ß_2$ integrin (CR3)-mediated phagocytosis by neutrophils is triggered by a non-restricted Ca^{2+} signal: Ca^{2+} controls time not space. J Cell Sci. 116: 2857-2865

Dewitt S, Tian W, Hallett MB. (2006) Localised $PI(3,4,5)P_3$ at the phagocytic cup is required for both phagosome closure and Ca^{2+} signalling in HL60 neutrophils. J Cell Sci 119 443-451

Ding AH, Porteu F. (1992) Regulation of tumor necrosis factor receptors on phagocytes. Proc Soc Exp Biol Med. 200: 458-465.

DiPolo R, Requena J, Brinkley FJ, et al. (1976) Ionized calcium concentrations in squid axons. J Gen Physiol 67: 433-467.

DiVirgilio F, Lew PD, Andersson T, Pozzan T. (1987) Plasma membrane potential modulates chemotactic peptide-stimulated cytosolic free Ca^{2+} changes in human neutrophils. J Biol Chem 262: 4574-9.

DiVirgilio F, Vicentini LM, Treves S, et al. (1985) Inositol phosphate formation in f-met-leu-phe stimulated human neutrophils does not require an increase in the cytosolic free Ca^{2+} concentration. Biochem J 229: 361-366.

Dougherty RW, Godfrey PP, Hoyle PC, et al. (1984) Secretagogue-induced phosphoinositol metabolism in human leukocytes. Biochem J 222: 307-312.

Dusi S, Donini M, Dell Bianca V, et al. (1994) Tyrosine phosphorylation of phospholipase$C\gamma$-2 is involved in the activation of phosphoinositide hydrolysis by Fc receptors in human neutrophils. Biochem Biophys Res Commun 201:1100-1108.

Ehrlich P. (1898): Ueber den Zusammenhang von chemischer Constitution und Wirkung. Münchener medizinische Wochenschrift: 1654-1655

Elsbach D, Schwartz IL. (1959) Studies on sodium and potassium transport in rabbit polymorphonuclear leukocytes. J Gen Physiol 42: 883-891.

Fallman M, Andersson R, Andersson T. (1993) Signalling properties of CR3 (CD11b/CD18) and CR-1 (CD35) in relation to phagocytosis of complement opsonised particles. J Immunol 151: 330-338

Fallman M, Gullberg M, Hellberg C, et al. (1992) Complement receptor-mediated phagocytosis is associated with accumulation of phosphatidyl choline-derived diglyceride in human neutrophils. J Biol Chem 267: 2665-2663.

Favre CJ, Jerstrom P, Foti M, et al. (1996) Organization of Ca^{2+} stores in myeloid cell: association of SERCA2b and the type-1 inositol 1,4,5-trisphosphate receptor. Biochem J 316: 137-142.

Foder B, Scharff O, Thastrup O. (1989) Ca^{2+} transients and Mn^{2+} entry in human neutrophils induced by thapsigargin. Cell Calcium 10: 477-490.

Foreman JC, Hallett MB, Mongar JL. (1977) The relationship between histamine secretion and ^{45}calcium uptake by mast cells. J Physiol 271: 193-214.

Gandola P, Rosen BP. (1987) Maintenance of intracellular calcium in Eschericia coli. J. Biol Chem, 262 12570-12574

Gennaro R, Pozzan T, Romeo D. (1984) Monitoring of cytosolic free Ca^{2+} in C5a-stimulated neutrophils: Loss of receptor-modulated Ca^{2+} stores and Ca^{2+} uptake in granule-free cytoplasts. Proc Natl Acad Sci USA 81: 1416-1420.

Gerard C, Gerard NP. (1994) C5a and its receptor. Ann Rev Immunol 12: 775-888.

Gerard NP, Gerard C. (1991) The chemotactic recptor for human C5a anaphylotoxin. Nature 1991; 349: 614-617.

Gilbert SH, Perry K, Fay FS. (1994) Mediation of chemoattractant-induced changes in $[Ca^{2+}]_i$ and cell shape, polarity and locomotion in IP_3, DAG and protein kinase C in newt eosinophils. J Cell Biol 127: 489-503.

Hallett MB. (1989) The unpredictability of cellular behavior: trivial or of fundamental importance to cell biology? Perspect Biol Med 33, 110-119

Hallett MB, Campbell AK. (1984) Is intracellular calcium the trigger for oxygen radical production by polymorphonuclear leucocytes? Cell Calcium 5: 1-19.

Hallett MB, Davies EV, Campbell AK. (1990) Oxidase activation in individual neutrophils is dependent on the onset and magnitude of the Ca^{2+} signal. Cell Calcium 11: 655-663.

Hallett MB, Dewitt S. (2007) Ironing out the wrinkles of neutrophil phagocytosis: Trends in Cell Biology

Hallett MB, Lloyds D. (1995) Neutrophil priming; the cellular signals which say "amber" but not "green". Immunology Today 16: 264-268.

Hallett MB, Pettit EJ (1997) Stochastic events underlie Ca^{2+} signalling in neutrophils. J Theor Biol 186, 1-6

Hallett MB, Pettit EJ, Davies EV. (1996) Capacitative Ca^{2+} influx and a diffusible influx factor. Biochem. J. 314: 1054-1055

Hallett MB, von Ruhland, CJ, Dewitt S. (2008) Chemotaxis and the cell surface area problem. Nature Rev Mol Cell Biol 9: 662-663

Hamachi T, Hirata M, Koga T. (1986) Origin of intracellular calcium and quantitation of mobilizable calcium in neutrophils stimulated with chemotactic peptide. Biochim Biophys Acta 889: 136-142.

Haslett C. (1992) Resolution of acute inflammation and the role of apoptosis in the tissue fate of granulocytes. Clin Sci (London) 83, 639-648

Haughland RP. (2002) In Handbook of fluorescent probes. (9th Edition). Molecular Probes Oregon USA 776-780.

Heiner I, Eisfeld J, Halaszovich CR, et al. (2003b) Expression profile of the transient receptor potential (TRP) family in neutrophil granulocytes: evidence for currents through long TRP channel 2 induced by ADP-ribose and NAD. Biochem J 371: 1045-1053

Heiner I, Eisfeld J, Luckhoff A. (2003a) Role and regulation of TRP channels in neutrophil granulocytes. Cell Calcium 33: 533-540

Hellberg C, Molony L, Zheng L, et al. (1996) Ca^{2+} signalling mechanisms of the ß2 integrin on neutrophils: involvement of phospholipaseCγ2 and IP_3. Biochem J 317: 403-409.

Hirsch JG, Cohn ZA. (1960) Degranulation of polymorphonuclear leukocytes following phagocytosis of microorganisms. J Exp Med 112, 1005

Hoffstein ST. (1979) Ultrastructural demonstration of calcium loss from local regions of the plasma membrane of surface stimulated human granulocytes. J Immunol 123: 1395-1402.

Hogg JC. (1987) Neutrophil kinetics and lung injury. Physiological Review 67, 1249-1295

Hokin MR, Hokin LE. (1953) Enzyme secretion and the incorporation of ^{32}P into phosophatides of pancreas slices. J Biol Chem 203: 967-977.

Holmes WE, Lee J, Kwang WJ, et al. (1991) Structure and functional expression of a human interleukin-8 receptor. Science 253: 1278-1280.

Horne JH, Meyer T. (1997) Elementary calcium-release units induced by inositol trisphosphate. Science 276: 1690-1693.

Huang JB, Kindzelskii AL, Clark AJ, Petty HR. (2004) Identification of channels promoting calcium spikes and waves in HT1080 tumor cells: Their apparent roles in cell motility and invasion. Cancer Res. 64 2482-2489.

Hynes RO. (1992) Integrins: versatility, modulation and signaling in cell adhesion. Cell 69: 11-25.

Insall RH, Jones GE, (2006) Moving matters: signals and mechanisms in directed cell migration. Nature Cell Biology 8 776 - 779.

Jackowski S, Petro K, Sha'afi RI. (1979) A Ca^{2+}-stimulated ATP-ase activity in rabbit neutrophil membranes. Biochim Biophys Acta 558: 348-354.

Jaiswal JK. (2001) Calcium – How and Why? J. Biosci. 26 357-363

Jog N, Rane MJ, Lominadze G, et al. (2007) The actin cytoskeleton regulates exocytosis of all neutrophil granule subsets. Am J Physiol Cell Physiol 292, C1690-700

Kantari C, Pederzoli-Ribeil M, Witko-Sarsat V. (2008) The role of neutrophils and monocytes in innate immunity. Contrib Microbiol 15, 118-46

Karnovsky ML, Wallach DFH. (1961) the metabolic basis of phagocytosis: incorporation of inorganis phosphate into various classes of phophatides during phagocytosis. J Biol Chem 236: 1895-1903.

Kasai H, Augustine GL. (1990) Cytosolic free Ca^{2+} gradients triggering unidirectional fluid secretion from exocrine pancreas. Nature 348: 735-738.

Kim KH, Kim JW, Zilberstein A, et al. (1991) PDGF stimulation of inositol phospholipid hydrolysis requires phospholipase C γ-1 phosphorylation of tyrosine residues 783 and 1254. Cell 65: 435-441.

Kindzelskii AL, Petty HR. (2002).Apparent role of traveling metabolic waves in oxidant release by living neutrophils Proc Natl Acad Sci (USA) 99, 9207-9212

Kindzelskii AL, Petty HR. (2003) Intracellular calcium waves accompany neutrophil polarization, formylmethionylleucylphenylalanine stimulation, and phagocytosis: A high speed microscopy study. J. Immunol. 170, 64-72.

Kindzelskii AL, Petty HR. (2004) Fluorescence spectroscopic detection of mitochondrial flavoprotein redox oscillations and transient reduction of the NADPH oxidase-associated flavoprotein in leukocytes. Eur Biophys J Biophys Lett 33 (2002) 291-299.

Kindzelskii AL, Petty HR. (2005) Ion channel clustering enhances weak electric field detection by neutrophils: apparent roles of SKF96365-sensitive cation channels and myeloperoxidase trafficking in cellular responses. Eur Biophys J Biophys Lett 35 1-26.

Kindzelskii AL, Sitrin RG, Petty HR. (2004) Optical micro-spectrophotometry supports the existence of gel phase lipid rafts at the lamellipodium of neutrophils: Apparent role calcium signaling. J Immunol 172 4681-4685.

Kippert F. (1987) Endoctyobiotic coordination, intracellular calcium signalling, and the origin of endogenous rythms, Ann NY Acad, Sci 503 476-495

Klempner MS. (1985) An ATP-dependent calcium pump in human neutrophil lysosomes. J Clin Invest 76: 303-310.

Krause K-H, Lew DP. (1987) Subcellular distribution of Ca^{2+} pumping sites in human neutrophils. J Clin Invest 80: 107-116.

Krause K-H, Pittet D, Volpe P, et al. (1989) Calciosome, a sarcoplasmic reticulum like organelle involved in intracellular Ca^{2+}-handling by non-muscle cells: studies in human neutrophils and HL-60 cells. Cell Calcium 10: 351-361.

Krause K-H, Schlegel W, Wollheim CB, et al. (1985) Chemotactic peptide activation of human neutrophils and HL-60 cells. Pertussis toxin reveals correlation between inositol tris-phosphate generation, calcium ion transients, and cellular activation. J Clin Invest 76: 1-11.

Kretsinger RH, Nockolds CE. (1973) Carp muscle calcium-binding protein. II. Structure determination and general description J Bio Chem 248 pp 3313-3326

Kruskal BA, Maxfield FR. (1987) Cytosolic free calcium increases before and oscillates during frustrated phagocytosis in macrophages. J Cell Biol 105 2685-2693

Kruskal BA, Shak S, Maxfield FR. (1986) Spreading of huiman neutrophils is preceded by a large increase in cytosolic free calcium Proc. Natl Acad Sci (USA) 83 2919-2923

Lad PM, Olson CV, Smiley PA. (1985) Assocaition of the N-formyl-met-leu-phe reeptor in human neutrophils with a GTP-binding protein sensitive to pertussis toxin. Proc Natl Acad Sci USA 82: 1348-1382.

Laffafian I, Hallett MB. (1995) Does cytosolic free Ca^{2+} signal neutrophil chemotaxis? J. Cell Sci.108: 3199- 3205

Laffafian I, Hallett MB. (1998) Lipid-assisted microinjection: introducing material into the cytosol and membranes of small cells. Biophys J. 75 2558-2563.

Lawrence MB, Springer TA. (1991) Leukocytes roll on a selectin at physiological flow rates: distinction from and prerequisite for adhesion through integrin. Cell 65, 859-873

Lee J-O, Rieu P, Arnaout MA, et al. (1995) Crystal structure of the A domain from the subunit of integrin CR3 (CD11b/CD18). Cell 80: 631-638.

Lehninger D, Cox AL, Nelson MM. (2004) Lehninger Principles of Biochemistry Published by W.H. Freeman & Company

Lew DP, Monod A, Krause K-H, et al. (1986) The role of cytosolic free Ca^{2+} in the generation of inositol 1,4,5-trisphosphate and inositol 1,3,4-trisphosphate in HL-60 cells. J Biol Chem 261: 13121-13128.

Ley K, Laudanna C, Cybulsky MI, Nourshargh S. (2007) Getting to the site of inflammation: the leukocyte adhesion cascade updated. Nature Reviews Immunol 7: 678-689

Lin G, Chattopadhay D, Maki M, et al. (1997) Crystal structure of calcium bound domain VI of calpain at 1.9Å resolution and its role in enzyme assembly, regulation, and inhibitor binding. Nature Struct. Biol. 4:539–547.

Lipp P, Thomas D, Berridge MJ, Bootman MD. (1997) Nuclear calcium signalling by individual cytoplasmic calcium puffs. EMBO J. 16 7166–7173.

Lloyds D, Brindle NJP, Hallett MB. (1995) Priming of human neutrophils by substance P and TNF-α is associated with tyrosine phosphorylation. Immunology 84: 220-226.

Lofgren R, Ng-Sikorski J, Sjolander A, et al. (1993) ß2 integrin engagement triggers actin polymerisation and phosphatidyl inositol tris phosphate in non-adherent neutrophils. J Cell Biol 123: 1597-1605.

Lominadze G, Powell DW, Luerman CG, et al. (2005) Proteomic Analysis of Human Neutrophil Granules. Mol. Cell. Proteomics 4 1503-1521.

Lorant DE, Zimmermann GA, McIntire TM, et al. (1995) Platelet-activating factor mediates procoagulant activity on the surface of endothelial cells by promoting leukocyte adhesion. Sem Cell Biol 6, 295-303

Macconi D, Foppolo M, Paris S, et al. (1995) PAF mediates neutrophil adhesion to thrombin or TNF stimulated endothelial cells under shear stress. Am J Physiol 269: C46-C47.

Marshall MS. (1995) Ras target proteins in eukaryotic cells. FASEB J 9: 1311-1318.

Mason MJ, Garcia-Rodriguez C, Grinstein S. (1991) Coupling between intracellular Ca^{2+} stores and the Ca^{2+} permeability of the plasma membrane. J Biol Chem 266: 20856-20862.

McEver RP. (1991) Selectins: novel receptors that mediate leukocyte adhesion during inflammation. Throm Haemostas 65: 223-228

Merritt JE, Armstrong WP, Benham J, et al. (1990) SKF 96365: a novel inhibitor of receptor-mediated calcium entry. Biochem J 271: 515-522

Merritt JE, Jacob R, Hallam TJ. (1989)Use of manganese to distinguish calcium influx from mobilisation from internal stores in stimulated human neutrophil. J Biol Chem 264: 1522-1527.

Metchnikoff E. (1892) Leçons sur la pathologie comparée de l'inflammation (Lectures on the Comparative Pathology of Inflammation).

Metchnikoff E. (1901) L'Immunité dans les maladies infectieuses (Immunity in Infectious Diseases),

Metchnikoff E. (1905) Études sur la nature humaine (The Nature of Man).. Translated by Cambridge University Press

Metzger H. (1992) Transmembrane signalling:the joy of aggregation. J Immunol; 149:1477-1487.

Meyer T, Stryer L. (1991) Calcium spiking. Ann Rev Biophys Biophys Chem 20: 153-174.

Michelangeli F, Ogunbayo OA, Wootten LA, (2005) A Plethora Of Interacting Organellar Ca^{2+} Stores, Current Opinion in Cell Biology 17 135-140

Michetti M, Salamino F, Minafra R, et al. (1997) Calcium binding properties of human erythrocyte calpain. Biochem. J. 325:721–726.

Mong S, Ch-Rosso G, Miller J, et al. (1986) Leukotriene B4 induces formation of inositol phosphates in rat polymorphonuclear leukocytes. Mol Pharmacol 30: 235-241.

Morgan BP, van der Berg CW, Davies EV, et al. (1993) Cross-linking of CD59 and other glycosyl phosphatidylinositol-anchored molecules on neutrophils triggers cell activation via tyrosine kinase. Eur J Immunol 23: 2841-2845.

Murphy PM, Tiffany HL. (1991) Cloning of complementary DNA encoding a functional human interleukin-8 receptor. Science 253: 1281-1283.

Murphy PM. (1994) The molecular biology of chemoattractant receptors. Ann Rev Immunol 12: 593-633.

Naccache PH, Molski MM, Volpi M, et al. (1985) Unique inhibitory profile of platelet activating factor induced calcium mobilisation and granule secretion in rabbit neutrophils toards pertussis toxin and phorbol ester. Biochem Biophys Res Commun 130: 677-682.

Naccache PH, Showell H, Becker EL, et al. (1977) Changes in ionic movements across rabbit polymorphonuclear leukocyte membranes during lysosomal enzyme release. J Cell Biol 75: 635-643.

Nakamura M, Honda Z, Izumi T, et al. (1991) Molecular cloning and expression of platelet activating factor from human leukocytes. J Biol Chem 266: 20400-20405.

Nasmith PE, Grinstein S. (1987) Are Ca^{2+} channels in neutrophil activated by a rise in cytosolic free Ca^{2+} ? FEBS Lett 221: 95-100.

Ng-Sikorski J, Andersson R, Patarroyo M, et al. (1991) Calcium signalling capacity of the CD11b/CD18 integrin on human neutrophils. Expt Cell Res 195: 504-509.

Niedergerke R. (1963) Movement of Ca^{2+} in beating ventricles of frog heart. J Physiol 167: 551-580.

Niggli E. (1999) Localized intracellular calcium signaling in muscle: Calcium sparks and calcium quarks. Ann. Rev. Physiol. 61 311-335.

Ohta H, Okajima F, Ui M. (1985) Inhibition by islet activating factor of a chemotactic peptide-induced early breakdown of inositol phospholipids and Ca^{2+} mobilisation in guinea pig neutrophils. J Biol Chem 260: 15771-15780.

Okuda K, Sanghera JS, Pelech SL, et al. (1992) Granulocyte-macrophage colony stimulating factor, interleukin-3, and steel-factorm rapid tyrosine phosphorylation of p42 and p44 MAP kinase. Blood 79, 2880-2887

Osipchuk YV, Wak M, Yule DI, Gallacher DV, Petersen OH. (1990) Cytosolic Ca^{2+} oscillations evoked by receptor stimulation, G-protein activation, internal application of

IP_3 or Ca^{2+} simultaneous microfluorimetry and Ca^{2+} dependent Cl-current recording in single pancreatic cells. EMBO J 9, 697-704

Parekh AB, Terlau H, Stuhmer W. (1993) Depletion of IP_3 stores activates a Ca^{2+} and K^+ current by means of a phosphatase and a diffusible messenger. Nature 364: 814-818.

Parekh AB. (2006) Cell biology - Cracking the calcium entry code. Nature 441, 163-164

Parekh AB. (2007) Functional consequences of activating store-operated CRAC channels. Cell Calcium 42, 111-21.

Park MK, Ashby MC, Erdemli G, et al. (2001) Perinuclear, perigranular and sub-plasmalemmal mitochondria have distinct functions in the regulation of cellular calcium transport EMBO J. 20 1863-1874.

Parker I, Choi J, Yao Y. (1996) Elementary events of InsP(3)-induced Ca^{2+} liberation in Xenopus oocytes: Hot spots, puffs and blips. Cell Calcium 20, 105-12.

Perraud AL, Fleig A, Dunn CA, et al. (2001) ADP-ribose gating of the calcium-permeable LTRPC2 channel revealed by Nudix motif homology. Nature 411:542-3.

Petersen M, Williams JD, Hallett MB. (1993) Cross-linking of CD11b or CD18 signals release of localised Ca^{2+} from intracellular stores in neutrophils. Immunology 80: 157-159.

Petersen OH. (2005) Ca^{2+} signalling and Ca^{2+}-activated ion channels in exocrine acinar cells. Cell calcium 38, 171-200

Petroski RJ, Becker EL, Sha'afi RI. (1963) Effects of the chemotactic peptide and cytochalasin B on the cellular level of calcium in rabbit neutrophils. FEBS Lett 100: 161-165.

Pettit EJ, Hallett MB. (1995) Early Ca^{2+} signalling events in neutrophils detected by rapid confocal laser scanning. Biochem J 310: 445-448.

Pettit EJ, Hallett MB. (1996a) Localised and global cytosolic Ca^{2+} changes in neutrophils during engagement of CD11b/CD18 integrin visualised using confocal laser scanning reconstruction. J Cell Sci 109: 1689-1694.

Pettit EJ, Hallett MB. (1996b) Temporal and spatial resolution of Ca^{2+} release and influx in human neutrophils using a novel confocal laser scanning mode. Biochem Biophys Res Commun 229: 109-113.

Pettit EJ, Hallett MB. (1997) Pulsatile Ca^{2+} influx in human neutrophils undergoing CD11b/CD18 integrin engagement. Biochem Biophys Res Commun 1997 230: 258-261

Pettit EJ, Hallett MB. (1998) Release of 'caged' cytosolic Ca^{2+} triggers rapid spreading of human neutrophils adherent via integrin engagement . J Cell Sci 111 2209-2215.

Petty HR, Liang B, Maher RJ. (1992) Mapping the entry of reactive oxygen metabolites into target erythrocytes during neutrophil-mediated antibody-dependent cellular cytotoxicity. J Cell Physiol 150: 447-450.

Prentki M, Wollheim CB, Lew DP. (1984) Ca^{2+} homeostasis in permeabilised human neutrophils: characterisation of Ca^{2+} sequestering pools and the action of inositol 1,4,5-trisphosphate. J Biol Chem 259; 255: 777-784.

Prossnitz ER, Quehenberger O, Cochrane CG, et al. (1993) The role of the third intracellular loop of the N-formyl peptide receptor in G protein coupling. Biochem J 294:581-587.

Pryzwansky KB, MacRae EK, Spritznagel JK, Cooney MH. (1979) Early degranulation of human neutrophils; immunochemical studies of surface and intracellular phagocytic events. Cell 18, 1025-1033.

Putney JW Jr, McKay RR. (1999) Capacitative Calcium Entry Channels. Bioessays 21, 38-46

Rabinovitch M. (1995) Professional and non-professional phagocytes: introduction. Trends Cell Biol, 5, 85-87

Randriamampita C, Tsein RY. (1993) Emptying of intracellular Ca^{2+} stores releases a novel small messenger that stimulates Ca^{2+} influx. Nature;364: 809-814.

Rhee SG, Choi KD. (1992) Regulation of inositol phospholipid specific phospholipase C isozymes. J Biol Chem 267: 12393-12396.

Rickard JE, Sheterline P. (1985) Evidence that phorbol ester interferes with stimulated Ca^{2+} redistribution by activating Ca^{2+} efflux in neutrophil leucocytes. Biochem J 231: 623-628.

Roberts G, Davies EV, Pettit EJ, et al. (1997) The timing and magnitude of Ca^{2+} signalling by CD32 depends on its redistribution on the cell surface. Exptl Cell Res 230: 303-306.

Roberts GM, Davies EV, Hallett MB. (1995) Slow Ca^{2+} waves in large myeloid cells as a result of a diffusible cytosolic factor. J Leukoc Biol 57: 837-841

Robinson RA, Stokes RH. (1968) Electrolyte solutions. Butterworths, London.

Rooney TA, Sass EJ, Thomas AP. (1990) Agonist-induced cytosolic oscillations originate from specific locations in single hepatocytes. J Biol Chem 265: 10792-10796.

Rosales C, Jones SL, McCourt D et al. (1994) Bromophenacyl bromide binding to the actin-bundling protein 1-plastin inhibits IP_3-independent increase in Ca^{2+} in human neutrophils. Proc Natl Acad Sci USA 91: 3534-3538.

Sage SO, Pintado E, Mahaut-Smith MP, et al. (1990) Rapid kinetics of agonist-evoked cytosolic free Ca^{2+} concentration in fura2-loaded human neutrophils. Biochem J 265: 915-918.

Sano Y, Inamura K, Miyake A, et al. (2001) Immunocyte Ca^{2+} influx system mediated by LTRPC2. Science 293, 1327-30.

Saris NEL, Carafoli E. (2005) A Historical Review of Cellular Calcium Handling, with Emphasis on Mitochondria, Biochemistry (Moscow) Vol 70, No 2 pp187-194

Sbarra AJ, Karnovsky ML. (1960) The biochemical basis of phagocytosis. Incorporation of ^{14}C-labelled building blocks into lipid, protein and glycogen of leukocytes during phagocytosis. J Biol Chem 235: 2224-2231.

Scharff O, Foder B. (1993) Regulation of cytosolic Ca^{2+} in blood cells. Physiol. Rev. 73 547-582.

Schmid-Schonbein GW, Shih YY, Chen S. (1980) Morphometry of human leucocytes. Blood 56: 866-878.

Schneider C, Mottola C, Romeo D. (1979) Calcium dependent adenosine triphosphate activity and plasma membrane phosphorylation in the human neutrophil. Biochem J 182: 655-660.

Schwab JC, Leong DA, Mandell GL. (1992) A wave of elevated intracellular calcium spreads through human neutrophils during phagocytosis of zymosan. J Leukocyte Biol 51: 437,443.

Segal AW, Jones OT. (1978) Novel cytochrome b system in phagocytic vacuoles of human phagocytes. Nature 27, 515-518

Selvaraj P, Rosse WF, Silber R, et al. (1988) The major Fc receptor in blood has a phosphoinositol anchor and is deficient in paroxysmal nocturnal haemoglobinuria. Nature 333: 565-567.

Shaner NC, Steinbach PA, Tsien RY. (2005) A guide to choosing fluorescent proteins. Nature Methods 2: 905-909.

Simchowitz L, De Weer RI. (1986) Chloride movements in human neutrophils. J Gen Physiol 88: 167-175.

Simchowitz L, Roos A. (1985) Regulation of intracellular pH in human neutrophils. J Gen Physiol 85: 443-452.

Southwick FS, Stossel TP. (1983) Contractile proteins in leukocyte function. Sem Haematol 20, 305-321

Stehno-Bittel L, Perez C, Clapham DE. (1995) Diffusion across the nuclear envelope inhibited by depletion of the nuclear Ca^{2+} store. Science 270:1835-1838

Stendahl O, Krause K-H, Krischer J, et al. (1994) Redistribution of intracellular Ca^{2+} stores during phagocytosis in human neutrophils. Science 265: 1439-1441.

Stossel TP. (1989) From signal to pseudopod. J. Biol Chem 264, 18261-18264

Strosberg AD. (1991) Structure/function relationship of proteins belonging to the family of receptors coupled to GTP-binding proteins. Eur J Biochem 196: 1-10.

Styrt B, Klempner MS. (1998) Lysosomotropic amines modulate neutrophil calcium homeostasis. J. Cell Physiol. 135 309–316.

Taylor CW, Thorn P. (2001) Calcium Signalling: IP_3 rises again...and again May 1; 11 (9) R352-5

Terasaki M, Song J, Wong MR, et al. (1984) Localisation of endoplasmic reticulum in living and glutaraldehyde-fixed cells with fluorescent dyes. Cell 38: 101-109.

Thelen M, Dewald B, Baggiolini M. (1993) Neutrophil signal transduction and activation of the respiratory burst. Physiol Rev 73: 797-822.

Theler J-M, Lew DP, Jaconi ME, et al. (1995) Intracellular pattern of cytosolic Ca^{2+} changes during adhesion and multiple phagocytosis in human neutrophils. Dynamics of intracellular Ca^{2+} stores. Blood 85: 2194-2201.

Thomas D, Lipp P, Tovey SC, et al. (2000) Microscopic properties of elementary Ca^{2+} release sites in nonexcitable cells. Curr. Biol. 10 8-15.

Thorn P, Lawrie AM, Smith PM, Gallacher DV, Petersen OH. (1993) Local and global Ca^{2+} oscillations in exocrine cells evoked by agonist and IP_3. Cell 74, 661-668

Tian W, Laffafian I, Dewitt S, Hallett MB. (2003) Exclusion of exogenous PIP_3 from neutrophil polarizing pseudopodia: stabilisation of uropod and cell polarity. EMBO Reports 4, 10, 982–988

Tovey SC, de Smet P, Lipp P, et al. (2001) Calcium puffs are generic InsP(3)-activated elementary calcium signals and are down regulated by prolonged hormonal stimulation to inhibit cellular calcium responses. J. Cell Sci. 114 3979-3989.

Tsien RY. (1989) Fluorescent probes of cell signalling . Ann Rev Neurosci 12: 227-253

Ueda T, Rieu P, Brayer J, et al. (1994) Identification of the complement iC3b binding site in the ß2 integrin CR3 (CD11b/CD18). Proc Natl Acad Sci USA 91: 10680-10684.

van der Berg CW, Cinek T, Hallett MB, et al. (1995) Exogenous GPI-anchored CD59 associates with kinases in membrane clusters on U937 cells and becomes Ca^{2+}-signalling competent. J. Cell Biol. 331: 669-678.

Vander AJ, Sherman JH, Luciano DS. (1994) 'Defence Mechanisms Of The Body' in Human Physiology. Ed 6, 699-754. McGraw-Hill, Inc, USA.

Venkatachalam K, Montell C. (2007) TRP Channels. Ann. Rev. Biochem. 76:387–417

Verghese MW, Smith CD, Snyderman R. (1985) Potential role for guanine nucleotide regulatory protein in chemoattractant receptor mediated polyphosphoinositide metabolism, Ca^{2+} mobilisation and cellular responses by leukocytes. Biochem Biophys Res Commun 127: 450-455.

Volpe P, Krause KH, Hashimoto KS, et al. (1988) Calciosome, a cytoplasmic organelle: the inositol 1,4,5 trisphosphate-sensitive calcium store of non-muscle cells? Proc Natl Acad Sci USA 85: 1091-1095

Volpi M, Naccache PH, Molski TFP, et al. (1985) Pertussis toxin inhibits the f-met-leu-phe, but not the phorbol ester stimulated changes in ion fluxes, protein phosphorylation and phospholipid metabolism in rabbit neutrophils. Proc Natl Acad Sci USA 82: 2708-2713.

Volpi M, Naccache PH, Sha'afi RI. (1982) Preparation of inside out vesicles from neutrophils capable of actively transporting calcium. Biochem Biophys Res Commun 106: 123-130.

Volpi M, Naccache PH, Sha'afi RI. (1983) Calcium transport in inside-out membrane vesicles prepared from rabbit neutrophils. J Biol Chem 258: 4153-4158.

Volpi M, Yassin R, Naccache PH, et al. (1983) Chemotactic factor causes rapid decreases in phosphatidylinositol 4,5,-bisphosphate and phosphatidylinositol 4-monophosphate in rabbit neutrophil. Biochem Biophys Res Commun 112: 957-961.

Volpi M, Yassin R, Tao W, et al. (1984) Leukotriene B4 mobilises calcium without the breakdown of polyphosphoinositides and the production of phosphatidic acid. Proc Natl Acad Sci USA 81: 5966-5970.

von Tscharner V, Deranleau DA, Baggiolini M. (1986a) Calcium fluxes and calcium buffering in human neutrophils. J Biol Chem 261: 10163-10168.

von Tscharner V, Prod'hom B, Baggiolini M, et al. (1986b) Ion channels in human neutrophils are activated by a rise in the cytosolic free Ca^{2+} concentration. Nature 324: 369-373.

Waller A. (1846) Microscopic observation on the perforation of capaillaries by the corpuscles of blood and the origin of mucus and pus globules. Edinburgh Philos Mag Sci; 29: 271-280

Watkins NJ, Knight MR, Trewalas AJ, Campbell AK. (1995) Free calcium transients in chemotactic and non-chemotactic strains of Escherichia coli determined by using recombinant aequorin, Biochem J 306 865-869

Wegener J, Keese CR, Giaeverl I. (2000) Electric cell–substrate impedance Sensing (ECIS) as a non-invasive means to monitor the kinetics of cell spreading to artificial surfaces. Exptl Cell Res 259, 158–166

Williams LT, Snyderman R, Pike MC, et al. (1977) Specific receptor sites for chemotactic peptides on human polymorphonuclear leukocytes. Proc Natl Acad Sci USA 74: 1204-1208.

Williams RJ. (1970) Cation distributions and the energy status of cells. J Bioenerg. 1(2):215-25

Williams RJ. (1976) The neurobiology of lithium. III. Physical chemistry and transport. Ion complexing with proteins and other macromolecules. Neurosci Res Program Bull 14, 145-51

Williams RJ. (1994) Calcium-binding proteins in normal and transformed cells. Cell Calcium. 16, 339-46

Wills-Karp M. (2007) Complement activation pathways: a bridge between innate and adaptive immune responses in asthma. Proc Am Thorac Soc 4, 247-51

Wilson DG. (1957) Direct effect of corticoid steroids on the electrolyte content of rabbit leukocytes. Am J Physiol 43: 493-502.

Wilson DL, Mannery JF. (1947) Permeability of rabbit leucocytes to sodium, potassium and chloride. J Cell Comp Physiol 34: 493-450.

Wingrad S, Shanes AM. (1962) Calcium flux and contractility in guinea-pig atria. J Gen Physiol 54: 371-394.

Wintrobe MM. (1967) Clinical Haematology. Lea and Febiger, Philadelphia, p226

Worth RG, Kim KM, Kindzelskii AL, et al. (2003) Signal sequence within Fc gamma RIIA controls calcium wave propagation patterns: Apparent role in phagolysosome fusion . Proc. Natl. Acad. Sci. (USA) 100 533-4538.

Zigmond SH. (1977) The ability of polymorphonuclear leukocytes to orient in gradients of chemotactic factors. J Cell Biol 75: 606-617.